

UNIVERSITY OF LATVIA  
FACULTY OF MEDICINE

**Martins Rucins**

**DESIGN OF PHARMACOPHORIC  
GROUP CONTAINING 1,4-DIHYDROPYRIDINE  
DERIVATIVES AND DETERMINATION OF  
SPECTRUM OF PHARMACOLOGICAL ACTIVITIES**

Doctoral thesis

Submitted for the degree of Doctor of pharmacy

Subfield: pharmaceutical chemistry

Riga, 2017

This work was carried out in Latvian Institute of Organic Synthesis and University of Latvia, Faculty of Medicine during the period from the year 2012 until the year 2016.



IEGULDĪJUMS TAVĀ NĀKOTNĒ

This work has been supported by the European Social Fund within the project „Support for Doctoral Studies at University of Latvia” and by the young researcher grant of the Latvian Institute of Organic Synthesis (IG-2016-10).

Form of the thesis: collection of research papers for the degree of doctor of Pharmacy, subfield pharmaceutical chemistry.

Scientific supervisors: Dr. habil. biol. professor **Ruta Muceniece**

University of Latvia, Faculty of Medicine

Dr. chem. **Aiva Plotniece**

Latvian Institute of Organic Synthesis

Official reviewers: Dr. chem. professor **Māra Jure**

Riga Technical university

Dr. habil. biol. professor **Nikolajs Sjakste**

University of Latvia

Dr. professor **Saulius Grigalevičius**

Kaunas University of Technology

The thesis will be defended at the public session of the Promotion Board in Medicine, Biology and Pharmacy of the University of Latvia at 14:00 o'clock on April 7, 2017 in Academic Center for Natural Sciences of the University of Latvia, Riga, Jelgavas street 1, room Nr. 223.

The work and its summary can be viewed at the Library of the University of Latvia, Kalpaka blvd. 4.

Doctoral Committee of Medicine, Biology and Pharmacy of the University of Latvia

Chairman of the Doctoral Committee \_\_\_\_\_ Dr. med., prof. V. Pīrāgs

Secretary of the Doctoral Committee \_\_\_\_\_ Dr. pharm. K. Saleniece

## Publication and approbation of the doctoral thesis

### Publications

- A. Petrichenko O.; **Rucins M.**; Vezane A.; Timofejeva I.; Sobolev A.; Cekavicus B.; Pajuste K.; Plotniece M.; Gosteva M.; Kozlovskā T.; Plotniece A. Studies of the physicochemical and structural properties of self-assembling cationic pyridine derivatives as gene delivery agents. *Chem. Phys. Lip.*, 2015, 191, 25-37. doi:10.1016/j.chemphyslip.2015.08.005.
- B. **Rucins M.**; Gosteva M.; Belyakov S.; Sobolev A.; Pajuste K.; Plotniece M.; Cekavicus B.; Tirzite D.; Plotniece A. Evaluation of antiradical activity and reducing capacity of synthesised bispyridinium dibromides obtained by quaternisation of 4-pyridyl-1,4-dihydropyridines with propargyl bromide. *Aust. J. Chem.*, 2015, 68, 86-92. doi.org/10.1071/CH14033.
- C. **Rucins M.**; Gosteva M.; Domracheva I.; Kanepe-Lapsa I.; Belyakov S.; Plotniece M.; Pajuste K.; Cekavicus B.; Jekabsone M.; Sobolev A.; Shestakova I.; Plotniece A. Synthesis and evaluation of reducing capacity and calcium channel blocking activity of novel 3,5-dipropargylcarbonyl-substituted 1,4-dihydropyridines. *Хим. Гетероцикл. Коэд.*, 2014, N10, 1557-1568; *Chem. Heterocycl. Comp. (Engl. Ed.)* 2015, 50(10). 1431-1442. doi: 10.1007/s10593-014-1607-z.
- D. **Rucins M.**; Kaldre D.; Pajuste K.; Fernandes M.A.S.; Vicente J.A.F.; Klimaviciusa L.; Jaschenko E.; Kanepe-Lapsa I.; Shestakova I.; Plotniece M.; Gosteva M.; Sobolev A.; Jansone B.; Muceniece R.; Klusa V.; Plotniece A. Synthesis and studies of calcium channel blocking and antioxidant activities of novel 4-pyridinium and/or N-propargyl substituted 1,4-dihydropyridine derivatives. *C. R. Chimie*, 2014, 17, 69-80. doi.org/10.1016/j.crci.2013.07.003.
- E. Pajuste K.; Hyvönen Z.; Petrichenko O.; Kaldre D.; **Rucins M.**; Cekavicus B.; Ose V.; Skrīvele B.; Gosteva M.; Morin-Picardat E.; Plotniece M.; Sobolev A.; Duburs G.; Rūponen M.; Plotniece A. Gene delivery agents possessing antiradical activity: self-assembling cationic amphiphilic 1,4-dihydropyridine derivatives. *New J. Chem.*, 2013 37(10), 3062-3075. doi:10.1039/C3NJ00272A.
- F. **Rucins M.**; Petrichenko O.; Pajuste K.; Plotniece M.; Pajuste K.; Gosteva M.; Cekavicus B.; Sobolev A.; Plotniece A. Studies of preparation and stability of liposomes formed by 1',1,-[(3,5-didodecyloxycarbonyl)-4-phenyl-1,4-dihydropyridine-2,6-diil]-dimethylen]bispyridinium dibromide. *Adv. Materials Research*. 2013, 787, 157-162. doi:10.4028/www.scientific.net/AMR.787/157.

## Theses at scientific conferences

1. Plotniece A.; Pajuste Kl.; **Rucins M.**; Vezane A.; Timofejeva I.; Petrichenko O.; Vigante B.; Ose V.; Plotniece M.; Bandere D.; Gosteva M.; Sobolev A.; Kozlovskā T.; Pajuste K. Structure-activity relationships of a series of self-assembling compounds on 1,4-dihydropyridine core as delivery agents. In 30th Conference of The European Colloid and Interface Society, ECIS-2016, September 4-9, 2016: Rome, Italy, 2016; P6.60; 527.
2. Pajuste K.; Vezane A.; **Rucins M.**; Gosteva M.; Timofejeva I.; Pajuste Kl.; Petrichenko O.; Plotniece M.; Vigante B.; Kozlovskā T.; Sobolev A.; Plotniece A. Structure-activity relationships of a series designed cationic 1,4-dihydropyridines as gene delivery agent. In Book of Abstracts, 13th International Conference on Nanosciences & Nanotechnologies (NN16) July 5-8, 2016, Thessaloniki, Greece, 233.
3. Jēkabsone M.; **Ruciņš M.**; Gosteva M.; Muceniece R.; Plotniece A. Ar amīniem modificētu 1,4-dihidropiridīna atvasinājumu sintēze un īpašību pētījumi. Tēžu apkopojums, Latvijas Universitātes 74. Zinātniskā konference. Medicīnas sekcija. Stenda ziņojumi, 19. februārī, 2016: Rīga, LU, 2016; 113.
4. **Rucins M.**; Pajuste K.; Gosteva M.; Sobolev A.; Cekavicus B.; Pajuste Kl.; Vigante B.; Plotniece A. Nanoparticles formed by amphiphilic 1,4-dihydropyridine derivatives. <http://nanoapp.ios.si>. In 2nd International Conference on Nanomaterials & Applications Maribor, Slovenia, 23-26 June, P05, 2015.
5. **Ruciņš M.**; Gosteva M.; Pajuste K.; Sobolevs A.; Cekavicus B.; Muceniece R.; Plotniece A. Antioksidantu un antiradikālo īpašību noteikšana oriģināliem bispiridil-1,4-dihidropiridīnu dibromīdiem. In Latvijas Universitātes 72. Zinātniskā konference. Medicīnas sekcija. Stenda ziņojumi, Tēžu apkopojums, Latvijas Universitātes 72. Zinātniskā konference, Rīga, LU, 2014: Rīga, LU, 2014; 63.
6. **Rucins M.**; Gosteva M.; Belyakov S.; Sobolev A.; Pajuste K.; Plotniece M.; Cekavicus B.; Tīrzīte D.; Plotniece A. Synthesis of novel bispyridinium-1,4-dihydropyridine dibromides and evaluation of their antiradical activity and reducing capacity. In 21st Young Research Fellow Meeting (XXIemes Journées Jeunes Chercheurs SCT), In Assets of Chemistry in Drug Discovery, Montpellier, France, PO-58, 2014.
7. **Rucins M.**; Gosteva M.; Beliakov S.; Sobolev A.; Pajuste K.; Plotniece M.; Cekavicus B.; Tīrzīte D.; Plotniece A. Synthesis and studies of novel bispyridinium-1,4-dihydropyridine dibromides. /PO084/. In International Conference on Organic

- Synthesis, Balticum Organicum Syntheticum (BOS-2014), in Programm and Abstracts, Vilnius, Lithuania, 2014; 128.
8. **Rucins M.**; Pajuste K.; Klimaviciusa L.; Pajuste K.; Kanepe-Lapsa I.; Jansone B.; Sestakova I.; Cekavicus B.; Klusa V.; Gosteva M.; Sobolev A.; Muceniece R.; Plotniece A. Synthesis and Studies of Novel 1,4-Dihydropyridine Derivatives. In Program and Abstract Book, XVth International Conference Heterocycles in Bio-organic Chemistry, May 27th-30th (Poster presentations/PO 107), Riga, Latvia , 2013; 164.
  9. **Rucins M.**; Pajuste K. Synthesis and Studies of Novel Propargyl Group Containing 1,4-Dihydropyridine Derivatives. In Materials of the 8th Paul Walden Symposium on Organic Chemistry (P17), May 13-14, Riga, 2013; 94.
  10. **Ruciņš M.**; Kaldre D.; Skrīvele B.; Jaščenko E.; Jansone B.; Šestakova I.; Pajuste K.; Soboļevs A.; Plotniece A.; Muceniece R. Jaunu N-propargilaizvietotu 1,4-dihidropiridīna atvasinājumu sintēze un īpašību salīdzinājums ar N-neaizvietotiem analogiem. In Tēžu apkopojums, Latvijas Universitātes 71. Zinātniskā konference. Medicīnas sekcija, 15. februāris, Rīga, 2013; 40.
  11. **Rucins M.**; Pajuste K.; Cekavicus B.; Birkmane K.; Petrichenko O. ; Ose V.; Skrīvele B.; Kaldre D.; Gosteva M.; Kazuss E.; Pajuste K.; Plotniece M.; Duburs G.; Sobolev A.; Plotniece A. Synthesis and studies of properties of 1,4-dihydropyridine amphiphiles. In Program and Abstracts, International Conference on Organic Synthesis, Balticum Organicum Syntheticum (BOS-2012), 1-4 July, PO113, Tallinn, Estonia, 2012; 160.
  12. Kore K.; Vezane A.; **Rucins M.**; Cekavicus B.; Timofeeva I.; Gosteva M.; Pajuste K.; Jakovele L.; Pajuste K.; Plotniece M.; Kozlovska T.; Sobolev A.; Plotniece A. Synthesis and studies of new gene delivery agents on base of cationic 1,4-dihydropyridine derivatives. In Abstract book, International Conference in Pharmacology. Targeting cellular regulatory systems, 20-21 April, P15, Riga, Latvia , 2012; 46.
  13. Petr J.; **Rucins M.**; Ginterova P.; Hruzikova J.; Znaleziona J.; Pajuste K.; Plotniece A.; Ševčík J. Characterization of 1,4-dihydropyridine-derivative based liposomes by capillary electrophoresis. In Final Program, 27th International Symposium on MicroScale Bioseparations and Analyses [MSB2012], February 12-15, Geneva, 2012.

## TABLE OF CONTENTS

ANNOTATION .....	7
ABBREVIATIONS .....	9
INTRODUCTION.....	10
The aim of the work.....	11
Tasks to achieve the aim.....	11
Scientific novelty .....	11
Practical significance .....	12
LITERATURE REVIEW .....	13
1,4-Dihydropyridine pharmacological properties .....	13
1,4-Dihydropyridine synthesis.....	20
Propargyl moiety.....	23
Pyridinium moiety .....	24
Nanoparticles .....	25
MATERIALS AND METHODS .....	30
General.....	30
Synthesis .....	31
Evaluation of the compounds' reducing capacity.....	31
Antiradical activity studies .....	32
Intracellular Ca <sup>2+</sup> measurements.....	32
Nanoparticle preparation and studies .....	33
Atomic force microscopy.....	33
Transmission electron microscopy .....	33
Dynamic light scattering.....	34
RESULTS AND DISCUSSION .....	35
Synthesis of 1,4-DHP derivatives (publications A, B, C, D, E) .....	35
Assessment of calcium channel blocking activity (publications C, D) .....	44
Antiradical activity and reducing capacity (publications B, C, D, E).....	47
Nanoparticle studies (publications A, E, F).....	51
CONCLUSIONS .....	59
ACKNOWLEDGEMENTS.....	61
REFERENCES .....	62
APPENDIX.....	81

## ANNOTATION

**Design of pharmacophoric group containing 1,4-dihydropyridine derivatives and determination of spectrum of pharmacological activities.** Rucins M., supervisors Dr. habil. biol. professor Muceniec R., Dr. chem. Plotniece A. Doctoral thesis. 81 pages, 21 figures, 3 tables, 2 schemes, 255 literature references, 1 appendix. In English.

1,4-DIHYDROPYRIDINES, PYRIDINIUM, PROPARGYL GROUP, PHARMACOPHORE, CALCIUM CHANNEL ACTIVITY, ANTIRADICAL ACTIVITY, REDUCING CAPACITY, NANOPARTICLES

1,4-Dihydropyridine cycle is one of pharmacologically privileged structures acting on ion channels and various receptors. Modification of the 1,4-dihydropyridine cycle by synthesis of structural analogues, varying substituents in the molecule provides the approach to give a variety of pharmacologically active compounds. In this thesis were synthesized new, targeted designed, pharmacophoric group containing 1,4-dihydropyridine derivatives by purposeful changing of pharmacophoric groups (pyridinium and/or propargyl) and their location in the molecule. Analyzed a spectrum of pharmacological properties of synthesized compounds (calcium channel activity, antiradical activity and reducing capacity), created the structure-activity relationship model for search of new pharmacologically active compounds. Studied properties of nanoparticle formation and stability of synthesized self-assembling 1,4-dihydropyridine derivatives.

## ANOTĀCIJA

**Farmakoforas grupas saturošu 1,4-dihidropiridīna atvasinājumu dizains un to farmakoloģiskās darbības spektra noteikšana.** M. Ruciņš, darba vadītāji Dr. habil. biol. profesore R. Muceniece, Dr. ķīm. A. Plotniece. Disertācija. 81 lappuse, 21 attēls, 3 tabulas, 2 shēmas, 255 literatūras avoti, 1 pielikums. Angļu valodā.

1,4-DIHDROPIRIDĪNI, PIRIDĪNIJS, PROPARGILGRUPA, FARMAKOFORS, AKTIVITĀTE UZ KALCIJA KANĀLIEM, ANTIRADIKĀLĀ AKTIVITĀTE, REDUCĒJOŠĀ KAPACITĀTE, NANODAĻIŅAS

Vairākkārtīgi ir uzsvērts, ka 1,4-dihidropiridīna cikls ir viens no farmakoloģiski privilēģētām struktūrām, kas iedarbojas uz jonu kanāliem un dažādiem receptoriem, un kuru modificējot, sintezējot tās struktūras analogus, varējot aizvietotājus molekulā, būtu iespējams iegūt dažādus farmakoloģiski aktīvus savienojumus. Pētījumā ir sintezēti jauni, mērķtiecīgi dizainēti, farmakoforas grupas saturoši 1,4-dihidropiridīna atvasinājumi, sistemātiski mainot farmakoforās grupas (piridīniju un/vai propargil) un to atrašanās vietu molekulā. Izvērtēts sintezēto savienojumu farmakoloģiskās darbības spektrs (aktivitāte uz kalcija kanāliem, antiradikālā aktivitāte un reducējošā kapacitāte), veidots struktūras-aktivitātes likumsakarību modelis, meklējot jaunus farmakoloģiski aktīvus savienojumus. Pētīta pašasociējošos 1,4-dihidropiridīna atvasinājumu nanodaļiņu veidošanās un to stabilitāte.



## ABBREVIATIONS

1,4-DHP	1,4-dihydropyridine
<sup>13</sup> C-NMR	carbon nuclear magnetic resonance
<sup>1</sup> H-NMR	proton nuclear magnetic resonance
AA	ascorbic acid
AFM	atomic force microscopy
ARA	antiradical activity
CAD	coronary artery disease
CCB	calcium channel blocker
CDCl <sub>3</sub>	deuterated chloroform
CMC	critical micelle concentration
DHPs	dihydropyridines
DLS	dynamic light scattering
DMEM	dulbecco's modified Eagle medium
DMSO- <i>d</i> <sub>6</sub>	deuterated dimethyl sulfoxide
DNA	deoxyribonucleic acid
DOTAP	N-(1-(2,3-dioleoyloxy)propyl)-N,N,N-trimethyl ammonium methylsulfate
DPPH	1,1-diphenyl-2-picrylhydrazyl
EDTA	ethylenediaminetetraacetic acid
IL	ionic liquids
m.p.	melting point
MCRs	multicomponent reactions
NBS	N-bromosuccinimide
NP	nanoparticles
PDI	polydispersity index
pDNA	plasmid deoxyribonucleic acid
PEI 25	polyethylenimine 25 kDa
ppm	parts per million
RC	reducing capacity
ROS	reactive oxygen species
SD	standard deviation
TEM	transmission electron microscopy
UV	ultraviolet

## INTRODUCTION

Since discovery of nifedipine in 1969 1,4-dihydropyridine (1,4-DHP) derivatives started to play an important role in synthetic, medicinal, and bioorganic chemistry. 1,4-DHP derivatives are large group of structurally diverse compounds with a broad range of pharmacological activities. As an active linker, according to Triggle, 1,4-DHP is an intrinsic structural part of many pharmacologically active compounds and drugs (Triggle 2007; Triggle 2003b). Introduction and variation of the substituents at the 1,4-DHP ring can result in elaboration of the compounds which can be capable to interact at diverse receptors and ion channels. In the same way these activities depend on various structural parameters related to DHPs (presence and character of substituents), lipophilicity, and depth of the incorporation in the biological membranes. Additionally, the main structure element – the DHP cycle – can be regarded as a model of the redox coenzyme NAD(P)H or as analogue of 1,4-dihydronicotinic amide. 1,4-Dihydropyridines regulate redox reactions, possess free radical-scavenging properties, inhibit the peroxidation processes and protect biological membranes (Klusa 2016).

Recently it was demonstrated that 1,4-DHP molecule can also serves as template for construction of synthetic lipid-type compounds which act as non-viral gene delivery agents. The cationic amphiphiles based on 1,4-DHP core show self-assembling properties, which means the formation of liposomes in water, complex DNA and show high transfection efficiency (Hyvönen et al. 2000).

Since the end of the last century in the fields of medicinal and pharmaceutical sciences efforts directed toward the development of new technologies, including transport systems have increased significantly. Synthetic delivery systems most frequently are formed on amphiphilic compound basis such as cationic lipids, polymers etc. However, there is no sufficient data concerning to characterization of formed nanoparticles and the relationships between delivery-activity and properties of nanosystems.

In Latvia synthesis of novel DHP derivatives as antihypertensive agents was started at the Latvian Institute of Organic Synthesis, Membrane active compounds (MAS) in 1980s. During the last years the research team of MAS in cooperation with partners perform synthesis, studies and development of the original 1,4-DHP molecules acting as calcium channel antagonists (M. Rucins et al. 2015; Rucins et al. 2014; Garaliene et al. 2014), multidrug resistance modulators (Krauze et al. 2014; Krauze et al. 2015), putative neuroprotectors (Jansone et al. 2016; Jansone et al. 2015) and self-assembling compounds as gene delivery systems (Pajuste et al. 2013; Petrichenko et al. 2015; Rucins et al. 2013).

The objects of these studies are 1,4-dihydropyridine derivatives with propargyl and/or pyridinium moieties as pharmacophoric groups. The main goal was to evaluate synthesized 1,4-DHP derivatives properties and characterize nanoparticles formed by these compounds.

### **The aim of the work**

Design and synthesis of new 1,4-dihydropyridine derivatives by introducing in the molecule propargyl and/or pyridinium moieties as pharmacophoric groups, variation of moieties position and determination of the spectrum of pharmacological activities and self-assembling properties.

### **Tasks to achieve the aim:**

1. Develop synthetic procedures for preparation of propargyl and/or pyridinium moieties containing 1,4-dihydropyridine (1,4-DHP) derivatives.
2. Synthesize and characterize novel series of 1,4-dihydropyridines with:
  - propargyl moiety variations at positions 1 or 3 and 5, or 2 and 6 of the 1,4-DHP cycle;
  - pyridinium moiety variations at positions 4 or 2 and 6 of the 1,4-DHP cycle;
  - variation of alkyl substituent length at the quaternized N-atom at position 4 of the 1,4-DHP cycle.
3. Study of pharmacological properties of newly synthesized 1,4-DHP derivatives:
  - assessment of calcium channel blocking activity;
  - evaluation of antiradical activity and reducing capacity.
4. Estimate of self-assembling properties of newly synthesized 1,4-DHP derivatives:
  - studies of nanoparticle formation, nanoparticle characterization;
  - studies of stability of liposomes formed by 1,1'-[(3,5-didodecyloxycarbonyl-4-phenyl-1,4-dihydropyridine-2,6-diyl)dimethylen]bispyridinium dibromide.

### **Scientific novelty**

The main goal of this study is design and synthesis of new 1,4-dihydropyridine derivatives by introduction into the molecule pharmacophoric groups - propargyl and/or pyridinium moieties and characterization of the spectrum of pharmacological activities and self-assembling properties of newly synthesized compounds.

Obtained results underlined the following novelty:

- A series of original 1,4-DHP derivatives containing propargyl and/or pyridinium moieties were obtained by targeted variation of the substituents at different positions of the 1,4-DHP cycle.

- In the reaction between 4-pyridyl-1,4-DHP derivatives with propargyl bromide an unexpected course of quaternization was observed and new bispyridinium dibromides on the base of 1,4-DHP were obtained instead of the expected monomeric N-propargyl-pyridinium-1,4-DHP bromides.
- Evaluation of calcium channel blocking activity, antiradical activity and reducing capacity of new 1,4-DHP derivatives containing pharmacophoric moieties was carried out.
- New amphiphilic pyridine derivatives containing dodecyloxycarbonyl substituents at positions 3 and 5, and cationic moieties at positions 2 and 6 were synthesized for comparison studies of their and the corresponding 1,4-DHP as NAD/NADH analogues properties.
- Estimation of self-assembling properties of newly synthesized cationic compounds was performed, characterization of obtained nanoparticles was achieved.

### **Practical significance**

The results of performed work, obtained data and recommendations of structure-activity relationships for 1,4-DHP derivatives containing propargyl and/or pyridinium moieties as pharmacophoric groups including data about self-assembling properties of 1,4-DHP containing cationic moieties will be offered for applications in the scientific communities of Latvia and other countries for development of new pharmacologically active compounds on 1,4-DHP core. In the future these self-assembling compounds can find applications in medicine as various synthetic lipid-like transport molecules with defined pharmacological properties, including for development of theranostic nanosystems; in chemistry as nanoreactors for a number of reactions and organized ionic liquids; in material science as molecules with self-assembling properties.

## LITERATURE REVIEW

### 1,4-Dihydropyridine pharmacological properties

Heterocycles are central backbones of the main part of natural products, pharmaceutically active molecules and biologically relevant compounds. One of the most well-known small molecules, is 1,4-dihydropyridine (1,4-DHP) as privileged nitrogen containing heterocycle which showed up everywhere in drugs currently in use in clinics and biologically active compounds. (Ioan et al. 2011; Hu et al. 2015; Carosati et al. 2012) 1,4-DHPs exhibit a diverse range of biological activities such as those for the treatment of cardiovascular diseases and hypertension, (Shan et al. 2004) potent calcium channel antagonists and agonists. (Triggle & Rampe 1989) They also have potential applications in other pharmacological activities, (Hilgeroth & Lillie 2003; Abbas et al. 2010) such as neuroprotective, anti-inflammatory, anti-ischemic, anti-diabetic, and many other actions (Duburs et al. 2008; Rucins et al. 2014) After the first synthesis of dihydropyridine reported by Hantzsch (Hantzsch 1882), many synthetic efforts have been made from all over the world to access these compounds due to their medicinal and synthetic usefulness. (Debache et al. 2009; Khan & Musawwer Khan 2011; Kumar & Maurya 2008; Evdokimov et al. 2006) In the recent years new biological functions (anti-proliferative (Singh et al. 2015), multidrug resistance (Shekari et al. 2015; Cindric et al. 2010; Krauze et al. 2014) and anti-bacterial (Sirisha et al. 2011)) on 1,4-DHPs scaffolds have continuously been discovered along with the increasing availability of new synthetic strategies. (Hu et al. 2015; Khan & Musawwer Khan 2011)

Calcium ions act as an intracellular signal and play a critical role in biological functions including muscle contraction, release of neurotransmitters, calcium-dependent gene transcription, and the regulation of neuronal excitability. Several types of voltage-dependent calcium channels have been identified in native tissues and classified into at least five subtypes based on their pharmacological and functional properties: N-(Cav2.2), L-(Cav1.1-Cav1.4), P/Q-(Cav2.1), R-(Cav2.3) and T-type (Cav3.1-Cav3.3). (Yamamoto et al. 2008; Li et al. 2015; Leo et al. 2017; Neumaier et al. 2015) Voltage-gated calcium channels are integral membrane proteins that open via electrical depolarization of the plasma membrane and mediate the entry of calcium ions into the cell. (Fig. 1) Calcium channels are found in every excitable cell, including neurons, myocytes and pancreatic  $\beta$ -cells and form the most efficient molecular link between membrane depolarization and intracellular biochemical signaling. (Bülbül et al. 2009)

Voltage gated calcium channels (Fig. 1) are key mediators of depolarization induced calcium influx into excitable cells, which in turn mediates a wide array of physiological responses including the activation of calcium dependent enzymes, smooth muscle contraction, pacemaker activity and neurotransmitter release. (Cooper et al. 2010; Zhao et al. 2011; Marger et al. 2011)

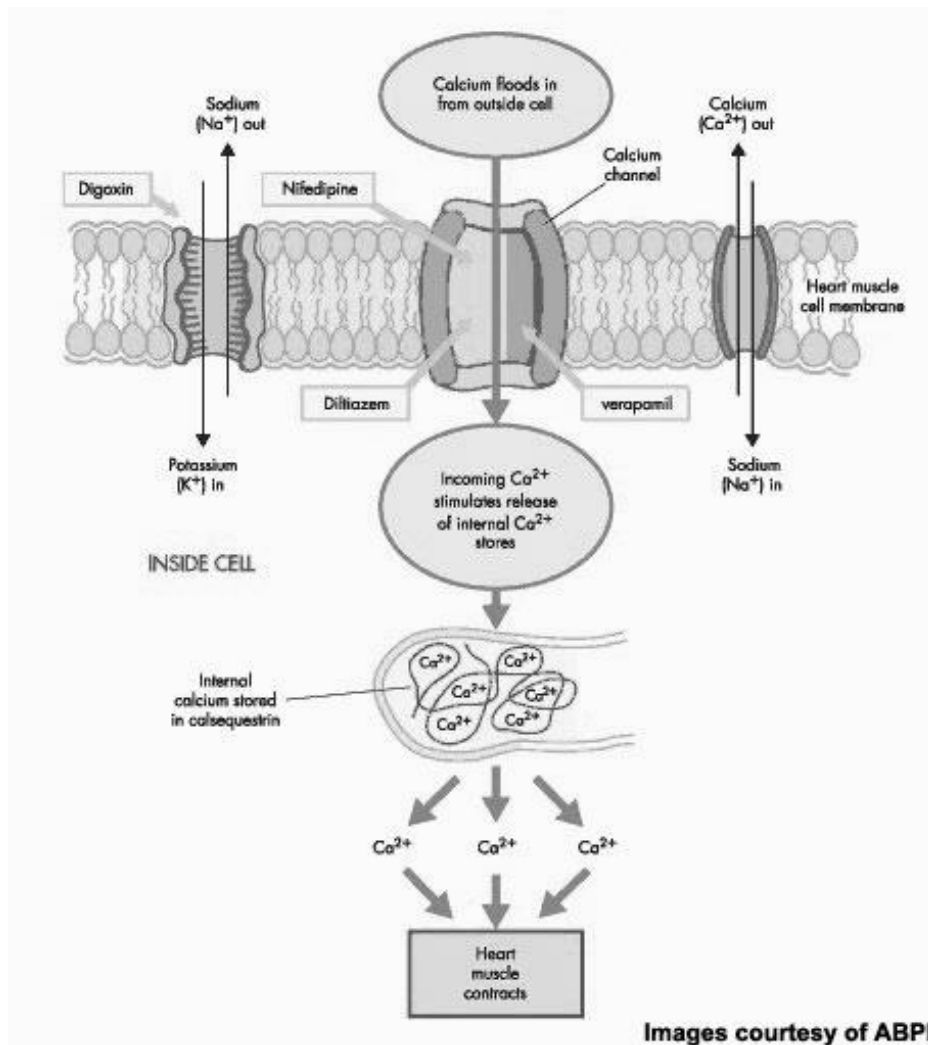


**Figure 1. Mechanism of action of calcium channel blockers in heart muscle cells**

Calcium channels are associated with a wide range of pathologies - pain, epilepsy, migraine, cardiac arrhythmias and autism. (Zamponi & Currie 2013; Tottene et al. 2011; Khosravani & Zamponi 2006; Liao & Soong 2010) Calcium channel blockers (CCB) are frequently prescribed for hypertension treatment, but their role in coronary artery disease (CAD) was previously limited due to the increased mortality and myocardial infarction risk observed in patients taking rapid release, short-acting dihydropyridines. Furthermore, findings from several large scale studies demonstrate long-acting CCB are as efficacious as beta-blockers for prevention of cardiovascular cases with comparable overall outcomes in patients with, or at risk for CAD. (Cooper-DeHoff et al. 2013; Hjemdahl et al. 2006; Dahlof et al. 2005)

**Cardioprotective activity.** Analyzing the literature sources about the properties of 1,4-DHP derivatives and to make some conclusions there are emerged main recommendations and trends in building the cardioprotective agents as 1,4-DHP derivatives (Fig. 2).

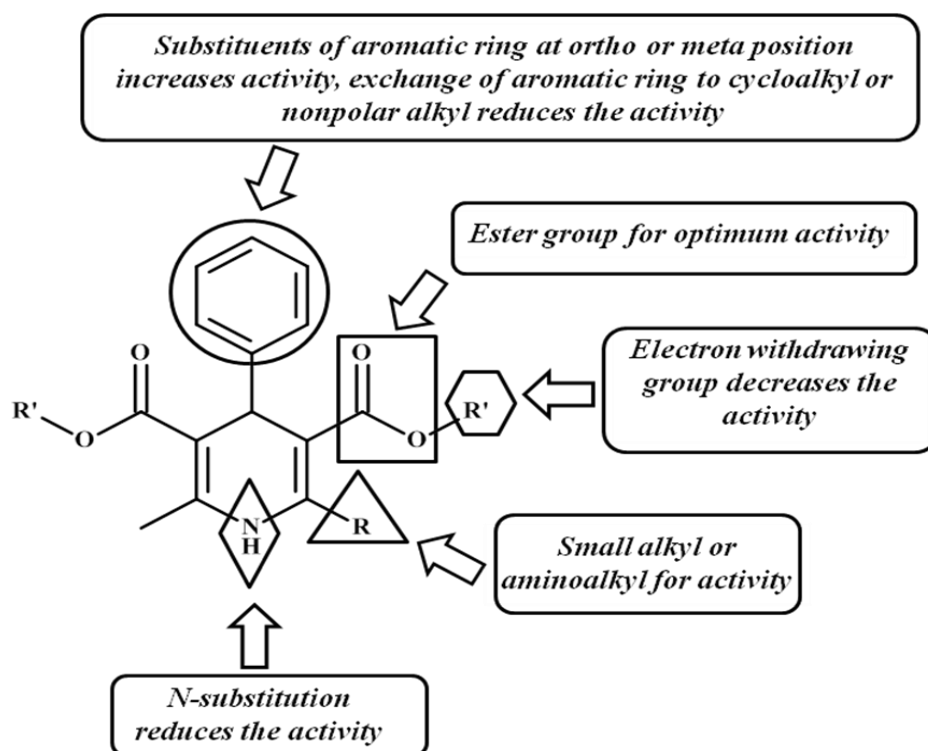


**Figure 2. Design of 1,4-DHP derivatives for cardioprotective activity** (Schade et al. 2012; Pedemonte et al. 2007; Edraki et al. 2009)

Structure-activity relationships of 1,4-DHP derivatives for cardioprotective activity: 1,4-DHP molecule needs to be decorated with ortho or meta position substituted aromatic ring at position 4 of the cycle, N substitution decreases the activity, optimum activity can be achieved by introduction of ester groups at the 3,5-positions, however R' electron withdrawing groups may decrease the activity. In the most cases R' groups are not identical and structurally R groups usually are small alkyls or aminoalkyls (Fig. 2). Therefore, the preparation of novel 1,4-DHP derivatives is challenging target in medicinal and synthetic organic chemistry. Many attempts to improve Hantzsch synthesis using green methods and alternative catalysts have been studied. (Nandi et al. 2010; Shen et al. 2010; Wang et al. 2011; Karlis Pajuste et al. 2011; Tamaddon et al. 2010; Palmisano et al. 2011; Safari et al. 2011; Kumar & Sharma 2011; Yang et al. 2013) The most efficient strategies for the synthesis of 1,4-DHPs are multicomponent reactions (MCRs) in terms of providing both sufficient structural diversity and a large number of compounds libraries. (Abdelhamid et al. 2015;

Shaaban 2014; Allais et al. 2014; Bugaut et al. 2013; Brauch et al. 2013; Dömling et al. 2012; Shiri 2012; Isambert et al. 2011; Candeias et al. 2010)

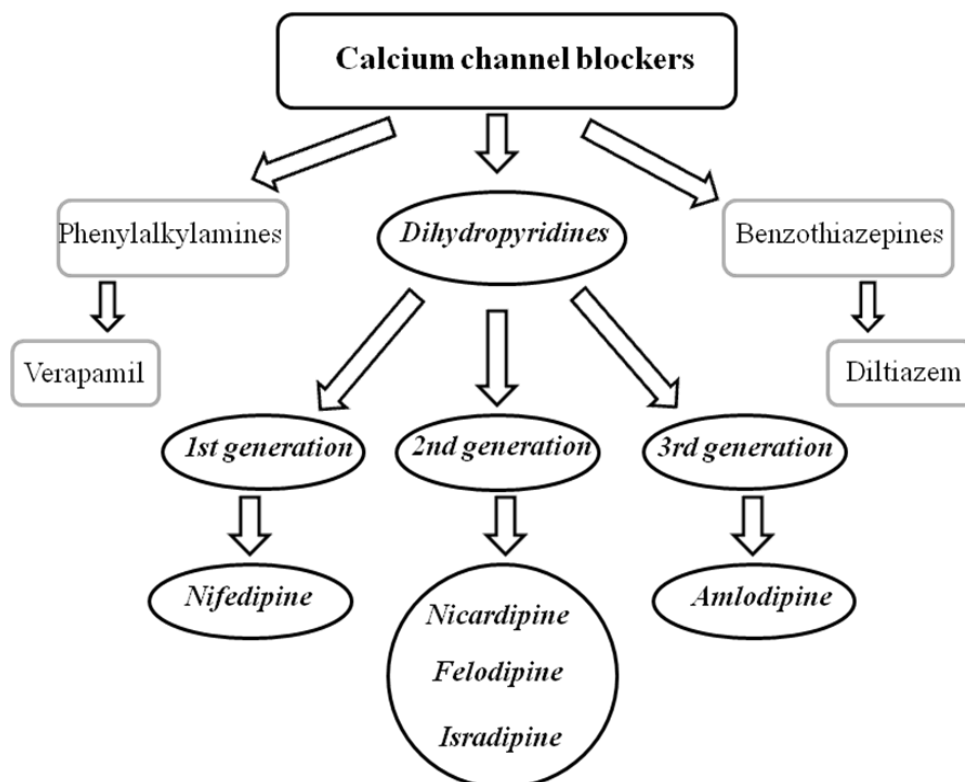


Figure 3. Calcium channel blockers (Whyte et al. 2016)

There are three classes of calcium channel blockers (phenylalkylamines, benzothiazepines and dihydropyridines), in this thesis interest is more focused on dihydropyridines. There are currently three generations of dihydropyridines: 1st generation with short half-life period <3 hours (nifedipine); 2nd generation with long half-life period <14 hours (isradipine); 3rd generation with very long half-life period >30 hours (amlodipine) (Fig. 3 and 4). (Zanchetti 2003)

Up to now 4-aryl-1,4-dihydropyridine-3,5-dicarboxylic esters of the nifedipine (Fig. 4) type are one of the most widely used and studied medications among calcium channel blockers. (Balalaie et al. 2013; Bossert & Vater 1989)



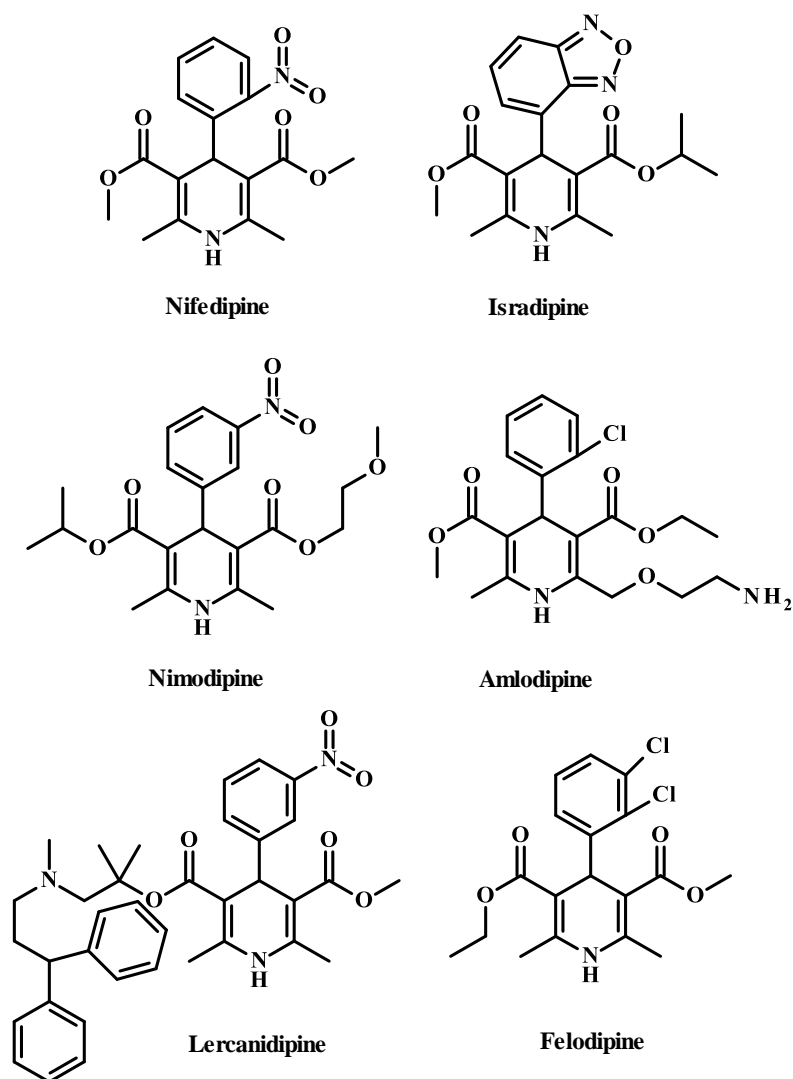


Figure 4. Structures of some calcium channel blockers – 1,4-DHP derivatives (Khairy et al. 2017; Qiu et al. 2016; Daschil & Humpel 2014; Triggle 2007)

It is worth to underline that the 1,4-DHP group is a privileged structure or scaffold and with appropriate substituents capable to interact with diverse receptors and ion channels. As an active linker, according to Triggle, 1,4-DHP is an intrinsic structural part of many pharmacologically active compounds and drugs. (Triggle 2007; Triggle 2003a)

**Neuroprotective activity.** During the last decades, interest has arisen to neurotropic effects of different 1,4-DHP derivatives, since experimental and clinical studies demonstrated their ability to penetrate the blood-brain barrier and reduce the risk of developing neurodegenerative diseases (Ritz et al. 2010; Becker et al. 2008). For example, about 27% reduction in Parkinson's disease risk was observed in patients who had taken centrally acting calcium channel blocking drugs (Simon et al. 2010). These drugs (e.g. isradipine Fig. 4) are found to be beneficial also for the Alzheimer's disease treatment strategy (Anekonda et al.

2011; Anekonda & Quinn 2011; Paris et al. 2011). 1,4-DHP derivatives of typical calcium antagonist (Miyazaki et al. 1999) or atypical (neuronally non-antagonist) class (Rumaks et al. 2012) showed neuroprotective properties also in ischemic stroke models. Search for memory-improving/dementia-preventing effects of 1,4-DHP derivatives are still on the agenda in experimental laboratories and clinics (Fournier et al. 2009). Taking into account mitochondrial abnormalities as the essential cause of neurodegeneration, particular importance is related to 1,4-DHP mitochondria-protecting effects. (Fernandes et al. 2005; Fernandes et al. 2009)

Some of 1,4-DHP derivatives (e.g. glutapyrone, cerebrocrast and 3',5'-bisethoxycarbonyl-2',6'-dimethyl-1-dodecyl-1',4-dihydro[3,4']bipyridinyl-1-ium bromide (AP-12)) which are synthesized at Latvian Institute of Organic synthesis also showed neuroprotection and memory stimulation. (Klusa 2016)

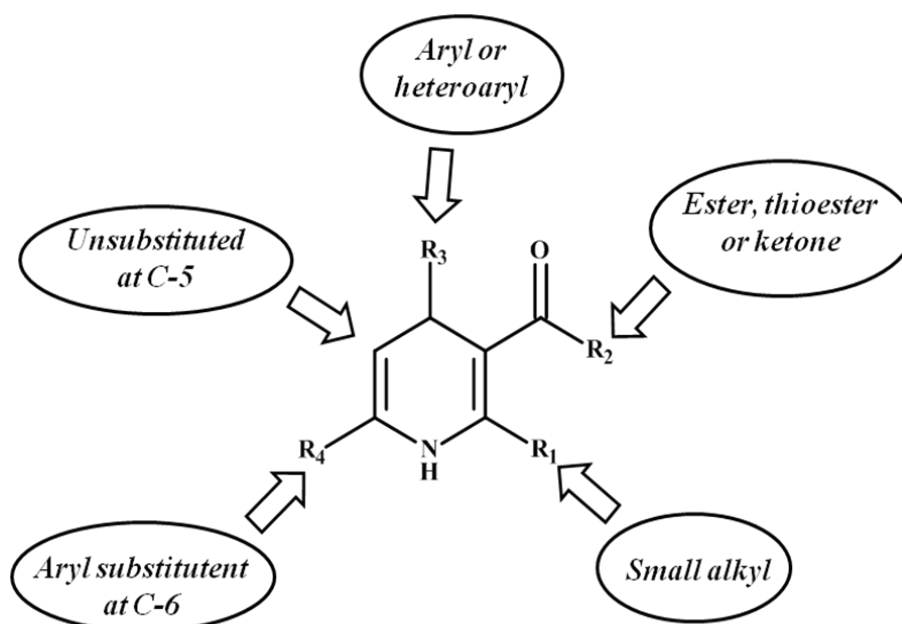


Figure 5. Design of 1,4-DHP derivatives for neuroprotective activity (Tenti et al. 2013)

Design of 1,4-dihydropyridine derivatives for neuroprotection is based on following structure-activity relationships: usually R<sub>1</sub> small alkyl; R<sub>2</sub> must be ester, thioester or ketone; R<sub>3</sub> aryl or heteroaryl; unsubstituted 1,4-DHP cycle at C-5 position and aryl substituent at R<sub>4</sub> (Fig. 5).

Felodipine and lercanidipine (Fig. 4) are usually used for treatment of hypertension and certain forms of angina (Tiwari 2015). Nifedipine (Fig. 4) is used for some types of angina (Canova et al. 2012). Nimodipine (Fig. 4) nowadays gives good results in preventing vasospasm associated with subarachnoid haemorrhage (Bele et al. 2015).

Photolability of dihydropyridines (DHPs) is well known, as well as the oxidation of the dihydropyridine ring to pyridine derivative as the main degradation mechanism is described (Maafi & Maafi 2013; Marinkovic et al. 2003). Pyridine by-products have been shown to have no therapeutic effects (Marinkovic et al. 2003; Ragno et al. 2003). Production of singlet oxygen and superoxide species has been observed during the photodegradation process, inducing peroxidation of fatty acids and leading dermatitis (Onoue et al. 2008). Furthermore, the same degradation mechanism has been observed in the liver metabolism of these drugs through oxidation catalysed by the analogue of cytochrome P-450 (Niwa et al. 1995). Photodegradation of the DHPs are particularly fast in solution (De Filippis et al. 2002), and this is the reason why most of the pharmaceuticals containing these drugs are marketed in solid formulations, usually tablets. (De Luca et al. 2016)

Additionally, the 1,4-DHP derivative containing COONa moiety at position 4 of the 1,4-DHP cycle synthesized at Latvian Institute of Organic Synthesis showed antimutagenic and deoxyribonucleic acid (DNA) repair stimulating activity. (Buraka et al. 2014)

***Antioxidant activity.*** The term antioxidant is commonly used in scientific literature but it can be defined in multiple ways according to the methods used to measure antioxidant activity. Therefore, Halliwell and Gutteridge (Halliwell & Gutteridge 1995) proposed a definition of an antioxidant as “any substance that delays, prevents or removes oxidative damage to a target molecule”. Physiological role of these compounds, as this definition suggests, is to prevent damage to cellular components arising as a consequence of chemical reactions involving free radicals (Procházková et al. 2011) In recent years, much information has appeared about the role of oxidative stress in the development of a number of serious illnesses, such as certain cancers, cardiovascular diseases and age-related degenerative diseases, and about the possible therapeutic value of antioxidants against these illnesses. (Andzi Barhé & Feuya Tchouya 2016)

In the last years, many studies have shown the relation between oxidative stress, cellular senescence and some diseases (Finkel & Holbrook 2000). In addition, current lifestyle is causing the overproduction of free radicals and reactive oxygen species (ROS) in our organism, increasing the physiological level of oxidative stress while decreasing the antioxidant activity (Ward et al. 2004). Free radicals and other ROS, such as singlet oxygen, hydroxyl radical, superoxide anion, and peroxy radical, can be generated from normal metabolism in the human body, and can cause oxidative damage to functional macromolecules such as DNA, proteins and lipids (Apel & Hirt 2004). This increases the chance of occurrence of neurodegenerative diseases, inflammation, atherosclerosis, cancer

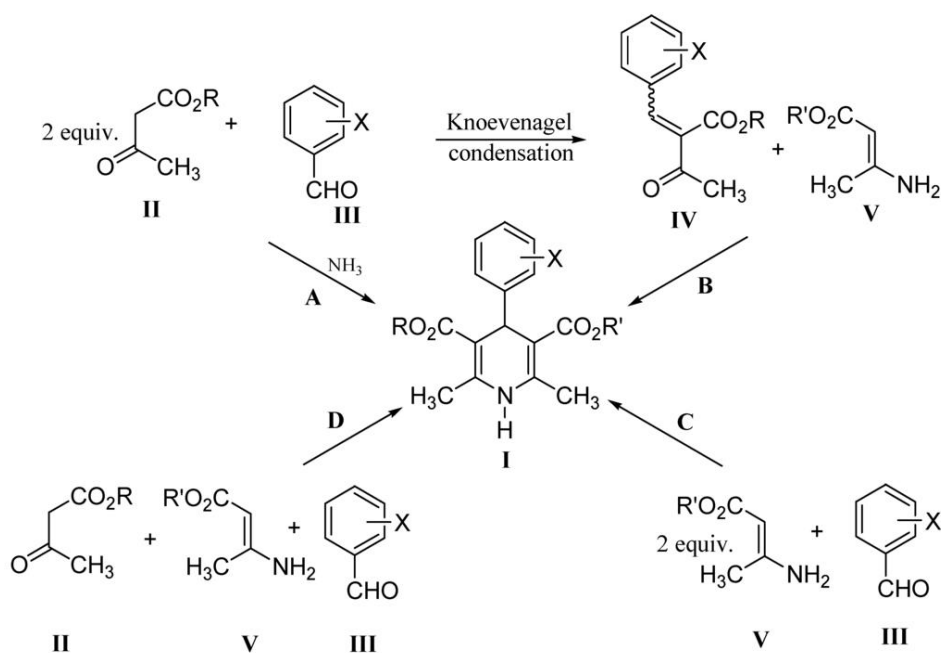
and age-related disorders. Antioxidants protect the human body from free radicals, preventing oxidative stress and associated diseases. (Jiménez-Zamora et al. 2016; Halliwell 1996)

Antioxidants are compounds which can inhibit or retard the oxidation of lipids and other biomolecules. They prohibit the start of an oxidizing chain reaction by radicals or quench the propagation. These reactions can cause functional damage to the human body, like cancer or cardiovascular diseases. Antioxidants can prevent this process due to their redox properties like reductive behavior, the donation of hydrogen or quenching of singlet oxygen. (Wollinger et al. 2016; Ismail et al. 2004)

According to various recommendations from literature concerning structure-activity relationships, the main task of this work is to perform design and synthesis of new 1,4-dihydropyridine derivatives by introducing propargyl and/or pyridinium moieties as pharmacophoric groups at various positions of 1,4-DHP cycle and to characterize spectrum of pharmacological activities of synthesized 1,4-DHP derivatives.

### **1,4-Dihydropyridine synthesis**

1,4-DHPs as the cyclic base donors are known as useful reactants in the synthesis of complex organic molecules. (Rudler et al. 2008; Schmaunz et al. 2014) In addition, they have been used as a hydride source for reductive amination (Hoffmann et al. 2006; Li & Antilla 2009) and used as synthetic intermediates. (Vicente-García et al. 2010; Chen & McNeil 2008) The versatile known utilities as well as the high application of 1,4-DHP cycle in different research areas have accordingly stimulated the timeless research interest in the synthesis of 1,4-DHPs, especially in the manner of diversity-oriented synthesis. (Stout & Meyers 1982; Wan & Liu 2012) As the first authentic diversity-oriented method toward 1,4-DHPs synthesis, the Hantzsch multicomponent reaction has hugely contributed to the chemistry of 1,4-DHPs, (Hantzsch 1882) which also inspired the excellent research advances in 1,4-DHPs synthesis with new approaches. During the past decade, a large number of outstanding works have been reported allowing the synthesis of 1,4-DHPs in great span of structural diversity, especially in the fashion of multicomponent reactions. (Wen et al. 2010; Wan et al. 2013; Kumar et al. 2014; Safari & Zarnegar 2013; Gati et al. 2012; Liu et al. 2013; Sun et al. 2011) A common feature of most known multicomponent methods, however, is that an aldehyde must be used to donate the formyl group. Such kind of synthetic methods result in the consequence of limited product diversity since most known multicomponent 1,4-DHPs syntheses provide 4-aryl or 4-alkyl 1,4-DHPs by relying on the aldehyde as the donor of C-4 fragment of the ring. (Hu et al. 2015)



*Scheme 1. Most common variations of the Hantzsch 1,4-DHP synthesis* (Filipan-Litvić et al. 2007)

As it seen from the Scheme 1, methods **A** (aldehyde **III** and two equivalents of acetoacetic acid ester **II**) or **C** (aldehyde **III** and two equivalents of  $\beta$ -aminocrotonic acid ester **V**) are only used for the synthesis of symmetrical, nonchiral 1,4-DHPs ( $R=R'$ ) (Affeldt et al. 2012), while methods **B** (two step synthesis *via* Knoevenagel intermediate **IV** and  $\beta$ -aminocrotonic acid ester **V**) or **D** (three component cyclocondensation; aldehyde **III**, acetoacetic acid ester **II** and  $\beta$ -aminocrotonic acid ester **V**) are usually used for the synthesis of 1,4-DHPs having different ester moieties ( $R\neq R'$ ) (Ghosh et al. 2013). In these studies the interest is more focused on symmetrically substituted 1,4-dihydropyridine cycle at the positions 3 and 5 or 2 and 6, therefore here mainly used modified methods A or C for design and synthesis of 1,4-DHP derivatives.

In view of the synthetic, industrial and biological importance of 1,4-DHP derivatives and polyhydroquinolines, several methods for synthesis have been reported. The classical Hantzsch reaction for the synthesis of 1,4-dihydropyridines is one-pot condensation of aldehyde with acetoacetic acid ester and ammonia at room temperature or by refluxing in alcohols for a long period of time (Loev & Snader 1965; Hantzsch 1882). This method involves harsh reaction conditions, long reaction times and low yields of products. Thereby several alternate and more efficient methods have been developed for the synthesis of dihydropyridine and polyhydroquinoline derivatives by using of conventional heating (Suárez et al. 1999), solar thermal energy (Mekheimer et al. 2008), ionic liquids (Fan et al. 2006; Priede & Zicmanis 2015), metal triflates (Wang et al. 2005; Donelson et al. 2006),

chlorotrimethylsilane and sodium iodide reagent system (Sabitha et al. 2003), grinding (Kumar et al. 2008), HY-Zeolite (Das et al. 2006), molecular iodine (Ko et al. 2005), polymers (Dondoni et al. 2004), cerium(IV) ammonium nitrate (Reddy & Raghu 2008), montmorillonite K-10 (Song et al. 2005), silica perchloric acid (Maheswara et al. 2006), *p*-toluenesulfonic acid (Cherkupally & Mekala 2008), L-proline and its derivatives (Evans & Gestwicki 2009; Kumar & Maurya 2007b), nickel nanoparticles (Sapkal et al. 2009), glycine (Singh & Singh 2010), Baker's yeast (Kumar & Maurya 2007a), and hafnium(IV) bis(perfluorooctanesulfonyl)imide complex in fluorous media (Hong et al. 2010) as well as microwave (Li et al. 2008) and ultrasound irradiation (Juncai 2001). Although most of these processes have distinct advantages, the use of high temperatures, expensive metal precursors, environmentally harmful catalysts, harsh reaction conditions, long reaction times and large quantity of volatile organic solvents limits the use of these methods. Furthermore, the main drawbacks of almost all existing methods are that the catalysts are destroyed in the work-up process and cannot be recovered and reused. (Nasr-Esfahani et al. 2014)

The design and efficient synthesis of bioactive compounds is one of the main objectives of organic and medicinal chemistry. In recent years, multicomponent reactions have become important implement in the preparation of structurally diverse chemical libraries of drug-like polyfunctional compounds. (Balalaie et al. 2013; Dömling et al. 2012)

Multicomponent reactions are one-pot processes that combine three or more building blocks simultaneously. (Heydari et al. 2009; Guillena et al. 2007; Dömling 2006) That kind of reactions play an important role in combinatorial chemistry for the efficient construction of highly complex molecules in a single procedural step from three or more reactants to synthesize target compounds, (Dömling et al. 2012; Touré & Hall 2009) thus avoiding the multiplex purification actions and allowing savings of both solvents and reagents, thereby enhancing the greenness of transformations. (Han et al. 2014; Ma et al. 2010; Staben & Blaquiere 2010) Multicomponent reactions offer a wide range of possibilities for the construction of highly complex molecules in a one step with high atom economy, minimum time, labor, cost and straight forward experimental procedures. (Rezvanian 2016; Sunderhaus & Martin 2009) Such processes are of a great interest in diversity-oriented synthesis, especially to generate compound libraries for screening purposes. (Heydari et al. 2009)

Combining two active pharmacophores into the molecule is one of the possibilities for drug design techniques which are used for drug discovery. (Martins Rucins et al. 2015) As it is described in various literature sources 1,4-DHP scaffold by it self is pharmacophore (Triggle 2003a; Triggle 2007; Carosati et al. 2012). Many pharmacophoric groups are reported previously (Praveena et al. 2015; Harel et al. 2013), therefore in this thesis have been

chosen two of them – propargyl and pyridinium moieties, which are specific themselves and with determined biological properties. Hybrid molecules which combine together 1,4-DHP cycle and one or both these pharmacophores were insufficiently investigated to this day, therefore further studies are necessary to make conclusions and recommendations for structure-activity relationships.

### Propargyl moiety

The propargyl moiety is known to play an important role in providing neuro- and mitochondria-protecting properties of propargyl group containing antidepressants, selegiline and rasagiline (Fig. 6). (Youdim et al. 2005; Weinreb et al. 2010) Propargylic compounds are common motifs in many natural products, fine chemicals, and synthetic pharmaceuticals, as well as useful synthetic intermediates in organic synthesis. (Zhang & Hu 2015)

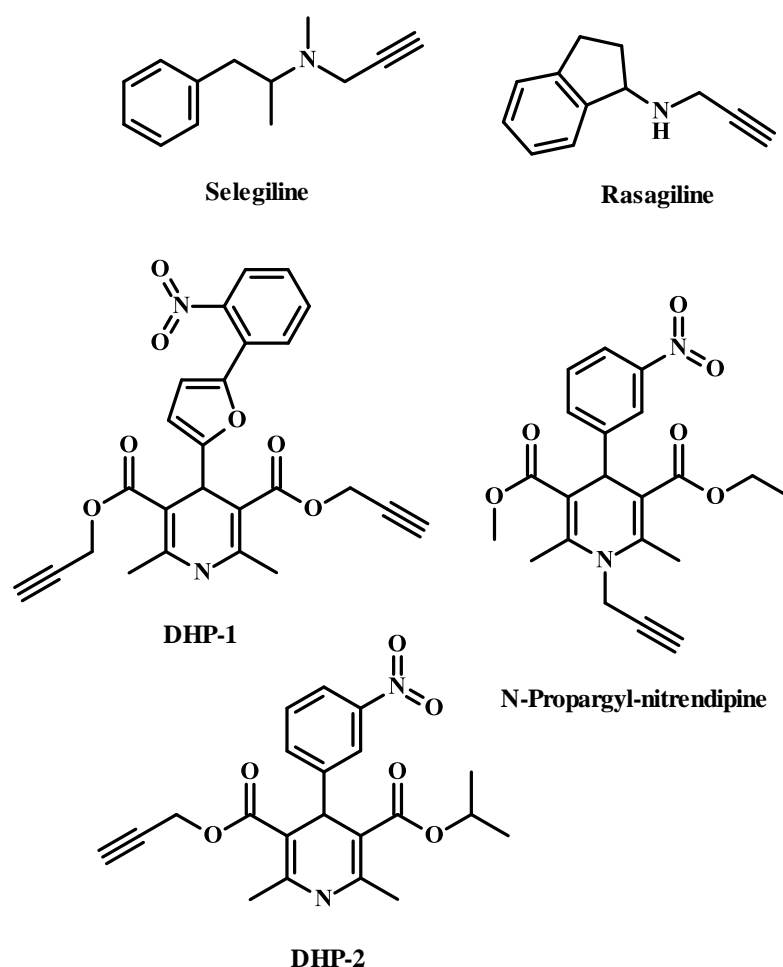


*Figure 6. Propargyl group containing representatives of pharmacologically active compounds (Harper et al. 2003; Cupka et al. 1987; AG 1976)*

Propargyl alcohol is an important moiety which has been routinely used as a scaffold for the synthesis of various heterocyclic compounds of biological interest. (Antony Savarimuthu et al. 2014; Rosenberg et al. 1991)

The one and only literature source about the N-propargyl group containing 1,4-DHP derivative – N-propargyl-nitrendipine (Fig. 6) – demonstrated the store-operated channel blocking effect in leukemic HL-60 cells. (Harper et al. 2003) There are also few literature sources about symmetrically (Fig. 6, DHP-1) and unsymmetrically (Fig. 6, DHP-2) propargyl moiety 3,5-substituted 1,4-DHP derivatives with cardiovascular and antihypertensive activities. (AG 1976; Aktiengesellschaft 1977; Tacke et al. 1983; Cupka et al. 1987)

### **Pyridinium moiety**

The significant interest in pyridinium and their salts is caused by high biological activity exhibited by these compounds containing these groups (Fujimoto et al. 2006; Ilies et al. 2006). Pyridine derivatives possess antimicrobial (Riahi et al. 2009), antitumor (Onnis et al. 2009; Pape et al. 2015) and carbonic anhydrases activating (Dave et al. 2011) properties, and are used for supplying genetic material *in vivo*. (Sharma et al. 2013; Fiscaro et al. 2017; Parvizi et al. 2014; Mamusa et al. 2016; Fiscaro et al. 2016) Pyridinium group can be used as a functional tool to enhance the bioactivity of the target compounds due to its positive charge. It can facilitate the interaction with anionic cell components and consequently conduce to the disruption of the innate defense system of bacterial membranes. The antibacterial activities are substantially enhanced after introducing the pyridinium group into 2,5-substituted-1,3,4-oxadiazole sulfoxide/sulfone, further suggesting that appreciable bioactivity can be achieved through introducing pyridinium group into heterocyclic systems. (Wang et al. 2016)

Pyridinium moiety containing compounds are quite often used as ionic liquids (IL) in organic synthesis. The interest of using pyridinium ILs is growing due to the wide range of applications in which pyridinium ionic liquids have been used in different fields such as nanotechnology, biotechnologies and in various organic reactions (Yoshida et al. 2007; Zhao et al. 2005). However, the toxicity data on pyridinium ILs is still incomplete. (Farouk et al. 2016)

Pyridine or pyridinium moiety/ies containing 1,4-dihydropyridine derivatives were not in detail studied previously. Thus, only few literature sources described studies of 4-pyridyl-1,4-DHP as calcium channel antagonists in the last decades. (Dagnino et al. 1987; Jensen et al. 2002) Synthesis (Makarova et al. 1997; K Pajuste et al. 2011) and influence of 4-pyridinium substituent containing 1,4-DHP derivatives on liposomes and erythrocyte membranes were studied by group from Latvian Institute of Organic Synthesis. Obtained data



confirmed a direct correlation between length of alkyl chain substituent at N-quaternized 4- $\beta$ -pyridyl-1,4-dihydropyridines and their improved membranotropic effects, such as incorporation in the liposomal membranes and bilayer fluidity. (Tirzite et al. 1998; Makarova et al. 1995) Additionally, N-quaternized 4-pyridyl-1,4-dihydropyridines showed gene delivery activity. (Hyvönen et al. 2000) During the last years one from representatives of N-quaternized 4- $\beta$ -pyridyl-1,4-DHP derivatives - 3',5'-bisethoxycarbonyl-2',6'-dimethyl-1-dodecyl-1',4-dihydro[3,4']bipyridinyl-1-ium bromide (AP-12) demonstrated the ability to cross the blood-brain barrier, improve spatial learning and memory in both mice strains, induce anxiolytic action in transgenic mice, and increase expression of hippocampal and cortical proteins (GAD67, Homer-1) related to synaptic plasticity (Jansone et al. 2015) and also in Tg female mice demonstrated spatial learning/memory-enhancing and anxiolytic effects with the predominant mechanisms based on regulation of GABAergic and synaptic plasticity processes in brain. (Jansone et al. 2016)

## **Nanoparticles**

Nanotechnology is rapidly expanding in the food and pharmaceutical industries (Neethirajan & Jayas 2011; Huang et al. 2010). One of the main applications of nanotechnology is nano-encapsulation of bioactive compounds for biological purposes. During nano-encapsulation process, besides bioactive protection, compounds bioavailability also is improved due to increase in surface to volume ratio by reducing particle size into nano-range. (Faridi Esfanjani & Jafari 2016; Raei et al. 2015; Shamsara et al. 2015; Mohammadi et al. 2016; Mehrnia et al. 2016) Various kinds of nanoparticle (NP)-based drug delivery systems have been constructed using novel nanomaterials. These NPs include liposomes, dendrimers, micelles, polymer nanoparticles and inorganic nanoparticles (Srikanth & Kessler 2012), which can carry therapeutic drugs or imaging probes and deliver them to target site (Gao 2016).

Different industries, especially medicine, have got the main benefits of this technology. There is enormous excitement regarding nanomedicine's potential impact on drug delivery and targeting (Singh & Lillard 2009), phototherapy (Paszko et al. 2011), biomedical imaging (Koo, Huh, Ryu, et al. 2011) and gene delivery (Jayakumar et al. 2010). Drug delivery *via* NPs presents novel therapeutic opportunities for active agents that were previously unsuited to traditional oral or injectable therapeutic formulations. (Najafi-Hajivar et al. 2016)

Typically, nanoparticles offer many advantages such as small particle size, greater drug efficacy, lower toxicity, enhanced drug solubility and stability. (Lakshmanan et al. 2011) According to the enhanced permeability and retention effect, nanoparticles can easily

accumulate at the tumor site at high concentrations due to the pathophysiological differences between normal tissues and tumor tissues; this phenomenon is known as passive targeting. (Jee et al. 2012) In addition, ligand-receptor, antigen-antibody and other forms of molecular identification by conjugation of targeting molecules onto nanoparticles to obtain targeted delivery systems of specific cells, tissues or organs are known as active targeting, which can maximize the drug therapeutic efficacy and reduce side effects. (Zhang et al. 2016; Slavoff & Saghatelian 2012; Chattopadhyay et al. 2012)

Currently, more than 1600 nano-based products have been introduced into the market (Vance et al. 2015) due to their properties, such as antimicrobial agents (Liu et al. 2012), color additives (Chen et al. 2013), ultraviolet (UV) filters (Newman et al. 2009; Al-Mubaddel et al. 2012), processing additives, agents for clarification, pH control (Grombe et al. 2014) or carrying flavours and aromas (Contado et al. 2013). Most commonly NPs are used in medicine (Au, CeO<sub>2</sub>), food (Ag, TiO<sub>2</sub>, SiO<sub>2</sub>, Fe), cosmetics (TiO<sub>2</sub>, ZnO), sports clothes (Ag), electronics, energy and fuel additives (CeO<sub>2</sub>), nutraceuticals and pharmaceuticals (silicate and aluminosilicate) and for wastewater treatment (Fe,TiO<sub>2</sub>). (De la Calle et al. 2016)

One important research direction in the nanomedicine field is nanoscale theranostics. Till today, theranostic has become a popular concept in which both diagnosis and therapy is simultaneously realized. Nanoscale theranostics usually refer to nano-agents with integrated imaging and therapy functions within single nanoparticle (Fig. 7) systems. (Chen et al. 2015; Bardhan et al. 2011)

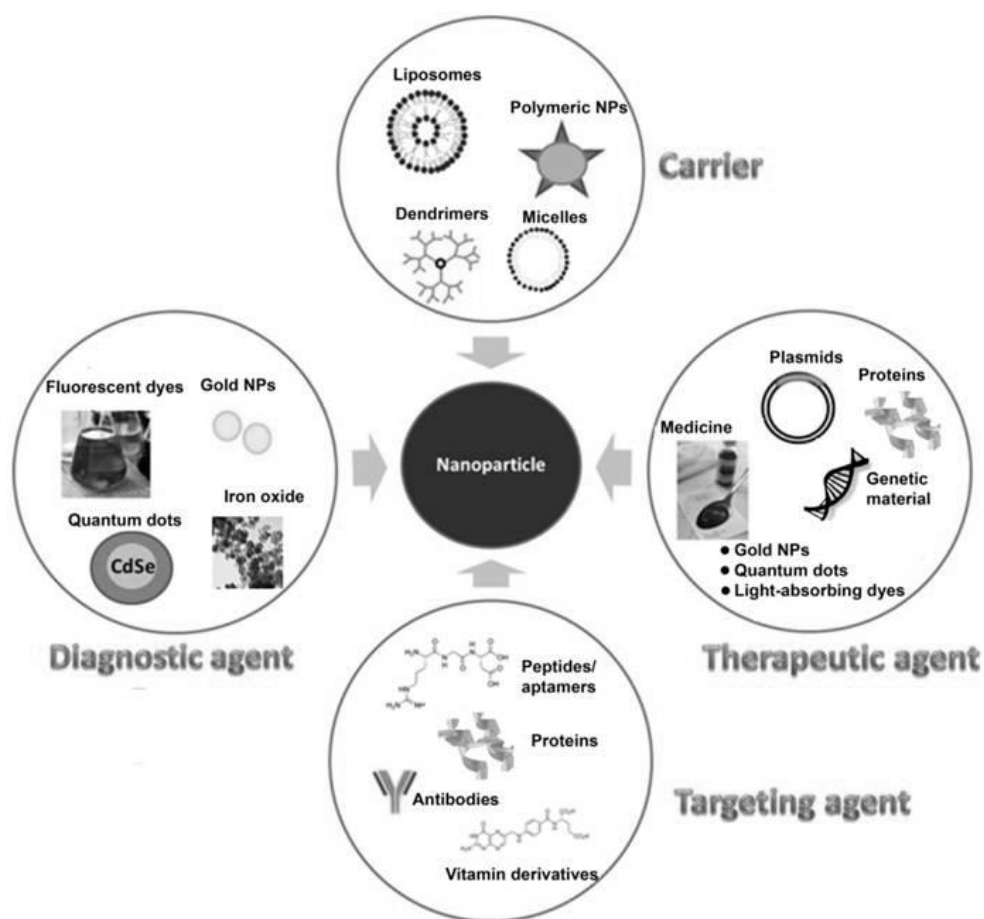
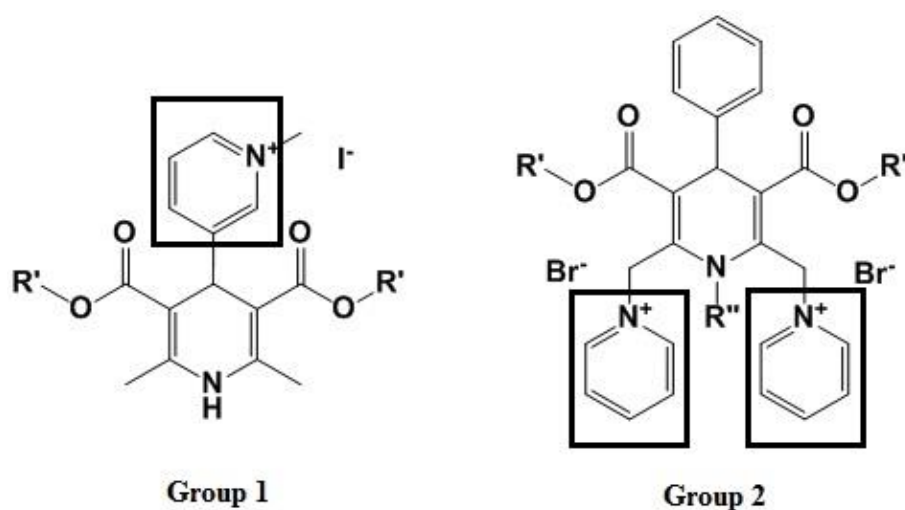


Figure 7. Design of nanoparticles (Menon et al. 2013)

The most often used nano-sized materials for theranostic purposes include: polymeric, lipid-based or metal oxide nanoparticles, dendrimers and cage proteins (Koo, Huh, Sun, et al. 2011; Cicha et al. 2014; Puri & Blumenthal 2011). These nanoparticles are attractive for the theranostic applications, mainly because of their ability to be located in pathological lesions rather than in normal tissues, particularly in the case of cancer or in dysfunctional endothelium. (Brigger et al. 2002; Wang et al. 2012) It is believed that theranostic approach can improve the outcome and increase the safety of medical procedures. It should allow identification and treatment of the diseases at their earliest stage when the chances for patient's recovery are relatively high and to monitor/correct the treatment. In that regard, theranostics can be very helpful in the development of personalized medicine which replaces the standard diagnostic and therapeutic strategies by individualized approach taking into account the inter-individual variability in therapeutic response. (Zapotoczny et al. 2015)

Cationic derivatives that possess self-assembling properties and are able to form liposomes in aqueous solutions have received widespread attention in gene delivery. Gene delivery studies have been focused on the design of synthetic cationic compounds, such as cationic amphiphilic ammonium (Peng et al. 2017) or pyridinium (Ilies et al. 2006; Fiscaro et

al. 2017) derivatives, polymers (Englert et al. 2016), peptides (Rea et al. 2009; Ishiguro et al. 2017) or dendrimers (Dufes et al. 2005; Abbasi et al. 2014), which would be able to overcome gene delivery barriers both *in vitro* and *in vivo*.



**Figure 8. Liposomes forming 1,4-DHP derivatives** (Hyvönen et al. 2000)

Previous studies performed by research groups from Latvian Institute of Organic synthesis and Kuopio University showed that studied cationic amphiphiles which have self-assembling properties and form liposomes in aqueous media can be divided into two main groups (Fig. 8). The compounds with the single charge (Fig. 8, group 1) have quaternized nitrogen atom at the 4-pyridyl ring and different alkyl chain length ( $C_{12} - C_{18}$ ) at positions 3 and 5 of the 1,4-DHP cycle. The compounds with double charge (Fig. 8, group 2) have two quaternized nitrogen atoms at positions 2 and 6 of the 1,4-DHP moiety and different length alkyl chains ( $C_{10} - C_{16}$ ) at positions 3 and 5 of 1,4-DHP ring. (Hyvönen et al. 2000) These amphiphiles have been demonstrated to condense and efficiently deliver plasmid DNA (pDNA) into different cell lines *in vitro*. (Pajuste et al. 2013; Hyvönen et al. 2002)

It is concluded, that the most active amphiphile from groups 1 and 2 - 1,1'-[(3,5-didodecyloxycarbonyl-4-phenyl-1,4-dihydropyridine-2,6-diyl)dimethylen]bispyridinium dibromide at optimal charge ratio (+/-4), was 2.5 times more effective than polyethylenimine 25 kDa (PEI 25) and 10 times better than N-(1-(2,3-dioleoyloxy)propyl)-N,N,N-trimethyl ammonium methylsulfate (DOTAP), well known efficient polymeric and liposomal transfection agents. The nanoparticle samples of single-charged compounds (Fig. 8, group 1) were heterogeneous, nevertheless the mean diameters of the liposomes were in the range of 15-30 nm. The double-charged amphiphiles (Fig. 8, group 2) formed liposomes with mean diameters in the range of 50-130 nm. (Hyvönen et al. 2000)

On this matter estimation of self-assembling properties of newly synthesized cationic moieties containing 1,4-DHP derivatives - detailed studies of nanoparticle formation and stability, nanoparticle characterization would be significant step for development of original delivery systems with perspective to use as composite nanosystems for diagnosis and therapy.

## MATERIALS AND METHODS

### General

All reagents were purchased from Acros Organics (Geel, Belgium), Sigma-Aldrich (St. Louis, MO, USA), Alfa Aesar (Lancashire, UK), or Merck KGaA (Darmstadt, Germany) and used without further purification. TLC was performed on silica gel 60 F254 aluminium sheets 20 × 20 cm (Merck KGaA, Darmstadt, Germany). <sup>1</sup>H-NMR (200 or 400 MHz) and <sup>13</sup>C-NMR (100.56 MHz) spectra were recorded with a Varian Mercury BB spectrometer (Agilent, Santa Clara, CA, USA) or <sup>1</sup>H-NMR (300 MHz) and <sup>13</sup>C-NMR (75 MHz) spectra were recorded with a Fourier 300 (Bruker, Billerica, MA, USA) spectrometer. The coupling constants are expressed in Hertz (Hz). The chemical shifts of the hydrogen and carbon atoms are presented in parts per million (ppm) and referred to the residual signals of the non-deuterated chloroform (CHCl<sub>3</sub>) (δ: 7.26) or partially deuterated dimethyl sulfoxide (DMSO) (δ: 2.50) solvent for <sup>1</sup>H-NMR spectra and CHCl<sub>3</sub> (δ: 77.0) or DMSO (δ: 39.5) solvent for <sup>13</sup>C-NMR, respectively. Multiplicities are abbreviated as s = singlet; d = doublet; t = triplet; m = multiplet; br = broad; dd = double doublet; dt = double triplet; td = triple doublet; tt = triple triplet; ddd = double double doublet. Mass spectral data were determined on an Acquity ultra performance liquid chromatography system (Waters, Milford, MA, USA) connected to a Waters SQ Detector-2 operating in the ESI positive or negative ion mode on a Waters Acquity UPLC<sup>®</sup> BEH C18 column (1.7 μm, 2.1 × 50 mm), using a gradient elution with acetonitrile (0.01% trifluoroacetic acid) in water (0.01% trifluoroacetic acid) at a flow rate of 0.5 mL/min. Liquid chromatography-mass spectrometry data were recorded with a Waters MassLynx 4.1 chromatography data system. The conversions of the reactions were analyzed by high-performance liquid chromatography on Waters Alliance 2695 system and Waters 2485 UV/Vis detector equipped with Alltima ODS-2 column (5 μm, 4.6 × 150 mm, Grace, Columbia, MD, USA) using a gradient elution with methanol/water (v/v), at a flow rate of 1 mL/min. Peak areas were determined electronically with Waters Empower 2 chromatography data system. Melting points (m.p.) of the synthesized compounds were determined on an OptiMelt (SRS Stanford Research Systems, Sunnyvale, CA, USA). Infrared spectra were recorded with a Prestige-21 FTIR spectrometer (Shimadzu, Kyoto, Japan). Elemental analyses were determined on an Elemental Combustion System ECS 4010 (Costech Instruments, Pioltello, Italy).

## Synthesis

The 1,4-DHP derivatives were synthesized *via* typical synthetic routes – the classical Hantzsch method (Hantzsch 1882), which involves the one-pot cyclocondensation of the corresponding acetoacetic acid ester, corresponding aldehyde and ammonia or ammonium acetate as nitrogen source in ethanol under reflux. The corresponding N-propargyl-substituted 1,4-DHP derivatives were obtained by analogy with the synthesis of other N-substituted 1,4-DHP ones – *via* modified Hantzsch-type cyclisation using propargyl amine hydrochloride as a nitrogen source instead of ammonia and pyridine as a solvent for the reaction mixture, under reflux. The synthesis of all the 4-pyridinium moieties containing 1,4-DHP derivatives were performed by alkylation of 4-pyridyl-1,4-DHP derivatives with the corresponding alkyl bromides in acetone under reflux. The typical procedure for the quaternization of pyridine derivatives has been reported by several research groups (Pijper et al. 2003; Meekel et al. 2000; Roosjen et al. 2002). Pyridinium betaines were obtained by treatment of the corresponding 4-(N-ethoxycarbonylmethyl)-pyridinium-1,4-DHP bromides with NaOH as a base, in analogy with the procedure described by Makarova et al (Makarova et al. 1997). The synthesis of 2,6-substituted amphiphilic 1,4-DHP derivatives was performed by bromination of 2,6-methyl groups of 1,4-DHP derivatives with N-bromosuccinimide at room temperature in methanol followed by nucleophilic substitution of bromine with various pyridine derivatives, pyrazine, N-methyl morpholine or N-methyl piperidine derivatives at room temperature in acetone. The corresponding bispyridinium dibromides were synthesized from 1,4-DHP derivatives in reaction with propargyl bromide in acetone under reflux. Synthesized amphiphilic pyridine derivatives with dodecyloxy carbonyl substituents at positions 3 and 5, and cationic moieties at positions 2 and 6 as NAD/NADH analogues were obtained from corresponding 2,6-bis(bromomethyl)-1,4-DHP followed by oxidation with *in situ* generated nitric oxide which resulted in the formation of the desired 2,6-bis(bromomethyl)-pyridine derivative. The bromine nucleophilic substitution reaction with N-containing heterocycles was performed at room temperature in acetone.

### Evaluation of the compounds' reducing capacity

The reducing capacity (RC) of the selected synthesized 1,4-DHP derivatives was studied using spectrophotometric quantitation of the RC through the formation a phosphomolybdenum complex. (Prieto et al. 1999) Stock solutions of the tested compounds and reference diludine of 1.0 mM were prepared in ethanol just before use. The final reagent solution contained 0.6 M sulfuric acid, 28 mM sodium phosphate, and 4 mM ammonium

molybdate solutions in water. An aliquot of 0.3 mL of the sample solution was combined in an eppendorf tube with 3 mL of the reagent solution. The tubes were capped and incubated in a thermal block at 95 °C for 90 min. After the samples were cooled to room temperature, the absorbance of each sample solution was measured at 695 nm against a blank sample using a UV/Vis Camspec M501 spectrometer (UK). A typical blank solution contained 3 mL of the reagent solution and the appropriate volume of ethanol (0.3 mL) as the solvent, and was incubated under the same conditions as the rest of the samples. Each assay was performed in triplicate. Results were expressed as a percentage.

### **Antiradical activity studies**

Free radical scavenging activity of the synthesized 1,4-DHP derivatives was evaluated by their ability to react with a stable radical of 1,1-diphenyl-2-picrylhydrazyl (DPPH). An aliquot (0.5 mL) of the tested 1,4-DHP derivative or diludine solution in ethanol (0.6 mM) was added to 3 mL of freshly prepared DPPH solution in EtOH (0.1 mM). The final concentration of the tested compound was 0.086 mM and the ratio of the tested compound and DPPH was equimolar. The solution was incubated for 30 min in the dark and changes in the optical density of solution were measured at 517 nm using a UV/Vis Camspec M501 spectrometer (UK). Each assay was performed in triplicate. The scavenging activity was defined as the decrease in sample absorbance versus absorbance of DPPH standard solutions. Results were expressed as a percentage of the DPPH free radical scavenging, which is defined by the following formula:

$$\text{ARA (\%)} = \frac{A_{\text{control}} - A_{\text{sample}}}{A_{\text{control}}} \times 100$$

where  $A_{\text{control}}$  is the absorbance of the standard solution of DPPH and  $A_{\text{sample}}$  is the absorbance value for the sample. (Abdelwahed et al. 2007)

### **Intracellular Ca<sup>2+</sup> measurements**

Fluo-4 NW Calcium Assay Kit was purchased from Invitrogen (Sweden), all the others from Sigma-Aldrich (St Louis, MO, USA). A7r5 (rat aorta smooth muscle cells) were obtained from the ATTC cell collection (USA), H9C2 (rat heart myoblast cells) and SH-SY5Y (human neuroblastoma cell line) from the European Collection of Animal Cell Cultures (ECACC, UK). The cells were grown at 37 °C in a humidified atmosphere with 5 % CO<sub>2</sub>/95 % air in Dulbecco's modified Eagle medium (DMEM), containing 2 mM of glutamine and



supplemented with 10 % fetal bovine serum. Cells were passaged once a week using 0.25 % trypsin, 0.53 mM ethylenediaminetetraacetic acid (EDTA) solution and grown in 75 mm<sup>2</sup> plastic culture flasks until confluence. For the experiment, SH-SY5Y cells were plated into 96-well plates at a density of 30000 cells per well and incubated for 24 h. A7r5 cells were seeded into 96-well plates at a density of 10000 cells per well and incubated for 72 h. Changes in intracellular [Ca<sup>2+</sup>]<sub>i</sub> concentration were studied using the Fluo-4 NW Calcium Assay Kit, accordingly to the manufacturer's instructions. The SH-SY5Y and A7r5 cells were loaded with Fluo-4 NW for 45 min. Then, the cells were pre-incubated in the dark for 15 min with the tested compounds at concentrations from 0.8 to 100 nM. The compounds were dissolved in dimethyl sulfoxide. Application of carbachol (100 nM) to Fluo-4 NW loaded SH-SY5Y cells was used to stimulate changes in the intracellular [Ca<sup>2+</sup>]<sub>i</sub> concentration, whereas A7r5 cells were treated with 1.5 mM CaCl<sub>2</sub> and KCl (50 mM) for 5 min to induce an increase in the [Ca<sup>2+</sup>]<sub>i</sub> concentration. The intracellular [Ca<sup>2+</sup>]<sub>i</sub> concentration was measured using the fluorescence spectrophotometer's (Thermo Asciant, Finland) settings appropriate for an excitation at 494 nm and an emission at 516 nm. Amlodipine, nimodipine were used as the positive control. IC<sub>50</sub> values as a mean ± standard deviation (SD) were calculated using GraphPad Prism 3.0 software.

### **Nanoparticle preparation and studies**

Samples for nanoparticle studies were prepared by dispersing selected 1,4-DHP amphiphiles or corresponding pyridine derivatives in an aqueous solution by sonication using a probe type sonicator (Cole Parmer ultrasonic processor CPX 130W (USA)) or a bath type sonicator (Cole Parmer Ultrasonic Cleaner 8891CPX (USA)). The settings for a probe type sonicator were as follows: amplitude 30 %, pulse 15 s on, 15 s off, 5 min or 15 min depending on 1,4-DHP derivatives and for pyridine derivatives with bath type sonicator 60 min at 60 °C.

**Atomic force microscopy (AFM).** Freshly cleaved mica plates were dipped into the solution of samples and kept for 30 s to allow the nanoparticles formed by 1,4-DHP amphiphiles stick to the negatively charged surface. The mica samples were dried at room temperature and visualized by AFM in tapping mode with an Asylum Research MFP-3D-BIOTM AFM in dynamic mode using Olympus AC240TM tips. The software IGOR Pro 6 was used for analysis of AFM images and characterization of average parameters of obtained nanoparticles.

**Transmission electron microscopy (TEM).** The morphology of nanoparticles formed by 1,4-DHP amphiphiles was studied by TEM applying a negative staining technique. One drop of the sample was adsorbed to a formvar carbon-coated copper grid and negatively

stained with 1 % aqueous solution of uranyl acetate. The grids were examined with a JEM-1230 TEM at 100 kV. The diameter of 400 nanoparticles of each negatively stained sample was measured from electron microscopic micrographs.

**Dynamic light scattering (DLS).** The DLS measurements of the nanoparticles formed by compounds were carried out in water using a Zetasizer Nano S90 instrument with Malvern Instruments Ltd software.

## RESULTS AND DISCUSSION

The study is devoted to the design, synthesis and biological studies of novel 1,4-DHP derivatives by adding to their structures some pharmacophore moieties:

- ✓ N-propargyl substituent at position 1 or propargyl moieties at positions 3 and 5, or 2 and 6;
- ✓ pyridinium moiety variations at positions 4 or 2 and 6 of the 1,4-DHP cycle;
- ✓ variation of alkyl substituent length at the quaternized N-atom of pyridinium at position 4.

### Synthesis of 1,4-DHP derivatives (publications A, B, C, D, E)

One of the main tasks of this work was to develop synthetic procedures for preparation of 1,4-DHP derivatives containing propargyl and/or pyridinium moieties with following characterization of their pharmacological properties. The first step of this study was to introduce propargyl group into the 1,4-DHP cycle at position 1. For comparison of the obtained biological data N-unsubstituted 1,4-DHP derivatives were synthesized as well. In this case, the 1,4-DHP derivatives **D1** and **D3** (Fig. 9) were synthesized with high yields, 92 % and 78 % respectively, *via* typical synthetic routes – the classical Hantzsch method (Hantzsch 1882), which involves the one-pot cyclocondensation of the corresponding aldehyde, ethyl acetoacetate and ammonia in ethanol under reflux for 5–7 h. The corresponding N-propargyl-substituted 1,4-DHP derivatives **D2** and **D4** (Fig. 9) were obtained by analogy with the synthesis of other N-substituted 1,4-DHP ones – *via* modified Hantzsch-type cyclisation using propargyl amine hydrochloride as a nitrogen source instead of ammonia and pyridine as a solvent for the reaction mixture, under reflux for 5–12 h. The one and only literature data about the synthesis and studies of N-propargyl-substituted 1,4-DHPs, such as N-propargyl nitrendipine demonstrated the alternative synthesis of N-substituted 1,4-DHP derivatives *via* N-alkylation of the corresponding N-unsubstituted 1,4-DHP derivative with propargyl bromide in the presence of NaH as a base with only 22 % yield of product (Harper et al. 2003). In this respect, the yields of synthesized N-propargyl-substituted 1,4-DHP derivatives – compounds **D2** and **D4** – were 19 % and 22 %, respectively. Hantzsch-type cyclisation was carried out with a propargyl amine hydrochloride refluxing the reaction mixture for 12 h. Meanwhile, the yields of the desired products **D2** and **D4** were increased to 40 % and 47 %, respectively; these reactions, when performed in a pressure tube as the reaction vessel, were completed in just 5 h. The synthesis of all the 1,4-

DHP derivatives containing pyridinium moieties **D5–14** (Fig. 9) were performed by alkylation of 4-pyridyl-1,4-DHP derivatives **D3** or **D4** with the corresponding alkyl bromides in acetone under reflux. The typical procedure for the quaternization of pyridine derivatives has been reported by several research groups (Pijper et al. 2003; Roosjen et al. 2002; Meekel et al. 2000). Reaction times and yields of the product are dependent on the structure of the alkyl halide. An excess of the alkylation agent was used to reduce the reaction time (Makarova et al. 1997). Compounds **D15** and **D16** (Fig. 9) were synthesized as synthones for the target products **D17** and **D18** (Fig. 9). Pyridinium betaines **D17** and **D18**, synthesized in 82 and 53 % yields, respectively, were obtained by treatment of the corresponding 4-(N-ethoxycarbonylmethyl) pyridinium-1,4-DHP bromides **D15** and **D16** with NaOH as a base, in analogy with the procedure described previously (Makarova et al. 1997).

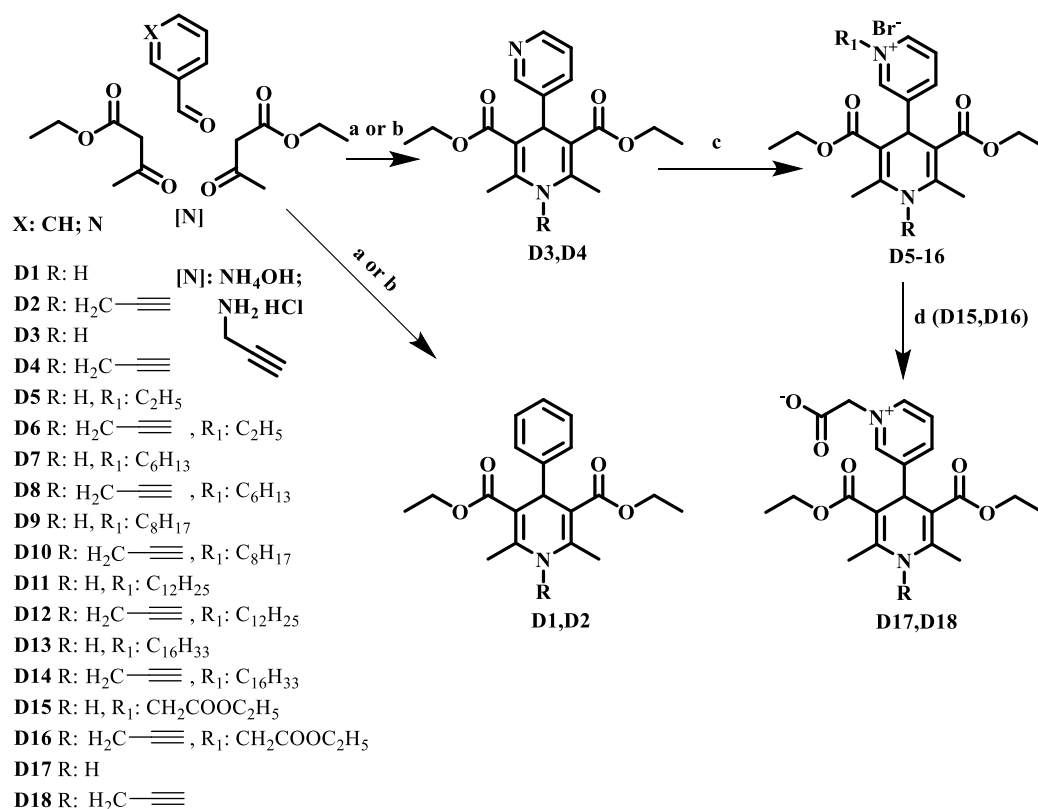


Figure continues on the next page

<i>Comp.</i>	<i>Yield (%)</i>	<i>M.p.</i>	<i>Comp.</i>	<i>Yield (%)</i>	<i>M.p.</i>
<b>D1</b>	92 (78 (Fox <i>et al.</i> 1951))	158-160 (153 (Fox <i>et al.</i> 1951))	<b>D10</b>	56	146-148
<b>D2</b>	19 (40*)	111-113	<b>D11</b>	68	162-164
<b>D3</b>	78 (80 (Wiley & Irick 1961))	189-191 (192- 194 (Wiley & Irick 1961))	<b>D12</b>	57	161-163
<b>D4</b>	22 (47*)	154-156	<b>D13</b>	60 (63 (Makarov <i>a et al.</i> 1995))	134-135 (135- 136 (Makarova <i>et al.</i> 1995))
<b>D5</b>	86	189-191	<b>D14</b>	76	149-151
<b>D6</b>	77	205 (decomp.)	<b>D15</b>	87 (88 (Makarov <i>a et al.</i> 1997))	210-212 (217 (decomp.) (Makarova <i>et al.</i> 1997))
<b>D7</b>	51	220-222	<b>D16</b>	78	157-159
<b>D8</b>	69	176-178	<b>D17</b>	82 (84 (Makarov <i>a et al.</i> 1997))	128-130 (128- 130 (Makarova <i>et al.</i> 1997))
<b>D9</b>	54	157-159	<b>D18</b>	53	105 (decomp.)

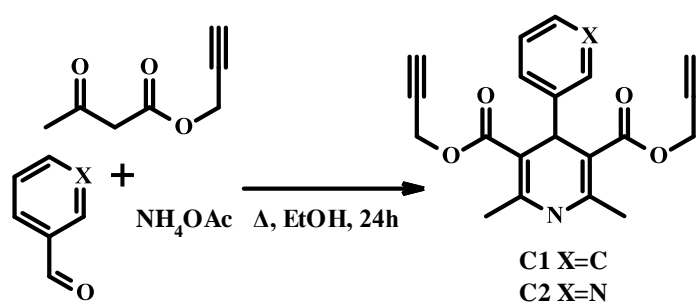
\*Yield of product, performing the reaction in a pressure tube as the reaction vessel.

**Figure 9. Synthesis of 1,4-DHP derivatives D1–18. Reactions conditions: a) comp. D1 and D3: EtOH, reflux for 5–7 h; b) comp. D2 and D4: pyridine, reflux for 5–12 h; c) alkylbromide, acetone, reflux for 5–26 h; d) NaOH, EtOH, water, 50 °C, 3 h**

All synthesized 1,4-DHP derivatives **D1-14**, **D17** and **D18** with introduced pharmacophore moieties into the 1,4-DHP cycle – at position 1 the propargyl moiety and at position 4 the pyridinium substituent with alkyl moieties of different lengths at quaternized nitrogen atom were used for studies of structure-activity relationships. For all the synthesized compounds calcium channel antagonistic properties and reducing capacity were tested. In addition *in vivo* subchronic toxicity test in mice was performed for safety of derivatives and the importance of amphiphilic substituent in the 1,4- DHP ring was showed. More detailed information can be found in appendix publication **D**.

At the next step in this work were obtained the 1,4-DHP derivatives with propargyl ester group at positions 3 and 5 of the 1,4-DHP cycle for further studies of pharmacological properties of these compounds and evaluation of propargyl moiety position influence on pharmacological properties. To obtain the target compounds was synthesized the non-commercial starting material acetoacetic acid propargyl ester according to the procedure described by Cruciani *et al.* (Cruciani & Stammer 1996) starting from propargyl alcohol and

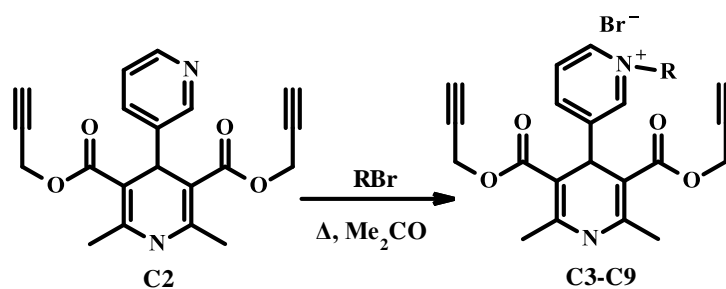
2,2,6-trimethyl-1,3-dioxin-4-one. Hantzsch-type 1,4-DHPs **C1** and **C2** for studies were synthesized with 61 and 82 % yields, respectively, *via* typical synthetic routes, such as the Hantzsch synthesis (Hantzsch 1882; Liepin'sh et al. 1989). It involves a one-pot cyclocondensation of the corresponding aldehyde, acetoacetic acid propargyl ester and ammonium acetate under 24 h reflux in ethanol (Scheme 2). In order to decrease the reaction time and improve the product yield, the synthesis of compound **C2** with the same reagent ratio was performed under microwave conditions. The irradiation during 30 min at 80 °C gave the 1,4-DHP derivative **C2** in 52 % isolated yield.



*Scheme 2. Synthesis of 3,5-propargyl moiety containing 1,4-DHP derivatives*

As the next step of these thesis, the synthesis of various N-alkylpyridinium-1,4-DHP salts **C3-9** was performed by alkylation of dipropargyl 1,4-DHP ester **C2** with the corresponding alkyl bromides in acetone under reflux (Fig. 10). The typical procedure for the quaternization of pyridine derivatives was described above in publication **D**. In this case, the solution of 2 to 8-fold excess of the corresponding alkyl bromide was added to the starting dipropargyl ester **C2**, and the reaction mixture was refluxed in a pressure tube for 75-222 h (Fig. 10). However, in a pressure tube the alkylation reactions were still found to be rather slow and proceeded with moderate yields of the products. In contrast, quaternization of the pyridine moiety of 3,5-diethoxycarbonyl-1,4-DHP with various alkyl bromides occurred in 5-26 h and with higher yields, corresponding derivatives from publication **D**.

New 1,4-DHP derivatives with propargyl ester group at positions 3 and 5 of the 1,4-DHP cycle **C3-9** were synthesized for evaluation of calcium channel antagonist/agonist properties and reducing capacity. More detailed information can be found in appendix publication **C**.



Comp.	R	Ratio of 1,4-DHP:RBr	Amount of RBr, mM/mL	Time, h	Yield, %
C3	C <sub>2</sub> H <sub>5</sub>	1:8	6.88/0.52	75	65
C4	C <sub>4</sub> H <sub>9</sub>	1:3	2.58/0.28	100	36
C5	C <sub>6</sub> H <sub>13</sub>	1:3	2.58/0.36	201	57
C6	C <sub>8</sub> H <sub>17</sub>	1:3	2.58/0.45	77	64
C7	C <sub>10</sub> H <sub>21</sub>	1:3	2.58/0.54	201	65
C8	C <sub>12</sub> H <sub>25</sub>	1:2	1.72/0.42	128	73
C9	C <sub>14</sub> H <sub>29</sub>	1:4	3.44/1.04	222	65

Figure 10. Characterization of alkylation reactions for synthesis of pyridinium 1,4-DHP derivatives C3-9

1,4-DHP derivatives with propargyl group at positions 2 and 6 of 1,4-DHP cycle (Fig. 11, group 3) and as substituent at phenyl group at position 4 of 1,4-DHP core (Fig. 11, group 4) were also synthesized (unpublished data) by following procedure: Hantzsch synthesis of corresponding acetoacetic acid ester, aldehyde and ammonium acetate as nitrogen source by reflux in ethanol for 24h, for further studies of pharmacological properties.

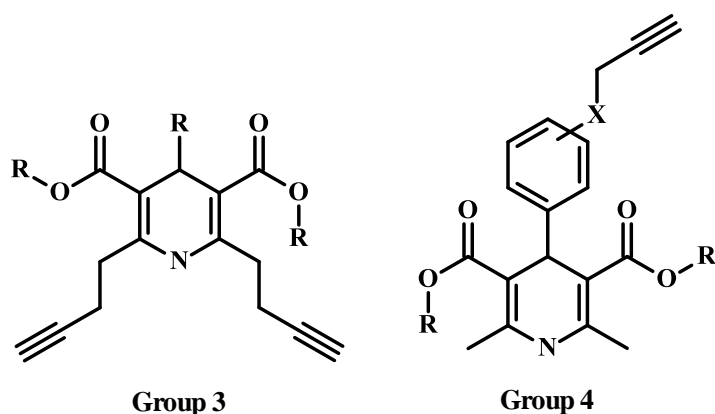
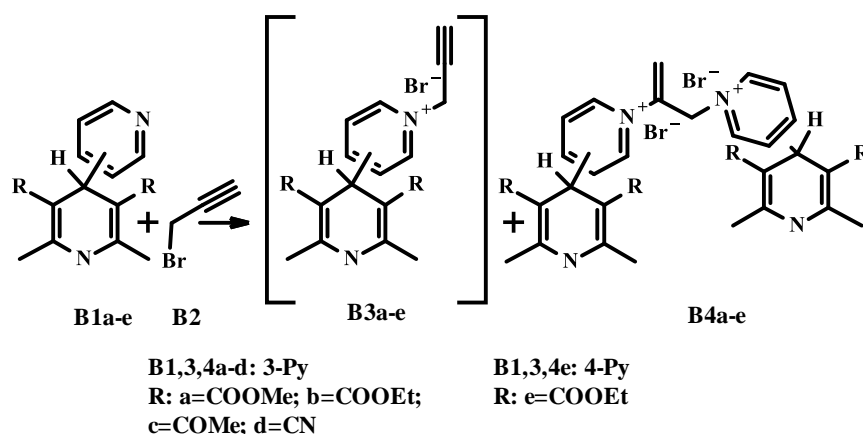


Figure 11. 1,4-DHP derivatives with propargyl moiety at positions 2 and 6 of 1,4-DHP ring (Group 3) or 4-phenyl substituent 1,4-DHP ring (Group 4)

The next step of this study was planned the propargyl moiety introduction into the pyridinium substituent at position 4 of the 1,4-DHP cycle. Initially, the main purpose of studies was the synthesis of the corresponding 1-prop-2-ynyl-pyridinium bromides **B3a-e** based on the 1,4-DHP cycle for further investigation of biological activity using the typical

procedure for the quaternization of pyridine derivatives which was described above in article **D**. In this case the first reaction was performed using the same conditions, and the starting 4-pyridyl-1,4-DHP derivative **B1b** was treated with 1.5 eq excess of propargyl bromide in acetone under reflux for 22 h (Figure 12).



Comp.	Het	R	Yield (%)
<b>B4a</b>	3-Py	COOMe	41
<b>B4b</b>	3-Py	COOEt	65
<b>B4c</b>	3-Py	COMe	68
<b>B4d</b>	3-Py	CN	72
<b>B4e</b>	4-Py	COOEt	59

**Figure 12. Synthesis of bispyridinium dibromides B4a-e. Reagents and conditions: 4-pyridyl-1,4-DHP derivative (0.66 mM (1 eq)) and 80 % solution of propargyl bromide in toluene (0.99 mM, 106  $\mu$ L (1.5 eq)) reflux under pressure in acetone for 22 h**

The obtained precipitate was filtered off and crystallized from a mixture of acetone/methanol. However, in the  $^1\text{H-NMR}$  spectra for solution of obtained compound in  $\text{DMSO-}d_6$  showed the evidence of other groups in molecule: AB-system in the 5.62 and 6.15 ppm with the coupling constant 3.1 Hz and singlet in the 6.06 ppm. The proton signals of pyridinium and 1,4-DHP moieties in the  $^1\text{H-NMR}$  spectra were found to be non-equivalent, the same occurrence was observed also for carbon signals in  $^{13}\text{C-NMR}$  spectra. For conclusive assessment of the structure of isolated compounds suitable crystals for X-ray crystallographic analysis were obtained by slow crystallization of the sample from hexane/dichloromethane. X-ray analysis of the crystals of the obtained compound was undertaken and confirmed structure of diethyl 4-(1-(2-(3-(3,5-bisethoxycarbonyl-2,6-dimethyl-1,4-dihydropyridin-4-yl)pyridin-1-ium-1-yl)allyl)pyridin-1-ium-3-yl)-2,6-dimethyl-1,4-dihydropyridine-3,5-dicarboxylate dibromide (**B4b**). It can be proposed, that

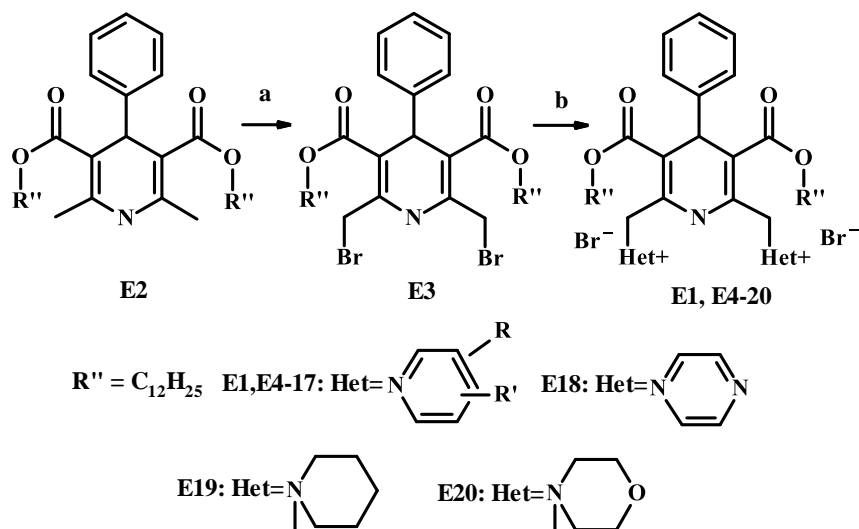


bispyridinium dibromide **B4b** perhaps is formed directly during quaternization reaction and further reaction of mono quaternized product – mono bromide **B3b** and starting 1,4-DHP **B1b** is less probable. Other 4-(3-pyridyl)-1,4-dihydropyridines **B1a**, **B1c**, **B1d** with various moieties at the positions 3 and 5 of 1,4-DHP cycle were also synthesized for studies of influence of electronic nature of substituents. The variation of position of pyridine cycle substituent was carried out, thus besides 4-(3-pyridyl)-1,4-dihydropyridine **B1b** its analogue 4-(4-pyridyl)-1,4-dihydropyridine **B1e** was also synthesized. Obtained products from quarterization reactions confirmed that in all cases instead of predicted mono derivatives **B3a**, **B3c–e** the formation of the corresponding bispyridinium dibromides **B4a**, **B4c–e** were observed (Fig. 12).

Generally, it could be concluded that variation of the substituent position at the pyridine (derivatives **B1d** and **B1e**) (Liepin'sh et al. 1989) as well as minor changes of electronic nature of 1,4-DHP cycle due to the difference of substituent at the positions 3 and 5 (derivatives **B1a–e**) did not affect the course of the reaction, the corresponding bispyridinium dibromides **B4a–e** were formed in all cases. However, it should be noted, that minor changes of electronic nature of 1,4-DHP cycle have influenced the yields of bispyridinium dibromides **B4a–e**, thus the highest yield (72 %) is obtained for bispyridinium dibromide **B4d**, and the lowest yield (41 %) for bispyridinium dibromide **B4a** respectively. Although the expected 1-prop-2-ynyl-pyridinium bromides **B3a–e** based on the 1,4-DHP core were not obtained, for synthesized bispyridinium dibromides **B4a–e** antiradical activity and reducing capacity were determined. More detailed information can be found in appendix publication **B**.

The next compound group - cationic moieties containing 1,4-DHP derivatives with modifications at positions 2 and 6 of the 1,4-DHP ring were obtained for studies of self-assembling and pharmacological properties. Previously Hyvonen et al. (Hyvönen et al. 2000) demonstrated that hydrophobic dodecyloxycarbonyl substituents at positions 3 and 5 of the 1,4-DHP ring are optimal for the expression of transfection efficiency *in vitro*. However, there are no data about the impact of the cationic part of the 1,4-DHP amphiphile on gene delivery and self-assembling properties of compounds. In order to investigate the effect of the substituents at the cationic head-group of the amphiphilic 1,4-DHP molecule was modified amphiphile **E1** at positions 2 and 6. The synthesis of amphiphilic compounds **E1** and **E4–20** is achieved *via* a multi-step sequence and showed in Figure 13. Nucleophilic substitution of bromine in the parent compound **E3** with various pyridine derivatives as well as pyrazine, N-methyl morpholine or N-methyl piperidine derivatives resulted in the target 1,4-DHP amphiphiles **E4–20**. Substitution reactions were performed at room temperature due to the fact that at temperatures above 50 °C lactonization of 2,6-di(bromomethyl) substituted 1,4-

DHP **E3** to 8-phenyl-5,8-dihydro-1H,3H-difuro-[3,4-b:3',4'-e]pyridine-1,7(4H)-dione occurs. (Skrastin'sh et al. 1991)

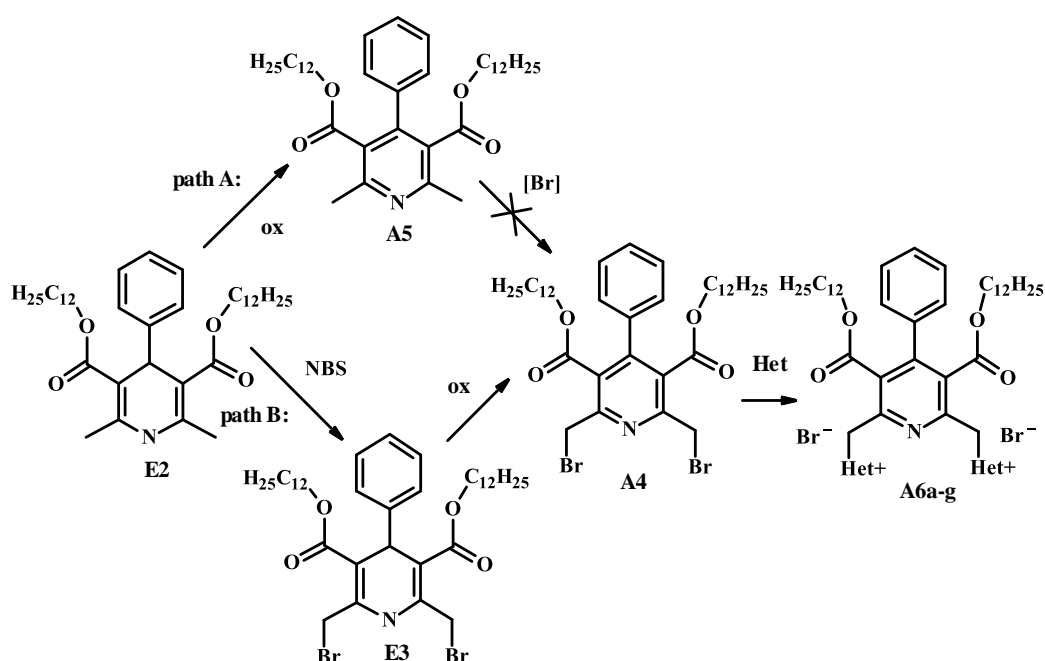


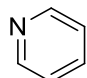
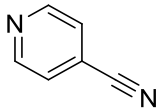
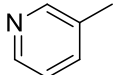
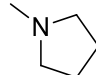
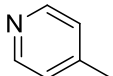
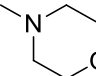
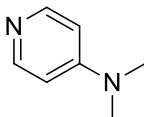
Comp.	R	R'	Yield (%)	Time (h)
<b>E1<sup>a</sup></b>	H	H	78	24
<b>E4</b>	4-CH <sub>3</sub>	H	68	24
<b>E5</b>	4-N(CH <sub>3</sub> ) <sub>2</sub>	H	65	24
<b>E6</b>	4-C(CH <sub>3</sub> ) <sub>3</sub>	H	30	48
<b>E7</b>	4-NH <sub>2</sub>	H	50	24
<b>E8</b>	4-CONH <sub>2</sub>	H	45	48
<b>E9</b>	4-COCH <sub>3</sub>	H	35	48
<b>E10</b>	4-CN	H	34	48
<b>E11</b>	3-CH <sub>3</sub>	H	65	24
<b>E12</b>	3-C <sub>6</sub> H <sub>5</sub>	H	60	48
<b>E13</b>	3-NH <sub>2</sub>	H	54	24
<b>E14</b>	3-CONH <sub>2</sub>	H	52	48
<b>E15</b>	3-COCH <sub>3</sub>	H	36	48
<b>E16</b>	3-CH <sub>3</sub>	4-CH <sub>3</sub>	47	24
<b>E17</b>	3-CH <sub>3</sub>	5-CH <sub>3</sub>	64	24
Comp.	Het		Yield (%)	Time (h)
<b>E18</b>	pyrazine		17	48
<b>E19</b>	N-CH <sub>3</sub> piperidine		79	24
<b>E20</b>	N-CH <sub>3</sub> morpholine		98	24

Figure 13. Synthesis of 1,4-DHP amphiphiles **E1**, **E4-20**. Reagents and conditions: a) N-bromosuccinimide, MeOH; b) substituted pyridine, pyrazine, N-methyl piperidine or N-methyl morpholine, acetone, room temperature.

For synthesized compounds antiradical activity was studied. That kind of 1,4-DHP derivatives are usually used as delivery agents, but in these thesis main emphasis was focused on characterization of self-assembling properties. More detailed information can be found in appendix publication **E**.

Oxidation of 1,4-dihydropyridines to the corresponding pyridine derivatives is the most typical and general reaction for this heterocyclic system. One of the main metabolic pathways of biologically active 1,4-DHP derivatives is the oxidation to their corresponding pyridines with Cytochrome P450 as catalyst (Guengerich et al., 1991). The aim of this part of study was to perform the synthesis of new amphiphilic pyridine derivatives **A6a-g** containing dodecyloxycarbonyl substituents at positions 3 and 5 and cationic moieties at positions 2 and 6. For comparison their and corresponding 1,4-DHP derivatives **E1**, **E4**, **E5**, **E10**, **E11**, **E20** NAD/NADH analogue properties were performed. For further transformations, firstly was performed oxidation of compound **E2** with *in situ* generated nitric oxide using the methodology described by Dubur and Uldrikis (Dubur & Uldrikis 1972) (Fig. 14) to obtain pyridine derivative **A5**. The next step bromination of compound **A5** with Br<sub>2</sub>/AcOH or N-bromosuccinimide (NBS) was unsuccessful and did not give the desired dibromide **A4**. Therefore, implementation of path B was another possibility for the synthesis of cationic pyridine derivatives **A6a-g** (Fig. 14). Bromination of the 2,6-methyl groups of compound **E2** was performed with NBS according to the reported method giving 2,6-bis(bromomethyl)-1,4-DHP **E3** (Pajuste et al., 2011) followed by oxidation with *in situ* generated nitric oxide which resulted in the formation of the desired 2,6-bis(bromomethyl)-pyridine **A4**. The bromine nucleophilic substitution reaction of compound **A4** was performed at room temperature in acetone with 25 – 83 % yields in 1-5 days depending on the nucleophile structure (Fig. 14). The yields of the obtained cationic pyridine derivatives **A6a-g** are slightly lower compared to the yields of the products of bromine nucleophilic substitution reaction of the corresponding 2,6-bis(bromomethyl)-1,4-DHP derivatives (from article E).



<i>Comp.</i>	<i>Het</i>	<i>Yield (%)</i>	<i>Time (days)</i>	<i>Comp.</i>	<i>Het</i>	<i>Yield (%)</i>	<i>Time (days)</i>
<b>A6a</b>		58	3	<b>A6e</b>		25	5*
<b>A6b</b>		49	5	<b>A6f</b>		60	1
<b>A6c</b>		55	2	<b>A6g</b>		83	2
<b>A6d</b>		58	1				

\*during last 2 days reaction was performed at 50 °C

**Figure 14. Synthesis of cationic pyridine derivatives A6a-g**

For example, reaction of 2,6-bis(bromomethyl)-pyridine **A4** with  $\gamma$ -picoline or *p*-dimethylaminopyridine proceeded within 2 or 1 day, with 55 and 58 % yield, respectively (Fig. 14, comp. **A6c**, **A6d**), while reaction of 2,6-bis(bromomethyl)-1,4-DHP with  $\gamma$ -picoline or *p*-dimethylaminopyridine occurred during 1 day, with 65 % yield in both cases (Fig. 13 compounds **E5** and **E11**); reaction of 2,6-bis(bromomethyl)-pyridine **A4** with *p*-cyanopyridine occurred during 5 days, with 25 % yield (Fig. 14, comp. **A6e**), on the other hand in the case of the corresponding 2,6-bis(bromomethyl)-1,4-DHP - during 2 days with 34 % yield (Fig. 13, compound **E10**).

For synthesized pyridine derivatives self-assembling properties were characterized. More detailed information can be found in appendix publication **A**.

In summary the synthesis of 3 and 5 propargyl ester group substituted 1,4-DHP derivatives proceed with higher yields than that of N-propargyl substituted 1,4-DHP derivatives. Nucleophilic substitution at positions 2 and 6 of the 1,4-DHP derivatives proceed in shorter reaction times and with higher yields compared with the pyridine ones. Quaternization reactions of pyridinium moiety at position 4 of 1,4-DHP cycle proceed in long reaction times with moderate to good yields.

#### **Assessment of calcium channel blocking activity (publications C, D)**

As it is written above one of the main 1,4-DHP derivatives pharmacological properties is calcium channel blocking activity, therefore this activity was evaluated for selected synthesized 1,4-DHP derivatives containing propargyl moieties. The influence of novel synthesized compounds on intracellular calcium  $[Ca^{2+}]_i$  concentration was assessed in both the neuroblastoma SH-SY5Y cells (containing L- and N-type  $Ca^{2+}$  channels) and the rat aorta

smooth muscle A7r5 cells, which express functional L-type  $\text{Ca}^{2+}$  channels. The well-known calcium channel inhibitors – amlodipine and nimodipine were used as the positive controls in this test. As it is shown in Table 1, the most potent calcium antagonistic properties in SH-SY5Y cells demonstrated that the 1,4-DHP derivatives contained at position 4 of the 1,4-DHP ring the N-octyl pyridinium group (compound **D10**) and the N-dodecyl pyridinium group (compounds **D11** and **D12**); these activities were comparable to that of amlodipine. Other compounds showed either weak calcium antagonism (compounds **D4**, **D8** and **D9**), or this activity was not obtained at all. Calcium antagonistic properties were found to be higher in A7r5 cells, indicating that compounds predominantly target the L-type calcium channels in vascular smooth muscles. The highest activity comparable to that of nimodipine was revealed for compound **D1**, which is a well-known 4-phenyl-1,4-DHP derivative with calcium antagonistic properties (Dagnino et al. 1986). In A7r5 cells, compounds **D11** and **D12** demonstrated at least 10-fold higher activity than that in SH-SY5Y cells, indicating their potential vasodilating activity, whereas compounds **D2**, **D3** and **D4** were about 3 to 4-fold less active than compounds **D11** and **D12**; others lacked activity.

Table 1.

**Calcium overload-preventing activity ( $\text{IC}_{50}$ ) of novel 1,4-DHP derivatives D1-18 in SH-SY5Y and A7r5 cells. Data are presented as a mean  $\pm$  SD**

Comp.	$\text{Ca}^{2+}$ antagonism, $\text{IC}_{50}$ ( $\mu\text{M}$ )	
	SH-SY5Y	A7r5
<b>D1</b>	#	0.0098 $\pm$ 0.0004*
<b>D2</b>	>100*	2 $\pm$ 0.2*
<b>D3</b>	#	1.5 $\pm$ 0.2*
<b>D4</b>	53 $\pm$ 8*	4.5 $\pm$ 1*
<b>D5</b>	#	#
<b>D6</b>	100 $\pm$ 8*	>100*
<b>D7</b>	#	#
<b>D8</b>	35 $\pm$ 3	#
<b>D9</b>	53 $\pm$ 8	#
<b>D10</b>	12 $\pm$ 3	#
<b>D11</b>	5 $\pm$ 0.8	0.7 $\pm$ 0.3*
<b>D12</b>	14 $\pm$ 5	0.6 $\pm$ 0.06*
<b>D13</b>	#	#
<b>D14</b>	#	#
<b>D15</b>	#	#
<b>D16</b>	#	#
<b>D17</b>	#	#
<b>D18</b>	#	#
Amlodipine	11 $\pm$ 5	0.140 $\pm$ 0.012
Nimodipine	53 $\pm$ 3*	0.008 $\pm$ 0.0014*

#No  $\text{Ca}^{2+}$  channel blocking activity was detected.

\* $p < 0.05$  vs. Amlodipine; Student's paired t-test, with a two-tailed distribution.

Compounds **D5**, **D7** and **D13–18** did not show calcium channel blocking activity in none of the used cell lines.

The obtained data demonstrated that propargyl group at position 1 of 1,4-DHP ring in general did not influence essentially the biological activity of the tested 1,4-DHP derivatives assessed in the used test systems. Among the tested N-alkyl-4-pyridinium-1,4-DHP the highest calcium channel blocking activity showed compounds with the N-dodecyl pyridinium moiety at position 4 of the 1,4-DHP cycle (compound **D11** and **D12**). This activity in smooth muscle cell line A7r5 was considerably higher than in neuroblastoma cell line SH-SY5Y, suggesting that these compounds are predominantly targeting L-type calcium channels. More detailed information can be found in appendix publication **D**.

Ca<sup>2+</sup> channel antagonist and agonist activities of compounds **C1–9** were assayed by changes in intracellular Ca<sup>2+</sup> ion concentration [Ca<sup>2+</sup>]<sub>i</sub> in H9C2 cells, derived from the embryonic rat ventricle, and A7r5 cells. The model for investigation of the Ca<sup>2+</sup> channel blocking activity of DHP derivatives is based on the analysis of the effect of KCl on intracellular Ca<sup>2+</sup> mobilization in H9C2 and A7r5 cells. The well-known calcium channel inhibitor – amlodipine was used as a positive control in this test. The results are summarized in Table 2. - none of 1,4-DHP derivatives **C1–9** in the tested concentrations showed antagonist effect in the H9C2 cell line, some of them, however, demonstrate such effect in A7r5 cells.

Table 2.

**Antagonist and agonist effects of 1,4-dihydropyridines C1-9 on [Ca<sup>2+</sup>]<sub>i</sub> in H9C2 and A7r5 cells**

<i>Comp.</i>	<i>Antagonist activity (IC<sub>50</sub>, μM)</i>		<i>Agonist activity (RFU, 100 μM)</i>	
	<i>H9C2</i>	<i>A7r5</i>	<i>H9C2</i>	<i>A7r5</i>
<i>Amlodipine</i>	*	0.14±0.01	<i>nt</i>	<i>nt</i>
<b>C1</b>	*	0.03±0.01	+	+
<b>C2</b>	*	0.60±0.06	*	*
<b>C3</b>	*	>100	*	*
<b>C4</b>	*	95±2	*	*
<b>C5</b>	*	2.5±0.6	*	*
<b>C6</b>	*	0.80±0.07	+	+
<b>C7</b>	*	0.70±0.05	+	+
<b>C8</b>	*	0.40±0.03	+	+
<b>C9</b>	*	0.50±0.05	+	+

nt – not tested

+ – activity was detected

\* – no activity was detected in tested concentrations

Furthermore, 1,4-DHP derivative **C1** demonstrated an activity 4.7 times higher than amlodipine, whereas 1,4-DHP derivatives **C2** and **C5-9** were about 3-8 times less active than amlodipine, and compounds **C3** and **C4** possessed low activity. The calcium channel agonist effect of 1,4-DHP derivatives **C1-9** was also tested on both cell lines. Studies of Ca<sup>2+</sup> channel antagonist and agonist activities of the 1,4-DHP derivatives indicate that the compounds target only calcium channels in vascular smooth muscle cells and do not affect calcium channels in cardiac cells. It has been found that from synthesized 1,4-DHP derivatives compound **C1** possess 4.7 times higher antagonist activity than amlodipine in the A7r5 cell line. More detailed information can be found in publication **C**.

In summary Ca<sup>2+</sup> channel antagonist activity on A7r5 cell line is more structure depending. According to obtained data, more pronounced Ca<sup>2+</sup> channel antagonist activity possess 1,4-DHP derivatives with propargyl ester group at positions 3 and 5 compared with 1-propargyl substituted 1,4-DHP derivatives.

Thank to Dr. chem. Ilona Domracheva Latvian Institute of Organic Synthesis experimental chemotherapy group for the obtained results of calcium channel activity.

#### **Antiradical activity and reducing capacity (publications B, C, D, E)**

As the additional biological properties for characterization of newly obtained 1,4-DHP derivatives antiradical activity (ARA) and reducing capacity (RC) were determined as well. The ARA of the synthesized 1,4-DHP derivatives from publications **B** and **E** was determined using a 1,1-diphenyl-2-picrylhydrazyl (DPPH) free radical scavenging test according to the procedure described in literature (Abdelwahed et al. 2007; Brand-Williams et al. 1995). This method is most frequently used for screening the ARA of compounds with different structures, including derivatives of 1,4-DHP. Test of the ability of 1,4-DHP derivatives to reduce the stable DPPH radical was carried out in ethanol at room temperature and determined photometrically with UV/Vis spectroscopy as reduction in absorption at 517 nm. In addition, the phosphomolybdenum complex method was used for the evaluation of the RC of the corresponding 1,4-DHP derivatives from publications **B**, **C** and **D**, according to a recommendation by Prieto et al (Prieto et al. 1999). The assay is based on the reduction of MoVI to MoV by the tested sample at acidic pH with the following formation of a green phosphate/MoV complex, with a characteristic absorbance maximum at 695 nm detectable by UV/Vis spectroscopy. Diludine, a well known 1,4-DHP derivative with antioxidant and antiradical properties, was used as a positive control in both cases. (Kouřimská et al. 1993) ARA and RC data obtained for bispyridinium 1,4-DHP dibromides **B4a-e** are summarized in Fig. 15. In turn, the obtained results (Fig. 15) showed that all the tested bispyridinium

dibromides based on the 1,4-DHP cycle **B4a-e** possess RC and antiradical properties. So, a low ARA (7–11 %) was determined for compounds **B4a-e**. However, the highest RC, which was comparable to that of diludine (40 %), was evidenced for the compound **B4d** (also 40 %) and moderate RC (25 %) for compound **B4c**, while other bispyridinium dibromides **B4a**, **B4b**, and **B4e** showed low RC (7–10 %).

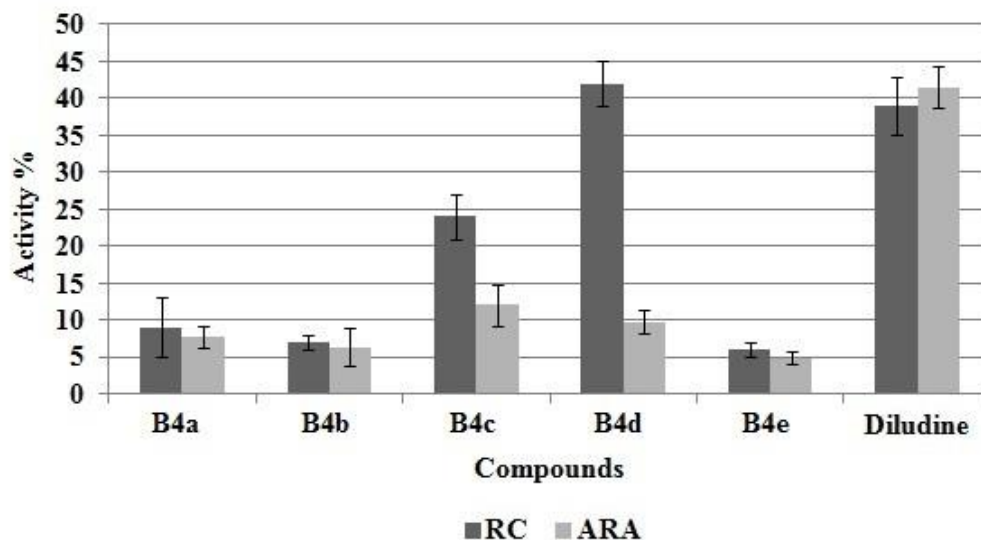


*Figure 15. Reducing capacity (RC) of the obtained bispyridinium derivatives B4a–e and diludine (at a concentration of 100  $\mu$ M); results are expressed as absorbance percentage (%) at 695 nm of sample against absorbance of a blank solution. Antiradical activity (ARA) of synthesized 1,4-DHP derivatives B4a–e and diludine. Results are expressed as an absorbance percentage (%) of the DPPH free radical scavenging at 517 nm. The untreated level of the DPPH radical is designated as 100 %. All data are presented as a mean  $\pm$  SD*

All the tested bispyridinium dibromides based on the 1,4-DHP cycle **B4a-e** possess RC and ARA. Highest RC, which was comparable to that of diludine (40 %), was detected for the compound **B4d** (also 40 %). More detailed information can be found in appendix publication **B**.

In this study, the phosphomolybdenum complex method was used also for the evaluation of reducing capacity of the synthesized 1,4-DHP derivatives **D1-18** using diludine as a positive control. The obtained results (Fig. 16) showed that all synthesized 1,4-DHP derivatives possessed antioxidant properties.

Highest activity (about 60–70 %) was evidenced for the N-unsubstituted derivatives – compounds **D1** and **D17**, containing the 4-phenyl or N-carboxymethyl pyridinium moiety, respectively. The RC of compounds **D3**, **D6** and **D15** was comparable to that of diludine. Other 1,4-DHP derivatives showed a lower reducing capacity than diludine and even



compounds that demonstrated a high calcium channel blocking activity (compounds **D11** and **D12**), indicating a lack of correlation between their RC and calcium antagonistic properties.

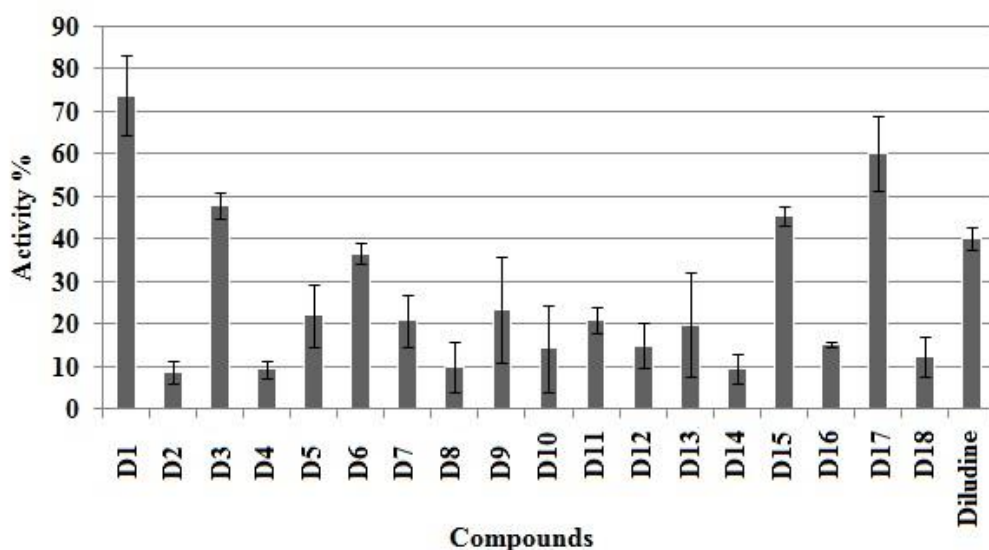


**Figure 16. Reducing capacity of 1,4-DHP derivatives D1–18 (at concentration 100  $\mu$ M) evaluated by phosphomolybdenum complex method. Results are expressed as absorbance percentage (%) (at 695 nm) of sample against absorbance of blank solution. Data are presented as a mean  $\pm$  SD. \* $p < 0.05$  vs. Diludine (taken as 100 %), one-way ANOVA followed by Bonferroni multiple comparison's test**

It is suggested that the reducing capacity of the tested 1,4-DHP derivatives is mainly related to the ability of their N–H group to protonate/deprotonate at the phosphomolybdenum complex test system. More detailed information can be found in appendix publication **D**.

Higher reducing capacity showed 1,4-DHP derivatives with unsubstituted N-atom compared with the N-propargyl substituted ones.

The obtained data on RC of the synthesized compounds **C1-9** are summarized in Figure 17. The obtained results showed that all synthesized 1,4-DHP derivatives **C1-9** possess reducing capacity under the tested conditions. It should be noted that RC of 1,4-DHP derivatives **C1** and **C2** was higher than that of diludine. Other 1,4-DHP derivatives **C3-9**, containing pyridinium moiety, showed lower RC values than diludine.

I expect that RC values of the tested 1,4-DHP derivatives are mainly related to the ability of their aromatization at the phosphomolybdenum complex system leading to full oxidation of dihydropyridine to the corresponding pyridine derivative (according to UV/Vis spectrum data).

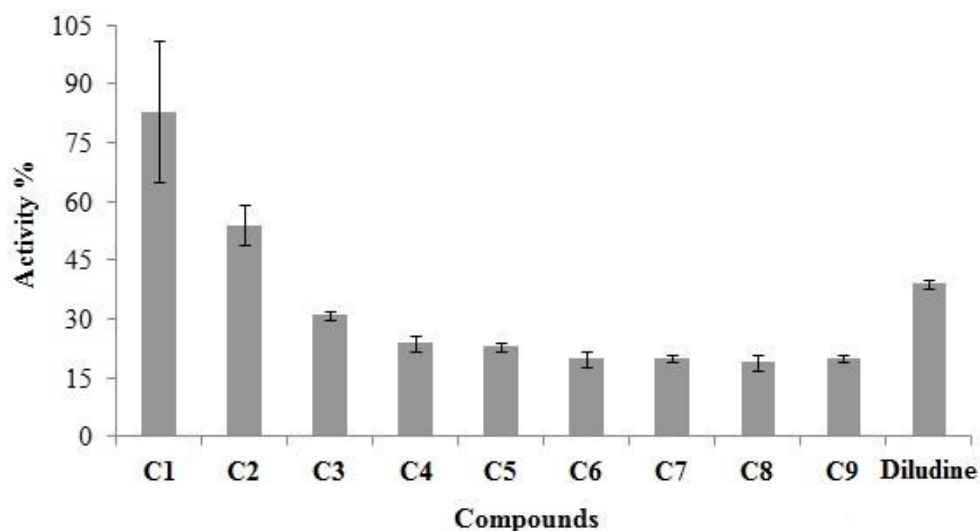


**Figure 17. RC of 1,4-DHP derivatives C1-9 and diludine (at 100  $\mu$ M concentration), evaluated by the phosphomolybdenum complex method; the results are expressed as absorbance percentage (%) of sample at 695 nm against absorbance of a blank solution. All data are presented as a mean  $\pm$  SD**

Higher activity was detected for non-quaternized 1,4-DHP derivatives at position 4 of 1,4-DHP cycle compared with quaternized ones. More detailed information can be found in appendix publication C.

Brief conclusion the 1,4-DHP derivatives with unsubstituted N-atom at position 1 possessed better reducing capacity activity than the N-substituted ones. Quaternized pyridinium moiety at position 4 of the 1,4-DHP cycle decreases the RC of compounds. Increasing the length of alkyl chain at quaternized pyridinium moiety at position 4 of the 1,4-DHP core did not significantly influence activity, but it is still less than the non-quaternized 1,4-DHP derivatives.

In this study interest was focused in whether the novel synthesized 1,4-DHP amphiphiles possess ARA and how the substituent at the cationic head-group of the 1,4-DHP carrier molecule affects the ability to scavenge free radicals. In this respect, both parent 1,4-DHP derivatives **E2** and **E3**, synthesized 1,4-DHP amphiphiles **E1**, **E4–20** as well as PEI 25 and DOTAP were tested as scavengers of the DPPH radical according to the above mentioned procedure. This method is widely used due to the stability and simplicity of the reaction system, which allows direct reaction between the radical and a potential antioxidant. (Noipa et al. 2011) The ARA of tested 1,4-DHP derivatives **E1–20** was compared with that of diludine and with the activity of ascorbic acid (AA), (Lo Scalzo 2008; Bendich et al. 1986) which is a well-known antioxidant and a free radical scavenger (Fig. 18). The results showed that among

the tested 1,4-DHP derivatives, amphiphiles **E1**, **E4–17** and **E19** possessed moderate ARA (25–60 %, Fig. 18) which are comparable with the ARA of diludine (40 %, Fig. 18).

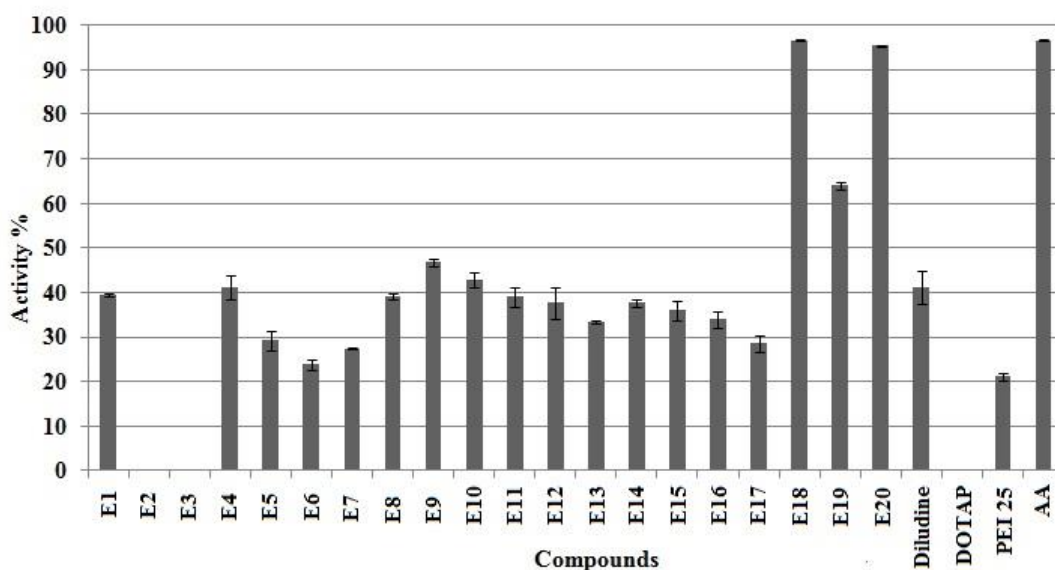


**Figure 18.** ARA of synthesized 1,4-DHP derivatives **E1–20**, **PEI 25**, **DOTAP**, **diludine** and **AA**, evaluated by their ability to react with the DPPH. Results are expressed as a percentage (%) of the DPPH free radical scavenging. The untreated level of the DPPH radical is designated as 100 %. Data are presented as a mean  $\pm$  SD

In contrast, parent compounds **E2** and **E3** without the cationic head-group in the molecule totally lacked ARA activity, suggesting that the cationic head-group within 1,4-DHP amphiphilic derivatives is an essential structural moiety for expression of ARA. Interestingly, also **PEI 25** showed minor ARA (20 %, Fig. 18), whereas **DOTAP** lacked ARA activity, as it was expected.

For ARA essential is cationic head-group at positions 2 and 6 of 1,4-DHP derivatives. More detailed information can be found in appendix publication **E**.

Brief conclusion the higher antiradical activity showed 1,4-DHP derivatives with cationic substituent at positions 2 and 6 of the 1,4-DHP cycle compared with compounds containing quaternized pyridinium moiety at position 4 of the 1,4-DHP core where this activity was very low or even not detected at all.

Thank to colleague M. Sc. Marina Gosteva for the obtained ARA and RC results.

### **Nanoparticle studies (publications A, E, F)**

Self-assembling properties of the compounds are important factor influencing the transfection efficiency. Cationic liposomes are the most extensively used non-viral systems for gene transfection *in vitro* and *in vivo*. (Hyvönen et al. 2000) To find new efficient and safe

agents for gene delivery in this thesis were synthesized and studied synthetic amphiphilic 1,4-DHP derivatives. In this part of work focus was on characterization of self-assembling properties depending from structure of cationic moiety of amphiphiles, stability of nanoparticles formed by amphiphile **E1** (1,1'-[(3,5-dido-decyloxycarbonyl-4-phenyl-1,4-dihydropyridine-2,6-diyl)dimethylen]-bispyridinium dibromide) for comparison of properties of cationic 1,4-DHP and corresponding cationic pyridines as NAD/NADH analogues. Due to the amphiphilic nature of the 1,4-DHP molecules it is predictable that they assemble spontaneously into nanoparticles in aqueous media. In previous work (Hyvönen et al. 2000) there was shown that cationic group containing 1,4-DHP derivatives forms liposomes, but there were little information about main nanoparticle formation characteristics. Therefore in this study more in detail were investigated formed liposomes of amphiphilic 1,4-DHP derivatives. At the beginning, samples from self-assembling 1,4-DHP amphiphile **E1** were prepared in aqueous media at concentrations 0.01 and 0.3 mg/mL and with sonication for 5 min. Stability of nanoparticles was tested every month during three month period. The obtained liposomes were visualized by atomic force microscopy (AFM) as images and vertical profiles of liposomes (Fig. 19).

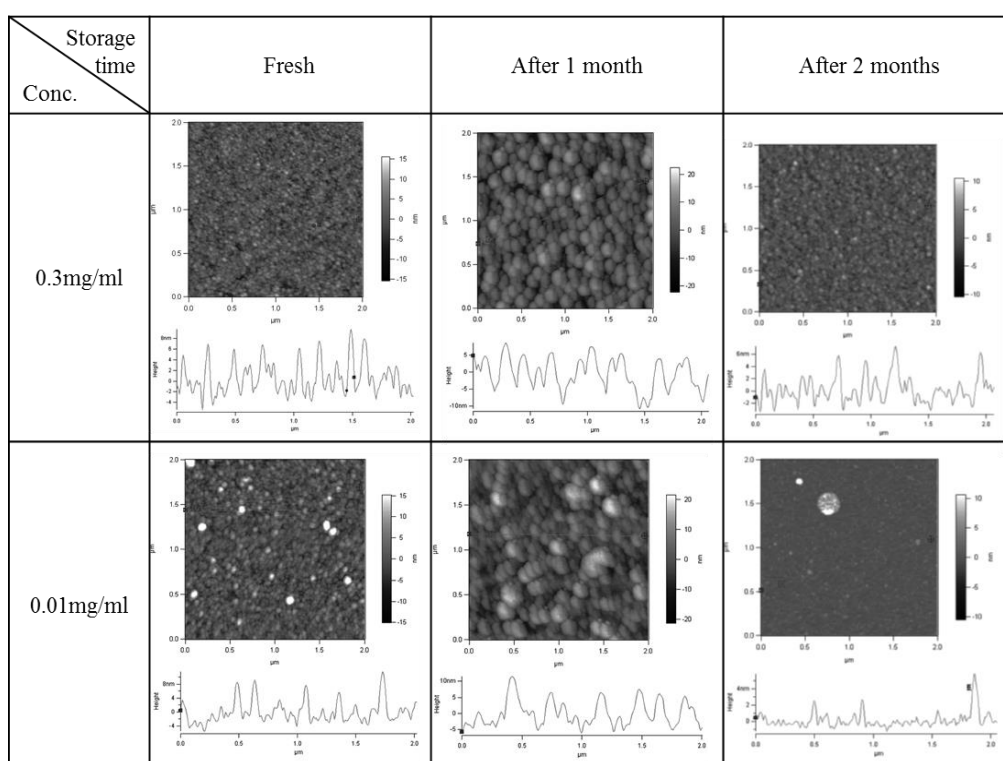


**Figure 19.** AFM images and vertical profiles of liposomes formed by 1,4-DHP amphiphile **E1** at the concentrations 0.01 or 0.3 mg/mL; liposomes adsorbed on a mica plates.

From obtained AFM data it was concluded that liposomes formed by 1,4-DHP amphiphile **E1** are with average diameter up to 100-150 nm and are stable at least for one month period. More detailed information can be found in appendix publication **F**.

In this study were tested the self-assembling properties of newly synthesized 1,4-DHP amphiphiles **E1**, **E4-20**. For more detailed studies of formed nanoparticles with atomic force microscopy, transmission electron microscopy (TEM) and dynamic light scattering (DLS) methods were selected six 1,4-DHP amphiphiles which readily formed most stable nanoparticles in water. The chosen amphiphiles were compounds **E5**, **E11**, **E12**, **E15** and **E20** with various structural modifications at the cationic head-group and 1,4-DHP amphiphile **E1** for comparison. For self-assembling compounds, the concentration above where micelles and other nanoparticles are formed, called the critical micelle concentration (CMC), is an important characterization. In this study CMC was determined for tested amphiphiles **E1**, **E5**, **E11** and **E15** in aqueous media by the DLS technique according to the procedure described by Topel et al (Topel et al. 2013). To determine CMC, an aqueous solution of amphiphiles was prepared within the concentration range of 0.5 mg/mL to  $0.1 \times 10^{-2}$  mg/mL starting from concentrated stock solution, which was subjected to a serial two-fold dilution each time with water.

According to AFM and TEM data, all studied nanoparticles formed by 1,4-DHP amphiphiles dispersed well without any aggregation and were homogeneous in morphology and shape (Fig. 20). The background between the nanoparticles appeared to be unstructured in TEM measurements. According to AFM data (Fig. 20A) amphiphile **5** formed rather small nanoparticles with an average size of 60–70 nm, whereas the nanoparticles formed by five amphiphiles **E1**, **E11**, **E12**, **E15** and **E20** were larger with an average diameter up to 170–200 nm. According to the TEM images (Fig. 20B), the average size of the nanoparticles formed by 1,4-DHP amphiphiles **E1**, **E11**, **E12**, **E15** and **E20** varied between 150 and 350 nm. Nanoparticles formed by 1,4-DHP amphiphile **E5** appeared to have an average diameter up to 330 nm. In conclusion, 1,4-DHP amphiphiles were able to self-aggregate and form nanoparticles in aqueous media with sizes between 60 and 350 nm. Zeta-potentials for six selected amphiphiles were determined by DLS (Fig. 21). The obtained data indicated that the nanoparticles formed by selected amphiphiles had quite similar surface characteristics and the surface charges were strongly positive.

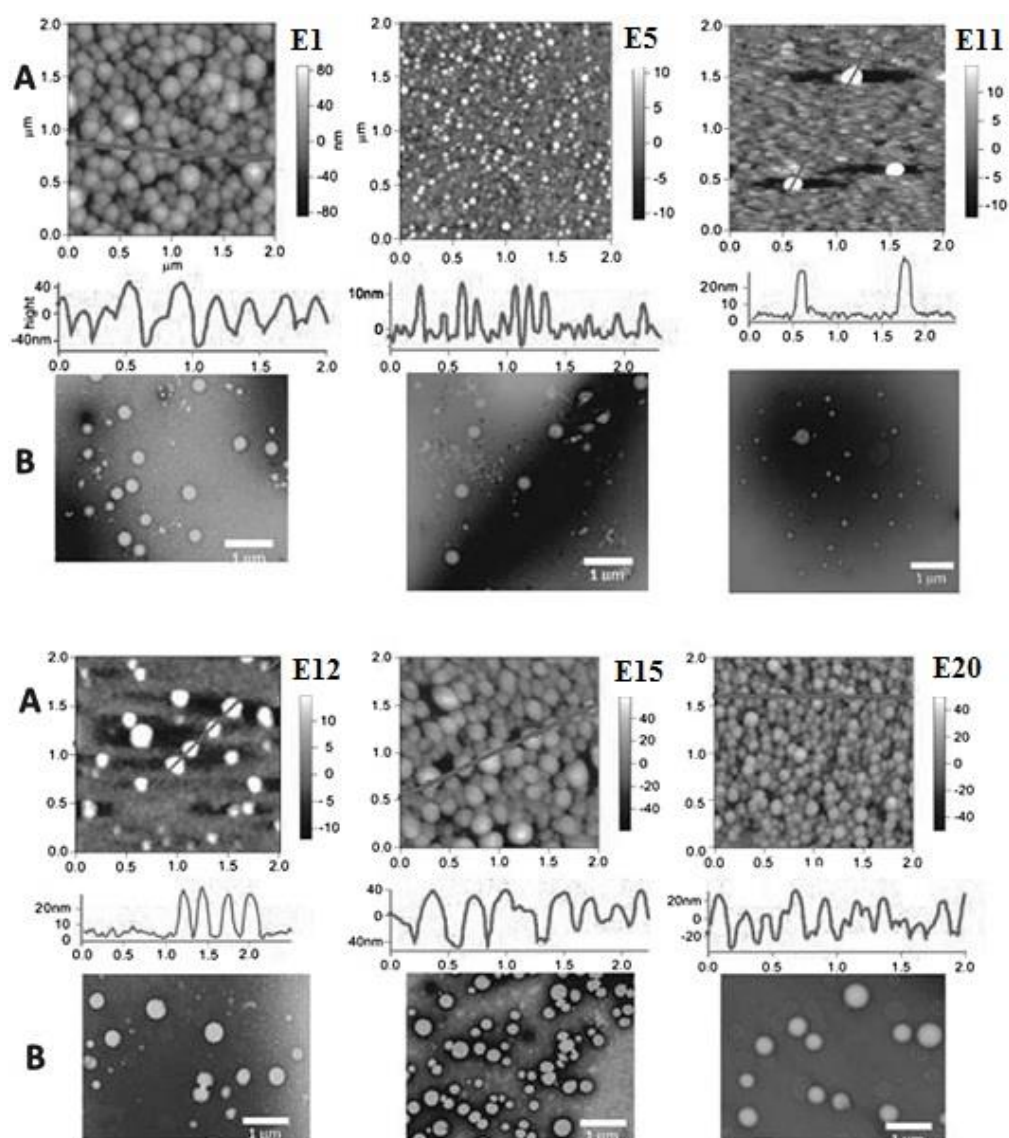
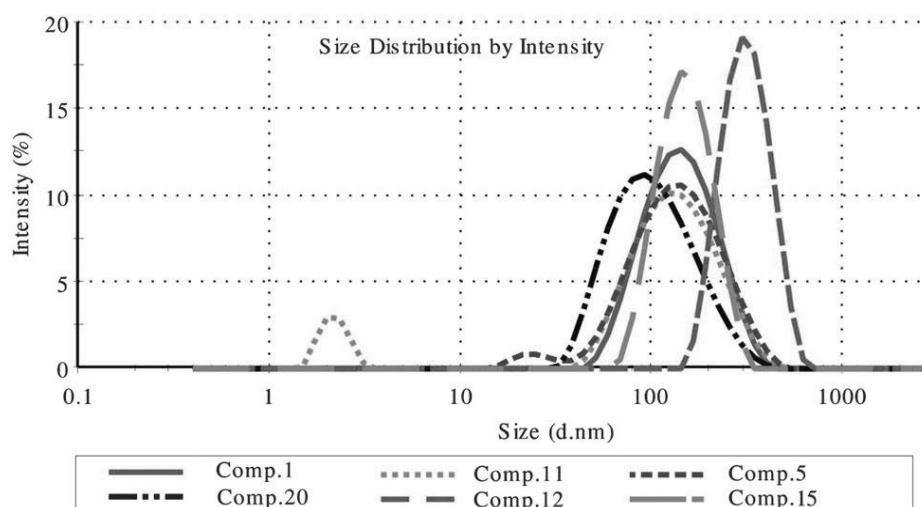


**Figure 20.** AFM images and vertical profiles of nanoparticles formed by 1,4-DHP amphiphiles **E1**, **E5**, **E11**, **E12**, **E15** and **E20** adsorbed on mica plates (A) and TEM images of formed nanostructures for the same amphiphiles **E1**, **E5**, **E11**, **E12**, **E15** and **E20** adsorbed to formvar carbon-coated copper grids and negatively stained with 1 % uranyl acetate aqueous solution; bars = 1000 nm (B). The samples were prepared by sonication in an aqueous solution at an amphiphile concentration of 0.5 mg/mL

Preliminary CMC values for tested 1,4-DHP amphiphiles **E1**, **E5**, **E11** and **E15** are 30, 35, 20 and 15 mM, respectively. In this case small changes in the structure of cationic part of the amphiphile have no a significant influence on CMC values for tested amphiphiles.

Zeta-potentials over 30 mV confirm that the formed nanoparticle solutions are relatively stable. The hydrodynamic diameters of the nanoparticles formed by selected 1,4-DHP amphiphiles **E1**, **E5**, **E11**, **E12**, **E15** and **E20** in water were determined also by DLS measurements (Fig. 21). Additionally, for all selected amphiphiles the polydispersity index was measured (Fig. 21). The results revealed that amphiphile **E11** possess a PDI of 0.607

shows rather broad particle size distribution. It seems from the obtained DLS data that compound **E11** forms micelles (diameter smaller than 5 nm) rather than vesicles in contrast to the other tested amphiphiles.



Comp.	$D_{[H]}$ Z-aver., nm	PDI	Distr. peak (max) mean $d_{[H]}$ , nm (%)		Zeta- potential, mV
			Peak 1	Peak 2	
<b>E1</b>	113	0.345	151 (98.9)	5210 (1.1)	82.1±9.54
<b>E5</b>	100	0.323	151 (96.6)	24.1 (3.4)	65.9±13.6
<b>E11</b>	75	0.607	147 (88.7)	2.21 (3.4)	67.0±11.7
<b>E12</b>	359	0.316	319 (100)	-	62.0±10.7
<b>E15</b>	150	0.270	154 (100)	-	61.0±11.7
<b>E20</b>	90	0.210	113 (100)	-	59.9±12.2

Figure 21. Size-distribution, polydispersity index (PDI), zeta-potential, Z-average diameter and intensity-weighted size distribution of nanoparticles formed by amphiphiles **E1**, **E5**, **E11**, **E12**, **E15** and **E20** were obtained by DLS measurements. Mean diameter depicts the hydrodynamic diameter of the main population of tested sample; PDI value describes polydispersity of sample; zeta-potential gives information about the surface charge of the nanoparticles; Z-average diameter represents the average hydrodynamic diameter of all nanoparticles in the sample

In summary, small changes in the chemical structure of amphiphiles are vitally important for the properties of the formed nanoparticles. It could be assumed that even small changes in the chemical structure of amphiphiles might bring changes in the properties of the formed nanoparticles. For amphiphiles **E1**, **E5** and **E12** PDI values were 0.345, 0.323 and 0.316, while the most homogeneous particles were formed by amphiphiles **E15** and **E20** with PDI of 0.270 and 0.210, respectively.

Generally, it could be concluded that the structure of the cationic head-group of 1,4-DHP amphiphiles affects the size of the formed nanoparticles. More detailed information can be found in appendix publication **E**.

The data about nanoparticle formation by amphiphile **E1** which is described in publication **F** correlate with the data showed in publication **E**, the average liposome size are about 150 nm.

The following studies of this thesis was to evaluate and characterize self-assembling properties and formation of nanoparticles of the corresponding pyridine derivatives **A6a–g** (Table 3) as oxidized forms of previously reported cationic 1,4-DHPs as NAD/NADH analogues and comparison of the obtained results with properties of 1,4-DHP amphiphile **E1** which was found to be most active gene delivery system among previously tested 1,4-DHP amphiphiles.

According to DLS data, the average size of the nanoparticles formed by pyridine derivatives **A6a–g** varied from 115 to 743 nm. Thus, for pyridines **A6b**, **A6c**, **A6d** (Table 3, entries 4–6) the average size of the nanoparticle diameters were comparable with the size of nanoparticles formed by 1,4-DHP amphiphile **E1**; for pyridines **A6a** and **A6g** sizes were slightly larger – 183 and 253 nm, while for pyridines **A6e** and **A6f** a significant increase of diameters was observed – 743 and 543 nm, respectively. The mean diameter which depicted the hydrodynamic diameter of the main population of nanoparticles for every sample varied between 118 and 389 nm. Thus, for 1,4-DHP amphiphile **1** the diameter of the formed nanoparticles was in the range of 130–150 nm these diameter values are similar to the hydrodynamic diameter of the main population of nanoparticles formed by pyridines **A6a–d** (Table 3, entries 3–6). For these samples the mean peak amounts were over 97 %. Only in the case of pyridine **A6g** two main populations of nanoparticles with hydrodynamic diameter 237 and 63 nm (Table 3, entry 9) were observed. The hydrodynamic diameter of the main population of nanoparticles for other pyridines **A6e** and **A6f** were 389 and 235 nm with the mean peak amount near 90 %. Additionally, for all pyridines **A6a–g** the polydispersity index was measured (Table 3).



Table 3.

Values of Z-average diameter, polydispersity index, mean diameter, zeta-potential and critical micelle concentration of nanoparticles formed by 1,4-DHP amphiphile E1 and new pyridine derivatives A6a–g obtained by DLS measurements

Entry	Comp.	Z-average diameter, nm	PDI	Mean diameter, nm	Zeta-potential, mV	CMC, $\mu$ M
1	<b>E1*</b>	113	0.345	151 (99%)	82±10	30
2	<b>E1</b>	110±10	0.345±0.06	134±5 (97%)	90±3	17
3	<b>A6a</b>	183±52	0.330±0.049	124±19 (100%)	66±1	34
4	<b>A6b</b>	118±14	0.383±0.058	126±4 (97%)	59±7	38
5	<b>A6c</b>	115±9	0.313±0.023	118±4 (97%)	79±4	33
6	<b>A6d</b>	120±1	0.227±0.002	151±5 (99%)	72±8	16
7	<b>A6e**</b>	743±64	0.668±0.008	389±8 (92%)	51±2	2
8	<b>A6f</b>	543±83	0.548±0.078	235±27 (89%)	48±3	67
9	<b>A6g</b>	253±25	0.373±0.029	237±21 (58%); 63±2 (42%)	57±7	16

\*according to literature data (Pajuste et al., 2013)

\*\*sample concentration – 0.1 mg/mL

The results showed a rather broad particle size distribution for pyridines **A6e** and **A6f** possessing a PDI of 0.668 and 0.548 (Table 3, entries 7 and 8), respectively. For 1,4-DHP amphiphile 1, pyridines **A6a–c** and **A6g** PDI values were in the range from 0.313 to 0.383 (Table 3, entries 1–5 and 9), while the most homogeneous particles were formed by pyridine **A6d** with PDI of 0.227 (Table 3, entry 6). The obtained data showed that values of zeta-potentials for the nanoparticles formed by pyridine derivatives were in the range of 48–79 mV, with the highest value for pyridine **A6c** (Table 3, entry 5) and lowest value for pyridine **A6f** (Table 3, entry 8). Zeta-potential values indicated that the nanoparticles formed by pyridine derivatives **A6a–g** had quite similar surface characteristics and the surface charges were strongly positive which would be a useful property for lipoplex formation with negatively charged DNA. In this study CMC was determined for synthesized pyridines **A6a–g** and 1,4-DHP amphiphile **E1** in aqueous media by the DLS technique according to the procedure described above. The obtained data showed that CMC values for the tested 1,4-DHP amphiphile **E1** and pyridines **A6a–g** are in the range of 2–67 mM (Table 3). Lower CMC value 2 mM was determined for pyridine **A6e** containing *p*-cyanopyridinium moieties

(Table 3, entry 7) which could involve poor solubility of this compound and also evident during the preparation of sample for DLS measurements, because in this case it was not possible to prepare a stock solution of the compound with concentration 0.5 mg/mL. Highest CMC value 67 mM was observed for pyridine **A6f** by introducing in the molecule N-methylpyrrolidinium moieties (Table 3, entry 8) whilst CMC values for other compounds were 16–38 mM. In this case small changes in the chemical structure of the pyridines have no significant influence on CMC values.

For some cationic moieties containing pyridines the average size of the formed nanoparticle diameters were comparable with the size of nanoparticles formed by 1,4-DHP amphiphile **E1**. More detailed information can be found in appendix publication A.

In summary all the tested 1,4-DHP and pyridine derivatives containing cationic moieties at positions 2 and 6 formed liposomes in aqueous media. In all cases the zeta-potential showed that formed nanoparticles are relatively stable. In most cases the formed liposomes of tested compounds are monodisperse. It could be proposed that even small changes in the chemical structure of 1,4-DHP or pyridine derivatives might bring changes in the properties of the formed nanoparticles.

Thank to Dr. habil. biol. Velta Ose-Klinklava Latvian Biomedical Research and Study Centre for the obtained TEM results and colleague Dr. chem. Karlis Pajuste for the obtained DLS results.

## CONCLUSIONS

1. The synthesis of novel original class of 1,4-DHP derivatives containing N-propargyl and 4-alkylpyridyl substituents has been developed, where the main step is Hantzsch-type cyclization with propargyl amine hydrochloride as nitrogen source in a pressure tube. Using these conditions allow to obtain the desired products in shorter time with higher yields in comparison with typical Hantzsch procedure.
2. Synthesis of new amphiphilic pyridine derivatives containing dodecyloxycarbonyl substituents at positions 3 and 5, and cationic moieties at positions 2 and 6 were elaborated by oxidation of the corresponding 2,6-bis(bromomethyl)-1,4-DHP instead of corresponding pyridine bromination. These compounds were obtained for studies of self-assembling properties and for comparison with self-assembling properties of the corresponding 1,4-DHP as NAD/NADH analogues. The made comparison shows that pyridine derivatives formed nanoparticles (120-253 nm) are with average diameter greater than 1,4-DHP analogues (90-113 nm), but the other parameters are comparable.
3. It has been shown that quaternization reaction of 4-pyridyl-1,4-DHP derivatives with propargyl bromide proceeded unexpectedly giving new bispyridinium dibromides on the base of 1,4-DHP instead of the expected monomeric N-propargyl-pyridinium-1,4-DHP bromides.
4. Assessment of calcium channel blocking activity of newly synthesized 1,4-DHP derivatives containing propargyl and/or pyridinium moieties confirmed, that:
  - propargyl group at the position 1 of 1,4-DHP ring did not influence essentially the biological activity of the tested 1,4-DHP derivatives in the used test systems; among the tested N-alkyl-4-pyridinium-1,4-DHP the highest calcium channel blocking activity was found for the compounds with the N-dodecyl pyridinium moiety at position 4 of the 1,4-DHP cycle; this activity in vascular smooth muscle cell line A7r5 was considerably higher than in neuroblastoma cell line SH-SY5Y, suggesting that these compounds predominantly target L-type calcium channels;
  - studies of calcium channel antagonist and agonist activities of the 1,4-DHP derivatives containing propargyl ester moieties at positions 3 and 5, assayed by changes in intracellular  $\text{Ca}^{2+}$  concentration in H9C2 and A7r5 cells, indicate that the compounds target only calcium channels in vascular smooth muscle cells and do not affect calcium channels in cardiac cells;
5. Assessment of antiradical activity using a 1,1-diphenyl-2-picrylhydrazyl free radical scavenging test confirmed that:

- only 1,4-DHP derivatives containing cationic moieties at the positions 2 and 6 possessed considerable radical scavenging properties (25-95 %), compared with diludine (40 %);
  - bispyridinium dibromides based on the 1,4-dihydropyridine cycle possessed low radical scavenging properties (5-10%).
6. Evaluation of reducing capacity by the phosphomolybdenum complex method confirmed that newly synthesized 1,4-DHP derivatives containing propargyl and/or pyridinium moieties as well as bispyridinium dibromides based on the 1,4-dihydropyridine cycle possessed this activity (6-80 %), compared with diludine (40 %).
7. Studies of self-assembling properties of newly synthesized 1,4-DHP derivatives with cationic moieties at the positions 2 and 6 as well as their oxidized analogues – corresponding cationic moieties containing pyridine derivatives confirmed that:
- all studied derivatives with cationic moieties at the positions 2 and 6 possessed self-assembling properties and formation of nanoparticles in aqueous media by the self-association; in all cases the values of zeta-potential (48-90 mV) confirmed that nanoparticles are relatively stable;
  - even small changes in the chemical structure of 1,4-DHP or pyridine derivatives may bring changes in the properties of the formed nanoparticles;
  - liposomes formed by 1,1'-[(3,5-didodecyloxycarbonyl-4-phenyl-1,4-dihydropyridine-2,6-diil)dimethylen]bispyridinium dibromide were with average diameter up to 100-150 nm and stable at least for one month period.

## ACKNOWLEDGEMENTS

The greatest thanks I would like to express to my supervisors Dr. chem. A. Plotniece and Dr. habil. biol. professor R. Muceniece for encouragement of all this process launch, known as thesis preparation time, and tips, hints and sharing of knowledge during the time of this work development.

Also I am very grateful to my family and friends for their understanding and support for the time of writing this thesis.

Thanks to the Latvian Institute of Organic Synthesis Membrane active compounds and  $\beta$ -diketones laboratory colleagues for support, sharing of experiences, fruitful discussions and recommendations.

I express my gratitude to the Latvian Biomedical Research and Study Centre researcher Dr. habil. biol. V. Ose-Klinklava for obtaining of TEM data.

I would like to thank my colleague M. Sc. M. Gosteva for the determination of antiradical activity and reducing capacity of synthesized compounds.

I am very grateful to Latvian Institute of Organic Synthesis Experimental chemotherapy group, especially Dr. chem. I. Domracheva, for the obtained data of calcium channel activity of synthesized compounds.

I am thankful to my colleagues Dr. chem. K. Pajuste and Dr. chem. O. Petrichenko for the obtained DLS data.

My gratitude goes to Dr. D. Erts and colleagues from the Institute of Chemical Physics, University of Latvia for assistance and training with AFM equipment.

## REFERENCES

1. Abbas, H.A.S. et al., 2010. Synthesis and antitumor activity of new dihydropyridine thioglycosides and their corresponding dehydrogenated forms. *European Journal of Medicinal Chemistry*, 45(3), pp.973–982.
2. Abbasi, E. et al., 2014. Dendrimers: synthesis, applications, and properties. *Nanoscale Research Letters*, 9(1), p.247.
3. Abdelhamid, I.A., Darweesh, A.F. & Elwahy, A.H.M., 2015. Synthesis and characterization of poly(2,6-dimethyl-4-phenyl-1,4-dihydropyridinyl)arenes as novel multi-armed molecules. *Tetrahedron letters*, 56(51), pp.7085–7088.
4. Abdelwahed, A. et al., 2007. Study of antimutagenic and antioxidant activities of Gallic acid and 1,2,3,4,6-pentagalloylglucose from *Pistacia lentiscus*: Confirmation by microarray expression profiling. *Chemico-Biological Interactions*, 165(1), pp.1–13.
5. Affeldt, R.F. et al., 2012. A new In-SiO<sub>2</sub> composite catalyst in the solvent-free multicomponent synthesis of Ca<sup>2+</sup> channel blockers nifedipine and nemadipine B. *New Journal of Chemistry*, 36(7), pp.1502–1511.
6. AG, F.B. ed., 1976. Pharmaceutical compositions containing unsymmetrical esters of 1,4-dihydropyridine 3,5-dicarboxylic acid. (US3932645).
7. Aktiengesellschaft, B. ed., 1977. 1,4-Dihydropyridines. (US4048171).
8. Al-Mubaddel, F.S. et al., 2012. Engineered nanostructures: A review of their synthesis, characterization and toxic hazard considerations. *Arabian Journal of Chemistry*, 10.1016/j.arabjc.2012.09.010.
9. Allais, C. et al., 2014. Metal-Free Multicomponent Syntheses of Pyridines. *Chemical Reviews*, 114(21), pp.10829–10868.
10. Andzi Barhé, T. et al., 2016. Comparative study of the anti-oxidant activity of the total polyphenols extracted from *Hibiscus Sabdariffa* L., *Glycine max* L. Merr., yellow tea and red wine through reaction with DPPH free radicals. *Arabian Journal of Chemistry*, 9(1), pp.1–8.
11. Anekonda, T.S. et al., 2011. L-type voltage-gated calcium channel blockade with isradipine as a therapeutic strategy for Alzheimer's disease. *Neurobiology of Disease*, 41(1), pp.62–70.
12. Anekonda, T.S. et al., 2011. Calcium channel blocking as a therapeutic strategy for Alzheimer's disease: The case for isradipine. *Biochimica et Biophysica Acta (BBA) - Molecular Basis of Disease*, 1812(12), pp.1584–1590.
13. Antony Savarimuthu, S. et al., 2014. Nucleophilic substitution of propargyl alcohols with aliphatic alcohols, aliphatic amines and heterocycles catalyzed by 4-nitrobenzenesulfonic acid: A scalable and metal-free process. *Tetrahedron Letters*, 55(21), pp.3213–3217.

14. Apel, K. et al., 2004. REACTIVE OXYGEN SPECIES: Metabolism, Oxidative Stress, and Signal Transduction. *Annual Review of Plant Biology*, 55(1), pp.373–399.
15. Balalaie, S. et al., 2013. Synthesis of polysubstituted 1,4-dihydropyridines via three-component reaction. *Tetrahedron*, 69(2), pp.738–743.
16. Bardhan, R. et al., 2011. Theranostic Nanoshells: From Probe Design to Imaging and Treatment of Cancer. *Accounts of Chemical Research*, 44(10), pp.936–946.
17. Becker, C. et al., 2008. Use of antihypertensives and the risk of Parkinson disease. *Neurology*, 70(16 Part 2), pp.1438–1444.
18. Bele, S. et al., 2015. Continuous intra-arterial nimodipine infusion in patients with severe refractory cerebral vasospasm after aneurysmal subarachnoid hemorrhage: a feasibility study and outcome results. *Acta Neurochirurgica*, 157(12), pp.2041–2050.
19. Bendich, A. et al., 1986. The antioxidant role of vitamin C. *Advances in Free Radical Biology & Medicine*, 2(2), pp.419–444.
20. Bossert, F. Et al., 1989. 1,4-Dihydropyridines—a basis for developing new drugs. *Medicinal Research Reviews*, 9(3), pp.291–324.
21. Brand-Williams, W. et al., 1995. Use of a free radical method to evaluate antioxidant activity. *LWT - Food Science and Technology*, 28(1), pp.25–30.
22. Brauch, S. Et al., 2013. Higher-order multicomponent reactions: beyond four reactants. *Chemical Society Reviews*, 42(12), pp.4948–4962.
23. Brigger, I. et al., 2002. Nanoparticles in cancer therapy and diagnosis. *Advanced Drug Delivery Reviews*, 54(5), pp.631–651.
24. Bugaut, X. et al., 2013. Michael addition-initiated sequential reactions from 1,3-dicarbonyls for the synthesis of polycyclic heterocycles. *Current Organic Chemistry*, 17(18), pp.1920–1928.
25. Bülbül, B. et al., 2009. Condensed 1,4-dihydropyridines with various esters and their calcium channel antagonist activities. *European Journal of Medicinal Chemistry*, 44(5), pp.2052–2058.
26. Buraka, E. et al., 2014. DNA-binding studies of AV-153, an antimutagenic and DNA repair-stimulating derivative of 1,4-dihydropyridine. *Chemico-Biological Interactions*, 220, pp.200–207.
27. Candeias, N.R. et al., 2010. Boronic Acids and Esters in the Petasis-Borono Mannich Multicomponent Reaction. *Chemical Reviews*, 110(10), pp.6169–6193.
28. Canova, D. et al., 2012. Cerebral oxygenation and haemodynamic effects induced by nimodipine in healthy subjects. *Functional Neurology*, 27(3), pp.169–176.
29. Carosati, E. et al., 2012. 1,4-Dihydropyridine scaffold in medicinal chemistry, the

- story so far and perspectives (part 2): action in other targets and antitargets. *Current Medicinal Chemistry*, 19(25), pp.4306–4323.
30. Chattopadhyay, N. et al., 2012. Role of antibody-mediated tumor targeting and route of administration in nanoparticle tumor accumulation in vivo. *Molecular Pharmaceutics*, 9(8), pp.2168–2179.
31. Chen, J. et al., 2008. Analyte-triggered gelation: Initiating self-assembly via oxidation-induced planarization. *Journal of the American Chemical Society*, 130(49), pp.16496–16497.
32. Chen, Q. et al., 2015. Nanoscale theranostics for physical stimulus-responsive cancer therapies. *Biomaterials*, 73, pp.214–230.
33. Chen, X.-X. et al., 2013. Characterization and preliminary toxicity assay of nano-titanium dioxide additive in sugar-coated chewing gum. *Small (Weinheim an der Bergstrasse, Germany)*, 9(9–10), pp.1765–74.
34. Cherkupally, S.R. et al., 2008. *P*-TSA catalyzed facile and efficient synthesis of polyhydroquinoline derivatives through hantzsch multi-component condensation. *Chemical and Pharmaceutical Bulletin*, 56(7), pp.1002–1004.
35. Cicha, I. et al., 2014. Cardiovascular therapy through nanotechnology - How far are we still from bedside? *European Journal of Nanomedicine*, 6(2), pp.63–87.
36. Cindric, M. et al., 2010. Reversal of multidrug resistance in murine lymphoma cells by amphiphilic dihydropyridine antioxidant derivative. *Anticancer Research*, 30(10), pp.4063–4069.
37. Contado, C. et al., 2013. Size characterization by Sedimentation Field Flow Fractionation of silica particles used as food additives. *Analytica Chimica Acta*, 788, pp.183–192.
38. Cooper-DeHoff, R.M. et al., 2013. Calcium antagonists in the treatment of coronary artery disease. *Current Opinion in Pharmacology*, 13(2), pp.301–308.
39. Cooper, P.J. et al., 2010. Excitation-contraction coupling in human heart failure examined by action potential clamp in rat cardiac myocytes. *Journal of Molecular and Cellular Cardiology*, 49(6), pp.911–917.
40. Cruciani, P. et al., 1996. New cobalt-catalyzed cycloisomerization of  $\epsilon$ -acetylenic  $\beta$ -keto esters. Application to a powerful cyclization reactions cascade. *The Journal of Organic Chemistry*, 61(8), pp.2699–2708.
41. Cupka et al., 1987. Synthesis and spectral properties of substituted 1,4-dihydropyridines and 1,4,5,6,7,8-hexahydroquinolines. *Collection of Czechoslovak Chemical Communications*, 52, pp.742–751.



42. Dagnino, L. et al., 1986. Synthesis and calcium channel antagonist activity of dialkyl 1,4-dihydro-2,6-dimethyl-4-(pyridinyl)-3,5-pyridinedicarboxylates. *Journal of Medicinal Chemistry*, 29(12), pp.2524–2529.
43. Dagnino, L. et al., 1987. Synthesis and calcium channel antagonist activity of dialkyl hexahydro-1,2',6'-trimethyl[bipyridine]-3',5'-dicarboxylates. *European Journal of Medicinal Chemistry*, 22(6), pp.499-503.
44. Dahlof, B. et al., 2005. Prevention of cardiovascular events with an antihypertensive regimen of amlodipine adding perindopril as required versus atenolol adding bendroflumethiazide as required, in the Anglo-Scandinavian Cardiac Outcomes Trial-Blood Pressure Lowering Arm (ASCOT-B. *Lancet (London, England)*, 366(9489), pp.895–906.
45. Das, B. et al., 2006. An efficient one-pot synthesis of polyhydroquinolines at room temperature using hy-zeolite. *Chemical and Pharmaceutical Bulletin*, 54(7), pp.1044–1045.
46. Daschil, N. Et al., 2014. Nifedipine and nimodipine protect dopaminergic substantia nigra neurons against axotomy-induced cell death in rat vibrosections via modulating inflammatory responses. *Brain Research*, 1581, pp.1–11.
47. Dave, K. et al., 2011. An inhibitor-like binding mode of a carbonic anhydrase activator within the active site of isoform II. *Bioorganic and Medicinal Chemistry Letters*, 21(9), pp.2764–2768.
48. Debache, A. et al., 2009. An efficient one-step synthesis of 1,4-dihydropyridines via a triphenylphosphine-catalyzed three-component Hantzsch reaction under mild conditions. *Tetrahedron Letters*, 50(37), pp.5248–5250.
49. Dömling, A., 2006. Recent Developments in Isocyanide Based Multicomponent Reactions in Applied Chemistry. *Chemical Reviews*, 106(1), pp.17–89.
50. Dömling, A. et al., 2012. Chemistry and Biology Of Multicomponent Reactions. *Chemical Reviews*, 112(6), pp.3083–3135.
51. Dondoni, A. et al., 2004. Multicomponent Hantzsch cyclocondensation as a route to highly functionalized 2- and 4-dihydropyridylalanines, 2- and 4-pyridylalanines, and their N-oxides: preparation via a polymer-assisted solution-phase approach. *Tetrahedron*, 60(10), pp.2311–2326.
52. Donelson, J.L. et al., 2006. An efficient one-pot synthesis of polyhydroquinoline derivatives through the Hantzsch four component condensation. *Journal of Molecular Catalysis A: Chemical*, 256(1-2), pp.309–311.
53. Dubur, G.Y. et al., 1972. The oxidation of 1,4-dihydropyridines. *Chemistry of Heterocyclic Compounds*, 6(1), pp.80–84.
54. Duburs, G. et al., 2008. Dihydropyridine derivatives as bioprotectors. *Chimica Oggi*,

26(2), pp.68–70.

55. Dufes, C. et al., 2005. Dendrimers in gene delivery. *Advanced drug delivery reviews*, 57(15), pp.2177–2202.
56. Edraki, N. et al., 2009. Dihydropyridines: evaluation of their current and future pharmacological applications. *Drug discovery today*, 14(21–22), pp.1058–66.
57. Englert, C. et al., 2016. Crossing the blood-brain barrier: Glutathione-conjugated poly(ethylene imine) for gene delivery. *Journal of Controlled Release*, 241, pp.1–14.
58. Evans, C.G. et al., 2009. Enantioselective organocatalytic hantzsch synthesis of polyhydroquinolines. *Organic Letters*, 11(14), pp.2957–2959.
59. Evdokimov, N.M. et al., 2006. One-step, three-component synthesis of pyridines and 1,4-dihydropyridines with manifold medicinal utility. *Organic Letters*, 8(5), pp.899–902.
60. Fan, X. S. et al., 2006. A n efficient and green synthesis of 1 , 4-dihydropyridine derivatives through multi-component reaction in ionic liquid. *Heteroatom Chemistry*, 17(5), pp.382–388.
61. Faridi Esfanjani, A. et al., 2016. Biopolymer nano-particles and natural nano-carriers for nano-encapsulation of phenolic compounds. *Colloids and Surfaces B: Biointerfaces*, 146, pp.532–543.
62. Farouk, N. et al., 2016. Ecotoxicity of Pyridinium Based ILs Towards Guppy Fish and Four Bacterial Strains. *Procedia Engineering*, 0, pp.830–838.
63. Fernandes, M.A.S. et al., 2005. Cerebrocrast promotes the cotransport of H<sup>+</sup> and Cl<sup>-</sup> in rat liver mitochondria. *Mitochondrion*, 5(5), pp.341–351.
64. Fernandes, M.A.S. et al., 2009. Effects of 5-acetyl(carbamoyl)-6-methylsulfanyl-1,4-dihydropyridine-5-carbonitriles on rat liver mitochondrial function. *Toxicology in Vitro*, 23(7), pp.1333–1341.
65. Filipan-Litvić, M. et al., 2007. Hantzsch synthesis of 2,6-dimethyl-3,5-dimethoxycarbonyl-4-(o-methoxyphenyl)-1,4-dihydropyridine; a novel cyclisation leading to an unusual formation of 1-amino-2-methoxycarbonyl-3,5-bis(o-methoxyphenyl)-4-oxa-cyclohexan-1-ene. *Molecules*, 12(11), pp.2546–2558.
66. De Filippis, P. et al., 2002. Photodegradation studies on lacidipine in solution: basic experiments with a cis–trans reversible photoequilibrium under UV-A radiation exposure. *Journal of Pharmaceutical and Biomedical Analysis*, 27(5), pp.803–812.
67. Finkel, T. et al., 2000. Oxidants, oxidative stress and the biology of ageing. *Nature*, 408(6809), pp.239–247.
68. Fisicaro, E. et al., 2017. Nonviral gene-delivery by highly fluorinated gemini bispyridinium surfactant-based DNA nanoparticles. *Journal of Colloid and Interface Science*,

487, pp.182–191.

69. Fisicaro, E. et al., 2016. Solution Thermodynamics of highly fluorinated gemini bispyridinium surfactants for biomedical applications. *Colloids and Surfaces A: Physicochemical and Engineering Aspects*, 507, pp.236–242.
70. Fournier, A. et al., 2009. Prevention of dementia by antihypertensive drugs: how AT1-receptor-blockers and dihydropyridines better prevent dementia in hypertensive patients than thiazides and ACE-inhibitors. *Expert Review of Neurotherapeutics*, 9(9), pp.1413–1431.
71. Fox, H.H. et al., 1951. Derivatives of 1,3-dimethyl-2-azafluorene (1,3-dimethyl-9-indeno[2,1-c]pyridine). *The Journal of Organic Chemistry*, 16(8), pp.1259–1270.
72. Fujimoto, K. et al., 2006. Antimalarial effect of bis-pyridinium salts, N,N'-hexamethylenebis(4-carbamoyl-1-alkylpyridinium bromide). *Bioorganic and Medicinal Chemistry Letters*, 16(10), pp.2758–2760.
73. Gao, H., 2016. Progress and perspectives on targeting nanoparticles for brain drug delivery. *Acta Pharmaceutica Sinica B*, 6(4), pp.268–286.
74. Garaliene, V. et al., 2014. The role of external Ca(2)(+) in the action of Ca(2)(+)-channel agonists and antagonists on isolated human thoracic arteries. *Journal of physiology and pharmacology: an official journal of the Polish Physiological Society*, 65(1), pp.31–35.
75. Gati, W. et al., 2012. Intramolecular carbolithiation of n-allyl-ynamides: an efficient entry to 1,4-dihydropyridines and pyridines - application to a formal synthesis of sarizotan. *Beilstein Journal of Organic Chemistry*, 8, pp.2214–2222.
76. Ghosh, P.P. et al., 2013. Light induced synthesis of symmetrical and unsymmetrical dihydropyridines in ethyl lactate–water under tunable conditions. *Tetrahedron Letters*, 54(2), pp.138–142.
77. Grombe, R. et al., 2014. Production of reference materials for the detection and size determination of silica nanoparticles in tomato soup. *Analytical and Bioanalytical Chemistry*, 406(16), pp.3895–3907.
78. Guillena, G. et al., 2007. Organocatalytic enantioselective multicomponent reactions (OEMCRs). *Tetrahedron Asymmetry*, 18(6), pp.693–700.
79. Halliwell, B., 1996. Antioxidants in human health and disease. *Annual Review of Nutrition*, 16(1), pp.33–50.
80. Halliwell, B. et al., 1995. The definition and measurement of antioxidants in biological systems. *Free radical biology & medicine*, 18(1), pp.125–126.
81. Han, C. et al., 2014. DMAP-catalyzed four-component one-pot synthesis of highly functionalized spirooxindole-1,4-dihydropyridines derivatives in aqueous ethanol. *Tetrahedron*, 70(45), pp.8768–8774.

82. Hantzsch, A., 1882. Synthesis of pyridine derivatives from ethyl acetoacetate and aldehydammonia. *Liebigs Annalen der Chemie*, 215, pp.1–82.
83. Harel, D. et al., 2013. New combination of pharmacophoric elements of potent  $\sigma_1$  ligands: Design, synthesis and  $\sigma$  receptor affinity of aminoethyl substituted tetrahydrobenzothiophenes. *European Journal of Medicinal Chemistry*, 69, pp.490–497.
84. Harper, J.L. et al., 2003. Dihydropyridines as inhibitors of capacitative calcium entry in leukemic HL-60 cells. *Biochemical Pharmacology*, 65(3), pp.329–338.
85. Heydari, A. et al., 2009. One-step, synthesis of Hantzsch esters and polyhydroquinoline derivatives in fluoro alcohols. *Journal of Fluorine Chemistry*, 130(7), pp.609–614.
86. Hilgeroth, A. et al., 2003. Structure-activity relationships of first bishydroxymethyl-substituted cage dimeric 4-aryl-1,4-dihydropyridines as HIV-1 protease inhibitors. *European Journal of Medicinal Chemistry*, 38(5), pp.495–499.
87. Hyvönen, Z. et al., 2002. Extracellular and intracellular factors influencing gene transfection mediated by 1,4-dihydropyridine amphiphiles. *European Journal of Pharmaceutical Sciences*, 15(5), pp.449–460.
88. Hyvönen, Z. et al., 2000. Novel cationic amphiphilic 1,4-dihydropyridine derivatives for DNA delivery. *Biochimica et Biophysica Acta - Biomembranes*, 1509(1–2), pp.451–466.
89. Hjemdahl, P. et al., 2006. Favourable long term prognosis in stable angina pectoris: an extended follow up of the angina prognosis study in Stockholm (APSIS). *Heart (British Cardiac Society)*, 92(2), pp.177–182.
90. Hoffmann, S. et al., 2006. Catalytic asymmetric reductive amination of aldehydes via dynamic kinetic resolution. *Journal of American Chemical Society*, 128(40), pp.13074–13075.
91. Hong, M. et al., 2010. Hafnium (IV) bis(perfluorooctanesulfonyl)imide complex catalyzed synthesis of polyhydroquinoline derivatives via unsymmetrical Hantzsch reaction in fluoruous medium. *Journal of Fluorine Chemistry*, 131(1), pp.111–114.
92. Hu, D. et al., 2015. An organocatalytic multi-molecular cascade reaction for the synthesis of acetate functionalized 1,4-dihydropyridines. *Tetrahedron*, 71(36), pp.6094–6098.
93. Huang, Q. et al., 2010. Bioavailability and delivery of nutraceuticals using nanotechnology. *Journal of food science*, 75(1), pp.R50–7.
94. Yamamoto, T. et al., 2008. The structure-activity relationship study on 2-, 5-, and 6-position of the water soluble 1,4-dihydropyridine derivatives blocking N-type calcium channels. *Bioorganic & medicinal chemistry letters*, 18(17), pp.4813–4816.
95. Yang, J. et al., 2013. A clean procedure for the synthesis of 1,4-dihydropyridines via

- Hantzsch reaction in water. *Green Chemistry Letters and Reviews*, 6(3), pp.262–267.
96. Ilies, M.A. et al., 2006. Lipophilic pyrylium salts in the synthesis of efficient pyridinium-based cationic lipids, gemini surfactants, and lipophilic oligomers for gene delivery. *Journal of Medicinal Chemistry*, 49(13), pp.3872–3887.
97. Ioan, P. et al., 2011. 1,4-dihydropyridine scaffold in medicinal chemistry, the story so far and perspectives (part 1): action in ion channels and gpcrs. *Current Medicinal Chemistry*, 18(32), pp.4901–4922.
98. Yoshida, M. et al., 2007. Oligomeric electrolyte as a multifunctional gelator. *Journal of the American Chemical Society*, 129(36), pp.11039–11041.
99. Youdim, M.B.H. et al., 2005. Rasagiline: neurodegeneration, neuroprotection, and mitochondrial permeability transition. *Journal of neuroscience research*, 79(1–2), pp.172–179.
100. Isambert, N. et al., 2011. Multicomponent reactions and ionic liquids: a perfect synergy for eco-compatible heterocyclic synthesis. *Chemical Society Reviews*, 40(3), pp.1347–1357.
101. Ishiguro, S. et al., 2017. Combined local pulmonary and systemic delivery of AT2R gene by modified tat peptide nanoparticles attenuates both murine and human lung carcinoma xenografts in mice. *Journal of Pharmaceutical Sciences*, 106(1), pp.385–394.
102. Ismail, A. et al, 2004. Total antioxidant activity and phenolic content in selected vegetables. *Food Chemistry*, 87(4), pp.581–586.
103. Jayakumar, R. et al., 2010. Chitosan conjugated DNA nanoparticles in gene therapy. *Carbohydrate Polymers*, 79(1), pp.1–8.
104. Jansone, B. et al., 2015. A novel 1,4-dihydropyridine derivative improves spatial learning and memory and modifies brain protein expression in wild type and transgenic APPSweDI mice. *PloS one*, 10(6). DOI: 10.1371/journal.pone.0127686
105. Jansone, B. et al., 2016. Memory-enhancing and brain protein expression-stimulating effects of novel calcium antagonist in Alzheimer's disease transgenic female mice. *Pharmacological research*, 113(Pt B), pp.781–787.
106. Jee, J.-P. et al., 2012. Cancer targeting strategies in nanomedicine: Design and application of chitosan nanoparticles. *Current Opinion in Solid State and Materials Science*, 16(6), pp.333–342.
107. Jensen, B. et al. Chemical compounds having ion channel blocking activity for the treatment of immune dysfunction. 2002, (US 20020119989 A1).
108. Jiménez-Zamora, A. et al., 2016. Antioxidant capacity, total phenols and color profile during the storage of selected plants used for infusion. *Food Chemistry*, 199, pp.339–346.

109. Juncai, T. et al., 2001. One step synthesis of 4-aryl polyhydroquinoline derivatives using microwave irradiation. *Chin. J. Org. Chem.*, 21(4), pp.313–316.
110. Khairy, M. et al., 2017. Sensitive determination of amlodipine besylate using bare/unmodified and DNA-modified screen-printed electrodes in tablets and biological fluids. *Sensors and Actuators B: Chemical*, 239, pp.768–775.
111. Khan, A.T. et al., 2011. Sequential three-component reactions: synthesis, regioselectivity and application of functionalized dihydropyridines (DHPs) for the creation of fused naphthyridines. *Tetrahedron Letter*, 52(27), pp.3455–3459.
112. Khosravani, H. Et al., 2006. Voltage-gated calcium channels and idiopathic generalized epilepsies. *Physiological reviews*, 86(3), pp.941–966.
113. Klusa, V., 2016. Atypical 1,4-dihydropyridine derivatives, an approach to neuroprotection and memory enhancement. *Pharmacological Research*, 113, pp.754–759.
114. Ko, S. et al., 2005. Molecular iodine-catalyzed one-pot synthesis of 4-substituted-1,4-dihydropyridine derivatives via Hantzsch reaction. *Tetrahedron Letters*, 46(34), pp.5771–5774.
115. Koo, H. et al., 2011. In vivo targeted delivery of nanoparticles for theranosis. *Accounts of Chemical Research*, 44(10), pp.1018–1028.
116. Koo, H. et al., 2011. Nanoprobes for biomedical imaging in living systems. *Nano Today*, 6(2), pp.204–220.
117. Kouřimská, L. et al., 1993. The antioxidant activity of 2,6-dimethyl-3,5-diethoxycarbonyl-1,4-dihydropyridine in edible oils. *Food/Nahrung*, 37(1), pp.91–93.
118. Krauze, A. et al., 2015. Synthesis of polysubstituted pyridines as potential multidrug resistance modulators. *Heterocyclic Communications*, 21, p.93.
119. Krauze, A. et al., 2014. Thieno[2,3-b]pyridines: A new class of multidrug resistance (MDR) modulators. *Bioorganic & Medicinal Chemistry*, 22(21), pp.5860–5870.
120. Kumar, A. et al., 2007a. Bakers' yeast catalyzed synthesis of polyhydroquinoline derivatives via an unsymmetrical Hantzsch reaction. *Tetrahedron Letters*, 48(22), pp.3887–3890.
121. Kumar, A. et al., 2008. Organocatalysed three-component domino synthesis of 1,4-dihydropyridines under solvent free conditions. *Tetrahedron*, 64(16), pp.3477–3482.
122. Kumar, A. et al., 2007b. Synthesis of polyhydroquinoline derivatives through unsymmetric Hantzsch reaction using organocatalysts. *Tetrahedron*, 63(9), pp.1946–1952.
123. Kumar, A. et al., 2011. A grinding-induced catalyst- and solvent-free synthesis of highly functionalized 1,4-dihydropyridines via a domino multicomponent reaction. *Green Chemistry*, 13(8), pp.2017–2020.

124. Kumar, R. et al., 2014. Multicomponent diversity-oriented synthesis of symmetrical and unsymmetrical 1,4-dihydropyridines in recyclable glycine nitrate (GlyNO<sub>3</sub>) ionic liquid: a mechanistic insight using Q-TOF, ESI-MS/MS. *RSC Advances*, 4(37), pp.19111–19121.
125. Kumar, S. et al., 2008. An efficient, catalyst- and solvent-free, four-component, and one-pot synthesis of polyhydroquinolines on grinding. *Tetrahedron*, 64(3), pp.536–542.
126. De la Calle, I. et al., 2016. Current trends and challenges in sample preparation for metallic nanoparticles analysis in daily products and environmental samples: A review. *Spectrochimica Acta Part B: Atomic Spectroscopy*, 125, pp.66–96.
127. Lakshmanan, V.-K. et al., 2011. Chitosan-based nanoparticles in cancer therapy. *Chitosan for Biomaterials I*, 243, pp. 55–91.
128. Leo, M. et al., 2017. Cisplatin-induced neuropathic pain is mediated by upregulation of N-type voltage-gated calcium channels in dorsal root ganglion neurons. *Experimental Neurology*, 288, pp.62–74.
129. Li, G. et al., 2009. Highly enantioselective hydrogenation of enamides catalyzed by chiral phosphoric acids. *Organic Letters*, 11(5), pp.1075–1078.
130. Li, M. et al., 2008. Microwave-assisted combinatorial synthesis of hexa-substituted 1,4-dihydropyridines scaffolds using one-pot two-step multicomponent reaction followed by a S-alkylation. *Journal of Combinatorial Chemistry*, 10(3), pp.436–441.
131. Li, Z. et al., 2015. The inhibition of high-voltage-activated calcium current by activation of MrgC11 involves phospholipase C-dependent mechanisms. *Neuroscience*, 300, pp.393–403.
132. Liao, P. et al., 2010. CaV1.2 channelopathies: From arrhythmias to autism, bipolar disorder, and immunodeficiency. *Pflugers Archiv European Journal of Physiology*, 460(2), pp.353–359.
133. Liepin'sh, E. et al., 1989. <sup>13</sup>C-NMR spectra of substituted 1,4-dihydropyridines. *Chemistry of Heterocyclic Compounds*, 25(9), pp.1032–1037.
134. Liu, J. et al., 2012. Methods for separation, identification, characterization and quantification of silver nanoparticles. *TrAC Trends in Analytical Chemistry*, 33, pp.95–106.
135. Liu, L. et al., 2013. Sc(OTf)<sub>3</sub>-catalyzed three-component cyclization of arylamines, β,γ-unsaturated α-ketoesters, and 1,3-dicarbonyl compounds for the synthesis of highly substituted 1,4-dihydropyridines and tetrahydropyridines. *The Journal of Organic Chemistry*, 78(11), pp.5751–5755.
136. Loev, B. et al., 1965. The Hantzsch Reaction. I. Oxidative Dealkylation of Certain Dihydropyridines. *The Journal of Organic Chemistry*, 30(6), pp.1914–1916.
137. De Luca, M. et al., 2016. Photostabilization studies of antihypertensive 1,4-

dihydropyridines using polymeric containers. *International Journal of Pharmaceutics*, 505(1), pp.376–382.

138. Ma, N. et al., 2010. New multicomponent domino reactions (MDRs) in water: highly chemo-, regio- and stereoselective synthesis of spiro{[1,3]dioxanopyridine}-4,6-diones and pyrazolo[3,4-b]pyridines. *Green Chemistry*, 12(8), pp.1357–1361.

139. Maafi, W. et al., 2013. Modelling nifedipine photodegradation, photostability and actinometric properties. *International Journal of Pharmaceutics*, 456(1), pp.153–164.

140. Maheswara, M. et al., 2006. An efficient one-pot synthesis of polyhydroquinoline derivatives via Hantzsch condensation using a heterogeneous catalyst under solvent-free conditions. *Arkivoc*, 2006(2), pp.201–206.

141. Makarova, N. V et al., 1995. Synthesis of 1,4-dihydropyridines having an N-alkylpyridinium substituent at the 4-position and their affinity towards liposomal membranes. *Chemistry of Heterocyclic Compounds*, 31(8), pp.969–973.

142. Makarova, N. V et al., 1997. Some transformations of N-ethoxycarbonylmethylpyridinium bromides with a pyridyl or 1,4-dihydropyridyl substituent at position 3. *Chemistry of Heterocyclic Compounds*, 33(2), pp.175–183.

143. Mamusa, M. et al., 2016. Interaction between a cationic bolaamphiphile and DNA: The route towards nanovectors for oligonucleotide antimicrobials. *Colloids and Surfaces B: Biointerfaces*, 143, pp.139–147.

144. Marger, L. et al., 2011. Pacemaker activity and ionic currents in mouse atrioventricular node cells. *Channels (Austin, Tex.)*, 5(3), pp.241–250.

145. Marinkovic, V.D. et al., 2003. Photochemical degradation of solid-state nisoldipine monitored by HPLC. *Journal of Pharmaceutical and Biomedical Analysis*, 32(4), pp.929–935.

146. Meekel, A.A.P. et al., 2000. Synthesis of pyridinium amphiphiles used for transfection and some characteristics of amphiphile/DNA complex formation. *European Journal of Organic Chemistry*, 2000(4), pp.665–673.

147. Mehrnia, M.-A. et al., 2016. Crocin loaded nano-emulsions: Factors affecting emulsion properties in spontaneous emulsification. *International Journal of Biological Macromolecules*, 84, pp.261–267.

148. Mekheimer, R.A. et al., 2008. Solar thermochemical reactions: four-component synthesis of polyhydroquinoline derivatives induced by solar thermal energy. *Green Chemistry*, 10(5), pp.592–593.

149. Menon, J.U. et al., 2013. Nanomaterials for photo-based diagnostic and therapeutic applications. *Theranostics*, 3(3), pp.152–166.



150. Miyazaki, H. et al., 1999. Neuroprotective effects of a dihydropyridine derivative, 1,4-dihydro-2,6-dimethyl-4-(3-nitrophenyl)-3,5-pyridinedicarboxylic acid methyl 6-(5-phenyl-3-pyrazolyloxy)hexyl ester (CV-159), on rat ischemic brain injury. *Life Sciences*, 64(10), pp.869–878.
151. Mohammadi, A. et al., 2016. Nano-encapsulation of olive leaf phenolic compounds through WPC–pectin complexes and evaluating their release rate. *International Journal of Biological Macromolecules*, 82, pp.816–822.
152. Najafi-Hajivar, S. et al., 2016. Overview on experimental models of interactions between nanoparticles and the immune system. *Biomedicine and Pharmacotherapy*, 83, pp.1365–1378.
153. Nandi, G.C. et al., 2010. Biginelli and Hantzsch-type reactions leading to highly functionalized dihydropyrimidinone, thiocoumarin, and pyridopyrimidinone frameworks via ring annulation with  $\beta$ -oxodithioesters. *The Journal of Organic Chemistry*, 75(22), pp.7785–7795.
154. Nasr-Esfahani, M. et al., 2014. Magnetic Fe<sub>3</sub>O<sub>4</sub> nanoparticles: Efficient and recoverable nanocatalyst for the synthesis of polyhydroquinolines and Hantzsch 1,4-dihydropyridines under solvent-free conditions. *Journal of Molecular Catalysis A: Chemical*, 382, pp.99–105.
155. Neethirajan, S. et al., 2011. Nanotechnology for the Food and Bioprocessing Industries. *Food and Bioprocess Technology*, 4(1), pp.39–47.
156. Neumaier, F. et al., 2015. Voltage-gated calcium channels: Determinants of channel function and modulation by inorganic cations. *Progress in Neurobiology*, 129, pp.1–36.
157. Newman, M.D. et al., 2009. The safety of nanosized particles in titanium dioxide– and zinc oxide–based sunscreens. *Journal of the American Academy of Dermatology*, 61(4), pp.685–692.
158. Niwa, T. et al., 1995. Species and sex differences of testosterone and nifedipine oxidation in liver microsomes of rat, dog and monkey. *Xenobiotica*, 25(10), pp.1041–1049.
159. Noipa, T. et al., 2011. New approach for evaluation of the antioxidant capacity based on scavenging DPPH free radical in micelle systems. *Food Research International*, 44(3), pp.798–806.
160. Omnis, V. et al., 2009. Synthesis and evaluation of anticancer activity of 2-arylamino-6-trifluoromethyl-3-(hydrazonocarbonyl)pyridines. *Bioorganic & Medicinal Chemistry*, 17(17), pp.6158–6165.
161. Onoue, S. et al., 2008. In vitro phototoxicity of dihydropyridine derivatives: A photochemical and photobiological study. *European Journal of Pharmaceutical Sciences*,

33(3), pp.262–270.

162. Pajuste, K. et al., 2011. Effect of the solvent nature on the course of quaternization of 3,5-diethoxycarbonyl-2,6-dimethyl-4-(3-pyridyl)-1,4-dihydropyridine. *Chemistry of Heterocyclic Compounds*, 47(5), p.597.

163. Pajuste, K. et al., 2013. Gene delivery agents possessing antiradical activity: self-assembling cationic amphiphilic 1,4-dihydropyridine derivatives. *New Journal of Chemistry*, 37(10), p.3062.

164. Pajuste, K. et al., 2011. Use of pyridinium ionic liquids as catalysts for the synthesis of 3,5-bis(dodecyloxycarbonyl)-1,4-dihydropyridine derivative. *Central European Journal of Chemistry*, 9(1), pp.143–148.

165. Palmisano, G. et al., 2011. Ultrasound-enhanced one-pot synthesis of 3-(Het)arylmethyl-4-hydroxycoumarins in water. *Ultrasonics Sonochemistry*, 18(2), pp.652–660.

166. Pape, V.F.S. et al., 2015. Synthesis and characterization of the anticancer and metal binding properties of novel pyrimidinylhydrazone derivatives. *Journal of Inorganic Biochemistry*, 144, pp.18–30.

167. Paris, D. et al., 2011. Selective antihypertensive dihydropyridines lower A $\beta$  accumulation by targeting both the production and the clearance of A $\beta$  across the blood-brain barrier. *Molecular Medicine*, 17(3–4), pp.149–162.

168. Parvizi, P. et al., 2014. Aspects of nonviral gene therapy: Correlation of molecular parameters with lipoplex structure and transfection efficacy in pyridinium-based cationic lipids. *International Journal of Pharmaceutics*, 461(1), pp.145–156.

169. Paszko, E. et al., 2011. Nanodrug applications in photodynamic therapy. *Photodiagnosis and Photodynamic Therapy*, 8(1), pp.14–29.

170. Pedemonte, N. et al., 2007. Structure-Activity Relationship of 1,4-Dihydropyridines as Potentiators of the Cystic Fibrosis Transmembrane Conductance Regulator Chloride Channel. *Molecular Pharmacology*, 72(1), pp.197–207.

171. Peng, S. et al., 2017. Hybrid liposomes composed of amphiphilic chitosan and phospholipid: Preparation, stability and bioavailability as a carrier for curcumin. *Carbohydrate Polymers*, 156, pp.322–332.

172. Petrichenko, O. et al., 2015. Studies of the physicochemical and structural properties of self-assembling cationic pyridine derivatives as gene delivery agents. *Chemistry and Physics of Lipids*, 191, pp.25–37.

173. Pijper, D. et al., 2003. Novel Biodegradable Pyridinium Amphiphiles for Gene Delivery. *European Journal of Organic Chemistry*, 2003(22), pp.4406–4412.

174. Praveena, K.S.S. et al., 2015. Design of new hybrid template by linking quinoline, triazole and dihydroquinoline pharmacophoric groups: A greener approach to novel polyazaheterocycles as cytotoxic agents. *Bioorganic & medicinal chemistry letters*, 25(5), pp.1057-1063.
175. Priede, E. et al., 2015. One-pot three-component synthesis of hantzsch 1,4-dihydropyridines promoted by dimethyl phosphate ionic liquids. *Helvetica Chimica Acta*, 98(8), pp.1095–1103.
176. Prieto, P. et al., 1999. Spectrophotometric quantitation of antioxidant capacity through the formation of a phosphomolybdenum complex: specific application to the determination of vitamin E. *Analytical Biochemistry*, 269(2), pp.337–341.
177. Procházková, D. et al., 2011. Antioxidant and prooxidant properties of flavonoids. *Fitoterapia*, 82(4), pp.513–523.
178. Puri, A. et al., 2011. Polymeric Lipid Assemblies as Novel Theranostic Tools. *Accounts of Chemical Research*, 44(10), pp.1071–1079.
179. Qiu, X.-Y. et al., 2016. The inhibitory effects of nifedipine on outward voltage-gated potassium currents in mouse neuroblastoma N2A cells. *Pharmacological Reports*, 68(3), pp.631–637.
180. Raei, M. et al., 2015. Nano-encapsulation of isolated lactoferrin from camel milk by calcium alginate and evaluation of its release. *International Journal of Biological Macromolecules*, 79, pp.669–673.
181. Ragno, G. et al., 2003. Design and monitoring of photostability systems for amlodipine dosage forms. *International Journal of Pharmaceutics*, 265(1), pp.125–132.
182. Rea, J.C. et al., 2009. Self-assembling peptide–lipoplexes for substrate-mediated gene delivery. *Acta biomaterialia*, 5(3), pp.903–912.
183. Reddy, C.S. et al., 2008. Cerium(IV) ammonium nitrate catalysed facile and efficient synthesis of polyhydroquinoline derivatives through Hantzsch multicomponent condensation. *Chinese Chemical Letters*, 19(7), pp.775–779.
184. Rezvanian, A., 2016. An expedient synthesis strategy to the 1,4-dihydropyridines and pyrido[1,2-a]quinoxalines: iodine catalyzed one-pot four-component domino reactions. *Tetrahedron*, 72(41), pp.6428–6435.
185. Riahi, A. et al., 2009. Synthesis and antimicrobial activity of 4-hydroxy-4-(pyridyl)alk-3-en-2-ones. *Bioorganic & Medicinal Chemistry*, 17(13), pp.4323–4326.
186. Ritz, B. et al., 2010. L-type calcium channel blockers and parkinson disease in Denmark. *Annals of Neurology*, 67(5), pp.600–606.
187. Roosjen, A. et al., 2002. Synthesis and characteristics of biodegradable pyridinium

- amphiphiles used for in vitro DNA delivery. *European Journal of Organic Chemistry*, 2002(7), pp.1271–1277.
188. Rosenberg, S.H. et al., 1991. Design of a well-absorbed renin inhibitor. *Journal of Medicinal Chemistry*, 34(1), pp.469–471.
189. Rucins, M. et al., 2015. Evaluation of antiradical activity and reducing capacity of synthesised bispyridinium dibromides obtained by quaternisation of 4-pyridyl-1,4-dihydropyridines with propargyl bromide. *Australian Journal of Chemistry*, 68(1), pp.86–92.
190. Rucins, M. et al., 2015. Synthesis and evaluation of reducing capacity and calcium channel blocking activity of novel 3,5-dipropargylcarbonyl-substituted 1,4-dihydropyridines. *Chemistry of Heterocyclic Compounds*, 50(10), pp.1431–1442.
191. Rucins, M. et al., 2014. Synthesis and studies of calcium channel blocking and antioxidant activities of novel 4-pyridinium and/or N-propargyl substituted 1,4-dihydropyridine derivatives. *Comptes Rendus Chimie*, 17(1), pp.69–80.
192. Rucins, M. et al., 2013. Studies of preparation and stability of liposomes formed by 1,1'-[(3,5-didodecylloxycarbonyl-4-phenyl-1,4-dihydropyridine-2,6-diyl)-dimethylen]bispyridinium dibromide. *Advanced Materials Research*, 787, pp.157–162.
193. Rudler, H. et al., 2008. Lactonizations of carboxylic acid-substituted 3-fluorodihydropyridines with electrophiles: peculiar behaviour of F<sup>+</sup>. *Chemical Communications*, (35), pp.4150–4152.
194. Rumaks, J. et al., 2012. Search for stroke-protecting agents in endothelin-1-induced ischemic stroke model in rats. *Medicina (Lithuania)*, 48(10), pp.525–531.
195. Sabitha, G. et al., 2003. A novel TMSI-mediated synthesis of Hantzsch 1,4-dihydropyridines at ambient temperature. *Tetrahedron Letters*, 44(21), pp.4129–4131.
196. Safari, J. et al., 2011. Cellulose sulfuric acid catalyzed multicomponent reaction for efficient synthesis of 1,4-dihydropyridines via unsymmetrical Hantzsch reaction in aqueous media. *Journal of Molecular Catalysis A: Chemical*, 335(1), pp.46–50.
197. Safari, J. et al., 2013. A magnetic nanoparticle supported Ni<sup>2+</sup>-containing ionic liquid as an efficient nanocatalyst for the synthesis of Hantzsch 1,4-dihydropyridines in a solvent-free dry-system. *RSC Advances*, 3(48), pp.26094–26101.
198. Sapkal, S.B. et al., 2009. Nickel nanoparticle-catalyzed facile and efficient one-pot synthesis of polyhydroquinoline derivatives via Hantzsch condensation under solvent-free conditions. *Tetrahedron Letters*, 50(15), pp.1754–1756.
199. Lo Scalzo, R., 2008. Organic acids influence on DPPH scavenging by ascorbic acid. *Food Chemistry*, 107(1), pp.40–43.
200. Schade, D. et al., 2012. Synthesis and SAR of b-annulated 1,4-dihydropyridines define

- cardiomyogenic compounds as novel inhibitors of TGFβ signaling. *Journal of medicinal chemistry*, 55(22), pp.9946–9957.
201. Schmaunz, C.E. et al., 2014. Inter- and intramolecular [4+2]-cycloaddition reactions with 4,4-disubstituted N-silyl-1,4-dihydropyridines as precursors for N-protonated 2-azabutadiene intermediates. *Synthesis (Germany)*, 46(12), pp.1630–1638.
202. Shaaban, A. et al., 2014. Synthesis of pyrido- and pyrimido-fused heterocycles by multi-component reactions (Part 3). *Current Organic Synthesis*, 11(6), pp.835–873.
203. Shamsara, O. et al., 2015. Effect of ultrasonication, pH and heating on stability of apricot gum–lactoglobuline two layer nanoemulsions. *International Journal of Biological Macromolecules*, 81, pp.1019–1025.
204. Shan, R. et al., 2004. Syntheses, calcium channel agonist-antagonist modulation activities, and nitric oxide release studies of nitrooxyalkyl 1,4-dihydro-2,6-dimethyl-3-nitro-4-(2,1,3-benzoxadiazol-4-yl)pyridine-5-carboxylate racemates, enantiomers, and diastereomers. *Journal of medicinal chemistry*, 47(1), pp.254–261.
205. Sharma, V.D. et al., 2013. Interfacial engineering of pyridinium gemini surfactants for the generation of synthetic transfection systems. *Biomaterials*, 34(28), pp.6906–6921.
206. Shekari, F. et al., 2015. Cytotoxic and multidrug resistance reversal activities of novel 1,4-dihydropyridines against human cancer cells. *European Journal of Pharmacology*, 746, pp.233–244.
207. Shen, L. et al., 2010. K<sub>2</sub>CO<sub>3</sub>-assisted one-pot sequential synthesis of 2-trifluoromethyl-6-difluoromethylpyridine-3,5-dicarboxylates under solvent-free conditions. *Tetrahedron Letters*, 51(37), pp.4866–4869.
208. Shiri, M., 2012. Indoles in multicomponent processes (MCPs). *Chemical Reviews*, 112(6), pp.3508–3549.
209. Simon, K.C. et al., 2010. Calcium channel blocker use and risk of Parkinson's disease. *Movement disorders: official journal of the Movement Disorder Society*, 25(12), pp.1818–1822.
210. Singh, R. et al., 2009. Nanoparticle-based targeted drug delivery. *Experimental and Molecular Pathology*, 86(3), pp.215–223.
211. Singh, R.K. et al., 2015. Hybrid pharmacophore-based drug design, synthesis, and antiproliferative activity of 1,4-dihydropyridines-linked alkylating anticancer agents. *Medicinal Chemistry Research*, 24(4), pp.1534–1545.
212. Singh, S.K. et al., 2010. Glycine-catalyzed easy and efficient one-pot synthesis of polyhydroquinolines through hantzsch multicomponent condensation under controlled microwave. *Journal of Heterocyclic Chemistry*, 47(1), pp.194–198.

213. Sirisha, K. et al., 2011. Synthesis, antibacterial and antimycobacterial activities of some new 4-aryl/heteroaryl-2,6-dimethyl-3,5-bis-N-(aryl)-carbamoyl-1,4-dihydropyridines. *European Journal of Medicinal Chemistry*, 46(5), pp.1564–1571.
214. Skrastin'sh, I.P. et al., 1991. Bromination of 4-aryl-3,5-dialkoxycarbonyl-2,6-dimethyl-1,4-dihydropyridines. *Chemistry of Heterocyclic Compounds*, 27(9), pp.989–994.
215. Slavoff, S.A. et al., 2012. Discovering ligand-receptor interactions. *Nat Biotech*, 30(10), pp.959–961.
216. Song, G. et al., 2005. Montmorillonite K10 clay: an effective solid catalyst for one-pot synthesis of polyhydroquinoline derivatives. *Synthetic Communications*, 35(22), pp.2875–2880.
217. Srikanth, M. et al., 2012. Nanotechnology[mdash]novel therapeutics for CNS disorders. *Nat Rev Neurol*, 8(6), pp.307–318.
218. Staben, S.T. et al., 2010. Four-component synthesis of fully substituted 1,2,4-triazoles. *Angewandte Chemie (International ed. in English)*, 49(2), pp.325–328.
219. Stout, D.M. et al., 1982. Recent advances in the chemistry of dihydropyridines. *Chemical Reviews*, 82(2), pp.223–243.
220. Suárez, M. et al., 1999. A joint experimental and theoretical structural study of novel substituted 2,5-dioxo-1,2,3,4,5,6,7,8-octahydroquinolines. *Tetrahedron*, 55(3), pp.875–884.
221. Sun, J. et al., 2011. Selective synthesis of fused 1,4- and 1,2-dihydropyridines by domino reactions of arylamines, acetylenedicarboxylate, aldehydes, and cyclic 1,3-diketones. *European Journal of Organic Chemistry*, 2011(34), pp.6952–6956.
222. Sunderhaus, J.D. & Martin, S.F., 2009. Applications of multicomponent reactions to the synthesis of diverse heterocyclic scaffolds. *Chemistry (Weinheim an der Bergstrasse, Germany)*, 15(6), pp.1300–1308.
223. Tacke et al., 1983. Sila-pharmaca, XXV. Sila-analogues of nifedipine-like dialkyl 2,6-dimethyl-4-aryl-1,4 dihydropyridine-3,5-dicarboxylates, III. *European Journal of Medicinal Chemistry*, 18(2), pp.155–161.
224. Tamaddon, F. et al., 2010. Synthesis of 3,4-dihydropyrimidin-2(1H)-ones and 1,4-dihydropyridines using ammonium carbonate in water. *Tetrahedron Letters*, 51(8), pp.1187–1189.
225. Tenti, G. et al., 2013. Identification of 4,6-diaryl-1,4-dihydropyridines as a new class of neuroprotective agents. *Medicinal Chemical Communications*, 4(3), pp.590–594.
226. Tirzite, D. et al., 1998. Influence of some quaternised 1,4-dihydropyridine derivatives on liposomes and erythrocyte membranes. *Biochemistry and molecular biology international*, 45(4), pp.849–856.

227. Tiwari, S. et al., 2015. Pharmacology, Efficacy and Safety of Felodipine with a Focus on Hypertension and Angina Pectoris. *Current Drug Safety*, 10(3), pp.194–201.
228. Topel, Ö. et al., 2013. Determination of critical micelle concentration of polybutadiene-block-poly(ethyleneoxide) diblock copolymer by fluorescence spectroscopy and dynamic light scattering. *Journal of Molecular Liquids*, 177, pp.40–43.
229. Tottene, A. et al., 2011. Role of different voltage-gated Ca<sup>2+</sup> channels in cortical spreading depression: specific requirement of P/Q-type Ca<sup>2+</sup> channels. *Channels (Austin, Tex.)*, 5(2), pp.110–114.
230. Touré, B.B. et al., 2009. Natural product synthesis using multicomponent reaction strategies. *Chemical Reviews*, 109(9), pp.4439–4486.
231. Triggle, D.J., 2003a. 1,4-dihydropyridines as calcium channel ligands and privileged structures. *Cellular and Molecular Neurobiology*, 23(3), pp.293–303.
232. Triggle, D.J., 2007. Calcium channel antagonists: Clinical uses—Past, present and future. *Biochemical Pharmacology*, 74(1), pp.1–9.
233. Triggle, D.J., 2003b. The 1,4-dihydropyridine nucleus: a pharmacophoric template part 1. Actions at ion channels. *Mini-Reviews in Medicinal Chemistry*, 3(3), pp.215–223.
234. Triggle, D.J. et al., 1989. 1,4-Dihydropyridine activators and antagonists: structural and functional distinctions. *Trends in Pharmacological Sciences*, 10(12), pp.507–511.
235. Vance, M.E. et al., 2015. Nanotechnology in the real world: Redeveloping the nanomaterial consumer products inventory. *Beilstein Journal of Nanotechnology*, 6, pp.1769–1780.
236. Vicente-García, E. et al., 2010. Unsaturated lactams: New inputs for Povarov-type multicomponent reactions. *Organic Letters*, 12(4), pp.860–863.
237. Wan, J.-P. et al., 2013. A “byproduct-intermediate-product” recycling strategy for multicomponent synthesis of 1,4-dihydropyridines. *RSC Advances*, 3(7), pp.2477–2482.
238. Wan, J.-P. et al., 2012. Recent advances in new multicomponent synthesis of structurally diversified 1,4-dihydropyridines. *RSC Advances*, 2(26), p.9763.
239. Wang, J.L. et al., 2011. *Candida antarctica* lipase B-catalyzed the unprecedented three-component Hantzsch-type reaction of aldehyde with acetamide and 1,3-dicarbonyl compounds in non-aqueous solvent. *Tetrahedron*, 67(14), pp.2689–2692.
240. Wang, L.-M. et al., 2005. Facile Yb(OTf)<sub>3</sub> promoted one-pot synthesis of polyhydroquinoline derivatives through Hantzsch reaction. *Tetrahedron*, 61(6), pp.1539–1543.
241. Wang, L.-S., et al., 2012. Nanotheranostics--a review of recent publications. *International journal of nanomedicine*, 7, pp.4679–4695.

242. Wang, P.Y. et al., 2016. Synthesis and antibacterial activity of pyridinium-tailored 2,5-substituted-1,3,4-oxadiazole thioether/sulfoxide/sulfone derivatives. *Bioorganic and Medicinal Chemistry Letters*, 26(4), pp.1214–1217.
243. Ward, N.C. et al., 2004. Oxidative stress in human hypertension: Association with antihypertensive treatment, gender, nutrition, and lifestyle. *Free Radical Biology and Medicine*, 36(2), pp.226–232.
244. Weinreb, O. et al., 2010. Rasagiline: A novel anti-Parkinsonian monoamine oxidase-B inhibitor with neuroprotective activity. *Progress in Neurobiology*, 92(3), pp.330–344.
245. Wen, L.-R. et al., 2010. Modulating the reactivity of heterocyclic ketene amins in mcr: selective construction of tetrahydrobenzo[b]imidazo[3,2,1-ij][1,8]naphthyridines. *The Journal of Organic Chemistry*, 75(22), pp.7605–7614.
246. Whyte, I., Buckley, N. & Dawson, A., 2016. Calcium channel blockers. *Medicine*, 44(3), pp.148–150.
247. Wiley, R. & Irick, G., 1961. Notes. 4[N, N-Bis(2-haloethyl)amino]benzaldehyde Derivatives. *The Journal of Organic Chemistry*, 26(2), pp.593–595.
248. Wollinger, A. et al., 2016. Antioxidant activity of hydro distillation water residues from *Rosmarinus officinalis* L. leaves determined by DPPH assays. *Comptes Rendus Chimie*, 19(6), pp.754–765.
249. Zamponi, G.W. et al., 2013. Regulation of Cav2 calcium channels by G protein coupled receptors. *Biochimica et Biophysica Acta (BBA) - Biomembranes*, 1828(7), pp.1629–1643.
250. Zanchetti, A., 2003. Emerging data on calcium-channel blockers: The COHORT study. *Clinical Cardiology*, 26(2 SUPPL.), pp.II17–II20.
251. Zapotoczny, S. et al., 2015. Nanoparticles in endothelial theranostics. *Pharmacological Reports*, 67(4), pp.751–755.
252. Zhang, D.Y. et al., 2015. Recent advances in copper-catalyzed propargylic substitution. *Tetrahedron Letters*, 56(2), pp.283–295.
253. Zhang, X. et al., 2016. Tumor targeting strategies for chitosan-based nanoparticles. *Colloids and Surfaces B: Biointerfaces*, 148, pp.460–473.
254. Zhao, X. et al., 2011. Molecular architecture of Ca<sup>2+</sup> signaling control in muscle and heart cells. *Channels (Austin, Tex.)*, 5(5), pp.391–396.
255. Zhao, Z. et al., 2005. Alkylation of  $\alpha$ -methylnaphthalene with long-chain alkenes catalyzed by butylpyridinium bromochloroaluminate ionic liquids. *Journal of Molecular Catalysis A: Chemical*, 231(1–2), pp.137–143.



## APPENDIX

## **Publication**

### **A**

Studies of the physicochemical and structural properties of self-assembling cationic pyridine derivatives as gene delivery agents.

*Chem. Phys. Lip.*, 2015, 191, 25-37.



## Studies of the physicochemical and structural properties of self-assembling cationic pyridine derivatives as gene delivery agents



Oksana Petrichenko<sup>a,b</sup>, Martins Rucins<sup>a</sup>, Aleksandra Vezane<sup>c</sup>, Irena Timofejeva<sup>c</sup>, Arkadij Sobolev<sup>a</sup>, Brigita Cekavicus<sup>a</sup>, Karlis Pajuste<sup>a</sup>, Mara Plotniece<sup>a</sup>, Marina Gosteva<sup>a</sup>, Tatjana Kozlovska<sup>c</sup>, Aiva Plotniece<sup>a,\*</sup>

<sup>a</sup> Latvian Institute of Organic Synthesis, Aizkraukles str. 21, Riga LV-1006, Latvia

<sup>b</sup> Laboratory of Magnetic Soft Matter, Department of Physics, University of Latvia, Zellu str. 8, Riga LV-1002, Latvia

<sup>c</sup> Latvian Biomedical Research and Study centre, Ratsupites str. 1, Riga LV-1067, Latvia

### ARTICLE INFO

#### Article history:

Received 18 June 2015

Received in revised form 5 August 2015

Accepted 6 August 2015

Available online 10 August 2015

#### Keywords:

Self-assembling pyridines

Synthetic lipids

Thermogravimetric analysis

Liposomes

Dynamic light scattering

DNA delivery

### ABSTRACT

New amphiphilic pyridine derivatives containing dodecyloxycarbonyl substituents at positions 3 and 5 and cationic moieties at positions 2 and 6 have been designed and synthesised. Compounds of this type can be considered as synthetic lipids. The corresponding 1,4-dihydropyridine (1,4-DHP) derivatives have earlier been proposed as a promising tool for plasmid DNA (pDNA) delivery in vitro. In this work studies of the self-assembling properties of amphiphilic pyridine derivatives leading to the formation of liposomes, determination of particle size, zeta-potential and critical micelle concentration (CMC) with dynamic light scattering (DLS) measurements are described. Furthermore, thermal analysis of pyridine derivatives was performed using thermogravimetry analysis (TGA) and differential thermal analysis (DTA) as well as the ability to deliver the pEGFP-C1 plasmid DNA (that encodes GFP reporter) into the Baby hamster kidney-derived (BHK-21) cell line was used for evaluation of gene delivery properties. We have revealed that the new pyridine derivatives possessed self-assembling properties which were proved by formation of nanoparticles with the average size from 115 to 743 nm, the zeta-potentials in the range of 48–79 mV and CMC values in the range of 2–67  $\mu$ M. DTA data showed that all processes were endothermic for all compounds. Additionally, we established that among the tested pyridines the representatives with *N*-methylpyrrolidinium or pyridinium moieties as cationic head-group at the positions 2 and 6 possessed higher pEGFP-C1 transfection activity into the BHK-21 cell line. Nevertheless, the obtained results indicated that correlation of the physicochemical, structural properties and gene delivery activities of the tested compounds were not completely elucidated yet. On the other hand, the synthesised pyridines as possible metabolites of promising delivery systems on the 1,4-DHP core possessed lower pDNA transfection activity than the corresponding 1,4-DHP amphiphiles.

© 2015 Elsevier Ireland Ltd. All rights reserved.

### 1. Introduction

Gene therapy relies on successful delivery of therapeutic DNA into the nuclei of target cells. The first successful in vitro delivery of DNA by liposome-mediated gene transfer was demonstrated in 1980 (Fraleigh et al., 1980). Based on these initial findings, the search and studies for optimal delivery agents have been continued into various directions. However, understanding of structure–activity relationships (SAR) is limited despite the development of an important number of non-viral delivery systems varying in chemical functionalisation of molecules and compositions of

reagents (van Gaal et al., 2011). Over the past decades, development of new non-viral vectors as gene delivery systems and liposomal drug delivery systems has resulted in elaboration of various nanopharmaceutical applications and become a competitive field for different research groups. Interest is growing towards the design of synthetic cationic lipid-like compounds as potential drug and gene delivery agents for transfer of genetic materials including high molecular weight DNA molecules into cells (Felgner et al., 1987) and for diagnostic applications (Marqués-Gallego and de Kroon, 2014). These lipid-like delivery systems are relatively non-toxic and non-immunogenic, moreover it is easy to use and produce them on a large scale (Al-Dosari and Gao, 2009; Guo and Huang, 2012; Lasic and Templeton, 1996; Margus et al., 2012; Rea et al., 2009).

\* Corresponding author.

E-mail address: [aiva@osi.lv](mailto:aiva@osi.lv) (A. Plotniece).

Lipoplexes formation of cationic non-viral vectors with negatively charged DNA is an important requirement for successful gene delivery. Molecular structure, the shape and thermal stability of liposome forming compounds, their zeta-potential, particle size, critical micelle concentration (CMC) have been found to be important factors influencing their self-assembling and DNA complexation properties, and subsequent gene delivery activity (Aravindan et al., 2009; Lv et al., 2006). Therefore, it is highly important to understand the correlations between structural, physicochemical and DNA transporting properties for different groups of non-viral vectors.

Previously, our group has developed and studied multiple cationic 1,4-dihydropyridine (1,4-DHP) amphiphiles (Fig. 1), which were capable of transfecting plasmid DNA (pDNA) into different cell lines in vitro (Hyvonen et al., 2000; Pajuste et al., 2013).

Variation of alkyl chain lengths at positions 3 and 5 and the amount of cationic moieties in the 1,4-DHP scaffold have been performed at the beginning of our studies. After which we have concluded that two cationic moieties at positions 2 and 6 as well as dodecyloxycarbonyl substituents at positions 3 and 5 were optimal for these kinds of synthetic lipid-like compounds. Thus, 1,1'-[(3,5-bis(dodecyloxycarbonyl)-4-phenyl-1,4-dihydropyridine-2,6-diyl)dimethylen]-bispyridinium dibromide (1,4-DHP amphiphile **1a**, Fig. 1) was found to be more active among the tested 1,4-DHP amphiphiles (Hyvonen et al., 2000). The next step of these studies involved modification of the substituents at the cationic head-group of the amphiphilic 1,4-DHP molecule. After these studies it was established that the electronic nature of the substituent of the pyridinium moieties as the cationic head-group of the 1,4-DHP derivatives strongly affected the ability of these compounds to bind pDNA and transfer it into the cells. In this way, we have demonstrated that compounds with electron-donating substituents at para- or meta-position of the above mentioned groups (1,4-DHP amphiphiles **1b** and **c**, Fig. 1) showed high gene transfection efficacy (Pajuste et al., 2013). Obtained data showed that the novel 1,4-DHP amphiphiles **1a–c** appeared to be more active than commercially available cationic lipid DOTAP (*N*-(1-(2,3-dioleoyloxy) propyl)-*N,N,N*-trimethyl ammonium methylsulfate) and cationic polymer PEI 25 (polyethyleneimine of 25 kDa). For example, at the charge ratio 2 the transfection efficiency of 1,4-DHP amphiphile **1a** was about 5 times better than that of DOTAP and 45 times more effective than that of PEI 25 (Pajuste et al., 2013). Some basic structure–activity relationships have been already found for cationic 1,4-DHP derivatives as gene delivery systems and shown how the chemical structure affected self-assembling properties, pDNA binding ability and properties of formed 1,4-DHP amphiphile–pDNA complexes (Hyvonen et al., 2000; Pajuste et al., 2013). It would be beneficial for more profound SAR conclusions to continue studies on the influence of oxidised forms of cationic 1,4-DHP derivatives on the mentioned activities and characterisation of physicochemical properties of the corresponding cationic pyridine compounds.

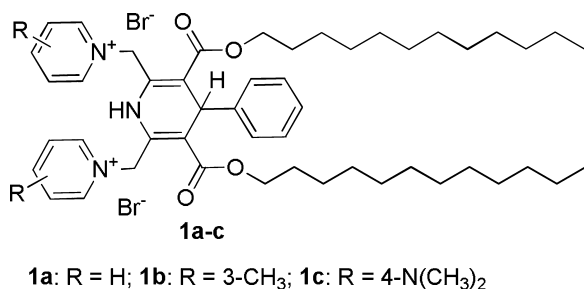


Fig. 1. Structures of cationic 1,4-dihydropyridine amphiphiles **1a–c** (Hyvonen et al., 2000; Pajuste et al., 2013).

Encouraged by these results, we have decided to obtain a novel group of delivery agents based on amphiphilic pyridine derivatives containing dodecyloxycarbonyl substituents at positions 3 and 5 and cationic moieties at positions 2 and 6, which would be structurally closely related to the most efficient 1,4-DHP derivative for pDNA delivery (1,4-DHP amphiphile **1a**, Fig. 1). Additionally, the self-assembling properties such as particle size, zeta-potential, critical micelle concentration of the synthesised pyridine derivatives were characterised by dynamic light scattering (DLS) measurements. The thermal analysis of liposome forming cationic compounds was performed using thermogravimetry analysis (TGA) and differential thermal analysis (DTA). The ability to deliver pEGFP-C1 plasmid DNA (that encodes GFP reporter) into the Baby hamster kidney-derived (BHK-21) cell line was used as a test for evaluation of gene delivery properties of lipid-like pyridine derivatives **6a–g**.

Characterisation of physicochemical properties of amphiphiles and understanding of the structure–activity relationships of these carriers in cells is essential for further improving design and functionality in order to develop new delivery systems using non-viral lipid-like compounds.

## 2. Materials and methods

### 2.1. General

<sup>1</sup>H and <sup>13</sup>C NMR spectra were recorded on a Varian Mercury BB (400 and 100.56 MHz, respectively) spectrometer. The chemical shifts of the atoms are reported in parts per million (ppm) relative to the residual signals of the solvent: DMSO-d<sub>6</sub> (δ 2.50 ppm) or CDCl<sub>3</sub> (δ 7.26 ppm) for <sup>1</sup>H NMR spectra and DMSO-d<sub>6</sub> (δ 39.5 ppm) or CDCl<sub>3</sub> (δ 77.2 ppm) for <sup>13</sup>C NMR spectra. Multiplicities are abbreviated as s, singlet; d, doublet; t, triplet; q, quartet; m, multiplet; dd, doublet of doublets; br, broad. The coupling constants are expressed in Hertz. Mass spectra were obtained on a Waters Acquity UPLC system connected to Waters SQ Detector-2 operating in the ESI positive ion mode on Waters Acquity UPLC<sup>®</sup> BEH C18 column (1.7 μm, 2.1 × 50 mm) using a gradient elution with acetonitrile (0.01% CF<sub>3</sub>COOH) in water (0.01% CF<sub>3</sub>COOH) at a flow rate 0.5 mL/min and processed with Waters MassLynx 4.1 chromatography data system. Elemental analyses were determined on an Elemental Combustion System ECS 4010 (Costech Instruments). Melting points were determined on a SRS OptiMelt system (SRS Stanford Research Systems). The compounds were analysed by HPLC on a Waters Alliance 2695 system equipped with Waters 2485 UV–vis detector and Alltima CN column (5 μm, 4.6 × 150 mm, Grace) using gradient elution with acetonitrile (0.1% H<sub>3</sub>PO<sub>4</sub>) in water, at a flow rate of 1 mL/min. Peak areas were determined electronically with Waters Empower 2 chromatography data system. TLC was performed on Silica gel 60 F<sub>254</sub> aluminium sheets 20 × 20 cm (Merck), spots were visualised with UV light (254 and 365 nm).

All chemical reagents were purchased from Acros, AlfaAesar or Sigma–Aldrich and used without further purification.

### 2.2. Synthesis

#### 2.2.1. Synthesis of compounds **2** and **5**

The 3,5-bis(dodecyloxycarbonyl)-2,6-dimethyl-4-phenyl-1,4-dihydropyridine (**2**) was obtained from acetoacetic acid dodecyl ester, benzaldehyde and ammonia via classical Hantzsch synthesis according to the already reported method (Hyvonen et al., 2000). The bromination of 2,6-methyl groups of compound **2** was performed with NBS according to the reported method giving 2,6-bis(bromomethyl)-3,5-bis(dodecyloxycarbonyl)-4-phenyl-1,4-dihydropyridine (**5**) (Pajuste et al., 2011). <sup>1</sup>H and <sup>13</sup>C NMR spectra

data of compounds **2** and **5** were identical to those reported in the literature (Pajuste et al., 2011).

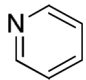
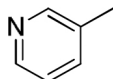
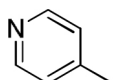
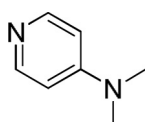
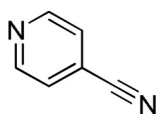
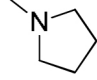
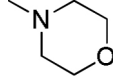
### 2.2.2. 2,6-Dimethyl-4-phenyl-pyridine-3,5-dicarboxylic acid didodecyl ester (**3**)

To the solution of 3,5-bis(dodecyloxycarbonyl)-2,6-dimethyl-4-phenyl-1,4-dihydropyridine (**2**) (0.20 g, 0.33 mmol) in glacial acetic acid (25 mL) sodium nitrite (0.05 g, 0.73 mmol) was added in several portions during 10 min, after which the reaction mixture was refluxed for 1 h. The resulting mixture was poured into ice water (30 mL) and extracted with  $\text{CHCl}_3$  ( $3 \times 20$  mL). The combined organic extracts were washed with water (20 mL) and brine, dried over  $\text{MgSO}_4$  and the solvent was removed in vacuo to give the product **3** as a yellowish oil (0.15 g, 75%).  $^1\text{H NMR}$  ( $\text{CDCl}_3$ ,  $\delta$ ): 0.88 (t, 6H,  $J=6.7$  Hz, 3,5- $\text{CH}_3$ ); 1.00–1.08 (m, 4H, 3,5- $\text{CH}_2\text{CH}_3$ ); 1.13–1.34 (m, 36H, 3,5- $(\text{CH}_2)_9$ ); 2.60 (s, 6H, 2,6- $\text{CH}_3$ ); 3.92 (t, 4H,  $J=6.7$  Hz, 3,5- $\text{OCH}_2$ ); 7.24–7.27 (m, 2H, 2,6-H 4-Ar); 7.33–7.37 (m, 3H, 3,4,5-H 4-Ar).  $^{13}\text{C NMR}$  ( $\text{CDCl}_3$ ,  $\delta$ ): 14.9; 23.4; 23.5; 26.4; 28.8; 29.9; 30.1; 30.2; 30.3; 30.4; 30.5; 32.7; 66.4; 127.9; 128.8; 128.9; 129.3; 133.5; 137.3; 156.0; 168.7. MS (+ESI)  $m/z$  (relative intensity) 608 ( $[\text{M}]^+$ , 100%). Anal. calcd for  $\text{C}_{39}\text{H}_{61}\text{NO}_4 \times \text{H}_2\text{O}$ : C, 74.84; H, 10.14; N, 2.24; found: C, 74.97; H, 9.99; N, 2.37.

### 2.2.3. 2,6-Bis(bromomethyl)-4-phenyl-pyridine-3,5-dicarboxylic acid didodecyl ester (**4**)

2,6-Bis(bromomethyl)-3,5-bis(dodecyloxycarbonyl)-4-phenyl-1,4-dihydropyridine (**5**) (0.50 g, 0.65 mmol) was dissolved in acetic acid (100 mL) at 45 °C, after which heating was discontinued and sodium nitrite (0.10 g, 2.22 mmol) was added in several portions during 10 min. The reaction mixture was stirred at room temperature for 2 h, then was poured into ice water (150 mL). After being stirred for the next 1 h the reaction mixture was extracted with  $\text{CHCl}_3$  ( $3 \times 30$  mL), the combined organic phase was washed with water ( $2 \times 20$  mL), dried over  $\text{MgSO}_4$  and evaporated. The residue was triturated with ethyl acetate–hexane mixture, giving the product **4** as a yellowish solid (0.56 g, 72%); mp 43–45 °C.  $^1\text{H NMR}$  ( $\text{CDCl}_3$ ,  $\delta$ ): 0.88 (t, 6H,  $J=6.7$  Hz, 3,5- $\text{CH}_3$ ); 0.98–1.06 (m, 4H, 3,5- $\text{CH}_2\text{CH}_3$ ); 1.10–1.32 (m, 36H, 3,5- $(\text{CH}_2)_9$ ); 3.94 (t, 4H,  $J=6.7$  Hz, 3,5- $\text{OCH}_2$ ); 4.69 (s, 4H, 2,6- $\text{CH}_2$ ); 7.24–7.29 (m, 2H, 2,6-H 4-Ar); 7.36–7.40 (m, 3H, 3,4,5-H 4-Ar).  $^{13}\text{C NMR}$  ( $\text{CDCl}_3$ ,  $\delta$ ): 14.3; 22.8; 25.8; 28.1; 29.2; 29.5; 29.6; 29.7; 29.8; 29.9; 30.7; 32.1; 66.3; 128.1; 128.5; 129.1; 129.4; 136.1; 148.4; 154.8; 166.7. MS (+ESI)  $m/z$  (relative intensity) 764 ( $2 \times ^{79}\text{Br}$ ), 766 ( $^{79}\text{Br}$  and  $^{81}\text{Br}$ ), 768 ( $2 \times ^{81}\text{Br}$ ) ( $[\text{M}]^+$ ), 51/100/49%. Anal. calcd for  $\text{C}_{39}\text{H}_{59}\text{Br}_2\text{NO}_4$ : C, 61.18; H, 7.77; N, 1.83; found: C, 61.29; H, 7.82; N, 1.77.

**Table 1**  
Structure, yield of pyridine derivatives **6a–g** and reaction time of the synthesis.

Entry	Comp.	Het	Formula	$\text{H}_2\text{O}$ cont. (%)	Yield (%)	Reaction time (days)
1	<b>6a</b>		$\text{C}_{49}\text{H}_{69}\text{Br}_2\text{N}_3\text{O}_4 \times \text{H}_2\text{O}$	1.9	58	3
2	<b>6b</b>		$\text{C}_{51}\text{H}_{73}\text{Br}_2\text{N}_3\text{O}_4 \times 2\text{H}_2\text{O}$	3.6	49	5
3	<b>6c</b>		$\text{C}_{51}\text{H}_{73}\text{Br}_2\text{N}_3\text{O}_4 \times 2\text{H}_2\text{O}$	3.6	55	2
4	<b>6d</b>		$\text{C}_{53}\text{H}_{79}\text{Br}_2\text{N}_5\text{O}_4 \times 2\text{H}_2\text{O}$	3.4	58	1
5	<b>6e</b>		$\text{C}_{51}\text{H}_{67}\text{Br}_2\text{N}_5\text{O}_4 \times \text{H}_2\text{O}$	3.7	25	5 <sup>a</sup>
6	<b>6f</b>		$\text{C}_{49}\text{H}_{81}\text{Br}_2\text{N}_3\text{O}_4 \times 2\text{H}_2\text{O}$	3.7	60	1
7	<b>6g</b>		$\text{C}_{49}\text{H}_{81}\text{Br}_2\text{N}_3\text{O}_6 \times \text{H}_2\text{O}$	1.8	83	2

<sup>a</sup> During last 2 days reaction was performed at 50 °C.

#### 2.2.4. General method for the synthesis of compounds **6a–g**

To a solution of 2,6-bis(bromomethyl)-4-phenyl-pyridine-3,5-dicarboxylic acid didodecyl ester (**4**) (0.10 g, 0.13 mmol) in acetone (10 mL), the corresponding N-containing heterocyclic compound (0.26 mmol) was added. The resulting mixture was stirred at room temperature until monitoring by TLC indicated that all of the starting material had disappeared after 1–5 days (Table 1). After cooling until 0 °C the precipitate was filtered off, washed with acetone, recrystallised from methanol and dried in vacuo.

#### 2.2.5. 1,1'-((3,5-Bis(dodecyloxycarbonyl)-4-phenylpyridine-2,6-diyl)bis(methylene))bis(pyridin-1-ium)dibromide (**6a**)

Yield: 58%; mp 158–160 °C. <sup>1</sup>H NMR (CDCl<sub>3</sub>, δ): 0.87 (t, 6H, J = 7.0 Hz, 3,5-CH<sub>3</sub>); 1.03–1.31 (m, 40H, 3,5-(CH<sub>2</sub>)<sub>10</sub>); 3.99 (t, 4H, J = 7.0 Hz, 3,5-OCH<sub>2</sub>); 6.37 (s, 4H, 2,6-CH<sub>2</sub>); 7.17–7.20 (m, 2H, 2,6-H 4-Ar); 7.39–7.41 (m, 3H, 3,4,5-H 4-Ar); 8.23 (dd, 4H, J = 7.8 and 5.8 Hz, 3-H Py); 8.73 (t, 2H, J = 7.8 Hz, 4-H Py); 9.37 (d, 4H, J = 5.8 Hz, 2-H Py). <sup>13</sup>C NMR (CDCl<sub>3</sub>, δ): 14.2; 22.8; 25.6; 27.9; 29.3; 29.5; 29.6; 29.7; 29.8; 29.9; 32.0; 62.2; 67.5; 127.8; 128.8; 128.9; 129.4; 129.5; 135.9; 146.3; 146.7; 149.8; 150.9; 166.2. MS (+ESI) *m/z* (relative intensity) 878 (<sup>79</sup>Br) ([M-2Br + CF<sub>3</sub>COOH]<sup>+</sup>, 5%; 382 ([M-2Br]<sup>+</sup>/2, 100%). Anal. calcd for C<sub>49</sub>H<sub>69</sub>Br<sub>2</sub>N<sub>3</sub>O<sub>4</sub> × H<sub>2</sub>O: C, 62.48; H, 7.60; N, 4.46; found: C, 62.21; H, 7.67; N, 4.40.

#### 2.2.6. 1,1'-((3,5-Bis(dodecyloxycarbonyl)-4-phenylpyridine-2,6-diyl)bis(methylene))bis(3-methylpyridin-1-ium)dibromide (**6b**)

Yield: 49%; mp 162–164 °C. <sup>1</sup>H NMR (CDCl<sub>3</sub>, δ): 0.87 (t, 6H, J = 6.9 Hz, 3,5-CH<sub>3</sub>); 1.05–1.31 (m, 40H, 3,5-(CH<sub>2</sub>)<sub>10</sub>); 2.68 (s, 6H, β-CH<sub>3</sub>-Py); 3.96 (t, 4H, J = 6.9 Hz, 3,5-OCH<sub>2</sub>); 6.37 (s, 4H, 2,6-CH<sub>2</sub>); 7.18–7.21 (m, 2H, 2,6-H 4-Ar); 7.40–7.43 (m, 3H, 3,4,5-H 4-Ar); 8.08 (dd, 2H, J = 8.0 and 6.2 Hz, 5-H Py); 8.33 (d, 2H, J = 8.0 Hz, 4-H Py); 9.25 (s, 2H, 2-H Py); 9.47 (d, 2H, J = 6.2 Hz, 6-H Py). <sup>13</sup>C NMR (CDCl<sub>3</sub>, δ): 13.2; 18.9; 22.5; 25.3; 27.5; 28.9; 29.1; 29.2; 29.3; 29.4; 29.5; 31.7; 61.4; 67.1; 127.4; 127.8; 128.5; 129.1; 129.4; 135.6; 139.6; 143.7; 144.9; 146.4; 149.5; 150.7; 166.2. MS (+ESI) *m/z* (relative intensity) 906 (<sup>79</sup>Br) ([M-2Br + CF<sub>3</sub>COOH]<sup>+</sup>, 5%; 396 ([M-2Br]<sup>+</sup>/2, 100%). Anal. calcd for C<sub>51</sub>H<sub>73</sub>Br<sub>2</sub>N<sub>3</sub>O<sub>4</sub> × 2H<sub>2</sub>O: C, 62.00; H, 7.86; N, 4.25; found: C, 62.17; H, 7.69; N, 4.19.

#### 2.2.7. 1,1'-((3,5-Bis(dodecyloxycarbonyl)-4-phenylpyridine-2,6-diyl)bis(methylene))bis(4-methylpyridin-1-ium)dibromide (**6c**)

Yield: 55%; mp 180–182 °C. <sup>1</sup>H NMR (CDCl<sub>3</sub>, δ): 0.86 (t, 6H, J = 7.0 Hz, 3,5-CH<sub>3</sub>); 1.02–1.30 (m, 40H, 3,5-(CH<sub>2</sub>)<sub>10</sub>); 2.72 (s, 6H, γ-CH<sub>3</sub>-Py); 3.95 (t, 4H, J = 7.0 Hz, 3,5-OCH<sub>2</sub>); 6.30 (s, 4H, 2,6-CH<sub>2</sub>); 7.13–7.19 (m, 2H, 2,6-H 4-Ar); 7.37–7.42 (m, 3H, 3,4,5-H 4-Ar); 7.93 (d, 4H, J = 6.7 Hz, 3,5-H Py); 9.33 (d, 4H, J = 6.7 Hz, 2,6-H Py). <sup>13</sup>C NMR (CDCl<sub>3</sub>, δ): 14.2; 22.8; 25.6; 27.8; 29.2; 29.3; 29.4; 29.5; 29.6; 29.7; 29.8; 32.0; 61.3; 67.4; 127.7; 128.8; 129.2; 129.4; 129.8; 135.8; 145.2; 149.8; 151.1; 160.2; 166.4. MS (+ESI) *m/z* (relative intensity) 906 (<sup>79</sup>Br) ([M-2Br + CF<sub>3</sub>COOH]<sup>+</sup>, 8%; 396 ([M-2Br]<sup>+</sup>/2, 100%). Anal. calcd for C<sub>51</sub>H<sub>73</sub>Br<sub>2</sub>N<sub>3</sub>O<sub>4</sub> × 2H<sub>2</sub>O: C, 62.00; H, 7.86; N, 4.25; found: C, 62.08; H, 7.66; N, 4.32.

#### 2.2.8. 1,1'-((3,5-Bis(dodecyloxycarbonyl)-4-phenylpyridine-2,6-diyl)bis(methylene))bis(4-(dimethylamino)pyridin-1-ium)dibromide (**6d**)

Yield: 58%; mp 200–202 °C. <sup>1</sup>H NMR (CDCl<sub>3</sub>, δ): 0.86 (t, 6H, J = 7.1 Hz, 3,5-CH<sub>3</sub>); 1.03–1.28 (m, 40H, 3,5-(CH<sub>2</sub>)<sub>10</sub>); 3.33 (s, 12H, 4-N(CH<sub>3</sub>)<sub>2</sub> Py); 3.91 (t, 4H, J = 7.1 Hz, 3,5-OCH<sub>2</sub>); 5.69 (s, 4H, 2,6-CH<sub>2</sub>); 7.07 (d, 4H, J = 7.4 Hz, 3,5-H Py); 7.16–7.19 (m, 2H, 2,6-H 4-Ar); 7.37–7.42 (m, 3H, 3,4,5-H 4-Ar); 8.49 (d, 4H, J = 7.4 Hz, 2,6-H Py). <sup>13</sup>C NMR (CDCl<sub>3</sub>, δ): 14.2; 22.8; 25.6; 27.9; 29.2; 29.4; 29.5; 29.6; 29.7; 29.8; 32.0; 40.9; 58.8; 67.1; 108.7; 127.8; 128.7; 129.0; 129.3; 135.9; 143.3; 149.2; 152.3; 156.7; 166.5. MS (+ESI) *m/z* (relative intensity) 964 (<sup>79</sup>Br) ([M-2Br + CF<sub>3</sub>COOH]<sup>+</sup>, 10%; 425 ([M-2Br]<sup>+</sup>/2, 100%). Anal.

calcd for C<sub>53</sub>H<sub>79</sub>Br<sub>2</sub>N<sub>5</sub>O<sub>4</sub> × 2H<sub>2</sub>O: C, 60.85; H, 8.00; N, 6.69; found: C, 60.79; H, 7.86; N, 6.54.

#### 2.2.9. 1,1'-((3,5-Bis(dodecyloxycarbonyl)-4-phenylpyridine-2,6-diyl)bis(methylene))bis(4-cyanopyridin-1-ium)dibromide (**6e**)

Yield: 25%; mp 211–213 °C. <sup>1</sup>H NMR (CDCl<sub>3</sub>, δ): 0.88 (t, 6H, J = 6.8 Hz, 3,5-CH<sub>3</sub>); 1.05–1.30 (m, 40H, 3,5-(CH<sub>2</sub>)<sub>10</sub>); 4.01 (t, 4H, J = 6.8 Hz, 3,5-OCH<sub>2</sub>); 6.56 (s, 4H, 2,6-CH<sub>2</sub>); 7.16–7.19 (m, 2H, 2,6-H 4-Ar); 7.38–7.42 (m, 3H, 3,4,5-H 4-Ar); 8.74 (d, 4H, J = 6.7 Hz, 3,5-H Py); 9.88 (d, 4H, J = 6.7 Hz, 2,6-H Py). <sup>13</sup>C NMR (CDCl<sub>3</sub>, δ): 14.0; 22.5; 25.3; 27.6; 28.9; 29.1; 29.2; 29.4; 29.5; 29.6; 31.7; 62.6; 67.4; 114.2; 127.5; 128.4; 128.5; 129.2; 130.0; 131.3; 135.4; 147.6; 149.8; 150.0; 165.8. MS (+ESI) *m/z* (relative intensity) 814 (<sup>79</sup>Br) ([M-2Br]<sup>+</sup>, 18%; 407 ([M-2Br]<sup>+</sup>/2, 100%). Anal. calcd for C<sub>51</sub>H<sub>67</sub>Br<sub>2</sub>N<sub>5</sub>O<sub>4</sub> × H<sub>2</sub>O: C, 61.75; H, 7.01; N, 7.06; found: C, 61.76; H, 6.83; N, 6.99.

#### 2.2.10. 1,1'-((3,5-Bis(dodecyloxycarbonyl)-4-phenylpyridine-2,6-diyl)bis(methylene))bis(1-methylpyrrolidin-1-ium)dibromide (**6f**)

Yield: 60%; mp 201–202 °C. <sup>1</sup>H NMR (CDCl<sub>3</sub>, δ): 0.86 (t, 6H, J = 6.9 Hz, 3,5-CH<sub>3</sub>); 1.02–1.28 (m, 40H, 3,5-(CH<sub>2</sub>)<sub>10</sub>); 2.21–2.45 (m, 8H, β-CH<sub>2</sub>-pyrrolidine); 3.31 (s, 6H, N-CH<sub>3</sub>); 3.86 (t, 4H, J = 6.9 Hz, 3,5-OCH<sub>2</sub>); 4.16–4.30 (m, 8H, α-CH<sub>2</sub>-pyrrolidine); 5.51 (s, 4H, 2,6-CH<sub>2</sub>); 7.16–7.20 (m, 2H, 2,6-H 4-Ar); 7.40–7.44 (m, 3H, 3,4,5-H 4-Ar). <sup>13</sup>C NMR (CDCl<sub>3</sub>, δ): 14.5; 21.8; 23.1; 25.9; 28.1; 29.5; 29.7; 29.8; 30.0; 30.1; 30.2; 32.3; 49.8; 64.4; 66.6; 67.7; 128.0; 129.2; 129.8; 132.6; 136.0; 149.1; 150.0; 167.0. MS (+ESI) *m/z* (relative intensity) 890 (<sup>79</sup>Br) ([M-2Br + CF<sub>3</sub>COOH]<sup>+</sup>, 13%; 388 ([M-2Br]<sup>+</sup>/2, 100%). Anal. calcd for C<sub>49</sub>H<sub>81</sub>Br<sub>2</sub>N<sub>3</sub>O<sub>4</sub> × 2H<sub>2</sub>O: C, 60.55; H, 8.81; N, 4.32; found: C, 60.41; H, 8.65; N, 4.30.

#### 2.2.11. 4,4'-((3,5-Bis(dodecyloxycarbonyl)-4-phenylpyridine-2,6-diyl)bis(methylene))bis(4-methylmorpholin-4-ium)dibromide (**6g**)

Yield: 83%; mp 200–202 °C. <sup>1</sup>H NMR (CDCl<sub>3</sub>, δ): 0.87 (t, 6H, J = 7.0 Hz, 3,5-CH<sub>3</sub>); 1.03–1.29 (m, 40H, 3,5-(CH<sub>2</sub>)<sub>10</sub>); 3.65 (s, 6H, N-CH<sub>3</sub>); 3.92 (t, 4H, J = 7.0 Hz, 3,5-OCH<sub>2</sub>); 4.03–4.19 (m, 12H, morpholine); 4.28–4.33 (m, 4H, morpholine); 5.53 (s, 4H, 2,6-CH<sub>2</sub>); 7.19–7.22 (m, 2H, 2,6-H 4-Ar); 7.40–7.45 (m, 3H, 3,4,5-H 4-Ar). <sup>13</sup>C NMR (CDCl<sub>3</sub>, δ): 14.6; 23.1; 25.9; 28.1; 29.5; 29.7; 29.8; 29.9; 30.0; 30.1; 30.2; 32.3; 48.6; 61.4; 62.2; 68.1; 128.2; 129.3; 130.0; 133.7; 135.7; 147.8; 150.5; 166.8. MS (+ESI) *m/z* (relative intensity) 922 (<sup>79</sup>Br) ([M-2Br + CF<sub>3</sub>COOH]<sup>+</sup>, 10%; 404 ([M-2Br]<sup>+</sup>/2, 100%). Anal. calcd for C<sub>49</sub>H<sub>81</sub>Br<sub>2</sub>N<sub>3</sub>O<sub>6</sub> × H<sub>2</sub>O: C, 59.69; H, 8.48; N, 4.26; found: C, 60.02; H, 8.38; N, 4.28.

### 2.3. Thermal analysis

Thermogravimetric (TG) and differential thermal analysis (DTA) were performed with SHIMADZU DTG-60 instrument in Ar atmosphere (Ar 5.0 from AGA Ltd.) with flow 50 mL/min at temperature range from 25 °C till 150 °C with heating rate 5 °C/min for compounds **1a**, **6a–d**, **6f** and **6g** and 2 °C/min for pyridine **6e**. Data files were transformed into an ASCII file format for further analysis by TA60 ver 2.10 software (Shimadzu Corporation, Japan).

### 2.4. Self-assembling properties

Samples for dynamic light scattering (DLS) studies were prepared by dispersing compounds in an aqueous solution at a concentration 0.5 mg/mL for compounds **1a**, **6a–d**, **6f** and **6g**, and 0.1 mg/mL for pyridine **6e** by sonication using a bath type sonicator (Cole Parmer Ultrasonic Cleaner 8891CPX (USA)). Samples were sonicated for 60 min at 60 °C.

## 2.5. Dynamic light scattering

The DLS measurements of the nanoparticles in an aqueous solution formed by compounds **1a**, **6a–d**, **6f** and **6g** at a concentration 0.5 mg/mL and for pyridine **6e**—0.1 mg/mL were carried out on a Zetasizer Nano ZSP instrument with Malvern Instruments Ltd. software 7.10. The zeta-potentials were determined via DLS measurements using a above mentioned Zetasizer apparatus with the following specifications: medium: water; refractive index: 1.590; viscosity: 0.8872 cP; temperature: 25 °C; dielectric constant: 78.5. Nanoparticles: liposomes; refractive index of materials: 1.60. A detection angle of 173°, a wavelength of 633 nm. Data were analysed using multimodal number distribution software included with the instrument. The measurements were repeated three times in order to check their reproducibility.

The critical micelle concentrations (CMC) were determined in aqueous media using a Zetasizer Nano ZSP instrument with Malvern Instruments Ltd. software 7.10 by procedure described by Topel et al (Topel et al., 2013). Briefly, a series of solutions of compound with concentrations ranging from 0.5 mg/mL to  $0.1 \times 10^{-2}$  mg/mL were prepared from a stock solution of compounds obtained as described above, and beginning concentration for pyridine **6e**—0.1 mg/mL. All next samples were prepared starting from the concentrated stock solution, which was subjected to a serial two-fold dilution each time with water. The intensity values of scattered light (kcps) as a function of concentration of

compounds were analysed. The scattering intensities detected for compound concentrations below CMC have an approximately constant value corresponding to water. The intensity starts to show a linear increase with concentration at the CMC, since the amount of nanoparticles increases in the solution. The intersection of the best fit lines drawn through the data points is the preliminary CMC value of compounds. The measurements were repeated three times in order to check their reproducibility.

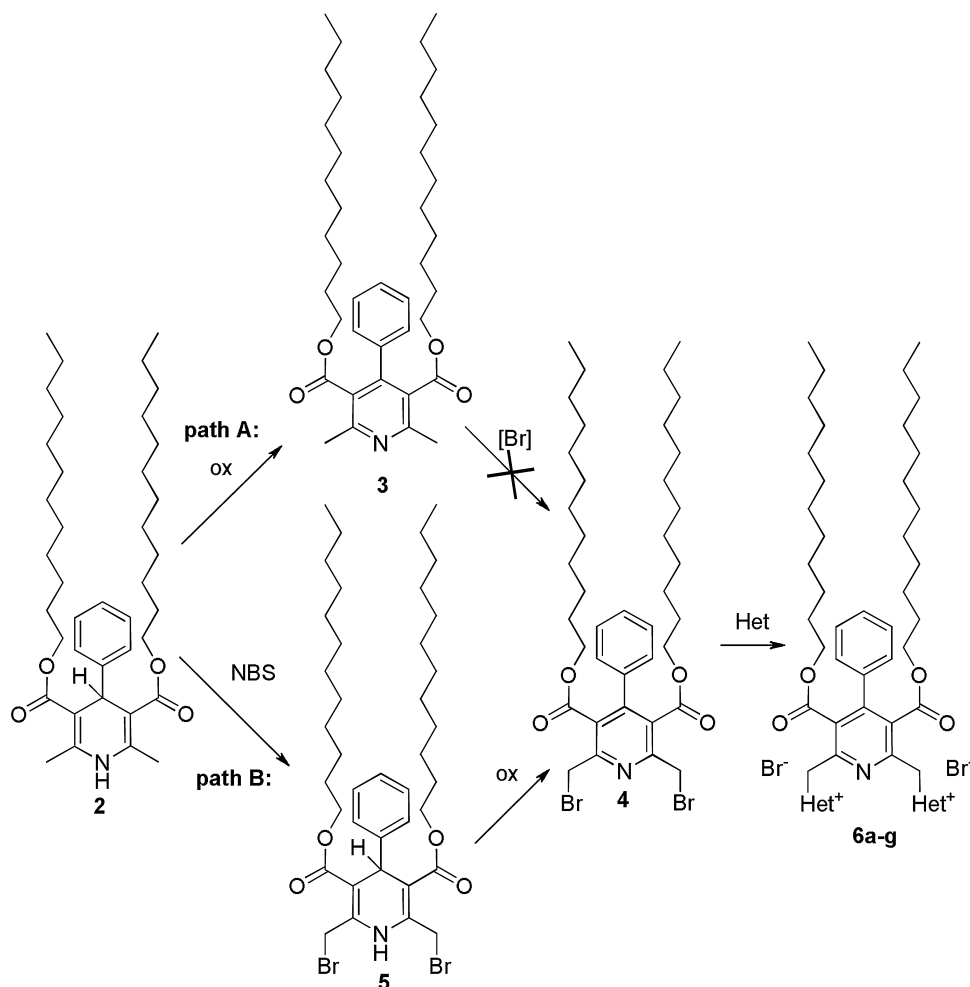
## 2.6. Transfection assay

### 2.6.1. Cell culture

Baby hamster kidney (BHK-21) cells (ATCC) were grown in BHK-21 medium (Glasgow MEM, USA) containing 5% fetal calf serum, 10% tryptose phosphate broth, 20 mM HEPES and 2 mM glutamine. Cells were incubated in a 5% CO<sub>2</sub> atmosphere at 37 °C.

### 2.6.2. Plasmids

pEGFP-C1 (Clontech, USA), was transformed in *Escherichia coli* strain DH5 $\alpha$  and amplified in lysogeny broth (LB) media (Sigma–Aldrich, USA) at 37 °C overnight. The plasmid was purified using an EndoFree plasmid purification system (Plasmid Maxi Kit; Qiagen, Germany). The concentration of DNA was measured by a NanoDrop 1000 Micro ultraviolet (UV) spectrophotometer (Thermo Electron Corporation, USA). Prepared plasmid DNA was stored at –20 °C before being used. Prior the transfection experiments, the purity



**Scheme 1.** Strategies for the synthesis of cationic pyridine derivatives **6a–g**.

and the quality of the plasmid DNA was confirmed by 1% agarose gel electrophoresis followed by EtBr staining.

#### 2.6.3. Determination of the N/P ratio

All samples of tested compounds were prepared as water solutions to a final concentration 1.0–0.5 mM (relative to the pyridine derivative). The optimal N/P ratio (the number of nitrogen residues in compound per DNA phosphate) for the best transfection results were determined for each compound. The various amounts of the compound to be mixed with constant amount of DNA and obtained N/P ratio were calculated using the following formula: compound ( $\mu\text{L}$ ) =  $3 \times D \times R/S$ , where  $D$  = total amount of pDNA used ( $\mu\text{g}$ ),  $R$  = N/P ratio;  $S$  = concentration of stock solution of compound (mM, expressed as nitrogen residues), taking into consideration that 1  $\mu\text{g}$  of DNA contains 3 nmoles of anionic phosphate.

#### 2.6.4. Preparation of compound–pDNA complexes

For preparation of the transfection complexes at 0.6, 1.8 and 3.0 N/P ratios the various amounts of tested compound stock solutions were mixed with constant amount (1  $\mu\text{g}$ ) of pEGFP-C1. Briefly, compound and pEGFP-C1 plasmid solutions were prepared separately in 100  $\mu\text{L}$  antibiotic-free, serum depleted BHK-21 media. After 5 min of incubation at ambient temperature, pEGFP-C1 solution was slowly added to the compound solution and the mixture was incubated at ambient temperature for another 15 min for formation of transfection complex.

#### 2.6.5. In vitro transfection experiment

24-Well plates were seeded with BHK-21 cell with antibiotic-free media 1 day before transfection until cells were reached of 70–80% confluence. Prior the transfection experiment, cell culture medium was removed and cells were washed once with serum-free medium. Transfection complexes in a total volume of 200  $\mu\text{L}$  were added to each well. Plates were transferred to 37 °C in a humidified atmosphere containing 5%  $\text{CO}_2$  for 1.5 h. After that, 500  $\mu\text{L}$  of the complete BHK-21 grow medium was added to each well and cells were cultivated for 24 h until subjected to fluorescent microscopic analysis. Each experiment was carried out several times; within a series, experiments were done in triplicate.

#### 2.6.6. Assessment of transfection efficiency

24 h after transfection, the microscopy images (fluorescent and phase contrast) were obtained at the magnification of 100 $\times$ , recorded with Leica DC 150 camera system (Switzerland) and processed with an open access image processing and analysing program ImageJ.

#### 2.6.7. Statistical analysis

Data statistical analysis was performed using open source programming language and software environment for statistical computing and graphics, program R. We performed two sample  $t$ -test, regression analysis, as well as analysis of covariance (ANCOVA). Statistical significance was set up at  $p < 0.05$ .

### 3. Results and Discussion

#### 3.1. Synthesis of compounds

Oxidation of 1,4-dihydropyridines to the corresponding pyridine derivatives is the most typical and general reaction for this heterocyclic system. One of the main metabolic pathways of biologically active 1,4-DHP derivatives is the oxidation to their corresponding pyridines with Cytochrome P450 (CYP) as catalyst (Guengerich et al., 1991). However, among the wide range of

studies regarding aromatisation of 1,4-DHP derivatives, there are only very few publications about oxidation of cationic 1,4-DHPs. Previously electrochemical oxidation of pyridinium moieties containing 1,4-dihydropyridines were achieved (Turovska et al., 2004). Thereafter, chemical and electrochemical oxidation of cationic moieties containing 1,4-DHP derivatives with ethoxycarbonyl substituent at the positions 3 and 5 as model compounds was reported by our research group (Plotniece et al., 2009). In the present study direct oxidation of cationic 1,4-DHP derivatives to the corresponding cationic pyridine derivatives failed. It can be assumed that direct oxidation does not occur due to the presence of didodecyloxycarbonyl substituents instead of the previously studied ethoxycarbonyl moieties which gave less sterical influence on 1,4-DHP system. It is an important task to elaborate a universal method for the convenient preparation of cationic moieties containing pyridine derivatives. Our synthetic plan is shown in Scheme 1.

The synthesis of the starting 1,4-dihydropyridine derivative **2** has already been reported in the literature (Pajuste et al., 2011). For further transformations, firstly we performed oxidation of compound **2** with in situ generated nitric oxide using the methodology described by Dubur and Uldrikis (1972) (Scheme 1, path A) to obtain pyridine derivative **3**. The next step—bromination of compound **3** with  $\text{Br}_2/\text{AcOH}$  or  $N$ -bromosuccinimide (NBS) was unsuccessful and did not give the desired dibromide **4**. Therefore, implementation of path B was another possibility for the synthesis of cationic pyridine derivatives **6** (Scheme 1). Bromination of the 2,6-methyl groups of compound **2** was performed with NBS according to the reported method giving 2,6-bis(bromomethyl)-1,4-DHP **5** (Pajuste et al., 2011) followed by oxidation with in situ generated nitric oxide which resulted in the formation of the desired 2,6-bis(bromomethyl)-pyridine **4**. The bromine nucleophilic substitution reaction of compound **4** was performed at room temperature in acetone with 25–83% yields in 1–5 days depending on the nucleophile structure (Table 1). The yields of the obtained cationic pyridine derivatives **6a–g** are slightly lower compared to the yields of the products of bromine nucleophilic substitution reaction of the corresponding 2,6-bis(bromomethyl)-1,4-DHP derivatives. For example, reaction of 2,6-bis(bromomethyl)-pyridine **4** with  $\gamma$ -picoline or  $p$ -dimethylaminopyridine proceeded within 2 or 1 day, with 55 and 58% yield, respectively (Table 1, entries 3 and 4), while reaction of 2,6-bis(bromomethyl)-1,4-DHP with  $\gamma$ -picoline or  $p$ -dimethylaminopyridine occurred during 1 day, with 65% yield in both cases (Pajuste et al., 2013); reaction of 2,6-bis(bromomethyl)-pyridine **4** with  $p$ -cyanopyridine occurred during 5 days, with 25% yield (Table 1, entry 5), on the other hand in the case of the corresponding 2,6-bis(bromomethyl)-1,4-DHP—during 2 days with 34% yield (Pajuste et al., 2013).

As evidenced in the  $^1\text{H}$  NMR spectra the signal of the 2,6-methylene groups of the synthesised pyridine derivatives **6a–g** was observed as a singlet with chemical shift in the range of 5.56–6.56 ppm, depending on the electronic nature of the heterocyclic substituent at the cationic part. In contrast to the pyridines **6a–g**, the  $^1\text{H}$  NMR signals of the 2,6-methylene groups of previously studied cationic 1,4-DHP derivatives were usually observed as AB-systems (Pajuste et al., 2013).

Structures of all the newly synthesised compounds were established and confirmed by  $^1\text{H}$  NMR,  $^{13}\text{C}$  NMR, MS and elemental analysis data. For the pyridine derivatives **6a–g** and parent compound **3** the elemental analyses showed that they were crystal hydrates, which was also confirmed by  $^1\text{H}$  NMR spectroscopic data. Molecular weights of compounds **6a–g** measured by LC-MS technique were in good agreement with the calculated values for all the derivatives. Details of the syntheses and full physicochemical characterisation for the newly synthesised compounds are given in the section Materials and Methods. The



purities of the studied compounds were at least 97% according to high-performance liquid chromatography (HPLC) data.

### 3.2. Thermal analysis

An effect of structure of the compounds on physicochemical properties of pyridine derivatives was examined by thermal analysis method. Thermogravimetric analysis (TGA) is the study of

the relationship between a sample's mass and temperature; differential thermal analysis (DTA) is the study of the energy change and temperature difference between a sample and an inert reference material, under identical heat conditions (Arseneau, 1961). These methods have been used in the determination of the thermal stability of simple molecules (Santos et al., 2012; Tomasic et al., 2013).

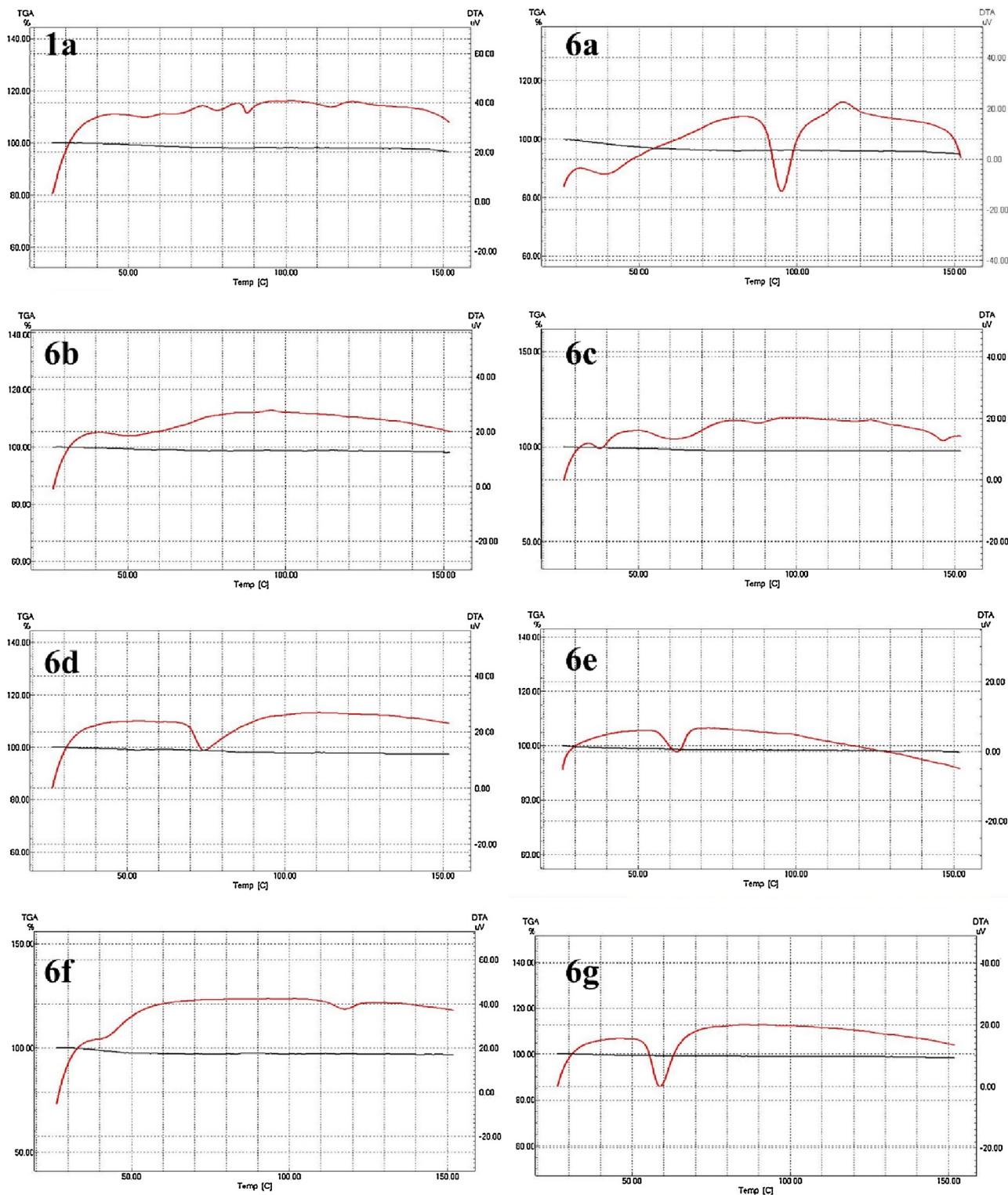


Fig. 2. A TGA-DTA thermograms profile of 1,4-DHP amphiphile **1a** and pyridines **6a–g**.

In this study we performed the thermal analysis of a previously reported 1,4-DHP amphiphile **1a** (Hyvonen et al., 2000; Pajuste et al., 2013) and the other prepared within this study novel pyridine derivatives **6a–g**. Approximately 5–7 mg of sample was heated over a temperature range of 25–150 °C under an argon atmosphere at a heating rate of 5 °C/min (a heating rate of 2 °C/min for **6e**). The temperature interval between 25 °C and 150 °C was chosen for TGA and DTA because it was lower than the melting point values of tested compounds and excluded full decomposition of samples. Differential thermal analysis curves were obtained simultaneously. In our case Al<sub>2</sub>O<sub>3</sub> was used as an inert reference material. The thermograms of 1,4-DHP amphiphile **1a** and pyridine derivatives **6a–g** are presented in Fig. 2 and all TGA and DTA data are summarised in Table 2.

Analysis of TGA data showed insignificant weight loss of samples in the tested temperature range—1.6% till 4.6%. These weight losses were related to the loss of water from samples. As mentioned above 1,4-DHP derivative **1a** (Hyvonen et al., 2000; Pajuste et al., 2013) and all synthesised pyridine derivatives **6a–g** were crystal hydrates with water content from 1.8% to 3.7% (data from Table 1) and 3.7% for derivative **1a** (Pajuste et al., 2013). In case of compounds **1a** and **6a** weight loss were approximately 1% higher than necessary and possibly related to the hygroscopicity of these derivatives. In the case of compounds **6f** and **6g** almost all amount of water was lost during thermogravimetric analysis, while for other amphiphiles—compounds **6b–e** only half of the water weight was lost.

Differential thermal analysis data showed that all processes were endothermic for all the samples of compounds—1,4-DHP **1a** and pyridines **6a–g** (Table 2, Fig. 2). Behaviour of the tested compounds was more or less similar due to their related chemical structure and could be dependent on the effect of the cationic head group forming heterocycles. Thus, the 1st transition peak for all derivatives containing pyridinium moieties (compounds **1a** and **6a**) or  $\beta$ - or  $\gamma$ -picolinium moieties (compounds **6b** and **6c**) were located in the 48–50 °C temperature range, for other pyridines, *p*-dimethylaminopyridinium moieties (compound **6d**) and *p*-cyano-pyridinium moieties (compound **6e**) – 74 and 62 °C, respectively,

for other heterocycles: *N*-methylpyrrolidinium moieties (compound **6f**) and *N*-methylmorpholinium moieties (compound **6g**) – 49 and 59 °C, respectively. Interestingly, DTA curves were characterised by only one endothermic transition for each of the pyridine derivatives **6b**, **6d**, **6e** and **6g**, two endothermic transitions for pyridine derivatives **6a** and **6f** and four for 1,4-DHP amphiphile **1a** and pyridine derivative **6c**. On the other hand, data from DTA curves showed that 1st transition peak area for pyridine **6g** at the temperature range 55–64 °C, 2nd transition peak area for pyridine **6a** at the temperature range 91–100 °C and 1st transition peak area pyridine **6d** at the temperature range 70–87 °C indicated greater intensity than others. Transition peak areas—1st at the temperature range 43–74 °C for pyridine **6b**, 2nd at the temperature range 53–70 °C for pyridine **6c** and 1st at the temperature range 57–66 °C for pyridine **6e** indicated medium intensity, while others showed slight intensity for the transition peak areas. We suggest that these transition stages are related to the phase transitions of the tested synthetic lipid-like compounds. For obtaining of more reasonable conclusions concerning to phase transitions of tested compounds it would be necessary to perform additional experiments using also other analytical and physical methods. According to the literature data delivery activity and lipoplexes formation of cationic lipids were dependent on the lipid shape and lamellar-hexagonal transitions (Zuhorn et al., 2007) and the geometry of lipoplexes is mainly dominated by the pure lipid preferred phase (Dan and Danino, 2014; Kundu et al., 2014). These conclusions were also confirmed by theoretical calculations for macroscopic model of partially or non-interdigitated gel phase lipid bilayers, and of mixed interdigitated gel phase bilayers (Chen et al., 2001).

### 3.3. Self-assembling properties

Self-assembling properties of the lipid-like compounds are important factors which may influence the biological activity of the compounds, in this case—transfection efficiency. Therefore, nanosystem characterisation would be essential for better understanding of structure–activity relationships for these compounds.

**Table 2**  
Values obtained from thermogravimetric analysis (TGA) and differential thermal analysis (DTA) curves of 1,4-DHP amphiphile **1a** and pyridine derivatives **6a–g**, a temperature range of 25–150 °C at a heating rate of 5 °C/min.

Comp.	TGA	DTA			
	Weight loss (%)	Transition	Onset–endset (°C)	Temp. (°C)	Absorbed heat (J/g)
<b>1a</b>	–3.1	1st	49–72	55	–40
		2nd	74–82	78	–22
		3rd	86–90	88	–22
		4th	112–124	118	–28
<b>6a</b>	–4.6	1st	33–46	39	–53
		2nd	91–100	95	–312
<b>6b</b>	–1.7	1st	43–74	50	–107
<b>6c</b>	–1.8	1st	35–41	38	–20
		2nd	53–70	61	–101
		3rd	83–92	88	–17
		4th	142–149	146	–18
<b>6d</b>	–2.7	1st	70–87	74	–240
<b>6e<sup>a</sup></b>	–2.1	1st	57–66	62	–184
<b>6f</b>	–3.3	1st	37–64	49	–47
		2nd	112–121	118	–40
<b>6g</b>	–1.6	1st	55–64	59	–246

<sup>a</sup> Measured at a heating rate of 2 °C/min.

**Table 3**

Values of Z-average diameter, polydispersity index (PDI), zeta-potential and critical micelle concentration (CMC) of nanoparticles formed by 1,4-DHP amphiphile **1a** and new pyridine derivatives **6a–g** obtained by DLS measurements. The samples were prepared by sonication in an aqueous solution at a compound concentration of 0.5 mg/mL. The mean diameter depicts the hydrodynamic diameter of the main population of nanoparticles in the tested sample; the PDI value describes polydispersity of the sample; the zeta-potential gives information about the surface charge of nanoparticles; the Z-average diameter represents the average hydrodynamic diameter of all nanoparticles in the sample.

Entry	Comp.	Z-average diameter (nm)	PDI	Mean diameter (nm)	Zeta-potential (mV)	CMC ( $\mu$ M)
1	<b>1a</b> <sup>a</sup>	113	0.345	151 (99%)	82 $\pm$ 10	30
2	<b>1a</b>	110 $\pm$ 10	0.345 $\pm$ 0.06	134 $\pm$ 5 (97%)	90 $\pm$ 3	17
3	<b>6a</b>	183 $\pm$ 52	0.330 $\pm$ 0.049	124 $\pm$ 19 (100%)	66 $\pm$ 1	34
4	<b>6b</b>	118 $\pm$ 14	0.383 $\pm$ 0.058	126 $\pm$ 4 (97%)	59 $\pm$ 7	38
5	<b>6c</b>	115 $\pm$ 9	0.313 $\pm$ 0.023	118 $\pm$ 4 (97%)	79 $\pm$ 4	33
6	<b>6d</b>	120 $\pm$ 1	0.227 $\pm$ 0.002	151 $\pm$ 5 (99%)	72 $\pm$ 8	16
7	<b>6e</b> <sup>b</sup>	743 $\pm$ 64	0.668 $\pm$ 0.008	389 $\pm$ 8 (92%)	51 $\pm$ 2	2
8	<b>6f</b>	543 $\pm$ 83	0.548 $\pm$ 0.078	235 $\pm$ 27 (89%)	48 $\pm$ 3	67
9	<b>6g</b>	253 $\pm$ 25	0.373 $\pm$ 0.029	237 $\pm$ 21 (58%); 63 $\pm$ 2 (42%)	57 $\pm$ 7	16

<sup>a</sup> According to literature data (Pajuste et al., 2013).

<sup>b</sup> Sample concentration—0.1 mg/mL.

Previously Hyvonen et al. (2000) reported, that double charged 1,4-DHP amphiphiles with ester variations at positions 3 and 5 of the 1,4-DHP ring were able to form liposomes with mean diameters in the range of 50–130 nm. Our research group recently showed, that double charged 1,4-DHP amphiphiles with variation of different cationic head-groups at positions 2 and 6 of the 1,4-DHP ring also form nanoparticles with diameters in the range of 75–360 nm (Pajuste et al., 2013). The aim of this work was to study and characterise self-assembling properties and formation of nanoparticles of the corresponding pyridine derivatives **6a–g** as oxidised forms of previously reported cationic 1,4-DHPs and comparison of the obtained results with properties of 1,4-DHP amphiphile **1a** which was found to be more active among previously tested 1,4-DHP amphiphiles.

The hydrodynamic diameters, polydispersity index (PDI), zeta-potential and critical micelle concentration (CMC) of the nanoparticles formed by pyridine derivatives **6a–g** in water were determined by dynamic light scattering (DLS) method. The aqueous solutions of the compounds with concentration of 0.5 mg/mL were prepared by sonication during 60 min, with one exclusion for pyridine **6e** where the solution with concentration of 0.1 mg/mL was prepared due to poor solubility of the compound. DLS data for nanoparticles formed by cationic pyridine derivatives **6a–g** are presented in Table 3.

Characterisation of nanoparticles formed by 1,4-DHP amphiphile **1a** was repeated and compared to the previously obtained data (Pajuste et al., 2013). The results revealed that the same kind of nanoparticles were obtained as the values of Z-average diameter, PDI, zeta-potential and critical micelle concentration in both cases are comparable (Table 3, entries 1 and 2).

According to DLS data, the average size of the nanoparticles formed by pyridine derivatives **6a–g** varied from 115 to 743 nm.

Thus, for pyridines **6b**, **6c**, **6d** (Table 3, entries 4–6) the average size of the nanoparticle diameters were comparable with the size of nanoparticles formed by 1,4-DHP amphiphile **1a**; for pyridines **6a** and **6g** sizes were slightly larger – 183 and 253 nm, while for pyridines **6e** and **6f** a significant increase of diameters was observed – 743 and 543 nm, respectively. The mean diameter which depicted the hydrodynamic diameter of the main population of nanoparticles for every sample varied between 118 and 389 nm. Thus, for 1,4-DHP amphiphile **1a** the diameter of the formed nanoparticles was in the range of 130–150 nm these diameter values are similar to the hydrodynamic diameter of the main population of nanoparticles formed by pyridines **6a–d** (Table 3, entries 3–6). For these samples the mean peak amounts were over 97%. Only in the case of pyridine **6g** two main populations of nanoparticles with hydrodynamic diameter 237 and 63 nm (Table 3, entry 9) were observed. The hydrodynamic diameter of the main population of nanoparticles for other pyridines **6e** and **6f** were 389 and 235 nm with the mean peak amount near 90%. Additionally, for all pyridines **6a–g** the polydispersity index (PDI) was measured (Table 3). The results showed a rather broad particle size distribution for pyridines **6e** and **6f** possessing a PDI of 0.668 and 0.548 (Table 3, entries 7 and 8), respectively. For 1,4-DHP amphiphile **1a**, pyridines **6a–c** and **6g** PDI values were in the range from 0.313 to 0.383 (Table 3, entries 1–5 and 9), while the most homogeneous particles were formed by pyridine **6d** with PDI of 0.227 (Table 3, entry 6).

The obtained data showed that values of zeta-potentials for the nanoparticles formed by pyridine derivatives were in the range of 48–79 mV, with the highest value for pyridine **6c** (Table 3, entry 5) and lowest value for pyridine **6f** (Table 3, entry 8). Zeta-potential values indicated that the nanoparticles formed by pyridine derivatives **6a–g** had quite similar surface characteristics and

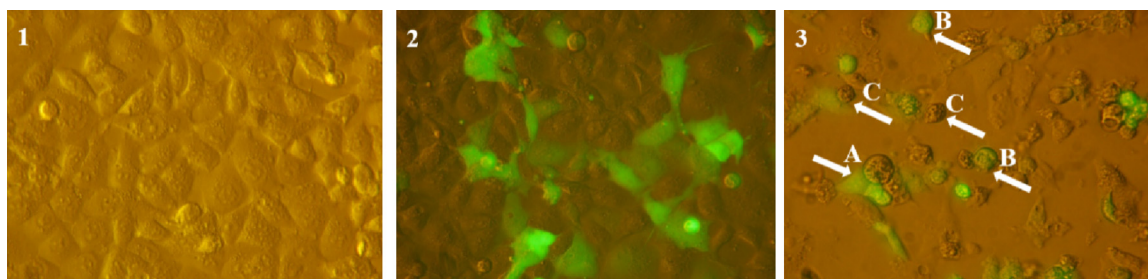


**Fig. 3.** Representative merge of phase contrast and fluorescence images of BHK-21 cells: illustration of cytotoxic effects of 1,4-DHP **1a**. Fluorescence and phase contrast images of BKH-21 cells were acquired sequentially 24 h post transfection. Image 1—confluent cell monolayer; image 2—cells transfected at N/P ratio 1.8, confluent cell monolayer without marked defects, GFP positive cells bear evidence of transfection; image 3—cells transfected at N/P ratio 3.0, decreased density of attached (living) cells (A) in comparison to Image 1, note also several rounded cells (B) and reattachment of them, apoptotic (shrink) cells (C), GFP signal present in the living as well in apoptotic cells.

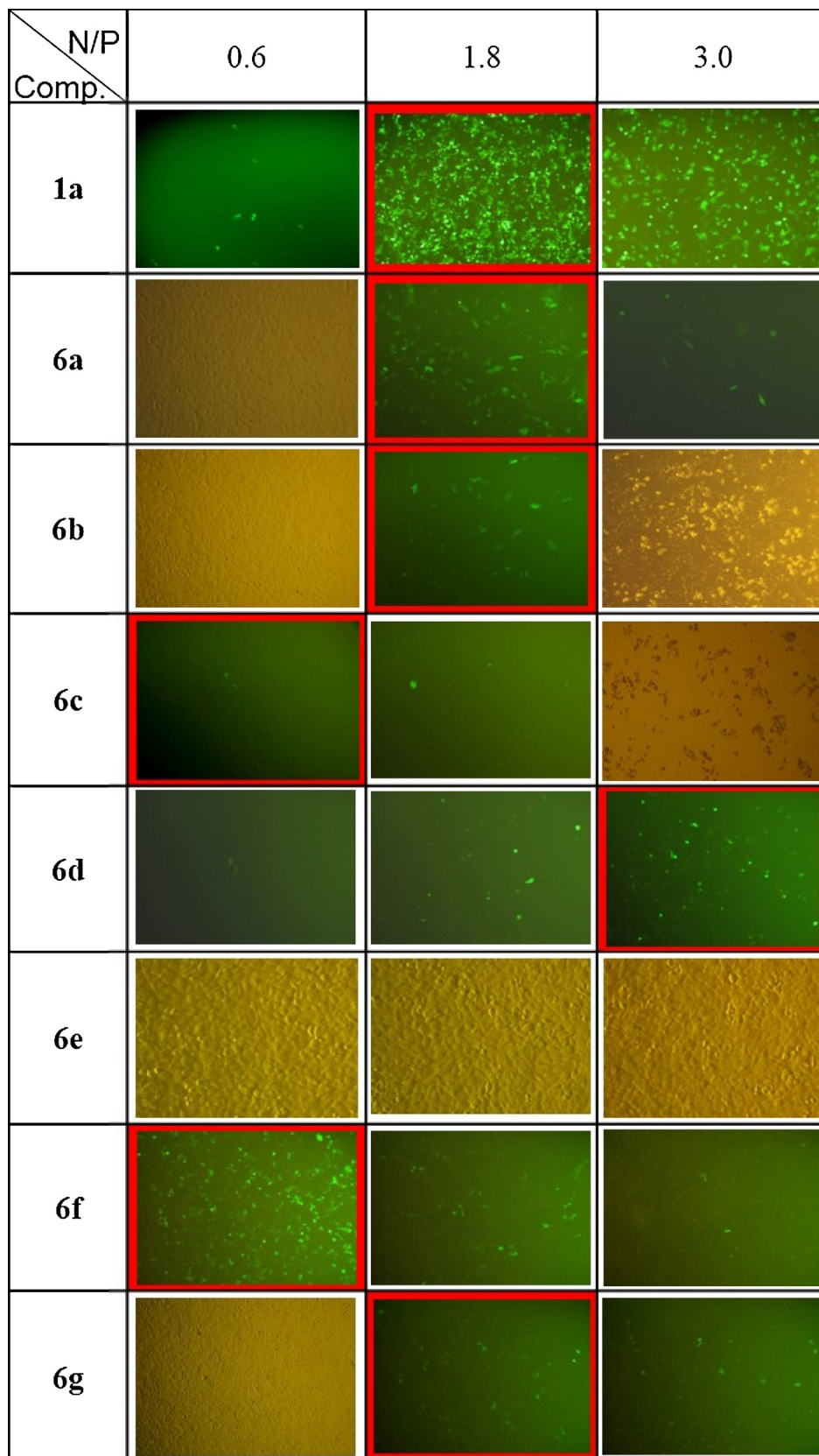


**Fig. 4.** Images for evaluation of gene transfection efficacy at three different N/P ratios of the tested pyridine derivatives **6a–g** and 1,4-DHP amphiphile **1a** (framed images depicted charge ratio (N/P) at highest gene transfection activity for individual amphiphiles). Optical images were added to substitute the fluorescent images for the cases when transfection results were negative (no GFP fluorescence).

the surface charges were strongly positive which would be a useful property for lipoplex formation with negatively charged DNA. According to the literature data it should be noted that the particles with zeta-potential values more positive than +30 mV or more negative than -30 mV are considered to be relatively stable (Markiewicz et al., 2013; Melendrez et al., 2010).

Nanoparticles in self-assembled compound solutions are formed only above a definite concentration, called the critical micelle concentration (CMC). CMC is an important characterisation for surfactants as delivery systems and crucial concerning formation and stability of nanoparticles. In this study CMC was determined for synthesised pyridines **6a–g** and 1,4-DHP amphiphile **1a** in aqueous media by the DLS technique according to the procedure described by Topel et al. (2013). To determine CMC, an aqueous solution of pyridines was prepared within the concentration range of 0.5 mg/mL (0.1 mg/mL for pyridine **6e**)– $0.1 \times 10^{-2}$  mg/mL starting from concentrated stock solution, which was subjected to a serial two-fold dilution each time with water. The obtained data showed that CMC values for the tested 1,4-DHP amphiphile **1a** and pyridines **6a–g** in aqueous media are in the range 2–67  $\mu$ M (Table 3). Lower CMC value—2  $\mu$ M was determined for pyridine **6e** containing *p*-cyanopyridinium moieties (Table 3, entry 7) which could involve poor solubility of this compound and also evident during the preparation of sample for DLS measurement because in this case it was not possible to prepare a stock solution of the compound with concentration 0.5 mg/mL. Highest CMC value—67  $\mu$ M was observed for pyridine **6f** by introducing in the molecule *N*-methylpyrrolidinium moieties (Table 3, entry 8) whilst CMC values for other compounds were 16–38  $\mu$ M. In this case small changes in the chemical structure of the pyridines have no significant influence on CMC values.

#### 3.4. Transfection activity

In order to test the transfection ability of synthesised pyridine derivatives **6a–g** to deliver the pEGFP-C1 plasmid DNA that encodes green fluorescent protein (GFP) reporter gene into the Baby hamster kidney-derived (BHK-21) cell line were performed. Transfection efficiencies of the novel pyridine derivatives **6a–g**

were compared with those of 1,4-DHP amphiphile **1a**, which is known to be the most efficient among the previously tested 1,4-DHP derivatives (Hyvonen et al., 2000; Pajuste et al., 2013).

In this respect different amounts of compounds were mixed with a constant amount of the plasmid DNA encoding for GFP to obtain three constant charge (N/P) ratios: 0.6, 1.8 and 3.0 and applied to the 70–80% confluent cell monolayers for 1.5 h contact in serum-free medium. GFP fluorescence was assessed by fluorescence microscopy 24 h later, after incubation at 37 °C in 5% CO<sub>2</sub>, and was evaluated digitally by the number of fluorescent cells using ImageJ software. Simultaneously, morphology of the cells (cells shape, and cell adhesion) was analysed using optical microscopy to estimate cytotoxicity of the tested compounds, as illustrated for 1,4-DHP amphiphile **1a** in the Fig. 3.

Generally, dose-dependent cytotoxicity, which appeared as decreased density of attached cells, increased quantity of oval cells and shranked cells with features of apoptosis, have been observed for pyridine derivatives **6b–d** and **6f**.

According to the obtained data, pyridine derivatives **6c** and **6d** have been found to be considerably cytotoxic to the cells at N/P ratio 1.8. For the compounds **6b** and **6f** the cytotoxic effect could be increased to N/P ratio 3.0, the same cytotoxic effect was observed also for the control compound **1a**. At the same time, pyridines **6a**, **6e** and **6g** were found to be relatively nontoxic at all N/P ratios tested in this study.

Gene transfection efficacy of the tested pyridine derivatives **6a–g** and 1,4-DHP amphiphile **1a** as the control is represented in Fig. 4.

The obtained results revealed that some of the tested pyridine derivatives showed significant gene transfection activities in vitro at distinct N/P ratios. Thus, pyridine **6f** was most efficient at charge ratio 0.6, the compounds **1a**, **6a**, **6b** and **6g** – at charge ratio 1.8, while derivative **6d** – at charge ratio 3.0. In turn, compounds **6c** and **6e** showed no transfection activity at the tested charge ratios. Comparison of transfection efficacy of the tested pyridine derivatives is represented in Fig. 5.

Transfection efficacy among tested compounds reduced in the order: amphiphile **1a** > **6f** > **6a** > **6d** ≥ **6b** > **6g** while pyridines **6c** and **6e** did not possess any transfection efficacy. None of the synthesised novel pyridine derivatives **6a–g** appeared to be more

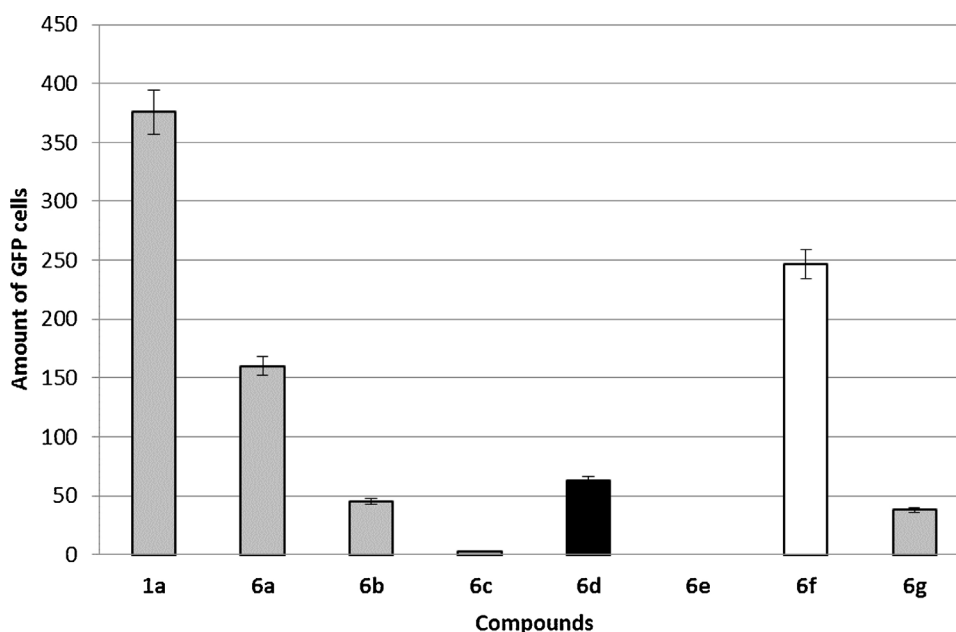


Fig. 5. Comparison of transfection efficiency of the compound–pDNA complexes for the tested pyridine derivatives **6a–g** and 1,4-DHP amphiphile **1a** evaluated by number of fluorescent cells. Used N/P ratios: black—3.0, grey—1.8 and white—0.6. Data are presented as mean ± SEM.

active than the previously tested 1,4-DHP amphiphile **1a**. The results presented at Fig. 5 showed that modifications of cationic head-groups of pyridine derivatives **6a–g** affected the delivery of pDNA. Compounds with pyridinium (compound **6a**) and N-methylpyrrolidinium (compound **6f**) moieties showed relatively high and rather comparable efficiency of gene transfer activity in vitro, whereas derivative **6c** with  $\gamma$ -methylpyridinium moieties possessed insignificant gene delivery activity—only few cells positive for GFP fluorescence were observed in the samples, and only compound **6e** with *p*-cyanopyridinium moieties proved incapable of transferring pDNA to the cells. Remarkably discrepancies between gene transfer activity of the pyridines **6a** and **6f** could be observed, compound **6f** displayed optimal transfection activity at N/P ratio 0.6, while compound **6a** was efficient only at higher N/P ratio—1.8. Moreover, increasing of the amount of a compound in transfection complexes (higher N/P ratios) in both variants did not improve transfection efficiency.

Generally, it could be concluded that among the tested pyridine derivatives compounds with *N*-methylpyrrolidinium moieties (compound **6f**) or pyridinium moieties (compound **6a**) as cationic head-group possessed higher pEGFP-C1 plasmid DNA transfection activity into the BHK-21 cell line. Interestingly, that other newly synthesised compounds with electron-donating substituent containing pyridinium moieties at the cationic part of amphiphiles (compounds **6b–d**) showed average or poor activity in contrast to the previously described 1,4-DHP amphiphiles, where  $\beta$ - or  $\gamma$ -picolinium or *p*-dimethylaminopyridinium moieties containing 1,4-DHP amphiphiles possessed delivery activity comparable with 1,4-DHP derivative **1a**, while 1,4-DHP derivatives containing saturated cationic heterocyclic moieties at the head-group did not show any delivery activity (Pajuste et al., 2011).

#### 4. Conclusions

In summary, based on the results we would propose that the difference in the transfection efficacy may be explained by diversity of physicochemical properties of pyridine derivatives which were tested by thermal analysis. For example, higher transfection efficiency possessing compounds **1a** and **6f** showed weak endothermic processes under differential thermal analysis, 22–47 J/g, while pyridines **6b**, **6d** and **6g** possessing low transfection activity—stronger endothermic processes, 107–246 J/g. In turn, with the results obtained for pyridine **6a** it is not possible to fit in this explanation. On the other hand, there is no clear correlation between self-assembling properties of compounds and their transfection efficacy. Comparable data of hydrodynamic diameters, polydispersity index, zeta-potential and critical micelle concentration were observed for higher transfection efficiency possessing compounds **1a** and **6a**, both compounds contain the same pyridinium moieties at the cationic part of molecule. DLS data for the other higher transfection efficiency possessing compound **6f** containing *N*-methylpyrrolidinium moieties is different. Nevertheless, the obtained results indicate that a correlation of the physicochemical, structural properties and gene delivery activities of tested compounds have not been completely elucidated yet. On the other hand, the synthesised pyridines **6a–g** as possible metabolites of previously studied promising delivery systems on the 1,4-DHP core (Hyvonen et al., 2000; Pajuste et al., 2013) possessed lower pDNA transfection activity than the corresponding 1,4-DHP amphiphiles.

#### Conflict of interest

The authors declare that there is no conflict of interests regarding the publication of this paper.

#### Acknowledgements

The authors are thankful for the financial support from the European Regional Development Fund (ERDF) project No. 2DP/2.1.1.1.0/14/APIA/VIAA/060, the Latvian National Research Programme BIOMEDICINE, and InnovaBalt (REGPOT-CT-2013-316149) project for O. Petrichenko as well as COST action CM1101 for fruitful discussion and possibility for dissemination of preliminary results. We are also grateful to Professor G. Duburs for initiation and support of development of these studies and to Dr. J. Kleperis of the Institute of Solid State Physics, University of Latvia for the use and assistance with the thermogravimetric measurements.

#### References

- Al-Dosari, M., Gao, X., 2009. Nonviral gene delivery: principle, limitations, and recent progress. *AAPS J.* 11, 671–681.
- Aravindan, L., Bicknell, K., Brooks, G., Khutoryanskiy, V., Williams, A., 2009. Effect of acyl chain length on transfection efficiency and toxicity of polyethylenimine. *Int. J. Pharm.* 378, 201–210.
- Arseneau, D.F., 1961. The differential thermal analysis of Wood. *Can. J. Chem.* 39, 1915–1919.
- Chen, L., Johnson, M., Biltonen, R., 2001. A macroscopic description of lipid bilayer phase transitions of mixed-chain phosphatidylcholines: chain-length and chain-asymmetry dependence. *Biophys. J.* 80, 254–270.
- Dan, N., Danino, D., 2014. Structure and kinetics of lipid-nucleic acid complexes. *Adv. Colloid Interface Sci.* 205, 230–239.
- Dubur, G.Y., Uldriks, Y.R., 1972. The oxidation of 1,4-dihydropyridines. *Chem. Heterocycl. Compd.* 6, 80–84.
- Felgner, P.L., Gadek, T.R., Holm, M., Roman, R., Chan, H.W., Wenz, M., Northrop, J.P., Ringold, G.M., Danielsen, M., 1987. Lipofection: a highly efficient, lipid-mediated DNA-transfection procedure. *Proc. Natl. Acad. Sci. U. S. A.* 84, 7413–7417.
- Fraleigh, R., Subramani, S., Berg, P., Papahadjopoulos, D., 1980. Introduction of liposome-encapsulated SV40 DNA into cells. *J. Biol. Chem.* 255, 10431–10435.
- Guengerich, F.P., Brian, W.R., Iwasaki, M., Sari, M.A., Bäärnhielm, C., Berntsson, P., 1991. Oxidation of dihydropyridine calcium channel blockers and analogues by human liver cytochrome P-450 IIIA4. *J. Med. Chem.* 34, 1838–1844.
- Guo, X., Huang, L., 2012. Recent advances in nonviral vectors for gene delivery. *Acc. Chem. Res.* 45, 971–979.
- Hyvonen, Z., Plotniece, A., Reine, I., Chekavichus, B., Duburs, G., Ursti, A., 2000. Novel cationic amphiphilic 1,4-dihydropyridine derivatives for DNA delivery. *Biochim. Biophys. Acta Biomembr.* 1509, 451–466.
- Kundu, S., Sharma, A., Lee, S., Sharma, G., Doss, C., Yagihara, S., Kim, D., Nam, J., Chakraborty, C., 2014. Recent trends of polymer mediated liposomal gene delivery system. *BioMed Res. Int.* 2014, 15. doi:<http://dx.doi.org/10.1155/2014/934605> 934605.
- Lasic, D., Templeton, N., 1996. Liposomes in gene therapy. *Adv. Drug Deliv. Rev.* 20, 221–266.
- Lv, H., Zhang, S., Wang, B., Cui, S., Yan, J., 2006. Toxicity of cationic lipids and cationic polymers in gene delivery. *J. Controll. Release* 114, 100–109.
- Margus, H., Padari, K., Pooga, M., 2012. Cell-penetrating peptides as versatile vehicles for oligonucleotide delivery. *Mol. Ther.* 20, 525–533.
- Markiewicz, M., Mroziak, W., Rezwani, K., Thoming, J., Hupka, J., Jungnickel, C., 2013. Changes in zeta potential of imidazolium ionic liquids modified minerals—implications for determining mechanism of adsorption. *Chemosphere* 90, 706–712.
- Marqués-Gallego, P., de Kroon, A.I., 2014. Ligation strategies for targeting liposomal nanocarriers. *BioMed Res. Int.* 2014, 12. doi:<http://dx.doi.org/10.1155/2014/129458> 129458.
- Melendrez, M., Cardenas, G., Arbiol, J., 2010. Synthesis and characterization of gallium colloidal nanoparticles. *J. Colloid Interface Sci.* 346, 279–287.
- Pajuste, K., Hyvonen, Z., Petrichenko, O., Kaldre, D., Rucins, M., Cekavichus, B., Ose, V., Skrivele, B., Gosteva, M., Morin-Picardat, E., Plotniece, M., Sobolev, A., Duburs, G., Ruponen, M., Plotniece, A., 2013. Gene delivery agents possessing antiradical activity: self-assembling cationic amphiphilic 1,4-dihydropyridine derivatives. *New J. Chem.* 37, 3062–3075.
- Pajuste, K., Plotniece, A., Kore, K., Intenberga, L., Cekavichus, B., Kaldre, D., Duburs, G., Sobolev, A., 2011. Use of pyridinium ionic liquids as catalysts for the synthesis of 3,5-bis(dodecyloxycarbonyl)-1,4-dihydropyridine derivative. *Cent. Eur. J. Chem.* 9, 143–148.
- Plotniece, A., Pajuste, K., Kaldre, D., Cekavichus, B., Vigante, B., Turovska, B., Belyakov, S., Sobolev, A., Duburs, G., 2009. Oxidation of cationic 1,4-dihydropyridine derivatives as model compounds for putative gene delivery agents. *Tetrahedron* 65, 8344–8349.
- Rea, J., Gibly, R., Barron, A., Shea, L., 2009. Self-assembling peptide-lipoplexes for substrate-mediated gene delivery. *Acta Biomater.* 5, 903–912.
- Santos, N., Cordeiro, A., Damasceno, S., Aguiar, R., Rosenhaim, R., Carvalho, J., Santos, I., Maia, A., Souza, A., 2012. Commercial antioxidants and thermal stability evaluations. *Fuel* 97, 638–643.

- Tomasic, V., Biliskov, N., Mihelj, T., Stefanic, Z., 2013. Thermal behaviour and structural properties of surfactant–picrate compounds: the effect of the ammonium headgroup number. *Thermochim. Acta* 569, 25–35.
- Topel, O., Cakir, B., Budama, L., Hoda, N., 2013. Determination of critical micelle concentration of polybutadiene-block-poly(ethyleneoxide) diblock copolymer by fluorescence spectroscopy and dynamic light scattering. *J. Mol. Liq.* 177, 40–43.
- Turovska, B., Stradins, J., Turovskis, I., Plotniece, A., Shmidlers, A., Duburs, G., 2004. Electrochemical oxidation of compounds containing 1,4-dihydropyridine and pyridinium rings—analogs of gene transfection agents. *Chem. Heterocycl. Compd.* 40, 753–758.
- van Gaal, E.V., van Eijk, R., Oosting, R.S., Kok, R.J., Hennink, W.E., Crommelin, D.J., Mastrobattista, E., 2011. How to screen non-viral gene delivery systems in vitro? *J. Control. Release* 154, 218–232.
- Zuhorn, I., Engberts, J., Hoekstra, D., 2007. Gene delivery by cationic lipid vectors: overcoming cellular barriers. *Eur. Biophys. J.* 36, 349–362.

## **Publication**

### **B**

Evaluation of antiradical activity and reducing capacity of synthesised bispyridinium dibromides obtained by quaternisation of 4-pyridyl-1,4-dihydropyridines with propargyl bromide.

*Aust. J. Chem.*, 2015, 68, 86-92.



# Evaluation of Antiradical Activity and Reducing Capacity of Synthesised Bispyridinium Dibromides Obtained by Quaternisation of 4-Pyridyl-1,4-dihydropyridines with Propargyl Bromide

Martins Rucins,<sup>A,B</sup> Marina Gosteva,<sup>A</sup> Sergey Belyakov,<sup>A</sup>  
Arkadij Sobolev,<sup>A</sup> Karlis Pajuste,<sup>A</sup> Mara Plotniece,<sup>A</sup>  
Brigita Cekavicus,<sup>A</sup> Dace Tirzite,<sup>A</sup> and Aiva Plotniece<sup>A,C</sup>

<sup>A</sup>Latvian Institute of Organic Synthesis, Aizkraukles str. 21, Riga, LV-1006, Latvia.

<sup>B</sup>Faculty of Medicine, University of Latvia, Raina blvd. 19, Riga, LV-1586, Latvia.

<sup>C</sup>Corresponding author. Email: aiva@osi.lv

New bispyridinium dibromides based on the 1,4-dihydropyridine (1,4-DHP) cycle were synthesised in the reaction between 4-pyridyl-1,4-DHP derivatives and propargyl bromide. It has been shown that variation of the substituent position on the pyridine as well as small changes in the electronic nature of the 1,4-DHP cycle as a result of the substituent nature at the 3 and 5 positions do not affect the course of the reaction and in all cases the corresponding bispyridinium dibromides **4a–e** were formed. The antiradical activity, using 1,1-diphenyl-2-picrylhydrazine as a free radical scavenger, and the reducing capacity using phosphomolybdenum complexes have been evaluated for the newly synthesised compounds **4a–e**. It has been shown that all tested 1,4-DHP bispyridinium dibromides **4a–e** possess reducing capacity and antiradical properties. Moreover, the reducing capacity results could be explained by the influence of the electronic nature of the substituent at the 3 and 5 positions of the 1,4-DHP cycle.

Manuscript received: 28 January 2014.

Manuscript accepted: 27 March 2014.

Published online: 7 May 2014.

## Introduction

1,4-Dihydropyridine (1,4-DHP) derivatives are a class of compounds playing an important role in synthetic, medicinal, and bioorganic chemistry.<sup>[1]</sup> It is worth emphasising that the 1,4-DHP group is a privileged structure or scaffold. As an active linker, according to Triggle, 1,4-DHP is an intrinsic structural part of many pharmacologically active compounds and drugs.<sup>[2]</sup> Thus, depending on the chemical structure peculiarities, dihydropyridines possess several activities: neuro- and radioprotection, anti-mutagenic, anti-diabetic, anti-inflammatory, anti-ischaemic/anti-anginal and anti-hypertensive actions, as well as gene transfection properties.<sup>[3]</sup> On the other hand, of increasing interest are pyridinium salts because of their high biological activity.<sup>[4]</sup> It is also known that pyridinium derivatives possess antitumour, antimicrobial, and acetylcholinesterase and/or butyrylcholinesterase inhibitor properties, and they are also used for transporting genetic material in vivo.<sup>[5]</sup>

Consequently, during the last decades development of new pyridinium moieties containing compounds based on a 1,4-DHP core has become an interesting area for medicinal chemistry research. Previously, our research group has developed multiple pyridinium moieties containing 1,4-DHP derivatives for studies of their membranotropic effects, such as incorporation in the liposomal membranes and influence on bilayer fluidity, gene delivery properties, and calcium channel blocking and

antioxidant activities.<sup>[6]</sup> Moreover, the propargyl moiety is known to play an important role in providing neuroprotecting properties of propargyl group-containing anti-depressants, such as selegiline and rasagiline.<sup>[7]</sup> The combination of two active pharmacophores into one molecule is one of the possibilities for drug designing techniques which are used for drug discovery.<sup>[8]</sup>

In this paper we describe the unexpected course of pyridine moiety quaternisation in 4-pyridyl-1,4-DHP derivatives with propargyl bromide, where instead of the expected monomeric compounds 1-prop-2-ynyl-pyridinium bromides **3**, we have obtained the corresponding bispyridinium dibromides **4** containing a 1,4-DHP moiety at position 3 or 4. The 1,4-DHP structure to some extent resembles 1,4-dihydronicotinamide, part of the coenzymes nicotinamide adenine dinucleotide (NADH) and nicotinamide adenine dinucleotide phosphate (NADPH), which are common mediators of biological processes in cells. Therefore the antiradical activity (ARA), using 1,1-diphenyl-2-picrylhydrazine (DPPH) as a free radical scavenger, and reducing capacity (RC), using a phosphomolybdenum complex of the newly synthesised compounds **4a–e**, were evaluated as well.

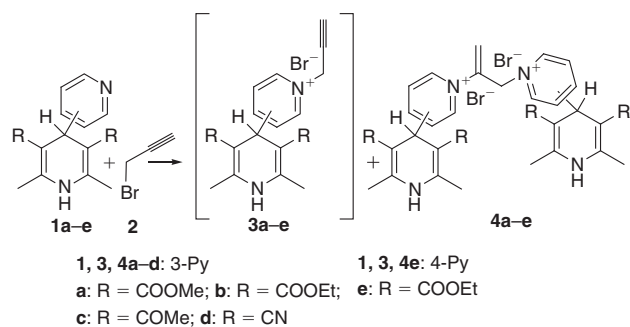
## Results and Discussion

### Synthesis

Initially, the main purpose of our studies was the synthesis of the corresponding 1-prop-2-ynyl-pyridinium bromides **3** based on

the 1,4-DHP cycle for further investigation of biological activity. The typical procedure for the quaternisation of pyridine derivatives has been reported by several research groups.<sup>[9]</sup> Previously, our research group carried out the quaternisation of the pyridyl moiety of 4-pyridyl-1,4-dihydropyridines with various alkyl halides in acetone under reflux.<sup>[6a,6d,10]</sup> In this case the first reaction was performed using the same conditions, and the starting 4-pyridyl-1,4-DHP derivative **1b** was treated with propargyl bromide in acetone under reflux for 22 h (Scheme 1). The obtained precipitate was filtered off and crystallised from an acetone/methanol mixture. However, the <sup>1</sup>H NMR spectra of the compound obtained in DMSO-*d*<sub>6</sub> solution showed evidence of other groups in the molecule: an AB-system at 5.62 and 6.15 ppm with a coupling constant 3.1 Hz and a singlet at 6.06 ppm. The proton signals for the pyridinium and 1,4-DHP moieties in the <sup>1</sup>H NMR spectra were found to be non-equivalent, and the same was observed for the carbon signals in the <sup>13</sup>C NMR spectra.

According to literature data the quaternisation of 1 equiv. of 3- or 4-hydroxypyridine with 1.5 equiv. of propargyl bromide when carried out in dry dichloromethane resulted in formation



**Scheme 1.** Synthesis of bispyridinium dibromides **4a-e**. Reagents and conditions: 4-pyridyl-1,4-dihydropyridine derivative (0.66 mM, 1 equiv.) and 80% solution of propargyl bromide in toluene (0.99 mM, 106  $\mu$ L, 1.5 equiv.) reflux under pressure in acetone for 22 h.

of the corresponding 1-(prop-2-ynyl)pyridinium salts with high yield, while in the case of quaternisation of 4-(3-phenylpropyl)pyridine another research group underlined that the corresponding substituted 1-(prop-2-ynyl)pyridinium salt was not isolated as a single compound, but as a mixture with its corresponding allene.<sup>[11]</sup> In turn, Katritzky et al. showed the influence of the substituent at position 4 of the pyridine ring on the pyridine reactivity with 2-propynyl halides.<sup>[12]</sup> Pyridines with strong electron donating substituents at position 4 gave the expected 1-(2-propynyl)pyridinium salts in good yields, while 4-methyl- or 4-phenylpyridine were much less reactive. In addition, extending the reaction time in some cases improved the yield of the corresponding 1-(2-propynyl)pyridinium salt, but in other cases nucleophilic attack of a second mole of pyridine derivative converted the 1-(2-propynyl)pyridinium salt into 1,3-propenediylbis(pyridinium) halides, especially for unsubstituted pyridine. However, Kanitskaya et al. proposed the formation of another product, 1-[(1,3,5)-6-pyridin-1-ium-1-ylhexa-1,3,5-trienyl]pyridin-1-ium dibromide in the reaction between pyridine and propargyl bromide in acetonitrile.<sup>[13]</sup> Analysis of the literature data suggest that the electronic nature of the pyridine substituent, ratio of reagents, and reaction media (solvent) affect the reaction progress and lead to different final products.

For conclusive assessment of the structure of obtained compounds **4**, suitable crystals of bispyridinium dibromide **4b** for X-ray crystallographic analysis were obtained by slow crystallisation from hexane/dichloromethane. X-Ray analysis of the crystals of the obtained compound was undertaken and the diethyl 4-(1-(2-(3-(3,5-bisethoxycarbonyl)-2,6-dimethyl-1,4-dihydropyridin-4-yl)pyridin-1-ium-1-yl)allyl)pyridin-1-ium-3-yl)-2,6-dimethyl-1,4-dihydropyridine-3,5-dicarboxylate dibromide (**4b**) structure was confirmed (Fig. 1).

It should be noted that there are no symmetry elements in the molecular structure of compound **4b** (point group of symmetry is  $C_1$ ). Nevertheless, in the crystal structure (space group is  $C2/c$ ) the molecular cations of compound **4b** lie in special positions (in symmetry axis of order 2). It is realised by crystal

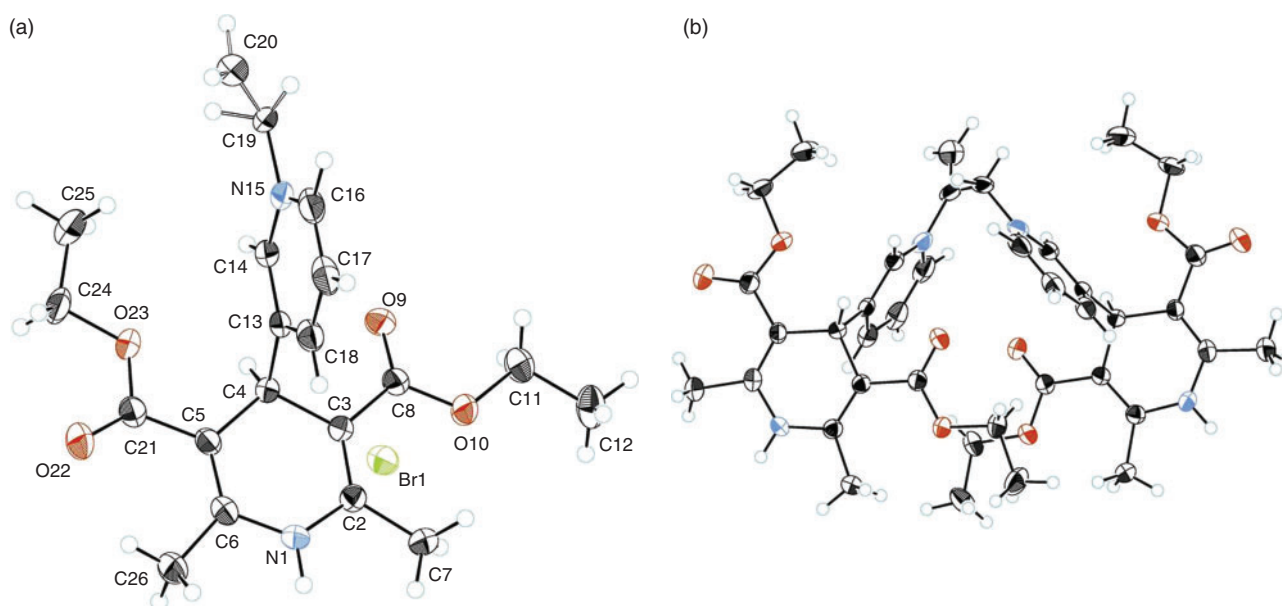


**Fig. 1.** (a) An ORTEP plot of the asymmetric unit of the bispyridinium dibromide **4b**, showing the atomic numbering scheme, and (b) a view of the doubly-charged molecular cation of compound **4b**.

structure disordering: the occupation  $g$ -factor of carbon atom C20 is 0.5. The same values of  $g$  occur for hydrogen atoms at C20 and C19.

The effect of the solvent and temperature on the course of the quaternisation reaction of 3,5-diethoxycarbonyl-2,6-dimethyl-4-(3-pyridyl)-1,4-dihydropyridine (**1b**) with propargyl bromide (**2**) has been investigated and the obtained results are presented in Table 1. The ratios of compounds **1b/3b/4b** were determined by ultra performance liquid chromatography–mass spectrometry (UPLC/MS).

The results in Table 1 (entries 1, 5, and 9) reveal that after 2 h of quaternisation reaction in acetone, acetonitrile, or dichloromethane at room temperature a large amount of the starting 1,4-DHP **1b**, minor amount or traces of mono bromide **3b**, and bispyridinium dibromide **4b** were detected. When the reaction time was increased to 22 h (Table 1, entries 2, 6, and 10) the bispyridinium dibromide **4b** was obtained with low yield (22–37%, depending on the solvent). In turn, the main product, bispyridinium dibromide **4b**, was formed in good yields (90, 92, and 83%, respectively) after 22 h at reflux of the reaction mixture under pressure (Table 1, entries 4, 8, and 12). In addition, the reaction mixture contained small amounts of the starting 3,5-diethoxycarbonyl-2,6-dimethyl-4-(3-pyridyl)-1,4-dihydropyridine (**1b**) and traces of mono quaternised product **3b** in acetone or dichloromethane (Table 1, entries 4 and 12). Traces of the starting 1,4-dihydropyridine **1b** and ~7% of mono bromide **3b** were detected when the reaction was refluxed in acetonitrile under pressure for 22 h (Table 1, entry 8). This result is in accordance with the studies of our research group where acetonitrile was recommended as a suitable solvent for alkylation of the pyridine fragment in 1,4-DHP.<sup>[14]</sup> However, further studies for optimisation of reaction conditions for synthesis of 1-prop-2-ynyl-pyridinium bromide **3b** are currently underway. UPLC/MS analyses of all reaction mixtures obtained by refluxing them under pressure for 2 h (Table 1, entries 3, 7, and 11) showed different ratios of starting compound **1b** and final bispyridinium salt **4b** and only traces of mono quaternised product **3b**.

It can be proposed that bispyridinium dibromide **4b** is perhaps formed directly during the quaternisation reaction and the further reaction of mono quaternised product, mono bromide **3b**, with starting 1,4-DHP **1b** is less probable. Other 4-(3-pyridyl)-1,4-dihydropyridines **1a**, **1c**, and **1d** with different moieties at positions 3 and 5 of the 1,4-DHP cycle were also

synthesised to study the influence of the electronic nature of the substituents. Variation of the pyridine cycle substituent position was carried out, thus besides 4-(3-pyridyl)-1,4-dihydropyridine **1b** its analogue 4-(4-pyridyl)-1,4-dihydropyridine **1e** was also synthesised. The obtained products from the quaternisation reactions confirmed that in all cases instead of the predicted mono derivatives **3a** and **3c–e** formation of the corresponding bispyridinium dibromides **4a** and **4c–e** were observed (Scheme 1).

Generally, it may be concluded that variation of the substituent position at the pyridine (derivatives **1b** and **1e**) as well as minor changes in the electronic nature of the 1,4-DHP cycle due to the different substituents at positions 3 and 5 (derivatives **1a–e**) did not affect the course of the reaction, the corresponding bispyridinium dibromides **4a–e** were formed in all cases.<sup>[15]</sup> However, it should be noted that minor changes in the electronic nature of the 1,4-DHP cycle have influenced the yields of bispyridinium dibromides **4**, thus the highest yield (72%) is obtained for 4-(1-(2-(3-(3,5-biscyano-2,6-dimethyl-1,4-dihydropyridin-4-yl)pyridin-1-ium-1-yl)allyl)pyridin-1-ium-3-yl)-3,5-biscyano-2,6-dimethyl-1,4-dihydropyridine dibromide (**4d**), and the lowest yield (41%) for dimethyl 4-(1-(2-(3-(3,5-bismethoxycarbonyl-2,6-dimethyl-1,4-dihydropyridin-4-yl)pyridin-1-ium-1-yl)allyl)pyridin-1-ium-3-yl)-2,6-dimethyl-1,4-dihydropyridine-3,5-dicarboxylate dibromide (**4a**).

Structures of all the newly synthesised derivatives of bispyridinium dibromides **4a–e** were established and confirmed by <sup>1</sup>H NMR, <sup>13</sup>C NMR, MS, IR and elemental analysis data. For the salts **4a** and **4e** elemental analysis showed that they were crystal hydrates, the compound **4d** was crystallised with 0.4 moles (3.3%) of acetone which was also confirmed by <sup>1</sup>H NMR spectroscopic data. Molecular weights of 1,4-DHP derivatives measured by a LC-MS technique were in good agreement with the calculated values for all the compounds. Details of the syntheses and full physical–chemical characterisation for the bispyridinium dibromides **4a–e** are given in the *Experimental* section. The purities of the studied compounds were at least 97% according to high-performance liquid chromatography (HPLC) data.

#### Antiradical Activity (ARA) and Reducing Capacity (RC)

1,4-DHP derivatives as nitrogen heterocycles are of great importance because of their role in biological systems. In

**Table 1.** The influence of the solvent and temperature on the reaction of 3,5-diethoxycarbonyl-2,6-dimethyl-4-(3-pyridyl)-1,4-dihydropyridine (**1b**) with propargyl bromide (**2**)

Entry	Solvent	Temperature	Time [h]	Ratio of compounds <sup>A</sup> [%]		
				<b>1b</b>	<b>3b</b>	<b>4b</b>
1	Acetone	Room temperature	2	95	traces	4
2	Acetone	Room temperature	22	59	4	37
3	Acetone	Reflux under pressure	2	67	traces	32
4	Acetone	Reflux under pressure	22	5	traces	90
5	Acetonitrile	Room temperature	2	92	7	traces
6	Acetonitrile	Room temperature	22	62	6	32
7	Acetonitrile	Reflux under pressure	2	9	13	78
8	Acetonitrile	Reflux under pressure	22	traces	7	92
9	Dichloromethane	Room temperature	2	98	traces	traces
10	Dichloromethane	Room temperature	22	76	traces	22
11	Dichloromethane	Reflux under pressure	2	82	traces	17
12	Dichloromethane	Reflux under pressure	22	16	traces	83

<sup>A</sup>Determined by ultra performance liquid chromatography–mass spectrometry.

particular, 1,4-DHP derivatives are known to be oxidised to the appropriate pyridine derivatives; in the case of 1,4-dihydropyridine (as part of redox coenzymes NADH or NADPH) reciprocal hydrogen transfer occurs. In addition, some of the dihydropyridine derivatives act as electron and hydrogen donors to oxidants, activated unsaturated compounds, free radicals, reactive oxygen species, and reactive nitrogen species, so antiradical and antioxidant properties of DHP derivatives have been discovered.<sup>[16]</sup> Oxidative aromatisation reactions of 1,4-DHP derivatives take place in biological systems in the presence of certain enzymes, for example Cytochrome P450 (CYP).<sup>[17]</sup> According to the literature, antioxidant or antiradical substances are able to diminish different radicals. Previously, Tirzitz et al. demonstrated ARA for 1,4-DHP derivatives, and revealed their singlet oxygen quenching activity as being similar to  $\alpha$ -tocopherol.<sup>[18]</sup>

The ARA of the synthesised compounds **4a–e** based on the 1,4-DHP core were determined using a DPPH free radical scavenging test.<sup>[19]</sup> This method is most frequently used for screening the ARA of compounds with different structures, including derivatives of 1,4-DHP. Testing the ability of bispyridinium-1,4-DHP derivatives **4a–e** to reduce the stable DPPH radical was carried out in ethanol at room temperature and determined photometrically with UV/Vis spectroscopy as reduction in absorption at 517 nm. In addition, the phosphomolybdenum complex method was used for the evaluation of the RC of the synthesised 1,4-DHP derivatives **4a–e**, according to a recommendation by Prieto et al.<sup>[20]</sup> The assay is based on the reduction of  $\text{Mo}^{\text{VI}}$  to  $\text{Mo}^{\text{V}}$  by the tested sample at acidic pH with the following formation of a green phosphate/ $\text{Mo}^{\text{V}}$  complex, with a characteristic absorbance maximum at 695 nm detectable by UV/Vis spectroscopy. Diludine (diethyl 1,4-dihydro-2,6-dimethyl-3,5-pyridinecarboxylate), a well known 1,4-DHP derivative with antioxidant and antiradical properties was used as a positive control in both cases.<sup>[21]</sup> ARA and RC data obtained are summarised in Fig. 2.

In turn, the obtained results (Fig. 2) showed that all the tested newly synthesised bispyridinium dibromides based on the 1,4-DHP cycle **4a–e** possess RC and antiradical properties. So, a low ARA (7–11 %) was determined for compounds **4a–e**.

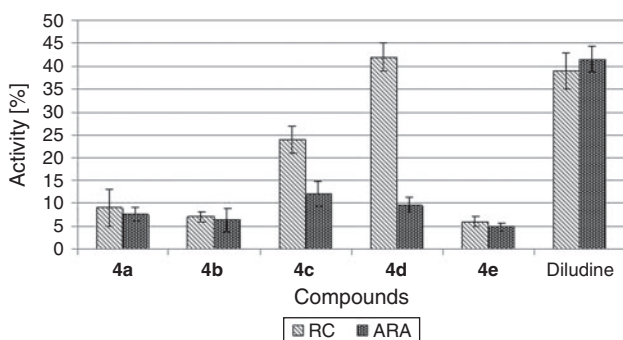


**Fig. 2.** Reducing capacity (RC) of the obtained bispyridinium moiety-containing 1,4-dihydropyridine (1,4-DHP) derivatives **4a–e** and Diludine (at a concentration of 100 mM), evaluated by the phosphomolybdenum complex method; results are expressed as absorbance percentage (%) at 695 nm of sample against absorbance of a blank solution. Antiradical activity (ARA) of synthesised 1,4-DHP derivatives **4a–e** and Diludine, evaluated by their ability to react with the 1,1-diphenyl-2-picrylhydrazine (DPPH) radical. Results are expressed as an absorbance percentage (%) of the DPPH free radical scavenging at 517 nm. The untreated level of the DPPH radical is designated as 100%. All data are presented as a mean  $\pm$  s.d.

However, the highest RC, which was comparable to that of Diludine (40%), was evidenced for the compound **4d** (also 40%) and moderate RC ( $\sim$ 25%) for compound **4c**, while other bispyridinium dibromides **4a**, **4b**, and **4e** showed low RC (7–10%). These data could be explained by the influence of the electronic nature of the substituent at positions 3 and 5 of the 1,4-DHP cycle. According to the literature data 1,4-DHP substituents that contain dialkoxycarbonyl moieties at positions 3 and 5 (analogues of compounds **4a** and **4b**) possess electron donating effects (for diethyl derivative  $\sigma_1 = -0.18$  or for dimethyl derivative  $\sigma_1 = -0.14$ ;  $\sigma_r = -0.08$  (for both) and diacetyl, an analogue of compound **4c** ( $\sigma_1 = -0.06$ ;  $\sigma_r = -0.09$ ), while introducing cyano moieties at positions 3 and 5 of the 1,4-DHP substituent made this system electron withdrawing in nature ( $\sigma_1 = 0.14$ ;  $\sigma_r = -0.06$ ).<sup>[15]</sup>

## Conclusion

In conclusion, during the reaction of 4-pyridyl-1,4-DHP derivatives with propargyl bromide an unexpected course of quaternisation was observed and new bispyridinium dibromides **4** were obtained instead of the expected monomeric compounds pyridinium bromides **3**. The variation of the substituent position at the pyridine as well as minor changes in the electronic nature of the 1,4-DHP cycle because of different substituents at the 3 and 5 positions did not affect the course of the reaction. The ARA and the RC of the synthesised bispyridinium dibromides **4a–e** were evaluated. The obtained results confirmed that all tested compounds **4a–e** possessed RC and antiradical properties. The RC results obtained for the compounds could be explained by the substituent's electronic influence at positions 3 and 5 of the 1,4-DHP cycle.

## Experimental

### General

All chemical reagents were purchased from Acros or Sigma-Aldrich and used without further purification.

TLC was performed on Silica gel 60 F254 Aluminium sheets 20  $\times$  20 cm (Merck).  $^1\text{H}$  and  $^{13}\text{C}$  NMR spectra were recorded with Varian Mercury BB spectrometer at 400 and 100.56 MHz, respectively. The chemical shifts of the atoms are reported in parts per million (ppm) relative to the residual signal of the solvent  $\text{DMSO}-d_6$ :  $\delta$  2.50 for  $^1\text{H}$  NMR spectra and 39.5 for  $^{13}\text{C}$  NMR spectra. Multiplicities are abbreviated as s = singlet, d = doublet, t = triplet, m = multiplet, br = broad, dd = doublet of doublets, dt = double of triplets. The coupling constants are expressed in Hertz. Mass spectrometric data were determined on a Waters Acquity UPLC system connected to Waters SQ Detector-2 operating in the electrospray ionisation (ESI) positive ion mode on a Waters Acquity UPLC BEH C18 column (1.7  $\mu\text{m}$ , 2.1  $\times$  50 mm) using a gradient elution with acetonitrile (0.01% trifluoroacetic acid) in water (0.01% trifluoroacetic acid) at a flow rate of 0.5 mL  $\text{min}^{-1}$ . LC-MS data were recorded with a Waters MassLynx 4.1 chromatography data system. The compounds were analysed by HPLC on a Waters Alliance 2695 system with a Waters 2485 UV/Vis detector equipped with an Alltima CN column (5  $\mu\text{m}$ , 4.6  $\times$  150 mm, Grace) using a gradient elution with acetonitrile/phosphoric acid (0.1%) in water, at a flow rate of 1 mL  $\text{min}^{-1}$ . Peak areas were determined electronically with a Waters Empower 2 chromatography data system. Infrared spectra ( $\nu_{\text{max}}$ ) were recorded with an FTIR spectrometer Prestige-21 (Shimadzu) and samples **4b–e** were analysed as thin films and **4a** as a Nujol mull. Melting points of

the synthesised compounds were determined on an OptiMelt (SRS Stanford Research Systems). Elemental analyses were performed on an EA 1106 (Carlo Erba Instruments).

### Synthesis

#### Synthesis of Compounds **1a–e**

The 1,4-DHP derivatives **1a**, **b**, and **e** were obtained from the corresponding acetoacetate, corresponding pyridinecarboxaldehyde, and ammonia by a classical Hantzsch synthesis in analogy with the literature. Using pentane-2,4-dione instead of acetoacetate led to the formation of 3,5-diacetyl-1,4-DHP derivative **1c**. 1,4-DHP derivative **1d** was synthesised starting from the 3-aminocrotonitrile and 3-pyridinecarboxaldehyde according to the literature.<sup>[6d,22]</sup>

#### General Method for Synthesis of Compounds **4a–e**

To a solution of the corresponding 1,4-DHP derivative (0.66 mM, 1 equiv.) in acetone (15 mL) was added a solution of propargyl bromide in toluene (0.99 mM, 106  $\mu$ L, 1.5 equiv.). The reaction mixture was refluxed in a pressure tube for 22 h, after which it was cooled to room temperature. The resulting precipitate was filtered off, washed with acetone, recrystallised from a mixture of acetone/methanol, and dried under vacuum.

#### Dimethyl 4-(1-(2-(3-(3,5-Bismethoxycarbonyl)-2,6-dimethyl-1,4-dihydropyridin-4-yl)pyridin-1-ium-1-yl)allyl)pyridin-1-ium-3-yl)-2,6-dimethyl-1,4-dihydropyridine-3,5-dicarboxylate Dibromide (**4a**)

Yield: 41 % (per 1,4-DHP derivative) of a brown powder. Mp 205°C (dec.).  $\nu_{\max}$  (Nujol)/ $\text{cm}^{-1}$  3404, 3161, 1699, 1619.  $\delta_{\text{H}}$  9.27 and 9.25 (2  $\times$  s, 2  $\times$  1H, NH) overlap, 9.05 and 8.98 (2  $\times$  d, *J* 6.3, 2  $\times$  1H, 6H-Py), 9.02 (br s, 2H, 2H-Py), 8.55 and 8.51 (2  $\times$  d, *J* 8.2, 2  $\times$  1H, 4H-Py), 8.21 and 8.17 (2  $\times$  dd, *J* 8.2 and *J* 6.3, 2  $\times$  1H, 5H-Py), 6.14 and 5.64 (AB-system, *J* 3.1, 2H, C=CH<sub>2</sub>), 6.00 (br s, 2H, N<sup>+</sup>-CH<sub>2</sub>), 5.04 and 4.98 (2  $\times$  s, 2  $\times$  1H, 4-H), 3.55 and 3.53 (2  $\times$  s, 2  $\times$  6H, 2,6-CH<sub>3</sub>) overlap, 2.31 and 2.30 (2  $\times$  s, 2  $\times$  6H, 3,5-CH<sub>3</sub>) overlap.  $\delta_{\text{C}}$  166.4 and 166.3 (C=O), 148.4 and 148.0, 147.9 and 147.8 (2,6-C-DHP), 143.6, 143.3 and 143.1, 142.5 and 141.4, 129.0 and 128.6, 99.2 and 99.1 (3,5-C-DHP), 96.5 and 96.4 (-CH<sub>2</sub>=C), 60.6 (N-CH<sub>2</sub>), 50.9 (OCH<sub>2</sub>), 37.9 and 37.8 (4-C-DHP), 18.2. *m/z* (ESI<sup>+</sup>) 644 (<sup>79</sup>Br) (5 %, [M-2Br]<sup>+</sup>), 322 (100, [M-2Br]<sup>+/2</sup>). Anal. Calc. for C<sub>35</sub>H<sub>40</sub>N<sub>4</sub>O<sub>8</sub>Br<sub>2</sub>·H<sub>2</sub>O: C 51.11, H 5.15, N 6.81. Found: C 50.85, H 5.17, N 6.54 %.

#### Diethyl 4-(1-(2-(3-(3,5-Bisethoxycarbonyl)-2,6-dimethyl-1,4-dihydropyridin-4-yl)pyridin-1-ium-1-yl)allyl)pyridin-1-ium-3-yl)-2,6-dimethyl-1,4-dihydropyridine-3,5-dicarboxylate Dibromide (**4b**)

Yield: 65 % (per 1,4-DHP derivative) of a yellowish powder. Mp 235°C (dec.).  $\nu_{\max}$  (film)/ $\text{cm}^{-1}$  3255, 3199, 1694, 1673.  $\delta_{\text{H}}$  9.23 and 9.21 (2  $\times$  s, 2  $\times$  1H, NH) overlap, 9.04 (m, 2H, 2H-Py) overlap, 9.03 and 8.98 (2  $\times$  s, 2  $\times$  1H, 6H-Py) overlap, 8.55 and 8.51 (2  $\times$  dt, *J* 8.2 and *J* 1.2, 2H, 4H-Py), 8.21 and 8.18 (2  $\times$  dd, *J* 8.2 and *J* 5.9, 2  $\times$  1H, 5H-Py), 6.15 and 5.62 (AB-system, *J* 3.1, 2H, C=CH<sub>2</sub>), 6.06 (br s, 2H, N<sup>+</sup>-CH<sub>2</sub>), 5.02 and 4.96 (2  $\times$  s, 2  $\times$  1H, 4-H), 4.00 (m, 8H, 3,5-CH<sub>2</sub>), 2.30 and 2.29 (2  $\times$  s, 2  $\times$  6H, 2,6-CH<sub>3</sub>) overlap, 1.13 and 1.12 (2  $\times$  t, *J* 7.0, 2  $\times$  6H, 3,5-CH<sub>3</sub>) overlap.  $\delta_{\text{C}}$  166.7 (C=O), 149.4 and 148.9, 148.4 and 148.2 (2,6-C-DHP), 147.3 and 146.7, 144.2 and 143.2, 129.6 and 129.2, 121.7, 100.1 and 100.0 (3,5-C-DHP), 99.9 and 99.8 (-CH<sub>2</sub>=C), 61.0 (N-CH<sub>2</sub>), 60.2 (OCH<sub>2</sub>), 38.9 and 38.8

(4-C-DHP), 19.0, 14.8. *m/z* (ESI<sup>+</sup>) 700 (<sup>79</sup>Br) (5 %, [M-2Br]<sup>+</sup>), 350 (100, [M-2Br]<sup>+/2</sup>). Anal. Calc. for C<sub>39</sub>H<sub>48</sub>N<sub>4</sub>O<sub>8</sub>Br<sub>2</sub>: C 54.43, H 5.62, N 6.51. Found: C 54.42, H 5.50, N 6.22 %.

#### 4-(1-(2-(3-(3,5-Bisacetyl-2,6-dimethyl-1,4-dihydropyridin-4-yl)pyridin-1-ium-1-yl)allyl)pyridin-1-ium-3-yl)-3,5-bisacetyl-2,6-dimethyl-1,4-dihydropyridine Dibromide (**4c**)

Yield: 68 % (per 1,4-DHP derivative) of a brown powder. Mp 90°C (dec.).  $\nu_{\max}$  (film)/ $\text{cm}^{-1}$  3314, 3267, 1664, 1622.  $\delta_{\text{H}}$  9.29 and 9.27 (2  $\times$  s, 2  $\times$  1H, NH) overlap, 8.95 and 8.86 (2  $\times$  m, 2  $\times$  1H, 6H-Py) overlap, 8.91 (br s, 2H, 2H-Py), 8.36 and 8.31 (2  $\times$  d, *J* 8.2, 2  $\times$  1H, 4H-Py), 8.11 and 8.05 (2  $\times$  m, 2  $\times$  1H, 5H-Py), 6.17 and 5.95 (AB-system, *J* 2.7, 2H, C=CH<sub>2</sub>), 6.06 (br s, 2H, N<sup>+</sup>-CH<sub>2</sub>), 5.15 and 5.09 (2  $\times$  s, 2  $\times$  1H, 4-H), 2.36 (s, 12H, 2,6-CH<sub>3</sub>), 2.22 (s, 12H, 3,5-CH<sub>3</sub>).  $\delta_{\text{C}}$  195.7 and 195.6 (C=O), 148.3 and 148.0, 147.7 and 147.6 (2,6-C-DHP), 143.8, 143.6 and 143.2, 142.3 and 142.2, 129.3 and 128.9, 111.6 and 111.4 (3,5-C-DHP), 111.0 and 110.4 (-CH<sub>2</sub>=C), 61.3 (N-CH<sub>2</sub>), 37.4 and 37.3 (4-C-DHP), 31.4, 19.9. *m/z* (ESI<sup>+</sup>) 580 (<sup>79</sup>Br) (3 %, [M-2Br]<sup>+</sup>), 290 (100 %, [M-2Br]<sup>+/2</sup>). Anal. Calc. for C<sub>35</sub>H<sub>40</sub>N<sub>4</sub>O<sub>4</sub>Br<sub>2</sub>: C 57.17, H 5.58, N 7.17. Found: C 56.77, H 5.44, N 7.57 %.

#### 4-(1-(2-(3-(3,5-Biscyano-2,6-dimethyl-1,4-dihydropyridin-4-yl)pyridin-1-ium-1-yl)allyl)pyridin-1-ium-3-yl)-3,5-biscyano-2,6-dimethyl-1,4-dihydropyridine Dibromide (**4d**)

Yield: 72 % (per 1,4-DHP derivative) of a brown powder. Mp: 203°C (dec.).  $\nu_{\max}$  (film)/ $\text{cm}^{-1}$  3464, 3176, 2199, 1660.  $\delta_{\text{H}}$  9.95 and 9.94 (2  $\times$  s, 2  $\times$  1H, NH) overlap, 9.28 (br s, 2H, 2-H-Py), 9.25 and 9.22 (2  $\times$  d, *J* 6.3, 2  $\times$  1H, 6H-Py), 8.81 and 8.77 (2  $\times$  d, *J* 8.2, 2  $\times$  1H, 4H-Py), 8.36 and 8.32 (2  $\times$  dd, *J* 8.2 and *J* 6.3, 2  $\times$  1H, 5H-Py), 6.35 and 6.08 (AB-system, *J* 2.7, 2H, C=CH<sub>2</sub>), 6.16 (br s, 2H, N<sup>+</sup>-CH<sub>2</sub>), 4.93 (br s, 2H, 4-H), 2.10–2.06 (m, 12H, 2,6-CH<sub>3</sub>).  $\delta_{\text{C}}$  149.7 and 149.5 (2,6-C-DHP), 147.9, 147.1, 145.9, 145.1, 144.3, 143.9, 143.8, 143.2, 142.2, 130.0 and 129.6, 124.3, 119.0 and 118.9 (CN), 103.8 and 103.7 (-CH<sub>2</sub>=C), 80.3 and 80.1 (3,5-C-DHP), 61.4 (N-CH<sub>2</sub>), 38.8 (4-C-DHP), 18.5. *m/z* (ESI<sup>+</sup>) 512 (<sup>79</sup>Br) (3 %, [M-2Br]<sup>+</sup>), 256 (100, [M-2Br]<sup>+/2</sup>). Anal. Calc. for C<sub>31</sub>H<sub>28</sub>N<sub>8</sub>Br<sub>2</sub>·0.4 (CH<sub>3</sub>)<sub>2</sub>CO: C 55.60, H 4.40, N 16.11. Found: C 55.61, H 4.38, N 15.76 %.

#### Diethyl 4-(1-(2-(4-(3,5-Bisethoxycarbonyl)-2,6-dimethyl-1,4-dihydropyridin-4-yl)pyridin-1-ium-1-yl)allyl)pyridin-1-ium-4-yl)-2,6-dimethyl-1,4-dihydropyridine-3,5-dicarboxylate Dibromide (**4e**)

Yield: 59 % (per 1,4-DHP derivative) of a yellowish powder. Mp: 176°C (dec.).  $\nu_{\max}$  (film)/ $\text{cm}^{-1}$  3246, 3191, 1691, 1634.  $\delta_{\text{H}}$  9.30 and 9.26 (2  $\times$  s, 2  $\times$  1H, NH), 9.04 and 8.97 (2  $\times$  d, *J* 7.0, 2  $\times$  2H, 2,6-H-Py), 7.92 (dd, *J* 7.0 and *J* 2.0, 4H, 3,5-H-Py), 6.25 and 5.76 (AB-system, *J* 3.1, 2H, C=CH<sub>2</sub>), 5.86 (br s, 2H, N<sup>+</sup>-CH<sub>2</sub>), 5.11 and 5.08 (2  $\times$  s, 2  $\times$  1H, 4-H), 4.02 (m, 8H, 3,5-CH<sub>2</sub>), 2.31 and 2.30 (2  $\times$  s, 2  $\times$  6H, 2,6-CH<sub>3</sub>) overlap, 1.13 and 1.11 (2  $\times$  t, *J* 7.0, 2  $\times$  6H, 3,5-CH<sub>3</sub>) overlap.  $\delta_{\text{C}}$  167.4 and 166.8, 166.2 and 166.1 (C=O), 148.4 and 148.2 (2,6-C-DHP), 145.2, 144.1, 142.8, 127.1 and 126.6, 99.1 and 99.0 (3,5-C-DHP), 98.9 and 98.8 (-CH<sub>2</sub>=C), 60.0 (N-CH<sub>2</sub>), 59.9 and 59.8 (OCH<sub>2</sub>), 40.8 and 40.7 (4-C-DHP), 18.6 and 18.5, 14.3. *m/z* (ESI<sup>+</sup>) 700 (<sup>79</sup>Br) (6 %, [M-2Br]<sup>+</sup>), 350 (100, [M-2Br]<sup>+/2</sup>). Anal. Calc. for C<sub>39</sub>H<sub>48</sub>N<sub>4</sub>O<sub>8</sub>Br<sub>2</sub>·2H<sub>2</sub>O: C 52.24, H 5.85, N 6.25. Found: C 52.14, H 5.55, N 6.09 %.

### X-Ray Crystallography

Diffraction data were collected at  $-100^{\circ}\text{C}$  on a Bruker-Nonius KappaCCD diffractometer using graphite monochromated  $\text{MoK}\alpha$  radiation ( $\lambda$  0.71073 Å). The crystal structure of bispyridinium dibromide **4b** was solved by direct methods and refined by full-matrix least-squares. All non-hydrogen atoms were refined in anisotropical approximation, all H-atoms were refined by riding model. Crystal data for bispyridinium dibromide **4b**: monoclinic;  $a$  16.3981(3),  $b$  12.3954(2),  $c$  19.9004(5) Å,  $\beta$  104.7206(7) $^{\circ}$ ;  $V$  3912.2(1) Å $^3$ ,  $Z$  4,  $\mu$  2.128 mm $^{-1}$ ,  $d_c$  1.461 g cm $^{-3}$ ; space group is  $C2/c$ . A total of 4672 independent reflection intensities were collected up to  $2\theta_{\text{max}}$  56 $^{\circ}$ ; for structure refinement 3436 reflections with  $I > 2\sigma(I)$  were used. The final  $R$ -factor is 0.0472. For further details, see crystallographic data for **4b** deposited with the Cambridge Crystallographic Data Centre as Supplementary Publication Number CCDC 978170. Copies of the data can be obtained, free of charge, on application to CCDC, 12 Union Road, Cambridge CB2 1EZ, UK.

### Evaluation of the Compounds' Reducing Capacity (RC)

The RC of the synthesised bispyridinium 1,4-DHP derivatives **4a–e** was studied using spectrophotometric quantitation of the RC through the formation a phosphomolybdenum complex.<sup>[20]</sup> Stock solutions of the tested compounds and reference Diludine of 1.0 mM were prepared in ethanol just before use. The final reagent solution contained 0.6 M sulfuric acid, 28 mM sodium phosphate, and 4 mM ammonium molybdate solutions in water. An aliquot of 0.3 mL of the sample solution was combined in an Eppendorf tube with 3 mL of the reagent solution. The tubes were capped and incubated in a thermal block at 95 $^{\circ}\text{C}$  for 90 min. After the samples were cooled to room temperature, the absorbance of each sample solution was measured at 695 nm against a blank sample using a UV/Vis Camspec M501 spectrometer (UK). A typical blank solution contained 3 mL of the reagent solution and the appropriate volume of ethanol (0.3 mL) as the solvent, and was incubated under the same conditions as the rest of the samples. Each assay was performed in triplicate. Results were expressed as a percentage.

### ARA Studies: DPPH Radical Scavenging Assay

Free radical scavenging activity of the synthesised 1,4-DHP derivatives **4a–e** was evaluated by their ability to react with a stable radical of DPPH. An aliquot (0.5 mL) of the tested 1,4-DHP derivative or Diludine solution in ethanol (0.6 mM) was added to 3 mL of freshly prepared DPPH solution in EtOH (0.1 mM). The final concentration of the tested compound was 0.086 mM and the ratio of the tested compound and DPPH was equimolar. The solution was incubated for 30 min in the dark and changes in the optical density of solution were measured at 517 nm using a UV/Vis Camspec M501 spectrometer (UK). Each assay was performed in triplicate. The scavenging activity was defined as the decrease in sample absorbance versus absorbance of DPPH standard solutions. Results were expressed as a percentage of the DPPH free radical scavenging, which is defined by the following formula:

$$\text{ARA (\%)} = \frac{A_{\text{control}} - A_{\text{sample}}}{A_{\text{control}}} \times 100$$

where  $A_{\text{control}}$  is the absorbance of the standard solution of DPPH and  $A_{\text{sample}}$  is the absorbance value for the sample.<sup>[23]</sup>

### Acknowledgements

This research work was supported by the European Social Fund Project Nr. ESF 2013/0002/1DP/1.1.1.2.0/13/APIA/VIAA/005 and the European Social Fund within the project 'Support for Doctoral Studies at University of Latvia' (for Martins Rucins). The authors gratefully acknowledge the generous assistance and valuable information provided by Dr Gunars Tirzitis and Dr Janis Uldrikis.

### References

- [1] (a) N. Edraki, A. R. Mehdipour, M. Khoshneviszadeh, R. Miri, *Drug Discov. Today* **2009**, *14*, 1058. doi:10.1016/J.DRUDIS.2009.08.004  
(b) R. Lavilla, *J. Chem. Soc., Perkin Trans. 1* **2002**, 1141. doi:10.1039/B101371H  
(c) P. Ioan, E. Carosati, M. Micucci, G. Cruciani, F. Broccatelli, B. S. Zhorov, A. Chiarini, R. Budriesi, *Curr. Med. Chem.* **2011**, *18*, 4901. doi:10.2174/092986711797535173  
(d) E. Carosati, P. Ioan, M. Micucci, F. Broccatelli, G. Cruciani, B. S. Zhorov, A. Chiarini, R. Budriesi, *Curr. Med. Chem.* **2012**, *19*, 4306. doi:10.2174/092986712802884204
- [2] (a) D. J. Triggles, *Cell. Mol. Neurobiol.* **2003**, *23*, 293. doi:10.1023/A:1023632419813  
(b) D. J. Triggles, *Mini Rev. Med. Chem.* **2003**, *3*, 215. doi:10.2174/1389557033488141
- [3] G. Duburs, B. Vīgante, A. Plotniece, A. Krauze, A. Sobolevs, J. Briede, V. Kluša, A. Velēna, *Chim. Oggi* **2008**, *26*, 68.
- [4] (a) K. Fujimoto, D. Morisaki, M. Yoshida, T. Namba, K. Hye-Sook, Y. Wataya, H. Kourai, H. Kakuta, K. Sasaki, *Bioorg. Med. Chem. Lett.* **2006**, *16*, 2758. doi:10.1016/J.BMCL.2006.02.030  
(b) M. A. Ilies, W. A. Seitz, B. H. Johnson, E. L. Ezell, A. L. Miller, E. B. Thompson, A. T. Balaban, *J. Med. Chem.* **2006**, *49*, 3872. doi:10.1021/JM0601755
- [5] (a) V. Onnis, M. T. Cocco, R. Fadda, C. Congiu, *Bioorg. Med. Chem.* **2009**, *17*, 6158. doi:10.1016/J.BMC.2009.07.066  
(b) A. A. Kalinin, A. D. Voloshina, N. V. Kulik, V. V. Zobov, V. A. Mamedov, *Eur. J. Org. Chem.* **2013**, *66*, 345. doi:10.1016/J.EJMECH.2013.05.038  
(c) A. Cornellas, L. Perez, F. Comelles, I. Ribosa, A. Manresa, M. T. Garcia, *J. Colloid Interface Sci.* **2011**, *355*, 164. doi:10.1016/J.JCIS.2010.11.063  
(d) K. Musilek, M. Komloova, V. Zavadova, O. Holas, M. Hrabnina, M. Pohanka, V. Dohnal, F. Nachon, M. Dolezal, K. Kuca, Y. S. Jung, *Bioorg. Med. Chem. Lett.* **2010**, *20*, 1763. doi:10.1016/J.BMCL.2010.01.034  
(e) V. Alptuzun, M. Prinz, V. Horr, J. Scheiber, K. Radacki, A. Fallarero, P. Vuorela, B. Engels, H. Braunschweig, E. Erciyas, U. Holzgrabe, *Bioorg. Med. Chem.* **2010**, *18*, 2049. doi:10.1016/J.BMC.2010.01.002  
(f) V. D. Sharma, E. O. Aifuwa, P. A. Heiney, M. A. Ilies, *Biomaterials* **2013**, *34*, 6906. doi:10.1016/J.BIOMATERIALS.2013.05.029
- [6] (a) D. Tirzite, J. Koronova, A. Plotniece, *IUBMB Life* **1998**, *45*, 849. doi:10.1080/15216549800203282  
(b) Z. Hyvonen, A. Plotniece, I. Reine, B. Chekavichus, G. Duburs, A. Urtti, *Biochim. Biophys. Acta* **2000**, *1509*, 451. doi:10.1016/S0005-2736(00)00327-8  
(c) K. Pajuste, Z. Hyvonen, O. Petrichenko, D. Kaldre, M. Rucins, B. Cekavicus, V. Ose, B. Skrivele, M. Gosteva, E. Morin-Picardat, M. Plotniece, A. Sobolev, G. Duburs, M. Ruponen, A. Plotniece, *New J. Chem.* **2013**, *37*, 3062. doi:10.1039/C3NJ00272A  
(d) M. Rucins, D. Kaldre, K. Pajuste, M. A. S. Fernandes, J. A. F. Vicente, L. Klimaviciusa, E. Jaschenko, I. Kanep-Lapsa, I. Shestakova, M. Plotniece, M. Gosteva, A. Sobolev, B. Jansone, R. Muceniece, V. Klusa, A. Plotniece, *C. R. Chim.* **2014**, *17*, 69. doi:10.1016/J.CRCI.2013.07.003
- [7] O. Weinreb, T. Amit, O. Bar-Am, M. B. Youdim, *Prog. Neurobiol.* **2010**, *92*, 330. doi:10.1016/J.PNEUROBIO.2010.06.008
- [8] L. Zhang, J. Dong, J. Liu, L. Kong, H. Yao, H. Sun, *Med. Chem.* **2013**, *9*, 118. doi:10.2174/157340613804488413

- [9] (a) A. A. P. Meekel, A. Wagenaar, J. Šmisterová, J. E. Kroeze, P. Haadsma, B. Bosgraaf, M. C. A. Stuart, A. Brisson, M. H. J. Ruiters, D. Hoekstra, J. B. F. N. Engberts, *Eur. J. Org. Chem.* **2000**, 2000, 665. doi:10.1002/(SICI)1099-0690(200002)2000:4<665::AID-EJOC665>3.0.CO;2-A  
(b) D. Pijper, E. Bulten, J. Šmisterová, A. Wagenaar, D. Hoekstra, J. B. F. N. Engberts, R. Hulst, *Eur. J. Org. Chem.* **2003**, 2003, 4406. doi:10.1002/EJOC.200300361
- [10] N. V. Makarova, Z. V. Koronova, A. V. Plotnietse, D. Y. Tirezite, G. D. Tirzitz, G. Y. Duburs, *Chem. Heterocycl. Compd.* **1995**, 31, 969. doi:10.1007/BF01170324
- [11] (a) Z. Jia, Q. Zhu, *Bioorg. Med. Chem. Lett.* **2010**, 20, 6222. doi:10.1016/J.BMCL.2010.08.104  
(b) W. Chen, S. A. Elfeky, Y. Nonne, L. Male, K. Ahmed, C. Amiable, P. Axe, S. Yamada, T. D. James, S. D. Bull, J. S. Fossey, *Chem. Commun.* **2011**, 47, 253. doi:10.1039/C0CC01420F
- [12] A. R. Katritzky, O. A. Schwarz, O. Rubio, D. G. Markees, *Helv. Chim. Acta* **1984**, 67, 939. doi:10.1002/HLCA.19840670404
- [13] L. V. Kanitskaya, V. N. Elokina, S. V. Fedorov, A. M. Shulunova, A. S. Nakhmanovich, V. K. Turchaninov, V. A. Lopyrev, *Russ. J. Gen. Chem.* **2002**, 72, 778. doi:10.1023/A:1019572605480
- [14] K. Pajuste, M. Gosteva, D. Kaldre, M. Plotniece, B. Cekavicus, A. Sobolev, A. Priksane, G. Tirzitis, G. Duburs, A. Plotniece, *Chem. Heterocycl. Compd.* **2011**, 47, 597. doi:10.1007/S10593-011-0803-3
- [15] E. E. Liepin'sh, R. M. Zolotoyabko, B. S. Chekavichus, A. E. Sausin, V. K. Lusic, G. Y. Dubur, *Chem. Heterocycl. Compd.* **1989**, 25, 1032. doi:10.1007/BF00487304
- [16] A. Augustyniak, G. Bartosz, A. Cipak, G. Duburs, L. Horakova, W. Luczaj, M. Majekova, A. D. Odysseos, L. Rackova, E. Skrzydlewska, M. Stefek, M. Strosova, G. Tirzitis, P. R. Venskutonis, J. Viskupicova, P. S. Vranka, N. Zarkovic, *Free Radic. Res.* **2010**, 44, 1216. doi:10.3109/10715762.2010.508495
- [17] (a) F. P. Guengerich, W. R. Brian, M. Iwasaki, M. A. Sari, C. Baarnhielm, P. Berntsson, *J. Med. Chem.* **1991**, 34, 1838. doi:10.1021/JM00110A012  
(b) R. H. Boecker, F. P. Guengerich, *J. Med. Chem.* **1986**, 29, 1596. doi:10.1021/JM00159A007
- [18] (a) G. D. Tirzitz, G. Y. Dubur, *Chem. Heterocycl. Compd.* **1972**, 8, 126. doi:10.1007/BF00478512  
(b) G. D. Tirzitz, I. M. Byteva, K. I. Salokhiddinov, G. P. Gurinovich, G. Y. Dubur, *Chem. Heterocycl. Compd.* **1981**, 17, 682. doi:10.1007/BF00506035  
(c) E. Y. Kazush, E. I. Sagun, G. D. Tirzitz, G. Y. Dabur, *Chem. Heterocycl. Compd.* **1994**, 30, 562. doi:10.1007/BF01169834
- [19] W. Brand-Williams, M. E. Cuvelier, C. Berset, *LWT - Food Sci. Technol.* **1995**, 28, 25. doi:10.1016/S0023-6438(95)80008-5
- [20] P. Prieto, M. Pineda, M. Aguilar, *Anal. Biochem.* **1999**, 269, 337. doi:10.1006/ABIO.1999.4019
- [21] (a) L. Kouřimská, J. Pokorný, G. Tirzitis, *Food/Nahrung* **1993**, 37, 91. doi:10.1002/FOOD.19930370121  
(b) G. Tirzitis, D. Tirzite, Z. Hyvönen, *Czech. J. Food Sci.* **2001**, 19, 81.
- [22] (a) N. V. Makarova, A. Plotnietse, G. Tirzitis, I. Turovskii, G. Dubur, *Chem. Heterocycl. Compd.* **1997**, 33, 175. doi:10.1007/BF02256759  
(b) U. Eisner, J. Kuthan, *Chem. Rev.* **1972**, 72, 1. doi:10.1021/CR60275A001  
(c) L. Dagnino, M. C. Li-Kwong-Ken, M. W. Wolowyk, H. Wynn, C. R. Triggle, E. E. Knaus, *J. Med. Chem.* **1986**, 29, 2524. doi:10.1021/JM00162A016
- [23] A. Abdelwahed, I. Bouhlel, I. Skandrani, K. Valenti, M. Kadri, P. Guiraud, R. Steiman, A. M. Mariotte, K. Ghedira, F. Laporte, M. G. Dijoux-Franca, L. Chekir-Ghedira, *Chem. Biol. Interact.* **2007**, 165, 1. doi:10.1016/J.CBI.2006.10.003

## **Publication**

### **C**

Synthesis and evaluation of reducing capacity and calcium channel blocking activity of novel 3,5-dipropargylcarbonyl-substituted 1,4-dihydropyridines.  
*Хим. Гетероцикл. Соед.*, 2014, N10, 1557-1568; *Chem. Heterocycl. Comp.*  
*(Engl. Ed.)* 2015, 50(10).



## SYNTHESIS AND EVALUATION OF REDUCING CAPACITY AND CALCIUM CHANNEL BLOCKING ACTIVITY OF NOVEL 3,5-DIPROPARGYLCARBONYL-SUBSTITUTED 1,4-DIHYDROPYRIDINES\*

M. Rucins<sup>1,2</sup>, M. Gosteva<sup>1</sup>, I. Domracheva<sup>1</sup>, I. Kanepe-Lapsa<sup>1</sup>, S. Belyakov<sup>1</sup>, M. Plotniece<sup>1</sup>,  
K. Pajuste<sup>1</sup>, B. Cekavicus<sup>1</sup>, M. Jekabsone<sup>2</sup>, A. Sobolev<sup>1</sup>, I. Shestakova<sup>1</sup>, and A. Plotniece<sup>1\*\*</sup>

*Novel pyridinium salts based on 4-(3-pyridyl)-3,5-dipropargylcarbonyl-1,4-dihydropyridine were obtained by quaternization of pyridine moiety with different alkyl halides. The reducing capacity of the synthesized compounds was evaluated using the phosphomolybdenum complex method. The obtained results confirmed that all tested compounds possessed reducing capacity. Ca<sup>2+</sup> channel antagonist and agonist activities of the compounds were additionally assayed by changes in intracellular Ca<sup>2+</sup> ion concentration in H9C2 and A7R5 cell lines. The obtained data confirmed that all synthesized 1,4-dihydropyridine derivatives have smooth muscle selective antagonist activities, and in the case of 4-phenyl derivative the activity was 4.7 times higher than that of amlodipine.*

**Keywords:** N-alkyl pyridinium, 1,4-dihydropyridines, calcium antagonists, Hantzsch synthesis, quaternization, reducing capacity.

The 1,4-dihydropyridine (1,4-DHP) derivatives are nitrogen-containing heterocyclic compounds playing an important role in medicinal, synthetic, and bioorganic chemistry [1-3]. Several representatives of 1,4-DHPs such as nifedipine, nitrendipine, amlodipine, and nisoldipine belong to the class of calcium channel modulating agents [4-6] used worldwide. Depending on the chemical structure peculiarities, dihydropyridine derivatives also possess other activities that are not related to calcium modulating, such as antimutagenic, antidiabetic, neuro- and radioprotective, anti-inflammatory, antianginal, and antihypertensive action, besides being regarded as perspective gene transfection agents [7]. The observation that 1,4-DHP derivatives, such as nifedipine [8], show activity as inhibitors of the multidrug resistance transporter has increased renewed interest for DHPs [9-11]. 1,4-DHPs are regarded as analogs of 1,4-dihydropyridinone and model compounds of redox coenzymes NAD(P)-H. Depending on their structure, 1,4-DHPs possess antioxidant, radical scavenging properties, and they quench reactive oxygen species [12]. Antiradical and antioxidant properties of

---

\*Dedicated to Academician Professor G. Duburs on the occasion of his 80th birthday.

\*\*To whom correspondence should be addressed, e-mail: aiva@osi.lv.

<sup>1</sup>Latvian Institute of Organic Synthesis, 21 Aizkraukles St., Riga LV-1006, Latvia.

<sup>2</sup>Faculty of Medicine, University of Latvia, 19 Raina Blvd., Riga LV-1586, Latvia; e-mail: rucins@osi.lv.

some representative of 1,4-DHPs have been discovered, as they act as hydrogen and electron donors to oxidants, reactive oxygen species, reactive nitrogen species, free radicals, or activated unsaturated compounds [13].

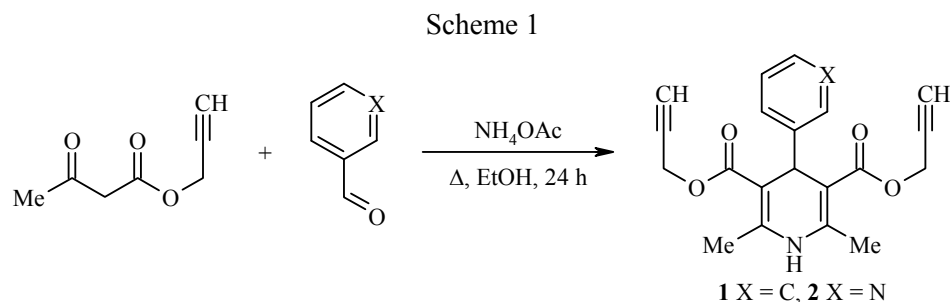
Changes in calcium level regulate important functions in the cells and in the organism. Dihydropyridines affect calcium levels, and they are widely used for treatment of many cardiovascular diseases [14]. Calcium channel blockers based on 1,4-DHP also selectively inhibit the influx of  $\text{Ca}^{2+}$  ions through calcium channels in the smooth muscle membrane, and they have been used in the therapy of angina pectoris and hypertension [15].

On the other hand, during the last decades the neurotropic properties of 1,4-DHP have been widely studied. Several research groups have experimentally demonstrated the ability of 1,4-DHPs to penetrate the blood-brain barrier [16, 17]. Moreover, the propargyl moiety is known to play an important role in providing neuroprotective properties in antidepressants, such as selegiline and rasagiline [18]. The combination of two active pharmacophore groups or compounds into the same molecule is one of the strategies in medicinal chemistry for drug design and drug discovery [19].

Our group has developed various pyridinium moiety-containing 1,4-DHPs for studies of their membranotropic effects [20]. Calcium antagonistic properties and antioxidant activity of 1,4-DHP derivatives containing a cationic pyridinium moiety at position 4 and *N*-propargyl group at position 1 of the 1,4-dihydropyridine cycle have also been studied by our research group giving a basic background which permits drawing conclusions concerning structure–activity relationships [21]. However, it would be beneficial to continue studies on the influence of propargyl substituent position in the 1,4-DHP molecule on the mentioned activities for final conclusions.

The aim of the present work was to obtain novel pyridinium salts based on 4-pyridyl-substituted 3,5-dipropargylcarbonyl-1,4-dihydropyridines, varying the substituent at the nitrogen atom in the pyridine ring by quaternization of the pyridine fragment of 2,6-dimethyl-3,5-dipropargylcarbonyl-4-(3-pyridyl)-1,4-dihydropyridine as potential biologically active compounds. Studies of reducing capacity (RC) and calcium channel blocking activity of the synthesized compounds were another objective of this work.

The propargyl acetoacetate was synthesized according to the procedure described by Cruciani et al. [22] starting from propargyl alcohol and 2,2,6-trimethyl-1,3-dioxin-4-one. Hantzsch-type 1,4-DHPs **1** and **2** for our studies were synthesized with 61 and 82% yields, respectively, *via* typical synthetic routes, such as the Hantzsch synthesis [23, 24]. It involves a one-pot cyclocondensation of the corresponding aldehyde, propargyl acetoacetate, and ammonium acetate under 24 h reflux in ethanol (Scheme 1).



In order to decrease the reaction time and improve the product yield, the synthesis of compound **2** with the same reagent ratio was performed under microwave conditions. The irradiation during 30 min at 80°C gave the 1,4-DHP derivative **2** in 52% isolated yield.

1,4-DHP derivative **1** has been described in the literature by Liepinsh et al. [24]. For this compound, only  $^{13}\text{C}$  NMR data and melting point (mp 143-144°C, recrystallized from ethanol) were reported previously [24]. In this case, the melting point of compound **1** was lower – 124-126°C. This could be explained by using a different technique for melting point determination and crystallization from methanol instead of ethanol. In the  $^1\text{H}$  NMR spectra, the signal of the CH proton of the propargyl groups was observed as a triplet at 2.41 ppm with

the coupling constant 2.4 and 2.5 Hz for 1,4-DHP derivatives **1** and **2**, respectively, while the signals for the CH<sub>2</sub> group protons were detected at 4.64 and 4.63 ppm with different multiplicities: an AB system of double doublets with coupling constants 15.6 and 2.4 Hz for compound **1** and a doublet with coupling constant 2.5 Hz for derivative **2**.

For an objective assessment of the structure of compounds **1** and **2**, an X-ray crystallographic analysis of the crystals of these compounds was undertaken. The crystal structure of compound **1** significantly differs from that of compound **2**. There are four independent molecules in the asymmetric unit in crystal of compound **1** (Fig. 1) The deviations of nitrogen atom N(1) from the C(2)–C(3)–C(5)–C(6) plane of dihydropyridine are

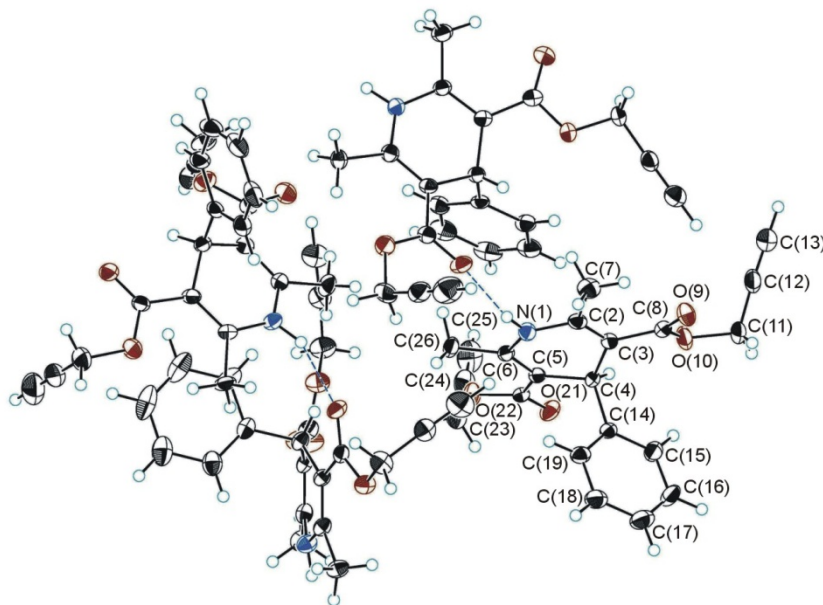


Fig. 1. Four independent molecules of the 1,4-DHP derivative **1** in the asymmetric unit; the atoms are represented as thermal vibration ellipsoids of 50% probability.

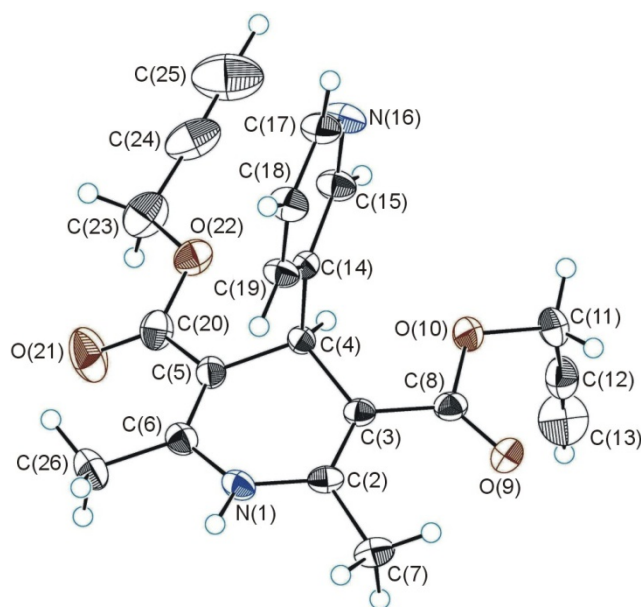


Fig. 2. Molecular structure of 1,4-DHP derivative **2** with atoms represented as thermal vibration ellipsoids of 50% probability.

TABLE 1. The Main Crystallographic Data and Refinement Parameters of the Structures of 1,4-DHP Derivatives **1** and **2**\*

Parameters	Compound <b>1</b>	Compound <b>2</b>
Empirical formula	C <sub>21</sub> H <sub>19</sub> NO <sub>4</sub>	C <sub>20</sub> H <sub>18</sub> N <sub>2</sub> O <sub>4</sub>
Molecular weight	349.39	350.37
Crystal system	Monoclinic	Monoclinic
<i>a</i> , Å	12.8538(1)	8.6757(3)
<i>b</i> , Å	11.8689(1)	15.4092(7)
<i>c</i> , Å	23.6725(3)	13.9313(7)
β, deg	93.9579(4)	97.882(2)
<i>V</i> , Å <sup>3</sup>	3602.87(6)	1844.8(1)
Space group	<i>Pc</i>	<i>P2<sub>1</sub>/a</i>
<i>Z</i>	8	4
μ, mm <sup>-1</sup>	0.089	0.089
<i>d</i> <sub>calc</sub> , g/cm <sup>3</sup>	1.288	1.262
2θ <sub>max</sub> for data, deg.	56.0	56.0
Reflections collected	26251	7652
Independent reflections	8585 ( <i>R</i> <sub>int</sub> 0.032)	4365 ( <i>R</i> <sub>int</sub> 0.036)
Reflections with <i>I</i> > 3σ( <i>I</i> )	7032	2782
Final <i>R</i> factor	0.071	0.053
<i>wR</i> <sub>2</sub> index for all data	0.201	0.238
CCDC deposit number	CCDC 1013346	CCDC 1013345

\*Crystal structure refinement was performed using SIR97 [27] and maXus [28] software.

different for each of the four molecules: 0.135(3), 0.149(3), 0.160(3), and 0.168(3) Å. The deviations of C(4) atom are 0.294(4), 0.304(4), 0.334(4), and 0.361(1) Å, respectively. The phenyl rings are nearly perpendicular to the mean planes of DHP. In the crystal structure, there are intermolecular hydrogen bonds between N–H group and carbonyl oxygen of ester group. The lengths of these hydrogen bonds are in the range from 2.890(3) to 2.985(3) Å.

Figure 2 shows a perspective view of the molecule of 1,4-DHP derivative **2** in a crystal. The dihydropyridine cycle is characterized by the usual boat conformation [25, 26]. The deviations of atoms N(1) and C(4) from the plane C(2)–C(3)–C(5)–C(6) are equal to 0.155(2) and 0.341(3) Å, respectively. The dihedral angle between pyridine ring and the mean plane of dihydropyridine cycle is 87.9(5)°. In the crystal structure of compound **2**, there are strong intermolecular hydrogen bonds of NH···N type between nitrogen atom N(16) and N(1)–H group; the length of this bond is 2.899(2) Å. By means of these bonds chains along crystallographic direction (100) are formed in the crystals. Basic crystallographic data, conditions, and parameters of the X-ray diffraction structure refinement of 1,4-DHP derivatives **1** and **2** are listed in Table 1.

As the next step of our work, the synthesis of various 1,4-DHP *N*-alkylpyridinium salts **3–9** was performed by alkylation of dipropargyl 1,4-DHP ester **2** with the corresponding alkyl bromides in acetone under reflux (Scheme 2, Table 2).

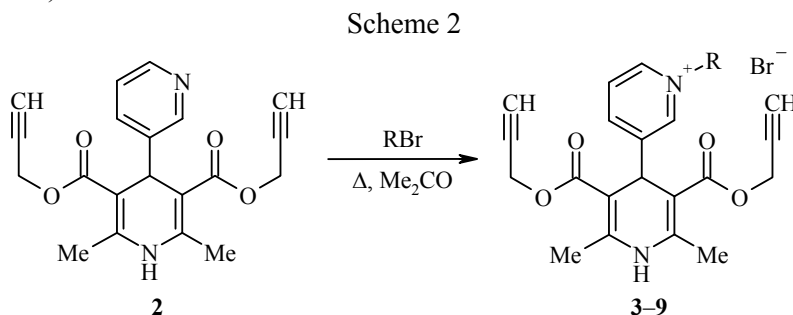


TABLE 2. Alkylation Reaction Parameters for the Synthesis of 1,4-DHP *N*-Alkylpyridinium Derivatives **3-9**

Com- pound	R	Ratio 1,4-DHP <b>2</b> – RBr	Amount of RBr, mmol/ml	Reaction time, h	Yield, %
<b>3</b>	Et	1:8	6.88/0.52	75	65
<b>4</b>	<i>n</i> -Bu	1:3	2.58/0.28	100	36
<b>5</b>	C <sub>6</sub> H <sub>11</sub>	1:3	2.58/0.36	201	57
<b>6</b>	C <sub>8</sub> H <sub>19</sub>	1:3	2.58/0.45	77	64
<b>7</b>	C <sub>10</sub> H <sub>21</sub>	1:3	2.58/0.54	201	65
<b>8</b>	C <sub>12</sub> H <sub>25</sub>	1:2	1.72/0.42	128	73
<b>9</b>	C <sub>14</sub> H <sub>29</sub>	1:4	3.44/1.04	222	65

The typical procedure for the quaternization of pyridine derivatives has been reported by several research groups [29]. Quaternization includes treating of pyridines with the corresponding alkyl halides in acetone under reflux. An approach to reduce the reaction time of quaternization by the use of an excess of alkyl bromide was also reported [30]. In our case, the solution of 2-8-fold excess of the corresponding alkyl bromide was added to the starting dipropargyl ester **2**, and the reaction mixture was refluxed in a pressure tube for 75-222 h (Table 2). However, in a pressure tube the alkylation reactions were still found to be rather slow and proceeded with moderate yields of the products. In contrast, quaternization of the pyridine moiety of 3,5-diethoxycarbonyl-1,4-DHP with various alkyl bromides occurred in 5-26 h and with higher yields [21].

In order to attempt optimization of reaction conditions for the quaternization reaction of the pyridyl moiety in compound **2** with tetradecyl bromide, the reaction was performed under microwave conditions using the same reagent ratio (1:4) as in the conventional quaternization procedure. The reaction course was monitored by HPLC every 15 min. It was found that the desired quaternized 1,4-DHP derivative **9** was formed in only 8% yield under microwave conditions in 1 h at 70°C.

All the synthesized 1,4-DHP alkylpyridinium salts **3-9** were crystalline substances. In the <sup>1</sup>H NMR spectra, characteristic signals for the NCH<sub>2</sub> group protons were observed at 4.56-4.73 ppm. On the other hand, the shift of the proton signals of the pyridine ring into the 8.05-8.93 ppm range confirms the presence of a positive charge on the nitrogen atom.

The structures of the synthesized new 1,4-DHP derivatives **2-9** and the already reported derivative **1** were confirmed by <sup>1</sup>H, <sup>13</sup>C NMR, MS, and elemental analysis data. Elemental analyses of 1,4-DHP derivatives were in accordance with the structures, with the exception for compound **3** where elemental analysis showed that this compound was crystallized with 0.1 mole of acetone. This was confirmed also by <sup>1</sup>H NMR data. The purities of the studied 1,4-DHP derivatives were at least 97% as detected by HPLC method. Molecular weights of all studied compounds were detected by LC/MS technique and the obtained values were in good agreement with the calculated ones.

1,4-DHP derivatives as nitrogen heterocycles play an important role in biological systems, for example, as part of redox coenzymes NAD-H or NADP-H. Oxidative aromatization reactions of 1,4-DHP derivatives take place in biological systems in the presence of certain enzymes, for example, Cytochrome P450 (CYP) [31]. Additionally, antiradical and antioxidant properties of DHP derivatives have also been discovered [12, 13, 32, 33].

The reducing capacity of the synthesized 1,4-DHP derivatives **1-9** was tested using the method reported by Prieto et al. [34]. The assay is based on the reduction of Mo(VI) with the subsequent formation of a green phosphate/Mo(V) complex, having a characteristic absorbance maximum at 695 nm, which can be detected by UV/Vis spectroscopy. Diludine (diethyl 1,4-dihydro-2,6-dimethyl-3,5-pyridinedicarboxylate), a well-known 1,4-DHP derivative with antioxidant and antiradical properties, was used as a positive control [35]. The obtained data on RC of the synthesized compounds are summarized in Figure 3.

The obtained results show that all synthesized 1,4-DHP derivatives **1-9** possess reducing capacity under the tested conditions. It should be noted that RC of 1,4-DHP derivatives **1** and **2** was higher than that of

diludine. Other 1,4-DHP derivatives **3-9**, containing pyridinium moiety, showed lower RC values than diludine. We assume that RC values of the tested 1,4-DHP derivatives are mainly related to the ability of their aromatization at the phosphomolybdenum complex system leading to full oxidation of dihydropyridine to the corresponding pyridine derivative (according to UV/Vis spectrum data).

Ca<sup>2+</sup> channel antagonist and agonist activities of compounds **1-9** were assayed by changes in intracellular Ca<sup>2+</sup> ion concentration [Ca<sup>2+</sup>]<sub>i</sub> in H9C2 cells, derived from the embryonic rat ventricle, and A7R5 cells (rat smooth muscle cells). The model for investigation of the Ca<sup>2+</sup> channel blocking activity of DHP derivatives is based on the analysis of the effect of KCl on intracellular Ca<sup>2+</sup> mobilization in H9C2 and A7R5 cells. The well-known calcium channel inhibitor – amlodipine (3-ethyl-5-methyl 2-(2-aminoethoxymethyl)-4-(2-chlorophenyl)-6-methyl-1,4-dihydropyridine-3,5-dicarboxylate) was used as a positive control in this test. The results are summarized in Table 3.

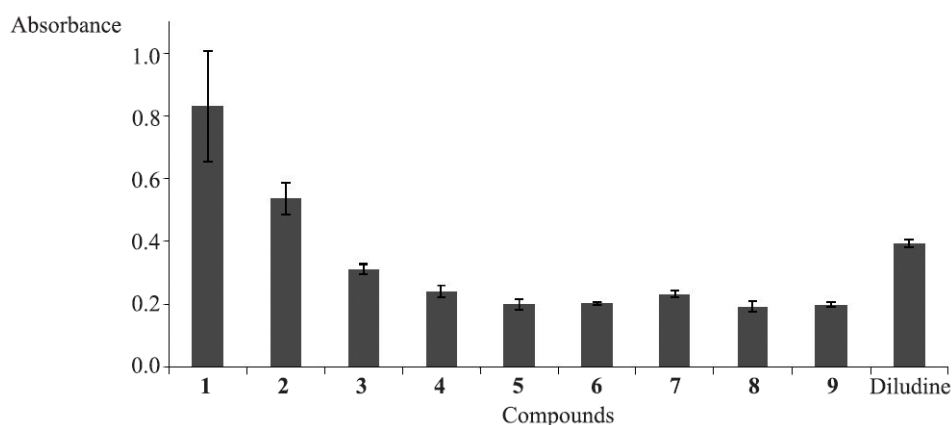


Fig. 3. RC of 1,4-DHP derivatives **1-9** and diludine (at 100 mM concentration), evaluated by the phosphomolybdenum complex method; the results are expressed as absorbance of sample at 695 nm against absorbance of a blank solution. All data are presented as a mean with standard deviation.

TABLE 3. Antagonist and Agonist Effects of 1,4-DHP Derivatives **1-9** on [Ca<sup>2+</sup>]<sub>i</sub> in H9C2 and A7R5 Cells

Compound	Antagonist activity (IC <sub>50</sub> , μM)		Agonist activity (RFU*, 100 μM)	
	H9C2	A7R5	H9C2	A7R5
Amlodipine	–	0.14±0.01	–	–
<b>1</b>	–	0.03±0.01	+	+
<b>2</b>	–	0.60±0.06	–	–
<b>3</b>	–	>100	–	–
<b>4</b>	–	95±2	–	–
<b>5</b>	–	2.5±0.6	–	–
<b>6</b>	–	0.80±0.07	+	+
<b>7</b>	–	0.70±0.05	+	+
<b>8</b>	–	0.40±0.03	+	+
<b>9</b>	–	0.50±0.05	+	+

+ – activity was detected.

– – no activity was detected in tested concentrations.

\*Relative fluorescence units.

As shown in Table 3, none of 1,4-DHP derivatives **1-9** in the tested doses showed antagonist effect in the H9C2 cell line, some of them, however, showed such effect in A7R5 cells. Furthermore, 1,4-DHP derivative **1** demonstrated an activity 4.7 times higher than amlodipine, whereas 1,4-DHP derivatives **2** and **5-9** were about 3-8 times less active than amlodipine, and compounds **3** and **4** possessed low activity. The obtained results indicate that the compounds target only calcium channels in vascular smooth muscle cells and do not affect calcium channels in cardiac cells.

The calcium channel agonist effect of 1,4-DHP derivatives **1-9** was also tested on both cell lines. Results are summarized in Table 3. The obtained time dependency data for one of the active compounds, 1,4-DHP derivative **7**, are represented in Fig. 4.

The obtained data show a rapid increase of  $[Ca^{2+}]_i$ , which subsequently turns into a "plateau". This is a classical "biphase" response confirming that in the response to the stimulus not only intracellular but also extracellular  $Ca^{2+}$  stores are involved. A similar effect was also observed for a known 1,4-DHP agonist BayK8644 [36].

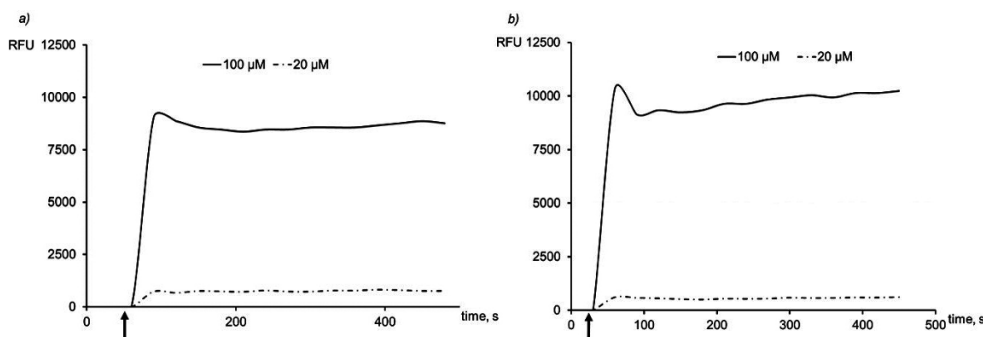


Fig. 4.  $Ca^{2+}$  responses by Fluo-4 NW-loaded cells (a) A7R5, (b) H9C2 stimulated by the addition of agonist **7** in concentrations 20 and 100  $\mu$ M. The arrow indicates the time of addition of compound **7**.

In summary, it has been established that all synthesized pyridinium salts based on 4-pyridyl-3,5-dipropargylcarbonyl-substituted 1,4-dihydropyridine with different alkyl substituents at the nitrogen atom possessed RC. Studies of  $Ca^{2+}$  channel antagonist and agonist activities of the compounds, assayed by changes in intracellular  $[Ca^{2+}]_i$  concentration in H9C2 and A7R5 cells, indicate that the compounds target only calcium channels in vascular smooth muscle cells and do not affect calcium channels in cardiac cells. It has been found that 1,4-DHP derivative **1** possess 4.7 times higher antagonist activity than amlodipine in the A7R5 cells. This study could serve as the basis for further design and synthesis of novel  $Ca^{2+}$  channel antagonist-agonist agents on the 1,4-DHP core.

## EXPERIMENTAL

$^1H$  and  $^{13}C$  NMR spectra were recorded on a Varian Mercury BB (400 and 100 MHz, respectively) or on a Bruker Fourier 300 (300 and 75 MHz, respectively) spectrometer. The chemical shifts of the atoms are reported relative to the residual signal of the solvent: DMSO- $d_6$  ( $\delta$  2.50 ppm) or  $CDCl_3$  ( $\delta$  7.26 ppm) for  $^1H$  NMR spectra and DMSO- $d_6$  ( $\delta$  39.5 ppm) or  $CDCl_3$  ( $\delta$  77.2 ppm) for  $^{13}C$  NMR spectra.  $^{13}C$  NMR signal assignments were based on the spectra of similar compounds [21, 37] and theoretical calculations according to [38]. Mass spectra were obtained on a Waters Acquity UPLC system connected to a Waters SQ Detector-2 operating in the ESI positive ion mode on a Waters Acquity UPLC<sup>®</sup> BEH C18 column (1.7  $\mu$ m, 2.1  $\times$  50 mm) using a gradient elution with MeCN (0.01%  $CF_3CO_2H$ ) in water (0.01%  $CF_3CO_2H$ ) at a flow rate 0.5 ml/min and processed with the Waters MassLynx 4.1 chromatography data system. Elemental analyses were performed on a Costech Instruments Elemental Combustion System ECS 4010 or on a Carlo Erba Instruments EA 1106

instrument. Melting points were determined on a SRS OptiMelt apparatus. The compounds were analyzed by HPLC on a Waters Alliance 2695 system equipped with a Waters 2485 UV/Vis detector and an Alltima CN column (5  $\mu$ m, 4.6 $\times$ 150 mm, Grace) using gradient elution with MeCN (0.1% H<sub>3</sub>PO<sub>4</sub>) in water, at a flow rate of 1 ml/min. Peak areas were determined electronically with the Waters Empower 2 chromatography data system. TLC was performed on Silica gel 60 F254 aluminum sheets 20 $\times$ 20 cm (Merck). Reducing capacity was measured at 695 nm using a UV/Vis Camspec M501 spectrometer. Calcium agonist activity was measured using a Thermo Ascient fluorescence spectrophotometer. Reactions under microwave conditions were performed on a Biotage<sup>®</sup> Initiator Classic microwave synthesizer with a single-mode microwave applicator.

Fluo-4 NW Calcium Assay Kit was purchased from Invitrogen (Sweden). H9C2 and A7R5 cell lines were obtained from European Collection of Animal Cell Cultures. All chemical reagents were purchased from Acros or Sigma-Aldrich and used without further purification.

**Bis(prop-2-ynyl) 2,6-dimethyl-4-phenyl-1,4-dihydropyridine-3,5-dicarboxylate (1)** was obtained from propargyl acetoacetate, benzaldehyde, and ammonia *via* classical Hantzsch synthesis following an already reported method [24]. Yield 0.64 g (61%), white crystals, mp 124-126 $^{\circ}$ C (MeOH) (mp 143-144 $^{\circ}$ C (EtOH) [24]). <sup>1</sup>H NMR spectrum (300 MHz, CDCl<sub>3</sub>),  $\delta$ , ppm (*J*, Hz): 2.35 (6H, s, 2,6-CH<sub>3</sub>); 2.41 (2H, t, *J* = 2.4, 2C $\equiv$ CH); 4.64 (4H, dd, AB system, *J* = 15.6, *J* = 2.4, 2CH<sub>2</sub>); 5.03 (1H, s, 4-CH); 5.78 (1H, s, NH); 7.10-7.16 (1H, m, H-4 Ph); 7.18-7.25 (2H, m, H-3,5 Ph); 7.27-7.33 (2H, m, H-2,6 Ph). <sup>13</sup>C NMR spectrum (100 MHz, CDCl<sub>3</sub>),  $\delta$ , ppm: 19.8 (2,6-CH<sub>3</sub>); 39.3 (C-4); 51.4 (2OCH<sub>2</sub>); 74.3 (2C $\equiv$ CH); 78.2 (2C $\equiv$ CH); 103.6 (C-3,5); 126.4 (C-4 Ph); 127.9 (C-3,5 Ph); 128.0 (C-2,6 Ph); 145.0 (C-2,6); 147.1 (C-1 Ph); 166.6 (2C=O). Mass spectrum, *m/z* (*I*<sub>rel</sub>, %): 350 [M+H]<sup>+</sup> (100). Found, %: C 72.11; H 5.49; N 4.01. C<sub>21</sub>H<sub>19</sub>NO<sub>4</sub>. Calculated, %: C 72.19; H 5.48; N 4.01.

**Bis(prop-2-ynyl) 2,6-dimethyl-4-(3-pyridyl)-1,4-dihydropyridine-3,5-dicarboxylate (2)** was synthesized from propargyl acetoacetate (1.50 g, 11.0 mmol), pyridine-3-carboxaldehyde (0.52 ml, 0.59 g, 5.5 mmol), and ammonium acetate (0.51 g, 6.6 mmol) in EtOH (50 ml). The reaction mixture was refluxed for 24 h and separated by flash chromatography (petroleum ether–EtOAc, 1:1 to 0:1); the obtained residue was recrystallized from MeOH. Yield 1.58 g (82%), yellow crystals, mp 180-182 $^{\circ}$ C (MeOH). <sup>1</sup>H NMR spectrum (300 MHz, CDCl<sub>3</sub>),  $\delta$ , ppm (*J*, Hz): 2.34 (6H, s, 2,6-CH<sub>3</sub>); 2.41 (2H, t, *J* = 2.5, 2C $\equiv$ CH); 4.63 (4H, d, *J* = 2.5, 2CH<sub>2</sub>); 5.01 (1H, s, 4-CH); 7.10 (1H, s, NH); 7.17 (1H, ddd, *J* = 7.8, *J* = 4.8, *J* = 0.7, H-5 Py); 7.66 (1H, ddd, *J* = 7.8, *J* = 2.4, *J* = 1.9, H-6 Py); 8.37 (1H, dd, *J* = 4.8, *J* = 1.6, H-4 Py); 8.54 (1H, d, *J* = 2.4, H-2 Py). <sup>13</sup>C NMR spectrum (100 MHz, CDCl<sub>3</sub>),  $\delta$ , ppm: 19.4 (2,6-CH<sub>3</sub>); 37.6 (C-4); 51.5 (2OCH<sub>2</sub>); 74.6 (2C $\equiv$ CH); 78.2 (2C $\equiv$ CH); 102.5 (C-3,5); 123.4 (C-5 Py); 136.0 (C-3 Py); 143.4 (C-4 Py); 146.5 (C-2,6); 147.3 (C-6 Py); 149.3 (C-2 Py); 166.3 (2C=O). Mass spectrum, *m/z* (*I*<sub>rel</sub>, %): 351 [M+H]<sup>+</sup> (100). Found, %: C 68.28; H 5.18; N 7.86. C<sub>20</sub>H<sub>18</sub>N<sub>2</sub>O<sub>4</sub>. Calculated, %: C 68.56; H 5.18; N 8.00.

**Synthesis of 1,4-DHP Alkylpyridinium Salts 3-9 (General Method).** The corresponding alkyl halide in 2-8-fold excess was added to a solution of 1,4-DHP derivative **2** (0.30 g, 0.86 mmol) in acetone (20 ml). The reaction mixture was refluxed in a pressure tube for 75-222 h (Table 2), then cooled to 0 $^{\circ}$ C. The resulting precipitate was filtered off, washed with cold acetone, recrystallized from acetone, and dried *in vacuo*.

**1-Ethyl-3-{2,6-dimethyl-3,5-bis[(prop-2-ynyloxy)carbonyl]-1,4-dihydropyridin-4-yl}-pyridinium Bromide (3).** Yield 0.26 g (65%), yellowish powder, mp 208-210 $^{\circ}$ C (Me<sub>2</sub>CO). <sup>1</sup>H NMR spectrum (400 MHz, DMSO-*d*<sub>6</sub>),  $\delta$ , ppm (*J*, Hz): 1.53 (3H, t, *J* = 7.1, N<sup>+</sup>CH<sub>2</sub>CH<sub>3</sub>); 2.31 (6H, s, 2,6-CH<sub>3</sub>); 3.46 (2H, t, *J* = 2.2, 2C $\equiv$ CH); 4.57-4.73 (6H, m, 2OCH<sub>2</sub>, N<sup>+</sup>CH<sub>2</sub>); 5.00 (1H, s, 4-CH); 8.05 (1H, dd, *J* = 7.9, *J* = 5.9, H-5 Py); 8.38 (1H, d, *J* = 7.9, H-6 Py); 8.88 (1H, s, H-2 Py); 8.92 (1H, d, *J* = 5.9, H-4 Py); 9.38 (1H, s, NH). <sup>13</sup>C NMR spectrum (75 MHz, DMSO-*d*<sub>6</sub>),  $\delta$ , ppm: 16.3 (N<sup>+</sup>CH<sub>2</sub>CH<sub>3</sub>); 17.9 (2,6-CH<sub>3</sub>); 37.4 (C-4); 50.7 (2OCH<sub>2</sub>); 55.9 (N<sup>+</sup>CH<sub>2</sub>); 74.8 (2C $\equiv$ CH); 78.4 (2C $\equiv$ CH); 98.5 (C-3,5); 127.9 (C-5 Py); 142.0 (C-3 Py); 142.2 (C-4 Py); 143.9 (C-6 Py); 147.6 (C-2 Py); 148.4 (C-2,6); 164.6 (2C=O). Mass spectrum, *m/z* (*I*<sub>rel</sub>, %): 379 [M-Br]<sup>+</sup> (100). Found, %: C 57.20; H 5.25; N 5.64. C<sub>22</sub>H<sub>23</sub>N<sub>2</sub>O<sub>4</sub>Br  $\cdot$  0.1 (CH<sub>3</sub>)<sub>2</sub>CO. Calculated, %: C 57.58; H 5.11; N 6.02.

**1-Butyl-3-{2,6-dimethyl-3,5-bis[(prop-2-ynyloxy)carbonyl]-1,4-dihydropyridin-4-yl}pyridinium Bromide (4).** Yield 0.15 g (36%), yellowish powder, mp 206-208 $^{\circ}$ C (Me<sub>2</sub>CO). <sup>1</sup>H NMR spectrum (400 MHz, DMSO-*d*<sub>6</sub>),  $\delta$ , ppm (*J*, Hz): 0.90 (3H, t, *J* = 7.3, CH<sub>3</sub>); 1.21-1.31 (2H, m, CH<sub>2</sub>CH<sub>3</sub>); 1.82-1.91 (2H, m,



$N^+CH_2CH_2$ ); 2.32 (6H, s, 2,6-CH<sub>3</sub>); 3.46 (2H, t,  $J = 2.4$ ,  $2C\equiv CH$ ); 4.58-4.70 (6H, m,  $2OCH_2$ ,  $N^+CH_2$ ); 4.99 (1H, s, 4-CH); 8.06 (1H, dd,  $J = 8.3$ ,  $J = 6.1$ , H-5 Py); 8.39 (1H, dt,  $J = 8.3$ ,  $J = 1.3$ , H-6 Py); 8.86 (1H, s, H-2 Py); 8.91 (1H, dt,  $J = 6.1$ ,  $J = 1.3$ , H-4 Py); 9.40 (1H, s, NH). <sup>13</sup>C NMR spectrum (75 MHz, DMSO-d<sub>6</sub>),  $\delta$ , ppm: 13.3 (CH<sub>3</sub>); 18.4 (2,6-CH<sub>3</sub>); 18.7 ( $CH_2CH_3$ ); 32.9 ( $N^+CH_2CH_2$ ); 37.8 (C-4); 51.1 ( $2OCH_2$ ); 60.4 ( $N^+CH_2$ ); 77.2 ( $2C\equiv CH$ ); 78.8 ( $2C\equiv CH$ ); 99.0 (C-3,5); 128.3 (C-5 Py); 142.6 (C-3 Py); 142.9 (C-4 Py); 144.4 (C-6 Py); 147.9 (C-2 Py); 148.8 (C-2,6); 165.0 ( $2C=O$ ). Mass spectrum,  $m/z$  ( $I_{rel}$ , %): 407 [ $M-Br$ ]<sup>+</sup> (100). Found, %: C 59.08; H 5.55; N 5.62. C<sub>24</sub>H<sub>27</sub>N<sub>2</sub>O<sub>4</sub>Br. Calculated, %: C 59.14; H 5.58; N 5.75.

**1-Hexyl-3-{2,6-dimethyl-3,5-bis[(prop-2-ynyloxy)carbonyl]-1,4-dihydropyridin-4-yl}-pyridinium Bromide (5).** Yield 0.25 g (57%), recrystallized twice, pale-yellow powder, mp 158-160°C (Me<sub>2</sub>CO). <sup>1</sup>H NMR spectrum (300 MHz, DMSO-d<sub>6</sub>),  $\delta$ , ppm ( $J$ , Hz): 0.85 (3H, t,  $J = 6.7$ , CH<sub>3</sub>); 1.17-1.32 (6H, m,  $(CH_2)_3CH_3$ ); 1.81-1.94 (2H, m,  $N^+CH_2CH_2$ ); 2.32 (6H, s, 2,6-CH<sub>3</sub>); 3.45 (2H, t,  $J = 2.4$ ,  $2C\equiv CH$ ); 4.57-4.71 (6H, m,  $2OCH_2$ ,  $N^+CH_2$ ); 5.00 (1H, s, 4-CH); 8.06 (1H, dd,  $J = 8.2$ ,  $J = 6.0$ , H-5 Py); 8.38 (1H, d,  $J = 8.2$ , H-6 Py); 8.85 (1H, s, H-2 Py); 8.92 (1H, d,  $J = 6.0$ , H-4 Py); 9.40 (1H, s, NH). <sup>13</sup>C NMR spectrum (100 MHz, DMSO-d<sub>6</sub>),  $\delta$ , ppm: 14.2 (CH<sub>3</sub>); 18.8 (2,6-CH<sub>3</sub>); 22.2 ( $CH_2CH_3$ ); 25.4 ( $N^+(CH_2)_3CH_2$ ); 30.9 ( $N^+(CH_2)_2CH_2$ ); 31.4 ( $N^+CH_2CH_2$ ); 38.3 (C-4); 51.5 ( $2OCH_2$ ); 61.0 ( $N^+CH_2$ ); 77.6 ( $2C\equiv CH$ ); 79.1 ( $2C\equiv CH$ ); 99.4 (C-3,5); 128.6 (C-5 Py); 143.0 (C-3 Py); 143.4 (C-4 Py); 144.7 (C-6 Py); 148.3 (C-2 Py); 149.1 (C-2,6); 165.4 ( $2C=O$ ). Mass spectrum,  $m/z$  ( $I_{rel}$ , %): 435 [ $M-Br$ ]<sup>+</sup> (100). Found, %: C 60.59; H 6.06; N 5.43. C<sub>26</sub>H<sub>31</sub>N<sub>2</sub>O<sub>4</sub>Br. Calculated, %: C 60.30; H 6.11; N 5.54.

**3-{2,6-Dimethyl-3,5-bis[(prop-2-ynyloxy)carbonyl]-1,4-dihydropyridin-4-yl}-1-octylpyridinium Bromide (6).** Yield 0.30 g (64%), pale-yellow powder, mp 182-184°C (Me<sub>2</sub>CO). <sup>1</sup>H NMR spectrum (300 MHz, DMSO-d<sub>6</sub>),  $\delta$ , ppm ( $J$ , Hz): 0.85 (3H, t,  $J = 6.7$ , CH<sub>3</sub>); 1.18-1.30 (10H, m,  $(CH_2)_5CH_3$ ); 1.82-1.93 (2H, m,  $N^+CH_2CH_2$ ); 2.32 (6H, s, 2,6-CH<sub>3</sub>); 3.46 (2H, t,  $J = 2.4$ ,  $2C\equiv CH$ ); 4.56-4.71 (6H, m,  $2OCH_2$ ,  $N^+CH_2$ ); 4.99 (1H, s, 4-CH); 8.05 (1H, dd,  $J = 8.1$ ,  $J = 6.0$ , H-5 Py); 8.38 (1H, d,  $J = 8.1$ , H-6 Py); 8.86 (1H, s, H-2 Py); 8.92 (1H, d,  $J = 6.0$ , H-4 Py); 9.40 (1H, s, NH). <sup>13</sup>C NMR spectrum (75 MHz, DMSO-d<sub>6</sub>),  $\delta$ , ppm: 13.9 (CH<sub>3</sub>); 18.3 ( $CH_2CH_3$ ); 22.0 (2,6-CH<sub>3</sub>); 25.3 ( $N^+(CH_2)_5CH_2$ ); 28.3 ( $N^+(CH_2)_4CH_2$ ); 28.4 ( $N^+(CH_2)_3CH_2$ ); 31.0 ( $N^+(CH_2)_2CH_2$ ); 31.1 ( $N^+CH_2CH_2$ ); 37.9 (C-4); 51.1 ( $2OCH_2$ ); 60.6 ( $N^+CH_2$ ); 77.2 ( $2C\equiv CH$ ); 78.7 ( $2C\equiv CH$ ); 99.0 (C-3,5); 128.3 (C-5 Py); 142.5 (C-3 Py); 143.0 (C-4 Py); 144.3 (C-6 Py); 147.9 (C-2 Py); 148.7 (C-2,6); 165.0 ( $2C=O$ ). Mass spectrum,  $m/z$  ( $I_{rel}$ , %): 463 [ $M-Br$ ]<sup>+</sup> (100). Found, %: C 61.87; H 6.50; N 5.11. C<sub>28</sub>H<sub>35</sub>N<sub>2</sub>O<sub>4</sub>Br. Calculated, %: C 61.88; H 6.49; N 5.15.

**1-Decyl-3-{2,6-dimethyl-3,5-bis[(prop-2-ynyloxy)carbonyl]-1,4-dihydropyridin-4-yl}pyridinium Bromide (7).** Yield 0.32 g (65%), pale-yellow powder, mp 182-184°C (Me<sub>2</sub>CO). <sup>1</sup>H NMR spectrum (300 MHz, DMSO-d<sub>6</sub>),  $\delta$ , ppm ( $J$ , Hz): 0.85 (3H, t,  $J = 6.7$ , CH<sub>3</sub>); 1.16-1.31 (14H, m,  $(CH_2)_7CH_3$ ); 1.81-1.94 (2H, m,  $N^+CH_2CH_2$ ); 2.32 (6H, s, 2,6-CH<sub>3</sub>); 3.45 (2H, t,  $J = 2.4$ ,  $2C\equiv CH$ ); 4.56-4.71 (6H, m,  $2OCH_2$ ,  $N^+CH_2$ ); 4.99 (1H, s, 4-CH); 8.06 (1H, dd,  $J = 8.2$ ,  $J = 6.0$ , H-5 Py); 8.38 (1H, d,  $J = 8.2$ , H-6 Py); 8.86 (1H, s, H-2 Py); 8.92 (1H, d,  $J = 6.0$ , H-4 Py); 9.40 (1H, s, NH). <sup>13</sup>C NMR spectrum (100 MHz, DMSO-d<sub>6</sub>),  $\delta$ , ppm: 14.4 (CH<sub>3</sub>); 18.8 ( $CH_2CH_3$ ); 22.5 (2,6-CH<sub>3</sub>); 25.7 ( $N^+(CH_2)_7CH_2$ ); 28.8 ( $N^+(CH_2)_6CH_2$ ); 29.1 ( $N^+(CH_2)_5CH_2$ ); 29.2 ( $N^+(CH_2)_4CH_2$ ); 29.3 ( $N^+(CH_2)_3CH_2$ ); 31.4 ( $N^+(CH_2)_2CH_2$ ); 31.7 ( $N^+CH_2CH_2$ ); 38.3 (C-4); 51.5 ( $2OCH_2$ ); 61.0 ( $N^+CH_2$ ); 77.6 ( $2C\equiv CH$ ); 79.2 ( $2C\equiv CH$ ); 99.4 (C-3,5); 128.7 (C-5 Py); 143.0 (C-3 Py); 143.4 (C-4 Py); 144.8 (C-6 Py); 148.3 (C-2 Py); 149.2 (C-2,6); 165.5 ( $2C=O$ ). Mass spectrum,  $m/z$  ( $I_{rel}$ , %): 491 [ $M-Br$ ]<sup>+</sup> (100). Found, %: C 62.92; H 6.82; N 4.88. C<sub>30</sub>H<sub>39</sub>N<sub>2</sub>O<sub>4</sub>Br. Calculated, %: C 63.04; H 6.88; N 4.90.

**1-Dodecyl-3-{2,6-dimethyl-3,5-bis[(prop-2-ynyloxy)carbonyl]-1,4-dihydropyridin-4-yl}-pyridinium Bromide (8).** Yield 0.38 g (73%), pale-yellow powder, mp 164-166°C (Me<sub>2</sub>CO). <sup>1</sup>H NMR spectrum (300 MHz, DMSO-d<sub>6</sub>),  $\delta$ , ppm ( $J$ , Hz): 0.85 (3H, t,  $J = 6.7$ , CH<sub>3</sub>); 1.17-1.30 (18H, m,  $(CH_2)_9CH_3$ ); 1.80-1.93 (2H, m,  $N^+CH_2CH_2$ ); 2.32 (6H, s, 2,6-CH<sub>3</sub>); 3.45 (2H, t,  $J = 2.4$ ,  $2C\equiv CH$ ); 4.56-4.71 (6H, m,  $2OCH_2$ ,  $N^+CH_2$ ); 4.99 (1H, s, 4-CH); 8.06 (1H, dd,  $J = 8.1$ ,  $J = 6.1$ , H-5 Py); 8.38 (1H, d,  $J = 8.1$ , H-6 Py); 8.86 (1H, s, H-2 Py); 8.93 (1H, d,  $J = 6.1$ , H-4 Py); 9.41 (1H, s, NH). <sup>13</sup>C NMR spectrum (100 MHz, DMSO-d<sub>6</sub>),  $\delta$ , ppm: 13.3 (CH<sub>3</sub>); 17.6 ( $CH_2CH_3$ ); 21.4 (2,6-CH<sub>3</sub>); 24.6 ( $N^+(CH_2)_9CH_2$ ); 27.7 ( $N^+(CH_2)_8CH_2$ ); 28.0 ( $N^+(CH_2)_7CH_2$ ); 28.1 ( $N^+(CH_2)_6CH_2$ ); 28.2 ( $N^+(CH_2)_5CH_2$ ); 28.3 ( $N^+(CH_2)_4CH_2$ ); 28.4 ( $N^+(CH_2)_3CH_2$ ); 30.3 ( $N^+(CH_2)_2CH_2$ ); 30.6 ( $N^+CH_2CH_2$ ); 37.2 (C-4); 50.4 ( $2OCH_2$ ); 59.9 ( $N^+CH_2$ ); 76.5 ( $2C\equiv CH$ ); 78.0 ( $2C\equiv CH$ ); 98.3 (C-3,5); 127.6

(C-5 Py); 141.9 (C-3 Py); 142.3 (C-4 Py); 143.6 (C-6 Py); 147.2 (C-2 Py); 148.1 (C-2,6); 164.3 (2C=O). Mass spectrum,  $m/z$  ( $I_{rel}$ , %): 519 [M-Br]<sup>+</sup> (100). Found, %: C 63.83; H 7.38; N 4.67. C<sub>32</sub>H<sub>43</sub>N<sub>2</sub>O<sub>4</sub>Br. Calculated, %: C 64.10; H 7.23; N 4.67.

**3-{2,6-Dimethyl-3,5-bis(prop-2-ynyloxy)carbonyl}-1,4-dihydropyridin-4-yl}-1-tetradecylpyridinium Bromide (9).** Yield 0.35 g (65%), pale-yellow powder, mp 153-155°C (Me<sub>2</sub>CO). <sup>1</sup>H NMR spectrum (300 MHz, DMSO-d<sub>6</sub>),  $\delta$ , ppm ( $J$ , Hz): 0.85 (3H, t,  $J$  = 6.7, CH<sub>3</sub>); 1.16-1.30 (22H, m, (CH<sub>2</sub>)<sub>11</sub>CH<sub>3</sub>); 1.80-1.94 (2H, m, N<sup>+</sup>CH<sub>2</sub>CH<sub>2</sub>); 2.32 (6H, s, 2,6-CH<sub>3</sub>); 3.45 (2H, t,  $J$  = 2.4, 2C≡CH); 4.56-4.71 (6H, m, 2OCH<sub>2</sub>, N<sup>+</sup>CH<sub>2</sub>); 4.99 (1H, s, 4-CH); 8.05 (1H, dd,  $J$  = 8.0,  $J$  = 6.0, H-5 Py); 8.38 (1H, d,  $J$  = 8.0, H-6 Py); 8.85 (1H, s, H-2 Py); 8.92 (1H, d,  $J$  = 6.0, H-4 Py); 9.40 (1H, s, NH). <sup>13</sup>C NMR spectrum (75 MHz, DMSO-d<sub>6</sub>),  $\delta$ , ppm: 13.9 (CH<sub>3</sub>); 18.3 (CH<sub>2</sub>CH<sub>3</sub>); 22.1 (2,6-CH<sub>3</sub>); 25.3 (N<sup>+</sup>(CH<sub>2</sub>)<sub>11</sub>CH<sub>2</sub>); 28.3 (N<sup>+</sup>(CH<sub>2</sub>)<sub>10</sub>CH<sub>2</sub>); 28.4 (N<sup>+</sup>(CH<sub>2</sub>)<sub>9</sub>CH<sub>2</sub>); 28.5 (N<sup>+</sup>(CH<sub>2</sub>)<sub>8</sub>CH<sub>2</sub>); 28.6 (N<sup>+</sup>(CH<sub>2</sub>)<sub>7</sub>CH<sub>2</sub>); 28.7 (N<sup>+</sup>(CH<sub>2</sub>)<sub>6</sub>CH<sub>2</sub>); 28.8 (N<sup>+</sup>(CH<sub>2</sub>)<sub>5</sub>CH<sub>2</sub>); 28.9 (N<sup>+</sup>(CH<sub>2</sub>)<sub>4</sub>CH<sub>2</sub>); 29.0 (N<sup>+</sup>(CH<sub>2</sub>)<sub>3</sub>CH<sub>2</sub>); 29.1 (N<sup>+</sup>(CH<sub>2</sub>)<sub>2</sub>CH<sub>2</sub>); 31.3 (N<sup>+</sup>CH<sub>2</sub>CH<sub>2</sub>); 37.8 (C-4); 51.1 (2OCH<sub>2</sub>); 59.8 (N<sup>+</sup>CH<sub>2</sub>); 77.1 (2C≡CH); 78.7 (2C≡CH); 99.0 (C-3,5); 128.2 (C-5 Py); 142.5 (C-3 Py); 143.0 (C-4 Py); 144.3 (C-6 Py); 147.9 (C-2 Py); 148.7 (C-2,6); 165.0 (2C=O). Mass spectrum,  $m/z$  ( $I_{rel}$ , %): 547 [M-Br]<sup>+</sup> (100). Found, %: C 64.83; H 7.78; N 4.38. C<sub>34</sub>H<sub>47</sub>N<sub>2</sub>O<sub>4</sub>Br. Calculated, %: C 65.06; H 7.55; N 4.46.

**X-ray diffraction** data were collected at -100°C on a Bruker-Nonius KappaCCD diffractometer using graphite monochromated MoK $\alpha$  radiation ( $\lambda$  0.71073 Å). The crystal structures were solved by direct methods and refined by full-matrix least squares. The main crystallographic data and refinement parameters of the crystal structures are listed in Table 1. For further details, see crystallographic data for these compounds deposited at the Cambridge Crystallographic Data Center.

**Evaluation of the Reducing Capacity.** The RC of the synthesized 1,4-DHP derivatives **1-9** was studied using spectrophotometric quantitation through the formation of phosphomolybdenum complex [34]. Stock solutions (1.0 mM) of the test compounds and reference compound diludine were prepared in EtOH just before use. The reagent solution contained sulfuric acid (0.6 M), sodium phosphate (28 mM), and ammonium molybdate (4 mM) in water. An aliquot of 0.3 ml of the sample solution was combined in an Eppendorf tube with 3 ml of the reagent solution. The tubes were capped and incubated in a thermal block at 95°C for 90 min. After the samples were cooled to room temperature, the absorbance of each sample solution was measured at 695 nm against a blank sample using a UV/Vis spectrometer. A typical blank solution contained 3 ml of the reagent solution and EtOH (0.3 ml), and was incubated under the same conditions as the rest of the samples. Each assay was performed in triplicate.

**Intracellular Ca<sup>2+</sup> measurements.** Cells were grown in Dulbecco's modified Eagle medium containing 1% non-essential amino acids and 2 mM glutamine, supplemented with 10% fetal bovine serum (Sigma) at 37°C under 5% CO<sub>2</sub>. Cells were passaged once a week using 0.25% trypsin and 0.53 mM EDTA solution and grown in 75 mm<sup>2</sup> plastic culture flasks until confluence and seeded in 96-well plates for experiments. Cells were seeded into 96-well plates at a density of 30,000 cells per well and incubated for 72 h. [Ca<sup>2+</sup>]<sub>i</sub> was measured in confluent cell monolayers with the Ca<sup>2+</sup>-sensitive fluorescent indicator Fluo-4 NW.

For investigation of Ca<sup>2+</sup> channel antagonist activity of compounds **1-9**, the cells were preincubated in the dark for 15 min with test compounds at concentrations from 0.16 to 100  $\mu$ M. KCl (50 mM for A7R5 cells and 200 mM for H9C2 cells) was applied to Fluo-4 NW-loaded cells to stimulate intracellular Ca<sup>2+</sup> mobilization. Amlodipine was used as the positive control.

For investigation of Ca<sup>2+</sup> channel agonist activity, Fluo-4 NW-loaded cells were stimulated by the addition of test compounds (concentration range from 4 to 100  $\mu$ M). BayK8644 was used as the positive control. Changes in [Ca<sup>2+</sup>]<sub>i</sub> were measured from the fluorescence emitted at 516 nm due to alternate excitation at 494 nm using a fluorescence spectrophotometer. IC<sub>50</sub> values for the tested compounds were calculated using GraphPad Prism 4.0 software.

This research work was supported by the European Social Fund Project No. ESF 2013/0002/1DP/1.1.1.2.0/13/APIA/VIAA/005 and the European Social Fund within the project "Support for Doctoral Studies at University of Latvia" (for Martins Rucins).

We are also grateful to Dr. Ilga Mutule for assistance in the work with MW equipment and B.Sc. Katrina Veinberga for technical assistance.

## REFERENCES

1. E. Carosati, P. Ioan, M. Micucci, F. Broccatelli, G. Cruciani, B. S. Zhorov, A. Chiarini, and R. Budriesi, *Curr. Med. Chem.*, **19**, 4306 (2012).
2. P. Ioan, E. Carosati, M. Micucci, G. Cruciani, F. Broccatelli, B. S. Zhorov, A. Chiarini, and R. Budriesi, *Curr. Med. Chem.*, **18**, 4901 (2011).
3. D. J. Triggle, *Biochem. Pharmacol.*, **78**, 217 (2009).
4. D. J. Triggle, *Biochem. Pharmacol.*, **74**, 1 (2007).
5. D. J. Triggle, *Mini-Rev. Med. Chem.*, **3**, 215 (2003).
6. N. Edraki, A. R. Mehdipour, M. Khoshneviszadeh, and R. Miri, *Drug Discovery Today*, **14**, 1058 (2009).
7. G. Duburs, B. Vīgante, A. Plotniece, A. Krauze, A. Sobolevs, J. Briede, V. Kluša, and A. Velēna, *Chim. Oggi*, **26**, 68 (2008).
8. S. Nobili, I. Landini, B. Giglioni, and E. Mini, *Curr. Drug Targets*, **7**, 861 (2006).
9. A. R. Mehdipour, K. Javidnia, B. Hemmateenejad, Z. Amirghofran, and R. Miri, *Chem. Biol. Drug Des.*, **70**, 337 (2007).
10. B. Voigt, C. Coburger, J. Monár, and A. Hilgeroth, *Bioorg. Med. Chem.*, **15**, 5110 (2007).
11. M. I. Szabon-Watola, S. V. Ulatowski, K. M. George, C. D. Hayes, S. A. Steiger, and N. R. Natale, *Bioorg. Med. Chem. Lett.*, **24**, 117 (2014).
12. G. D. Tirzit, I. M. Byteva, K. I. Salokhiddinov, G. P. Gurinovich, and G. Y. Dubur, *Chem. Heterocycl. Compd.*, **17**, 682 (1981). [*Khim. Geterotsikl. Soedin.*, 924 (1981).]
13. A. Augustyniak, G. Bartosz, A. Čipak, G. Duburs, L. Horáková, W. Łuczaj, M. Majekova, A. D. Odysseos, L. Rackova, E. Skrzydlewska, M. Stefek, M. Strosova, G. Tirzitis, P. R. Venskutonis, J. Viskupicova, P. S. Vraha, and N. Zarkovic, *Free Radical Res.*, **44**, 1216 (2010).
14. R. Miri, K. Javidnia, H. Mirkhani, F. Kazemi, B. Hemmateenejad, N. Edraki, and A. R. Mehdipour, *Daru, J. Pharm. Sci.*, **16**, 263 (2008).
15. W. A. Catterall and J. Striessnig, *Trends Pharmacol. Sci.*, **13**, 256 (1992).
16. C. Becker, S. S. Jick, and C. R. Meier, *Neurology*, **70**, 1438 (2008).
17. B. Ritz, S. L. Rhodes, L. Qian, E. Schernhammer, J. H. Olsen, and S. Friis, *Ann. Neurol.*, **67**, 600 (2010).
18. O. Weinreb, T. Amit, O. Bar-Am, and M. B. Youdim, *Prog. Neurobiol.*, **92**, 330 (2010).
19. Y. Bansal and O. Silakari, *Eur. J. Med. Chem.*, **76**, 31 (2014).
20. D. Tirzite, J. Koronova, and A. Plotniece, *Biochem. Mol. Biol. Int.*, **45**, 849 (1998).
21. M. Rucins, D. Kaldre, K. Pajuste, M. A. S. Fernandes, J. A. F. Vicente, L. Klimaviciusa, E. Jaschenko, I. Kanepe-Lapsa, I. Shestakova, M. Plotniece, M. Gosteva, A. Sobolev, B. Jansone, R. Muceniece, V. Klusa, and A. Plotniece, *C. R. Chim.*, **17**, 69 (2014).
22. P. Cruciani, R. Stammeler, C. Aubert, and M. Malacria, *J. Org. Chem.*, **61**, 2699 (1996).
23. A. Hantzsch, *Justus Liebigs Ann. Chem.*, **215**, 1 (1882).
24. E. E. Liepinsh, R. M. Zolotoyabko, B. S. Chekavichus, A. E. Sausin', V. K. Lasis, and G. Ya. Dubur, *Chem. Heterocycl. Compd.*, **25**, 1032 (1989). [*Khim. Geterotsikl. Soedin.*, 1232 (1989).]
25. S. Goldmann and J. Stoltefuss, *Angew. Chem., Int. Ed.*, **30**, 1559 (1991).
26. J. Kuthan and A. Kurfurst, *Ind. Eng. Chem. Prod. Res. Dev.*, **21**, 191 (1982).
27. A. Altomare, M. Burla, M. Camalli, G. Cascarano, C. Giacobuzzo, A. Guagliardi, A. G. G. Moliterni, and R. Spagna, *Appl. Cryst.*, **32**, 115 (1999).

28. S. Mackay, W. Dong, C. Edwards, A. Henderson, C. J. Gilmore, N. Stewart, K. Shankland, and A. Donald, *maXus: Integrated Crystallography Software*, Bruker-Nonius and University of Glasgow, 2003.
29. D. Pijper, E. Bulten, J. Šmisterová, A. Wagenaar, D. Hoekstra, J. B. F. N. Engberts, and R. Hulst, *Eur. J. Org. Chem.*, **2003**, 4406 (2003).
30. N. V. Makarova, A. Plotnietse, G. Tirzitis, I. Turovskii, and G. Dubur, *Chem. Heterocycl. Compd.*, **33**, 175 (1997). [*Khim. Geterotsikl. Soedin.*, 202 (1997).]
31. F. P. Guengerich, W. R. Brian, M. Iwasaki, M. A. Sari, C. Bäärnhielm, and P. Berntsson, *J. Med. Chem.*, **34**, 1838 (1991).
32. G. D. Tirzit and G. Ya. Dubur, *Chem. Heterocycl. Compd.*, **8**, 126 (1972). [*Khim. Geterotsikl. Soedin.*, 133 (1972).]
33. D. Ya. Tirzite, Zh. V. Khyuvonen, A. G. Schmidlers, G. D. Tirzitis, and G. Ya. Duburs, *Pharm. Chem. J.*, **34**, 297 (2000). [*Khim.-Farm. Zh.*, **34**, № 6, 17 (2000).]
34. P. Prieto, M. Pineda, and M. Aguilar, *Anal. Biochem.*, **269**, 337 (1999).
35. L. Kouřimská, J. Pokorný, and G. Tirzitis, *Nahrung*, **37**, 91 (1993).
36. R. W. Hadley and J. R. Hume, *Circ. Res.*, **62**, 97 (1988).
37. M. Rucins, M. Gosteva, S. Belyakov, A. Sobolev, K. Pajuste, M. Plotniece, B. Cekavicus, D. Tirzite, and A. Plotniece, *Aust. J. Chem.*, DOI: 10.1071/CH14033 (2014).
38. E. Pretsch, W. Simon, J. Seibl, and T. Clerc, in: W. Fresenius, J. F. K. Huber, E. Pungor, G. A. Rechnitz, W. Simon, and Th. S. West (editors), *Tables of Spectral Data for Structure Determination of Organic Compounds*, Springer-Verlag, Berlin, Heidelberg (1989).

## **Publication**

### **D**

Synthesis and studies of calcium channel blocking and antioxidant activities of novel 4-pyridinium and/or N-propargyl substituted 1,4-dihydropyridine derivatives.

*C. R. Chimie*, 2014, 17, 69-80.



ELSEVIER

Contents lists available at [SciVerse ScienceDirect](http://www.sciencedirect.com)

## Comptes Rendus Chimie

[www.sciencedirect.com](http://www.sciencedirect.com)

Full paper/Mémoire

# Synthesis and studies of calcium channel blocking and antioxidant activities of novel 4-pyridinium and/or N-propargyl substituted 1,4-dihydropyridine derivatives



Martins Rucins<sup>a</sup>, Dainis Kaldre<sup>a</sup>, Karlis Pajuste<sup>a,b</sup>, Maria A.S. Fernandes<sup>c</sup>,  
 Joaquim A.F. Vicente<sup>c</sup>, Linda Klimaviciusa<sup>b</sup>, Elina Jaschenko<sup>a</sup>,  
 Iveta Kanepe-Lapsa<sup>a</sup>, Irina Shestakova<sup>a</sup>, Mara Plotniece<sup>a</sup>,  
 Marina Gosteva<sup>a</sup>, Arkadij Sobolev<sup>a</sup>, Baiba Jansone<sup>b</sup>, Ruta Muceniece<sup>b</sup>,  
 Vija Klusa<sup>b,\*</sup>, Aiva Plotniece<sup>a,\*</sup>

<sup>a</sup>Latvian Institute of Organic Synthesis, Aizkraukles 21, Riga LV-1006, Latvia<sup>b</sup>Faculty of Medicine, University of Latvia, Sarlotes 1A, Riga LV-1001, Latvia<sup>c</sup>IMAR-CMA, Department of Life Sciences, University of Coimbra, 3001-401 Coimbra, Portugal

## ARTICLE INFO

## Article history:

Received 28 March 2013

Accepted after revision 8 July 2013

Available online 5 September 2013

## Keywords:

1,4-Dihydropyridines

N-Dodecyl pyridinium

Propargyl substituent

Calcium antagonists

Antioxidant activity

Mitochondrial processes

Structure–activity relationships

## ABSTRACT

The novel 1,4-dihydropyridine derivatives containing the cationic pyridine moiety at the position 4, and the *N*-propargyl group as a substituent at position 1 of the 1,4-DHP cycle were designed, synthesised, and assessed in biological tests. Among all the novel compounds, the 4-(*N*-dodecyl) pyridinium group-containing compounds **11** (without the *N*-propargyl group) and **12** (with the *N*-propargyl group) demonstrated the highest calcium antagonistic properties against neuroblastoma SH-SY5Y (IC<sub>50</sub> about 5–14 μM) and the vascular smooth muscle A7r5 cell (IC<sub>50</sub> – 0.6–0.7 μM) lines, indicating that they predominantly target the L-type calcium channels. These compounds showed a slight total antioxidant activity. At concentrations close to those of L-type calcium channel blocking ones, compound **12** did not affect mitochondrial functioning; also, no toxicity was obtained in vivo. The *N*-propargyl group as a substituent at position 1 of the 1,4-DHP cycle did not essentially influence the compounds' activity. The 4-(*N*-dodecyl) pyridinium moiety-containing compounds can be considered as prototype molecules for further chemical modifications and studies as cardioprotective/neuroprotective agents.

© 2013 Académie des sciences. Published by Elsevier Masson SAS. All rights reserved.

## 1. Introduction

Derivatives of 1,4-dihydropyridine (1,4-DHP) are one of the major categories of drugs with a wide variety of reported pharmacological activities, particularly due to

their calcium channel modulating properties, which are considered as the basis for 1,4-DHPs' cardioprotective [1,2], neuroprotective, anti-inflammatory, anti-ischemic, anti-diabetic, and many other actions [3]. The multifaceted effects of 1,4-DHPs were explained by the privileged structure of the 1,4-DHP scaffolds with appropriate substituents, capable of interacting with diverse receptors and ion channels [4]. During the last decade, interest has arisen to neurotropic effects of different 1,4-DHPs, since experimental and clinical studies demonstrated their ability to penetrate the blood–brain barrier and reduce the risk of developing neurodegenerative

\* Corresponding authors.

E-mail addresses: [vijklaus@latnet.lv](mailto:vijklaus@latnet.lv) (V. Klusa),[aiva@osi.lv](mailto:aiva@osi.lv) (A. Plotniece).<sup>1</sup> Biology.<sup>2</sup> Chemistry.

diseases [5,6]. For instance, about a 27% reduction in Parkinson's disease risk was observed in patients who had taken centrally acting calcium channel blocking drugs [7]. These drugs (e.g., isradipine) are found to be beneficial also for the Alzheimer's disease treatment strategy [8–10]. 1,4-DHP derivatives of typical calcium antagonist [11] or atypical (neuronally non-antagonist) class [12] showed neuroprotective properties also in ischemic stroke models. Search for memory-improving/dementia-preventing effects of 1,4-DHP derivatives is still on the agenda in experimental laboratories and clinics [13,14]. Taking into account mitochondrial abnormalities as the essential cause of neurodegeneration, particular importance is related to 1,4-DHP mitochondria-protecting effects [15–18].

The present study is devoted to the design, synthesis and biological studies of novel 1,4-DHP derivatives by adding to their structures some pharmacophore moieties:

- a pyridine substituent at position 4 (compounds **3** and **4**) or *N*-alkyl pyridinium moiety at the position 4 (compounds **5–18**);
- a *N*-propargyl substituent at position 1 (compounds **2**, **4**, **6**, **8**, **12**, **14**, **16**, **18**).

The propargyl moiety is known to play an important role in providing neuro- and mitochondria-protecting properties of propargyl group-containing anti-depressants, selegiline and rasagiline [19–21]. The one and only literature source about the propargyl group-containing 1,4-DHP derivative – propargyl nitrendipine – demonstrated the store-operated channel blocking effect in leukemic HL-60 cells [22]. In turn, the 4-(*N*-dodecyl) pyridinium group was considered as a lipophilicity-giving moiety for the improvement of 1,4-DHP derivative penetration through the membranes and easier delivery to cellular targets. The dodecyl chain is found as an optimal-length alkyl substituent of different alkylphosphonium compounds for improving their mitochondria-targeted antioxidative properties [23].

The aim of the present study was to find the structure–activity relationships and to identify the importance of structure moieties as the above-mentioned 1,4-DHP derivatives for the future design of novel cytoprotective drugs. The studies were performed in vitro to assess:

- the compounds' calcium antagonistic properties in neuroblastoma SH-SY5Y cells and smooth muscle A7r5 cell line;
- the compounds' antioxidant activity with the phosphomolybdenum complex method;
- the importance of the amphiphilic substituent in the 1,4-DHP ring. For that, two structurally similar compounds, **12** [the 4-(*N*-dodecyl) pyridinium group-containing derivative] and **4** (without 4-(*N*-dodecyl) pyridinium moiety), were tested and compared in isolated rat liver mitochondria;
- in addition, the safety of compound **12** – in vivo subchronic toxicity test in mice.

## 2. Results and discussion

### 2.1. Chemistry

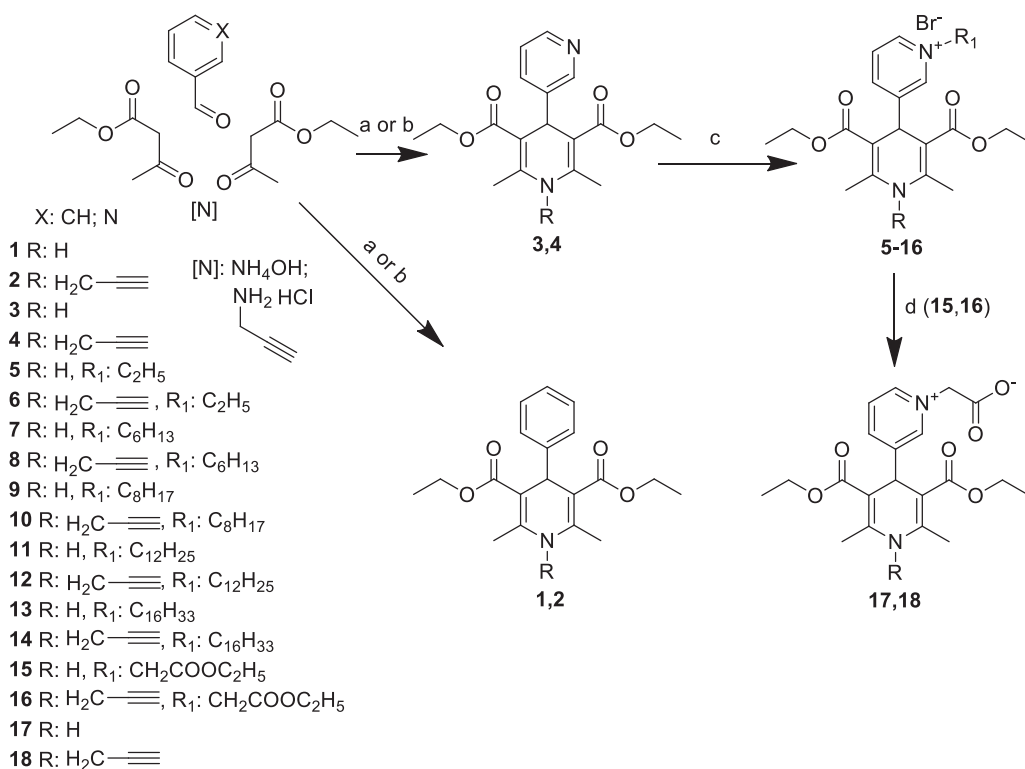
Different pharmacophore moieties were introduced into the 1,4-DHP cycle:

- at position 4, the pyridinium substituent with alkyl moieties of different lengths at quaternised nitrogen atom;
- at position 1, the propargyl moiety.

Previously, we had found a direct correlation between the length of the alkyl chain substituent at *N*-quaternised 4- $\beta$ -pyridyl-1,4-dihydropyridines and their improved membranotropic effects, such as incorporation in the liposomal membranes and bilayer fluidity [24]. Furthermore, the dodecyl substituent was shown as the optimal-length moiety among different alkyl groups in alkyltriphenylphosphonium or alkylrhodamine derivatives for their mitochondria-targeted antioxidant activity [23]. In the present study, some representative types of compounds containing a *N*-ethyl, *N*-hexyl, *N*-octyl, *N*-dodecyl or *N*-hexadecyl pyridinium moiety at position 4 of the 1,4-DHP ring (compounds **5–14**) were synthesised. The propargyl moiety was introduced in the 1,4-DHP molecule at position 1; better mitochondria-regulating properties were expected because this group was considered as essential in the antidepressant rasagiline molecule [20]. Moreover, *N*-alkylation of benzimidazole derivatives with propargyl halides led to more active compounds [25]. All 1,4-DHP derivatives were synthesised as *N*-H (*N*-unsubstituted) compounds (**1**, **3**, **5**, **7**, **9**, **11**, **13**, **15** and **17**) and *N*-propargyl substituted compounds (**2**, **4**, **6**, **8**, **10**, **12**, **14**, **16** and **18**). Our synthetic plan is shown in Scheme 1.

The structures and characterisation of synthesised novel and reference compounds: *N*-H (*N*-unsubstituted) and *N*-propargyl-substituted 1,4-DHP derivatives are presented in Table 1.

The data in the literature reported that the synthesis of the well-known 4-phenyl- (**1**) and 4-pyridyl- (**3**) substituted Hantzsch-type 1,4-DHP is usually performed via the classical synthetic procedures; they can be obtained in good (78–80%) yields [26,27]. In our case, the 1,4-DHP derivatives **1** and **3** were synthesised with high yields, 92% and 78% respectively, via typical synthetic routes – the classical Hantzsch method [30], which involves the one-pot cyclocondensation of the corresponding aldehyde, ethyl acetoacetate and ammonia in ethanol under reflux for 5–7 h. The corresponding *N*-propargyl-substituted 1,4-DHP derivatives **2** and **4** were obtained by analogy with the synthesis of other *N*-substituted 1,4-DHP ones [31] – via modified Hantzsch-type cyclisation using propargyl amine hydrochloride as a nitrogen source instead of ammonia and pyridine as a solvent for the reaction mixture, under reflux for 5–12 h. The one and only literature data about the synthesis and studies of *N*-propargyl-substituted 1,4-DHPs, such as *N*-propargyl nitrendipine (*N*-propargyl substituted (*RS*)-ethyl methyl-2,6-dimethyl-4-(3-nitrophenyl)-1,4-dihydropyridine-3,5-dicarboxylate) demonstrated the alternative synthesis of *N*-substituted



**Scheme 1.** Synthesis of 1,4-DHP derivatives **1–18**. Reactions conditions: (a) compounds **1** and **3**; EtOH, reflux for 5–7 h; (b) compounds **2** and **4**; pyridine, reflux for 5–12 h; (c) alkylbromide, acetone, reflux for 5–26 h; (d) NaOH, EtOH, water, 50 °C, 3 h.

**Table 1**  
Structures and characterisation of the studied 1,4-DHP derivatives **1–18**.

Compound	X	R	Yield (%)	Mp (°C)
<b>1</b>	CH	H	92 (78[26])	158–160 (153[26])
<b>2</b>	CH	–CH <sub>2</sub> C≡CH	19 (40 <sup>a</sup> )	111–113
<b>3</b>	N	H	78 (80[27])	189–191 (192–194[27])
<b>4</b>	N	–CH <sub>2</sub> C≡CH	22 (47 <sup>a</sup> )	154–156
<b>5</b>	N <sup>+</sup> –(CH <sub>2</sub> ) <sub>n</sub> CH <sub>3</sub> ; n = 1; Br <sup>–</sup>	H	86	189–191
<b>6</b>	N <sup>+</sup> –(CH <sub>2</sub> ) <sub>n</sub> CH <sub>3</sub> ; n = 1; Br <sup>–</sup>	–CH <sub>2</sub> C≡CH	77	205 (decomp.)
<b>7</b>	N <sup>+</sup> –(CH <sub>2</sub> ) <sub>n</sub> CH <sub>3</sub> ; n = 5; Br <sup>–</sup>	H	51	220–222
<b>8</b>	N <sup>+</sup> –(CH <sub>2</sub> ) <sub>n</sub> CH <sub>3</sub> ; n = 5; Br <sup>–</sup>	–CH <sub>2</sub> C≡CH	69	176–178
<b>9</b>	N <sup>+</sup> –(CH <sub>2</sub> ) <sub>n</sub> CH <sub>3</sub> ; n = 7; Br <sup>–</sup>	H	54	157–159
<b>10</b>	N <sup>+</sup> –(CH <sub>2</sub> ) <sub>n</sub> CH <sub>3</sub> ; n = 7; Br <sup>–</sup>	–CH <sub>2</sub> C≡CH	56	146–148
<b>11</b>	N <sup>+</sup> –(CH <sub>2</sub> ) <sub>n</sub> CH <sub>3</sub> ; n = 11; Br <sup>–</sup>	H	68	162–164
<b>12</b>	N <sup>+</sup> –(CH <sub>2</sub> ) <sub>n</sub> CH <sub>3</sub> ; n = 11; Br <sup>–</sup>	–CH <sub>2</sub> C≡CH	57	161–163
<b>13</b>	N <sup>+</sup> –(CH <sub>2</sub> ) <sub>n</sub> CH <sub>3</sub> ; n = 15; Br <sup>–</sup>	H	60 (63[28])	134–135 (135–136[28])
<b>14</b>	N <sup>+</sup> –(CH <sub>2</sub> ) <sub>n</sub> CH <sub>3</sub> ; n = 15; Br <sup>–</sup>	–CH <sub>2</sub> C≡CH	76	149–151
<b>15</b>	N <sup>+</sup> –CH <sub>2</sub> COOC <sub>2</sub> H <sub>5</sub> ; Br <sup>–</sup>	H	87 (88[29])	210–212 (217 (decomp.))[29]
<b>16</b>	N <sup>+</sup> –CH <sub>2</sub> COOC <sub>2</sub> H <sub>5</sub> ; Br <sup>–</sup>	–CH <sub>2</sub> C≡CH	78	157–159
<b>17</b>	N <sup>+</sup> –CH <sub>2</sub> COO <sup>–</sup>	H	82 (84[29])	128–130 (128–130[29])
<b>18</b>	N <sup>+</sup> –CH <sub>2</sub> COO <sup>–</sup>	–CH <sub>2</sub> C≡CH	53	105 (decomp.)

<sup>a</sup> Yield of product, performing the reaction in a pressure tube as the reaction vessel.



1,4-DHP derivatives via *N*-alkylation of the corresponding *N*-unsubstituted 1,4-DHP derivative with propargyl bromide in the presence of NaH as a base with only 22% yield of product [22]. In our hands, the yields of synthesised *N*-propargyl-substituted 1,4-DHP derivatives – 2,6-dimethyl-4-phenyl-1-prop-2'-ynyl-1,4-dihydropyridine-3',5'-dicarboxylic acid diethyl ester (**2**) and 2',6'-dimethyl-1'-prop-2-ynyl-1',4'-dihydro-[3,4']bipyridinyl-3',5'-dicarboxylic acid diethyl ester (**4**) – were 19% and 22%, respectively. Hantzsch-type cyclisation was carried out with a propargyl amine hydrochloride refluxing the reaction mixture for 12 h. Meanwhile, the yields of the desired products **2** and **4** were increased to 40% and 47%, respectively; these reactions, when performed in a pressure tube as the reaction vessel, were completed in just 5 h.

The synthesis of all the pyridinium moieties containing 1,4-DHP derivatives **5–14** were performed by alkylation of 4-pyridyl-1,4-DHP derivatives **3** or **4** with the corresponding alkyl bromides in acetone under reflux. The typical procedure for the quaternisation of pyridine derivatives has been reported by several research groups [32–34]. Reaction times and yields of the product are dependent on the structure of the alkyl halide. An excess of the alkylation agent was used to reduce the reaction time [29]. Compounds **15** and **16** were synthesised as synthones for the target products **17** and **18**. Pyridinium betaines **17** and **18**, synthesised in 82 and 53%, yields respectively, were obtained by treatment of the corresponding 4-(*N*-ethoxycarbonylmethyl) pyridinium-1,4-DHP bromides **15** and **16** with NaOH as a base, in analogy with the procedure described by our research group [29].

The structures of all newly synthesised derivatives **2, 4–12, 14, 16** and **18**, and of those already reported compounds **1** [26], **3**, [27], **13** [28], **15** [29] and **17** [29] were established and confirmed by <sup>1</sup>H NMR, <sup>13</sup>C NMR, MS and elemental analysis data. Molecular weights of 1,4-DHP derivatives measured by LC/MS technique were in good agreement with the calculated values for all the compounds. Details of the syntheses and full physically chemical characterisation for 1,4-DHPs **1–18** are given in Section 4. The purities of the studied compounds **1–18** were at least 97% according to high-performance liquid chromatography (HPLC) data.

## 2.2. Biology

### 2.2.1. Assessment of calcium channel blocking activity in SH-SY5Y and A7r5 cell lines

The influence of novel synthesised compounds on intracellular calcium [Ca<sup>2+</sup>]<sub>i</sub> concentration was assessed in both the neuroblastoma SH-SY5Y cells (containing L- and N-type Ca<sup>2+</sup> channels) and the rat aorta smooth muscle A7r5 cells, which express functional L-type Ca<sup>2+</sup> channels. The well-known calcium channel inhibitors – amlodipine and nimodipine – were used as the positive controls in this test.

As it is shown in Table 2, the most potent calcium antagonistic properties in SH-SY5Y cells demonstrated that the 1,4-DHP derivatives contained at position 4 of the 1,4-DHP ring the *N*-octyl pyridinium group (compound **10**)

**Table 2**

Calcium overload-preventing activity (IC<sub>50</sub>) of novel 1,4-DHP derivatives in SH-SY5Y and A7r5 cells.

Compound	Ca <sup>2+</sup> antagonism, IC <sub>50</sub> (μM)	
	Cell	
	SH-SY5Y	A7r5
<b>1</b>	#	0.0098 ± 0.0004*
<b>2</b>	> 100 <sup>†</sup>	2 ± 0.2 <sup>†</sup>
<b>3</b>	#	1.5 ± 0.2 <sup>†</sup>
<b>4</b>	53 ± 8 <sup>†</sup>	4.5 ± 1 <sup>†</sup>
<b>5</b>	#	#
<b>6</b>	100 ± 8 <sup>†</sup>	> 100 <sup>†</sup>
<b>7</b>	#	#
<b>8</b>	35 ± 3	#
<b>9</b>	53 ± 8	#
<b>10</b>	12 ± 3	#
<b>11</b>	5 ± 0.8	0.7 ± 0.3 <sup>†</sup>
<b>12</b>	14 ± 5	0.6 ± 0.06 <sup>†</sup>
<b>13</b>	#	#
<b>14</b>	#	#
<b>15</b>	#	#
<b>16</b>	#	#
<b>17</b>	#	#
<b>18</b>	#	#
Amlodipine	11 ± 5	0.140 ± 0.012
Nimodipine	53 ± 3 <sup>†</sup>	0.008 ± 0.0014 <sup>†</sup>

#: No Ca<sup>2+</sup>-channel blocking activity was detected. Data are presented as a mean ± SD.

<sup>†</sup> P < 0.05 vs. amlodipine; Student's paired *t*-test, with a two-tailed distribution.

and the *N*-dodecyl pyridinium group (compounds **11** and **12**); these activities were comparable to that of amlodipine. Other compounds showed either weak calcium antagonism (compounds **4, 8** and **9**), or this activity was not obtained at all. Calcium antagonistic properties were found to be higher in A7r5 cells, indicating that compounds predominantly target the L-type calcium channels in vascular smooth muscles. The highest activity comparable to that of nimodipine was revealed for compound **1**, which is a well-known 4-phenyl-1,4-DHP derivative with calcium antagonistic properties [35]. In A7r5 cells, compounds **11** and **12** demonstrated at least 10-fold higher activity than that in SH-SY5Y cells, indicating their potential vasodilating activity, whereas compounds **2, 3** and **4** were about 3–4-fold less active than compounds **11** and **12**; others lacked activity. Compounds **5, 7** and **13–18** did not show calcium channel blocking activity in none of the used cell lines.

Our results about compounds **1** and **3** are in good agreement with literature data, which demonstrated their calcium channel blocking activities [35,36].

The comparison of the Ca<sup>2+</sup>-channel blocking activity of structurally related compounds – *N*-H (*N*-unsubstituted) (compounds **1, 3, 5, 7, 9, 11, 13, 15**, and **17**) and *N*-propargyl-substituted (compounds **2, 4, 6, 8, 10, 12, 14, 16**, and **18**) 1,4-DHP derivatives shows either slightly increased blocking activity only for compounds **2, 4, 6** vs **1, 3, 5**, and **7** in SH-SY5Y cells, or decreased activity for compound **2** vs compound **1** in A7r5 cells.

### 2.2.2. Assessment of total antioxidant activity (AOA)

In this study, the phosphomolybdenum complex method was used for the evaluation of the total

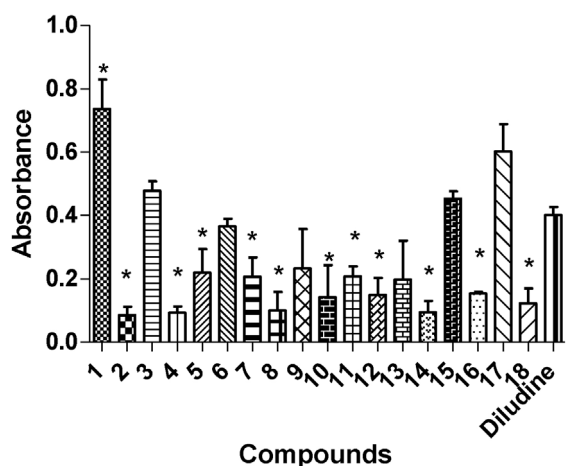


Fig. 1. Total antioxidant activity of 1,4-DHP derivatives **1–18** (at concentration 100  $\mu\text{M}$ ) evaluated by the phosphomolybdenum complex method. Results are expressed as absorbance unit (at 695 nm) of sample against absorbance of a blank solution. Data are presented as a mean  $\pm$  SD.  $P < 0.05$  vs diludine (taken as 100%), one-way ANOVA followed by Bonferroni's multiple-comparison test.

antioxidant activity of the synthesised 1,4-DHP derivatives. Diludine (diethyl-1,4-dihydro-2,6-dimethyl-3,5-pyridinecarboxylate), a well-known 1,4-DHP derivative with antioxidant properties [37,38], was used as a positive control. The obtained results (Fig. 1) show that all synthesised 1,4-DHP derivatives possessed antioxidant properties. The highest activity (about 0.5 absorbance units) was evidenced for the *N*-unsubstituted derivatives – compounds **1** and **17**, containing the 4-phenyl or *N*-carboxymethyl pyridinium moiety, respectively. The AOA of compounds **3**, **6** and **15** was comparable to that of diludine. Other 1,4-DHP derivatives showed a lower AOA than diludine and even compounds that demonstrated a high calcium channel blocking activity (compounds **11** and **12**), indicating a lack of correlation between their antioxidant and calcium antagonistic properties. We suggested that the AOA of the tested 1,4-DHP derivatives is mainly related to the ability of their *N*-H group to protonate/deprotonate at the phosphomolybdenum complex test system.

Table 3

Effects of compounds **12** and **4** on the respiratory parameters (states 2, 3, 4, FCCP), and respiratory indices RCR and ADP/O ratio using a glutamate/malate respiratory substrate.

Compound	Concentration ( $\mu\text{M}$ )	Oxygen consumption (% of control)				RCR	ADP/O
		State 2	State 3	State 4	State FCCP		
<b>12</b>	0 (control)	100.0 $\pm$ 0.0	100.0 $\pm$ 0.0	100.0 $\pm$ 0.0	100.0 $\pm$ 0.0	4.9 $\pm$ 0.5	3.2 $\pm$ 0.2
	1	110.8 $\pm$ 2.9	93.8 $\pm$ 5.5	110.6 $\pm$ 3.4	95.2 $\pm$ 2.3	4.5 $\pm$ 0.6	3.0 $\pm$ 0.2
	10	157.5 $\pm$ 25**	76.7 $\pm$ 2.7**	149.2 $\pm$ 18.4*	81.07 $\pm$ 4.9	2.5 $\pm$ 0.2**	2.4 $\pm$ 0.1*
<b>4</b>	0 (control)	100.0 $\pm$ 0.0	100.0 $\pm$ 0.0	100.0 $\pm$ 0.0	100.0 $\pm$ 0.0	7.9 $\pm$ 1.0	3.0 $\pm$ 0.05
	10	98.3 $\pm$ 2.4	93.8 $\pm$ 3.9	115.0 $\pm$ 10.0	100.1 $\pm$ 7.7	7.2 $\pm$ 1.1	2.9 $\pm$ 0.13

The values are given in percentage of control (without compounds). Control values are expressed in  $\text{nmol O}_2 \text{ mg}^{-1} \text{ protein min}^{-1}$ . Data are presented as a mean  $\pm$  SE, one-way ANOVA for multiple-comparisons, followed by Tukey's test. For compound **12**: state 2 = 7.9  $\pm$  0.4; state 3 = 44  $\pm$  0.2; state 4 = 9.4  $\pm$  0.9; FCCP = 70  $\pm$  8.8. ND: not determined. For compound **4**: state 2 = 7.32  $\pm$  0.49; state -3 = 43.67  $\pm$  3.47; state 4 = 4.27  $\pm$  0.49; state FCCP = 54.08  $\pm$  7.7.

\*  $P < 0.05$ .

\*\*  $P < 0.01$ .

### 2.2.3. Influence on mitochondrial functions of rat liver isolated mitochondria

Now it is known that 1,4-DHP compounds may penetrate the blood–brain barrier [5,6]. Moreover, they are capable of penetrating cell membranes, even those of organelles, reaching mitochondria and nucleus [39]. Suggesting that an amphiphilic (*N*-dodecyl pyridinium) group may dramatically increase the lipophilicity of compound **12** and enhance its mitochondria-penetrating ability, we tested it in rat liver isolated mitochondria and compared their action with that of compound **4**, which lacks this moiety. Both compounds also contain the *N*-propargyl group. We used a concentration close to  $\text{IC}_{50}$  obtained in the A7r5 cell line.

**2.2.3.1. Effects on mitochondrial bioenergetics.** Uncoupled respiration was initiated by the addition of 1  $\mu\text{M}$  of *p*-trifluoromethoxyphenylhydrazone (FCCP). The respiratory control ratio (RCR) and ADP-to-oxygen ratio (ADP/O) were calculated. The results, presented in Table 3, show that compound **12** at concentration 1  $\mu\text{M}$  did not affect mitochondrial bioenergetics; however, at higher concentration of 10  $\mu\text{M}$  (about 15 times higher than  $\text{IC}_{50}$  in A7r5 cells), it perturbed the respiration and phosphorylation efficiency of mitochondria by affecting the permeability (integrity) of the inner mitochondrial membrane to cations, as reflected by a stimulation of states-2 and 4 respiration rate, with a parallel decrease of state-3 one (but not FCCP state) and RCR and ADP/O ratio, when glutamate/malate (Table 3) or succinate (not shown) were used as the respiratory substrates. These data indicate that the *N*-dodecyl group plays some role in the compound's ability to influence mitochondrial bioenergetics at higher concentrations, while compound **4** (without this structural moiety) did not show any influence on mitochondrial bioenergetics.

**2.2.3.2. Influence on  $\text{Ca}^{2+}$ -induced mitochondrial pore transition (MPT).** The influences of compounds **12** and **4** were also studied on  $\text{Ca}^{2+}$ -induced MPT to evaluate their abilities to increase the susceptibility of mitochondria to MPT induction by measuring the increase in oxygen consumption, which is a typical phenomenon that follows the induction of MPT. Mitochondria can tolerate a certain amount of  $\text{Ca}^{2+}$ , but ultimately, their capacity of

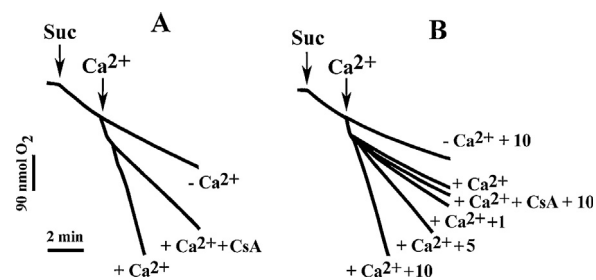


**Fig. 2.** A. Effects of compound **12** on MPT induction evaluated by measuring succinate (Suc)-supported mitochondrial respiration (oxygen consumption). Control assays show MPT induction by  $\text{Ca}^{2+}$  at a concentration of 100 nmol/mg protein and its inhibition by CsA (0.75 nmol/mg protein). B. Influence of compound **12** at concentrations 1, 5 and 10  $\mu\text{M}$  (1, 5, 10, respectively) on MPT induction at  $\text{Ca}^{2+}$  concentration of 60 nmol/mg protein. Assay conditions: + $\text{Ca}^{2+}$ : presence of calcium; - $\text{Ca}^{2+}$ : absence of calcium. The traces in experiments A and B are representative of assays performed with three different mitochondrial preparations.

$\text{Ca}^{2+}$ -loading is overwhelmed and mitochondria are completely uncoupled due to a change in the inner membrane permeability. This effect is prevented by cyclosporin A (CsA), a specific inhibitor of MPT. Assays in the absence and presence of  $\text{Ca}^{2+}$  (100 nmol/mg protein) as well as assays in the presence of  $\text{Ca}^{2+}$  (100 nmol/mg protein) plus CsA (0.75 nmol/mg protein) were used as the controls for MPT induction (Fig. 2A).

When the influence of compounds on MPT induction was tested, we used a  $\text{Ca}^{2+}$  concentration of 60 nmol/mg of protein that did not induce MPT by itself. The obtained results (Fig. 2B) showed that in the absence of calcium, compound **12**, even at the higher concentration of 10  $\mu\text{M}$ , did not induce MPT, while in the presence of calcium, this compound at concentrations 1, 5 and 10  $\mu\text{M}$  significantly potentiated calcium toxic effects. For instance, at concentration 10  $\mu\text{M}$ , the potentiating effect reached the control level when a concentration of 100 nmol  $\text{Ca}^{2+}$ /mg protein was used (Fig. 2A). CsA totally blocked the potentiating effect of compound **12** (Fig. 2B, + $\text{Ca}^{2+}$  + CsA + 10  $\mu\text{M}$ ), indicating that compound **12** has an ability to potentiate MPT induction. In

**Table 4**

Effect of compounds **12** and **4** on membrane lipid peroxidation of rat liver mitochondria induced by the pro-oxidant pair ADP/ $\text{Fe}^{2+}$  by evaluating TBARs formation.

Compound	Concentration ( $\mu\text{M}$ )	TBARs (nmol/mg protein, 10 min)
<b>12</b>	0	11.3 ± 0.5
	1	11.0 ± 0.2
	10	11.7 ± 1.0
	20	10.9 ± 1.3
	50	11.5 ± 1.6
	100	12.0 ± 1.1
<b>4</b>	0	11.3 ± 0.5
	60	10.4 ± 0.5
-ADP/ $\text{Fe}^{2+}$		0.44 ± 0.25

The data are presented as mean ± SE. Means were compared using one-way ANOVA for multiple-comparisons, followed by Tukey's test.

contrast, compound **4** neither protected MPT nor potentiated its induction (not shown).

Therefore, mitochondrial transition pore opening is not induced by compound **12** per se, indicating the mitochondria safety. Under certain pathological conditions (in our case, the calcium ion overload), it may potentiate calcium entry into mitochondria.

**2.2.3.3. Influence on mitochondrial oxidative stress.** The effects of compounds **12** and **4** on mitochondrial oxidative damage were assessed by detecting mitochondrial membrane lipid peroxidation induced by the pro-oxidant pair ADP/ $\text{Fe}^{2+}$  by evaluating the formation of thiobarbituric acid reactive substances (TBARs). Both compounds **12** and **4** did not affect TBARs formation, indicating that they do not possess mitochondrial antioxidant properties (Table 4).

### 2.3. Subchronic toxicity in mice for compound **12**

To clarify whether the changes in mitochondrial bioenergetics caused by compound **12** may play a crucial role in cell survival, we tested this compound in vivo for its subchronic toxicity. Compound **12** was administered for 7 days as a single daily intraperitoneal dose of 100 mg/kg. Mice were observed during 10 days. No toxic symptom was observed. Therefore, it can be considered that some toxic influences found in vitro at higher concentrations are not essential for cell-integrative in vivo processes, and the compound can be considered as a cell-safe agent.

## 3. Conclusions

The obtained data have demonstrated that among the tested *N*-quaternised 4- $\beta$ -pyridyl-1,4-dihydropyridines **5–14**, the highest calcium channel blocking activity was shown by compounds comprising the amphiphilic group – the *N*-dodecyl pyridinium moiety at position 4 of the 1,4-DHP cycle (compounds **11** and **12**). This activity, in smooth muscle cell line A7r5, was considerably higher than that in neuroblastoma cell line SH-SY5Y, suggesting that these compounds are predominantly targeting the L-type calcium channels. These compounds possessed low antioxidant activity if compared to 1,4-DHP derivatives **1**, **3** and **17**. Compound **12** at concentrations close to those of others demonstrating L-type calcium channel blocking activity did not affect mitochondrial functioning. This compound can be considered as a safe agent also in vivo (no toxicity up to 100 mg/kg). The propargyl group at position 1 of 1,4-DHP ring in general did not influence essentially the biological activity of the tested 1,4-DHP derivatives assessed in the used test systems. The compounds containing the *N*-dodecyl pyridinium moiety at position 4 of the 1,4-DHP cycle can be regarded as the prototype molecules for further chemical modifications and studies in animal models of cardiovascular or neurological diseases.

The structure–activity relationships of synthesised 4-pyridinium and/or *N*-propargyl substituted 1,4-DHP derivatives are summarised in Fig. 3.

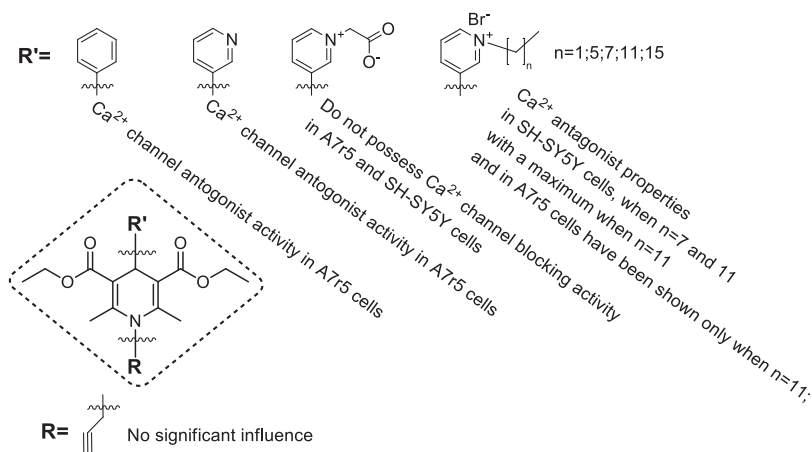


Fig. 3. Structure–activity relationships of the studied 4-pyridinium and/or N-propargyl-substituted 1,4-DHP derivatives.

## 4. Experimental

### 4.1. Chemistry

#### 4.1.1. General

All the reagents and solvents were purchased from commercial suppliers: Acros, Sigma–Aldrich, Alfa Aesar or Merck and used without further purification. TLC was performed on Silica gel 60 F254 Aluminium sheets  $20 \times 20$  cm (Merck). The purities of compounds were determined by HPLC on a Waters Alliance 2695 system and Waters 2489 UV–vis detector equipped with an Alltima C18 column,  $5 \mu\text{m}$ ,  $4.6 \times 150$  mm, using a gradient elution with acetonitrile/ $\text{H}_3\text{PO}_4$  (0.1%) in water, at a flow rate of 1 mL/min. Peak areas were determined electronically with a Waters Empower 2 chromatography data system.  $^1\text{H}$  NMR spectra were recorded on a Varian-Mercury BB (200 MHz or 400 MHz) spectrometer.  $^{13}\text{C}$  NMR spectra were recorded on a Varian-Mercury BB (100 MHz) spectrometer using  $\text{CDCl}_3$  or  $\text{DMSO}-d_6$  as the solvents. The chemical shifts of the atoms are reported in parts per million (ppm) relatively to the residual signals of the solvent:  $\text{CDCl}_3$  ( $\delta$ : 7.26) or  $\text{DMSO}-d_6$  ( $\delta$ : 2.50) for  $^1\text{H}$  NMR spectra and  $\text{CDCl}_3$  ( $\delta$ : 77.16) or  $\text{DMSO}-d_6$  ( $\delta$ : 39.52) for  $^{13}\text{C}$  NMR. Multiplicities are abbreviated as: s, singlet; d, doublet; t, triplet; q, quartet; quint, quintet; m, multiplet; dq, double quartet; dd, double doublet; dq, double quartet; bs, broad singlet. The coupling constants are expressed in Hz. Mass spectral data were determined on a Waters Alliance 2695 Separation module connected with a Micromass 3100 mass detector (Waters) operating in the ESI positive or negative ion mode on a Xbridge C18 column ( $5 \mu\text{m}$ ,  $2.1 \text{ mm} \times 50$  mm; Waters) using a gradient elution with acetonitrile/formic acid (0.1%) in water, at a flow rate of 0.6 mL/min. Melting points were determined on an OptiMelt (SRS Stanford Research Systems) equipment. Elemental analyses were determined on an Elemental Combustion System ECS 4010 (Costech Instruments) or on an EA 1106 (Carlo Erba Instruments).

#### 4.1.2. Synthesis

Compounds **1**, **3**, **13**, **15** and **17** were synthesised according to the literature. Briefly, the 2',6'-dimethyl-4-phenyl-1,4-dihydropyridine-3,5-dicarboxylic acid diethyl ester (**1**) [26,40] and 2',6'-dimethyl-1',4'-dihydro-[3,4]bipyridinyl-3',5'-dicarboxylic acid diethyl ester (**3**) [27] were obtained from the corresponding aldehyde, ethyl acetoacetate and ammonia in the classical Hantzsch synthesis; 3',5'-bisethoxycarbonyl-1-hexadecyl-2',6'-dimethyl-1',4'-dihydro-[3,4]bipyridinyl-1-ium bromide (**13**) and 3',5'-bisethoxycarbonyl-1-ethoxycarbonylmethyl-2',6'-dimethyl-1',4'-dihydro-[3,4]bipyridinyl-1-ium bromide (**15**) from 2',6'-dimethyl-1',4'-dihydro-[3,4]bipyridinyl-3',5'-dicarboxylic acid diethyl ester (**3**) and hexadecyl bromide [28] or ethyl bromoacetate [29], according to procedures described from Makarova et al., respectively; 1-carboxymethyl-2',6'-dimethyl-3',5'-bisethoxycarbonyl-1',4'-dihydro-[3,4]bipyridinyl-1-ium (**17**) from equimolar amounts of 3',5'-bisethoxycarbonyl-1-ethoxycarbonylmethyl-2',6'-dimethyl-1',4'-dihydro-[3,4]bipyridinyl-1-ium bromide (**15**) and metallic sodium in absolute ethanol, according to the procedure described by Makarova et al. [29].  $^1\text{H}$  NMR spectra data and elemental analysis of compounds **1**, **3**, **13**, **15** and **17** were in agreement with those reported in the corresponding literature.

4.1.2.1. 2',6'-Dimethyl-4-phenyl-1,4-dihydropyridine-3,5-dicarboxylic acid diethyl ester (**1**). Yield: 92%. Mp: 158–160 °C (78%; M: 153 °C [26].  $^1\text{H}$  NMR (400 MHz,  $\text{CDCl}_3$ )  $\delta$ : 1.20 (t, 6H,  $J = 7.4$ ); 2.29 (s, 6H); 4.01–4.12 (m, 4H); 4.97 (s, 1H); 5.85 (bs, 1H); 7.08–7.12 (m, 1H); 7.16–7.20 (m, 2H); 7.24–7.28 (m, 2H). MS (+ESI)  $m/z$  (relative intensity) 330 ( $[\text{M}]^+$ , 60%). Anal. calcd for  $\text{C}_{19}\text{H}_{23}\text{NO}_4$ : C, 69.28; H, 7.04; N, 4.25; found: C, 69.35; H, 7.04; N, 4.19.

4.1.2.2. 2',6'-Dimethyl-1',4'-dihydro-[3,4]bipyridinyl-3',5'-dicarboxylic acid diethyl ester (**3**). Yield: 78%. Mp: 189–191 °C (80%; M: 192–194 °C [27].  $^1\text{H}$  NMR (200 MHz,  $\text{CDCl}_3$ )  $\delta$ : 1.21 (t, 6H,  $J = 7.3$ ); 2.33 (s, 6H); 4.08 (q, 4H,

$J = 7.3$ ); 4.97 (s, 1H); 6.03 (bs, 1H); 7.12–7.18 (m, 1H); 7.57–7.61 (m, 1H); 8.36 (d, 1H,  $J = 5.1$ ); 8.52 (s, 1H).  $^{13}\text{C}$  NMR ( $\text{CDCl}_3$ )  $\delta$ : 14.24; 19.18; 37.87 (4-C-DHP); 59.80 (3,5-OCH<sub>2</sub>); 103.13 (3,5-C-DHP); 123.20; 135.95; 143.76; 145.05; 147.00; 149.40; 167.53 (C=O). MS (+ESI)  $m/z$  (relative intensity) 331 ( $[\text{M}]^+$ , 100%). Anal. calcd for  $\text{C}_{18}\text{H}_{22}\text{N}_2\text{O}_4$ : C, 65.44; H, 6.71; N, 8.48; found: C, 65.40; H, 6.73; N, 8.56.

4.1.2.3. *3',5'-Bisethoxycarbonyl-1-hexadecyl-2',6'-dimethyl-1',4'-dihydro-[3,4']bipyridinyl-1-ium bromide (13)*. Yield: 60%. Mp: 134–135 °C (63%; M: 135–136 °C [28]).  $^1\text{H}$  NMR (400 MHz, DMSO- $d_6$ )  $\delta$ : 0.84 (t, 3H,  $J = 7.0$ ); 1.12 (t, 6H,  $J = 7.0$ ); 1.18–1.26 (m, 26H); 1.85 (quint, 2H,  $J = 7.0$ ); 2.30 (s, 6H); 4.00 (dq, 4H,  $J = 7.0$  and  $J = 3.5$ ); 4.64 (t, 2H,  $J = 7.0$ ); 4.98 (s, 1H); 8.05 (dd, 1H,  $J = 8.2$  and  $J = 6.0$ ); 8.35 (d, 1H,  $J = 8.2$ ); 8.84 (bs, 1H); 8.92 (d, 1H,  $J = 6.0$ ); 9.20 (s, 1H).  $^{13}\text{C}$  NMR (DMSO- $d_6$ )  $\delta$ : 14.54; 14.76; 18.95; 22.70; 25.80; 28.98; 29.30; 29.36; 29.46; 29.56; 29.58; 29.61; 29.63; 29.64; 29.66; 31.50; 31.89; 38.71 (4-C-DHP); 60.03 ( $\text{N}^+\text{-CH}_2$ ); 61.09 (3,5-OCH<sub>2</sub>); 100.14 (3,5-C-DHP); 128.68; 143.25; 143.39; 144.82; 148.20; 148.99; 166.66 (C=O). MS (+ESI)  $m/z$  (relative intensity) 555 ( $^{79}\text{Br}$ ) ( $[\text{M-Br}]^+$ , 100%). Anal. calcd for  $\text{C}_{34}\text{H}_{55}\text{N}_2\text{O}_4\text{Br}$ : C, 64.24; H, 8.72; N, 4.41; found: C, 64.01; H, 8.78; N, 4.29.

4.1.2.4. *3',5'-Bisethoxycarbonyl-1-ethoxycarbonylmethyl-2',6'-dimethyl-1',4'-dihydro-[3,4']bipyridinyl-1-ium bromide (15)*. Yield: 87%. Mp: 210–212 °C. (88%; Mp: 217 °C (decomp.) [29]).  $^1\text{H}$  NMR (400 MHz, DMSO- $d_6$ )  $\delta$ : 1.10 (t, 6H,  $J = 7.0$ ); 1.23 (t, 3H,  $J = 7.0$ ); 2.30 (s, 6H); 3.99 (dq, 4H,  $J = 7.0$  and  $J = 3.5$ ); 4.22 (q, 2H,  $J = 7.0$ ); 5.00 (s, 1H); 5.70 (s, 2H); 8.13 (dd, 1H,  $J = 7.8$  and  $J = 5.9$ ); 8.45 (d, 1H,  $J = 7.8$ ); 8.84 (bs, 1H); 8.87 (d, 1H,  $J = 5.9$ ); 9.21 (s, 1H).  $^{13}\text{C}$  NMR (DMSO- $d_6$ )  $\delta$ : 13.67; 13.88; 18.12; 37.93 (4-C-DHP); 59.25 (3,5-OCH<sub>2</sub>); 60.05 ( $\text{N}^+\text{-...OCH}_2$ ); 62.12 ( $\text{N}^+\text{-CH}_2$ ); 99.25 (3,5-C-DHP); 127.30; 143.91; 144.31; 145.15; 147.44; 148.00; 165.78 (3,5-C=O); 166.16 ( $\text{N}^+\text{-...C=O}$ ). MS (+ESI)  $m/z$  (relative intensity) 417 ( $^{79}\text{Br}$ ) ( $[\text{M-Br}]^+$ , 100%). Anal. calcd for  $\text{C}_{22}\text{H}_{29}\text{N}_2\text{O}_6\text{Br}$ : C, 53.13; H, 5.88; N, 5.63; found: C, 52.73; H, 5.81; N, 5.47.

4.1.2.5. *1-Carboxymethyl-2',6'-dimethyl-3',5'-bisethoxycarbonyl-1',4'-dihydro-[3,4']bipyridinyl-1-ium (17)*. Yield: 82%. Mp: 128–130 °C (84%; M: 128–130 °C [29]).  $^1\text{H}$  NMR (200 MHz,  $\text{CDCl}_3$ )  $\delta$ : 1.22 (t, 6H,  $J = 7.0$ ); 2.28 (s, 6H); 4.06 (q, 4H,  $J = 7.0$ ); 5.04 (s, 1H); 5.16 (s, 2H); 7.67 (dd, 1H,  $J = 8.2$  and  $J = 5.9$ ); 8.29 (d, 1H,  $J = 8.2$ ); 8.37 (d, 1H,  $J = 5.9$ ); 8.77 (s, 1H); 9.39 (bs, 1H). MS (+ESI)  $m/z$  (relative intensity) 389 ( $[\text{M}]^+$ , 100%). Anal. calcd for  $\text{C}_{20}\text{H}_{24}\text{N}_2\text{O}_6$ : C, 56.69; H, 6.65; N, 6.60; found: C, 56.45; H, 6.60; N, 6.33.

4.1.2.6. *General method for synthesis of compounds (2 and 4)*. The solution of ethyl acetoacetate (14.2 g, 0.109 mol, 13.7 mL), propargylamine hydrochloride (5.0 g, 0.055 mol) and the corresponding aldehyde (benzaldehyde or pyridine-3-carboxaldehyde) (0.055 mol) in pyridine (15 mL) was refluxed for 5–12 h, the reaction mixture was poured in an ice/water mixture, extracted by diethyl ether (3  $\times$  15 mL), then the organic phase was dried over  $\text{Na}_2\text{SO}_4$ . The solvent was evaporated in vacuo, after which the

residue was recrystallized from ethyl acetate, then from ethanol, and dried in vacuo.

4.1.2.6.1. *2,6-Dimethyl-4-phenyl-1-prop-2'-ynyl-1,4-dihydropyridine-3',5'-dicarboxylic acid diethyl ester (2)*. Yield: 19 or 40%. Mp: 111–113 °C.  $^1\text{H}$  NMR (200 MHz, DMSO- $d_6$ )  $\delta$ : 1.14 (t, 6H,  $J = 7.3$ ); 2.51 (s, 6H); 3.50 (t, 1H,  $J = 2.2$ ); 4.04 (q, 4H,  $J = 7.3$ ); 4.50 (d, 2H,  $J = 2.2$ ); 4.93 (s, 1H); 7.10–7.20 (m, 5H).  $^{13}\text{C}$  NMR ( $\text{CDCl}_3$ )  $\delta$ : 14.22; 15.21; 36.38 ( $\text{N-CH}_2$ ); 38.52 (4-C-DHP); 60.21 (3,5-OCH<sub>2</sub>); 73.82 ( $\text{-C}\equiv$ ); 79.48 ( $\equiv\text{CH}$ ); 107.97 (3,5-C-DHP); 125.94; 127.25; 128.14; 146.11; 147.83; 167.78 (C=O). MS (+ESI)  $m/z$  (relative intensity) 368 ( $[\text{M}]^+$ , 30%). Anal. calcd for  $\text{C}_{22}\text{H}_{25}\text{NO}_4$ : C, 71.91; H, 6.86; N, 3.81; found: C, 71.59; H, 6.90; N, 3.77.

4.1.2.6.2. *2',6'-Dimethyl-1'-prop-2'-ynyl-1',4'-dihydro-[3,4']bipyridinyl-3',5'-dicarboxylic acid diethyl ester (4)*. Yield: 22 or 47%. Mp: 154–156 °C.  $^1\text{H}$  NMR (200 MHz,  $\text{CDCl}_3$ )  $\delta$ : 1.25 (t, 6H,  $J = 7.3$ ); 2.45 (t, 1H,  $J = 2.2$ ); 2.60 (s, 6H); 4.14 (q, 4H,  $J = 7.3$ ); 4.32 (d, 2H,  $J = 2.2$ ); 5.06 (s, 1H); 7.12 (dd, 1H,  $J = 8.1$  and  $J = 5.1$ ); 7.54 (d, 1H,  $J = 8.1$ ); 8.37 (dd, 1H,  $J = 5.1$  and  $J = 2.2$ ); 8.46 (d, 1H,  $J = 2.2$ ).  $^{13}\text{C}$  NMR ( $\text{CDCl}_3$ )  $\delta$ : 14.27; 16.18; 36.14 ( $\text{N-CH}_2$ ); 36.84 (4-C-DHP); 60.18 (3,5-OCH<sub>2</sub>); 73.93 ( $\text{-C}\equiv$ ); 79.00 ( $\equiv\text{CH}$ ); 106.98 (3,5-C-DHP); 123.08; 135.08; 141.37; 147.56; 148.47; 148.48; 149.30; 167.22 (C=O). MS (+ESI)  $m/z$  (relative intensity) 369 ( $[\text{M}]^+$ , 100%). Anal. calcd for  $\text{C}_{21}\text{H}_{24}\text{N}_2\text{O}_4$ : C, 68.46; H, 6.57; N, 7.60; found: C, 68.08; H, 6.57; N, 7.31.

4.1.2.7. *General method for synthesis of compounds (5–12, 14, 16)*. The corresponding alkyl (ethyl, hexyl, octyl, dodecyl or hexadecyl) bromide or ethyl bromoacetate (9.0 mmol) was added to a solution of the corresponding 2',6'-dimethyl-1',4'-dihydro-[3,4']bipyridinyl-3',5'-dicarboxylic acid diethyl ester (**3**) or 2',6'-dimethyl-1'-prop-2'-ynyl-1',4'-dihydro-[3,4']bipyridinyl-3',5'-dicarboxylic acid diethyl ester (**4**) (3.0 mmol) in acetone (30 mL). The mixture was refluxed for 5–26 h, cooled to 0 °C, the resulting precipitate was filtered off, washed with cooled acetone, recrystallized from acetone, and dried in vacuo.

4.1.2.7.1. *3',5'-Bisethoxycarbonyl-1-ethyl-2',6'-dimethyl-1',4'-dihydro-[3,4']bipyridinyl-1-ium bromide (5)*. Yield: 86%. Mp: 189–191 °C.  $^1\text{H}$  NMR (200 MHz,  $\text{CDCl}_3$ )  $\delta$ : 1.23 (t, 6H,  $J = 6.9$ ); 1.71 (t, 3H,  $J = 7.3$ ); 2.51 (s, 6H); 4.09 (q, 4H,  $J = 6.9$ ); 4.90 (q, 2H,  $J = 7.3$ ); 5.10 (s, 1H); 7.93 (dd, 1H,  $J = 8.0$  and  $J = 5.9$ ); 8.37 (bs, 1H); 8.39 (d, 1H,  $J = 8.0$ ); 8.85 (s, 1H); 9.10 (d, 1H,  $J = 5.9$ ).  $^{13}\text{C}$  NMR ( $\text{CDCl}_3$ )  $\delta$ : 14.29; 17.31; 19.48; 39.02 (4-C-DHP); 57.37 ( $\text{N-CH}_2$ ); 60.23 (3,5-OCH<sub>2</sub>); 99.99 (3,5-C-DHP); 127.99; 142.10; 142.33; 144.68; 148.67; 150.14; 167.15 (C=O). MS (+ESI)  $m/z$  (relative intensity) 359 ( $^{79}\text{Br}$ ) ( $[\text{M-Br}]^+$ , 100%). Anal. calcd for  $\text{C}_{20}\text{H}_{27}\text{N}_2\text{O}_4\text{Br}$ : C, 54.68; H, 6.19; N, 6.38; found: C, 54.77; H, 6.17; N, 6.32.

4.1.2.7.2. *3',5'-Bisethoxycarbonyl-1-ethyl-2',6'-dimethyl-1'-prop-2'-ynyl-1',4'-dihydro-[3,4']bipyridinyl-1-ium bromide (6)*. Yield: 77%. Mp: 205 °C (decomp.).  $^1\text{H}$  NMR (400 MHz,  $\text{CDCl}_3$ )  $\delta$ : 1.24 (t, 6H,  $J = 7.0$ ); 1.63 (t, 3H,  $J = 7.4$ ); 2.51 (t, 1H,  $J = 2.4$ ); 2.68 (s, 6H); 4.14 (q, 4H,  $J = 7.0$ ); 4.67 (d, 2H,  $J = 2.4$ ); 5.07 (q, 2H,  $J = 7.4$ ); 5.14 (s, 1H); 7.95 (dd, 1H,  $J = 8.2$  and  $J = 6.3$ ); 8.42 (d, 1H,  $J = 8.2$ ); 8.77 (s, 1H); 9.29 (d, 1H,  $J = 6.3$ ).  $^{13}\text{C}$  NMR ( $\text{CDCl}_3$ )  $\delta$ : 9.63; 12.06; 12.50; 33.14 ( $\text{N-CH}_2$ ); 33.23 (4-C-DHP); 52.60 ( $\text{N-CH}_2$ ); 55.96 (3,5-OCH<sub>2</sub>); 69.41 ( $\text{-C}\equiv$ ); 74.79 ( $\equiv\text{CH}$ ); 98.78 (3,5-C-DHP);

123.07; 137.48; 138.12; 140.01; 142.93; 146.58; 162.39 (C=O). MS (+ESI)  $m/z$  (relative intensity) 397 ( $^{79}\text{Br}$ ) ( $[\text{M}-\text{Br}]^+$ , 100%). Anal. calcd for  $\text{C}_{23}\text{H}_{29}\text{N}_2\text{O}_4\text{Br}$ : C, 57.87; H, 6.12; N, 5.87; found: C, 57.74; H, 6.08; N, 5.74.

4.1.2.7.3. *3',5'-Bisethoxycarbonyl-1-hexyl-2',6'-dimethyl-1',4'-dihydro-[3,4]bipyridinyl-1-ium bromide (7)*. Yield: 51%. Mp: 220–222 °C.  $^1\text{H}$  NMR (400 MHz,  $\text{DMSO}-d_6$ )  $\delta$ : 0.83 (t, 3H,  $J=7.0$ ); 1.11 (t, 6H,  $J=7.0$ ); 1.16–1.26 (m, 6H); 1.85–1.90 (quint, 2H,  $J=7.0$ ); 2.30 (s, 6H); 4.09 (dq, 4H,  $J=7.0$  and  $J=3.9$ ); 4.66 (t, 2H,  $J=7.0$ ); 4.78 (s, 1H); 8.06 (dd, 1H,  $J=8.2$  and  $J=5.9$ ); 8.35 (d, 1H,  $J=8.2$ ); 8.45 (bs, 1H); 8.94 (d, 1H,  $J=5.9$ ); 9.22 (s, 1H).  $^{13}\text{C}$  NMR ( $\text{DMSO}-d_6$ )  $\delta$ : 13.86; 14.24; 18.43; 21.90; 24.92; 30.60; 30.93; 38.18 (4-C-DHP); 59.53 (3,5-OCH<sub>2</sub>); 60.56 (N<sup>+</sup>-CH<sub>2</sub>); 99.60 (3,5-C-DHP); 128.14; 142.66; 142.93; 144.34; 147.71; 148.17; 166.15 (C=O). MS (+ESI)  $m/z$  (relative intensity) 415 ( $^{79}\text{Br}$ ) ( $[\text{M}-\text{Br}]^+$ , 100%). Anal. calcd for  $\text{C}_{24}\text{H}_{35}\text{N}_2\text{O}_4\text{Br}$ : C, 58.18; H, 7.12; N, 5.65; found: C, 58.18; H, 7.14; N, 5.55.

4.1.2.7.4. *3',5'-Bisethoxycarbonyl-1-hexyl-2',6'-dimethyl-1'-prop-2-ynyl-1',4'-dihydro-[3,4]bipyridinyl-1-ium bromide (8)*. Yield: 69%. Mp: 176–178 °C.  $^1\text{H}$  NMR (400 MHz,  $\text{DMSO}-d_6$ )  $\delta$ : 0.83 (t, 3H,  $J=6.7$ ); 1.18 (t, 6H,  $J=7.1$ ); 1.20–1.25 (m, 6H); 1.81–1.90 (m, 2H); 2.58 (s, 6H); 3.58 (s, 1H); 4.10 (q, 4H,  $J=7.1$ ); 4.60 (s, 2H); 4.66 (t, 2H,  $J=6.7$ ); 5.02 (s, 1H); 8.05 (dd, 1H,  $J=7.8$  and  $J=5.1$ ); 8.37 (d, 1H,  $J=7.8$ ); 8.73 (s, 1H); 8.97 (d, 1H,  $J=5.1$ ).  $^{13}\text{C}$  NMR ( $\text{DMSO}-d_6$ )  $\delta$ : 14.02; 14.37; 16.16; 22.07; 25.16; 30.80; 31.15; 36.55 (N-CH<sub>2</sub>); 37.09 (4-C-DHP); 60.36 (3,5-OCH<sub>2</sub>); 60.93 (N<sup>+</sup>-CH<sub>2</sub>); 76.69 (-C≡); 80.45 (≡CH); 103.80 (3,5-C-DHP); 128.46; 142.69; 143.34; 144.22; 146.42; 151.13; 163.30 (C=O). MS (+ESI)  $m/z$  (relative intensity) 453 ( $^{79}\text{Br}$ ) ( $[\text{M}-\text{Br}]^+$ , 100%). Anal. calcd for  $\text{C}_{27}\text{H}_{37}\text{N}_2\text{O}_4\text{Br}$ : C, 60.79; H, 6.99; N, 5.25; found: C, 60.59; H, 7.01; N, 5.12.

4.1.2.7.5. *3',5'-Bisethoxycarbonyl-2',6'-dimethyl-1-octyl-1',4'-dihydro-[3,4]bipyridinyl-1-ium bromide (9)*. Yield: 54%. Mp: 157–159 °C.  $^1\text{H}$  NMR (400 MHz,  $\text{DMSO}-d_6$ )  $\delta$ : 0.83 (t, 3H,  $J=7.0$ ); 1.11 (t, 6H,  $J=7.0$ ); 1.16–1.27 (m, 10H); 1.87 (quint, 2H,  $J=7.0$ ); 2.30 (s, 6H); 4.00 (dq, 4H,  $J=7.0$  and  $J=3.5$ ); 4.65 (t, 2H,  $J=7.0$ ); 4.98 (s, 1H); 8.05 (dd, 1H,  $J=8.2$  and  $J=6.0$ ); 8.35 (d, 1H,  $J=8.2$ ); 8.85 (bs, 1H); 8.95 (d, 1H,  $J=6.0$ ); 9.23 (s, 1H).  $^{13}\text{C}$  NMR ( $\text{DMSO}-d_6$ )  $\delta$ : 13.44; 13.72; 17.90; 21.58; 24.75; 27.89; 27.97; 30.47; 30.63; 37.65 (4-C-DHP); 58.99 (3,5-OCH<sub>2</sub>); 60.03 (N<sup>+</sup>-CH<sub>2</sub>); 99.08 (3,5-C-DHP); 127.62; 142.15; 142.40; 143.81; 147.19; 147.94; 165.62 (C=O). MS (+ESI)  $m/z$  (relative intensity) 443 ( $^{79}\text{Br}$ ) ( $[\text{M}-\text{Br}]^+$ , 100%). Anal. calcd for  $\text{C}_{26}\text{H}_{39}\text{N}_2\text{O}_4\text{Br}$ : C, 59.65; H, 7.51; N, 5.35; found: C, 59.52; H, 7.50; N, 5.24.

4.1.2.7.6. *3',5'-Bisethoxycarbonyl-2',6'-dimethyl-1-octyl-1'-prop-2-ynyl-1',4'-dihydro-[3,4]bipyridinyl-1-ium bromide (10)*. Yield: 56%. Mp: 146–148 °C.  $^1\text{H}$  NMR (400 MHz,  $\text{DMSO}-d_6$ )  $\delta$ : 0.84 (t, 3H,  $J=7.0$ ); 1.18 (t, 6H,  $J=7.0$ ); 1.19–1.27 (m, 10H); 1.85 (quint, 2H,  $J=7.0$ ); 2.58 (s, 6H); 3.58 (t, 1H,  $J=2.0$ ); 4.05 (dq, 4H,  $J=7.0$  and  $J=3.0$ ); 4.95 (d, 2H,  $J=2.0$ ); 4.65 (t, 2H,  $J=7.0$ ); 5.02 (s, 1H); 8.05 (dd, 1H,  $J=8.0$  and  $J=6.0$ ); 8.36 (d, 1H,  $J=8.0$ ); 8.73 (s, 1H); 8.96 (d, 1H,  $J=6.0$ ).  $^{13}\text{C}$  NMR ( $\text{DMSO}-d_6$ )  $\delta$ : 14.09; 14.30; 16.08; 22.22; 25.45; 28.54; 28.60; 31.12; 31.27; 36.46 (N-CH<sub>2</sub>); 37.02 (4-C-DHP); 60.28 (3,5-OCH<sub>2</sub>); 60.85 (N<sup>+</sup>-CH<sub>2</sub>); 76.60 (-C≡); 80.36 (≡CH); 103.75 (3,5-C-DHP); 128.39; 142.62; 143.22; 144.15; 146.39; 150.75; 166.22 (C=O). MS (+ESI)  $m/z$  (relative intensity) 481 ( $^{79}\text{Br}$ ) ( $[\text{M}-\text{Br}]^+$ , 100%). Anal.

calcd for  $\text{C}_{29}\text{H}_{41}\text{N}_2\text{O}_4\text{Br}$ : C, 62.03; H, 7.36; N, 4.99; found: C, 61.74; H, 7.41; N, 4.77.

4.1.2.7.7. *3',5'-Bisethoxycarbonyl-2',6'-dimethyl-1-dodecyl-1',4'-dihydro-[3,4]bipyridinyl-1-ium bromide*. Yield: 68%. Mp: 162–164 °C.  $^1\text{H}$  NMR (200 MHz,  $\text{CDCl}_3$ )  $\delta$ : 0.85 (t, 3H,  $J=7.4$ ); 1.21 (t, 6H,  $J=7.0$ ); 1.22–1.25 (m, 18H) overlap; 1.98 (quint, 2H,  $J=7.4$ ); 2.50 (s, 6H); 4.07 (q, 4H,  $J=7.0$ ); 4.78 (t, 2H,  $J=7.4$ ); 5.07 (s, 1H); 7.91 (dd, 1H,  $J=8.2$  and  $J=6.3$ ); 8.22 (d, 1H,  $J=8.2$ ); 8.48 (bs, 1H); 8.76 (s, 1H); 9.02 (d, 1H,  $J=6.3$ ).  $^{13}\text{C}$  NMR ( $\text{CDCl}_3$ )  $\delta$ : 14.07; 14.36; 19.44; 22.65; 26.03; 28.98; 29.00; 29.28; 29.31; 29.44; 29.51; 29.54; 31.84 (N<sup>+</sup>-CH<sub>2</sub>-CH<sub>2</sub>); 31.92 (4-C-DHP); 39.01 (N<sup>+</sup>-CH<sub>2</sub>); 60.21 (3,5-OCH<sub>2</sub>); 100.02 (3,5-C-DHP); 127.97; 141.81; 142.44; 144.62; 148.67; 149.91; 167.36 (C=O). MS (+ESI)  $m/z$  (relative intensity) 499 ( $^{79}\text{Br}$ ) ( $[\text{M}-\text{Br}]^+$ , 100%). Anal. calcd for  $\text{C}_{30}\text{H}_{47}\text{N}_2\text{O}_4\text{Br}$ : C, 62.34; H, 8.17; N, 4.83; found: C, 62.34; H, 8.22; N, 4.72.

4.1.2.7.8. *3',5'-Bisethoxycarbonyl-2',6'-dimethyl-1-dodecyl-1'-prop-2-ynyl-1',4'-dihydro-[3,4]bipyridinyl-1-ium bromide (12)*. Yield: 57%. Mp: 161–163 °C.  $^1\text{H}$  NMR (200 MHz,  $\text{CDCl}_3$ )  $\delta$ : 0.90 (t, 3H,  $J=6.6$ ); 1.22–1.39 (m, 22H); 1.50–1.65 (m, 2H); 1.99–2.04 (m, 2H); 2.51 (t, 1H,  $J=2.2$ ); 2.74 (s, 6H); 4.21 (q, 4H,  $J=7.3$ ); 4.70 (d, 2H,  $J=2.2$ ); 5.03 (t, 2H,  $J=6.6$ ); 5.20 (s, 1H); 8.01 (dd, 1H,  $J=8.1$  and  $J=5.9$ ); 8.33 (d, 1H,  $J=8.1$ ); 8.69 (s, 1H); 8.91 (d, 1H,  $J=5.9$ ).  $^{13}\text{C}$  NMR ( $\text{CDCl}_3$ )  $\delta$ : 14.07; 14.30; 16.79; 22.63; 25.98; 29.05; 29.28; 29.32; 29.44; 29.46; 29.52; 29.54; 31.84 (N<sup>+</sup>-CH<sub>2</sub>-CH<sub>2</sub>); 32.00 (N-CH<sub>2</sub>); 37.88 (4-C-DHP); 60.70 (N<sup>+</sup>-CH<sub>2</sub>); 62.04 (3,5-OCH<sub>2</sub>); 74.12 (-C≡); 79.54 (≡CH); 103.34 (3,5-C-DHP); 127.87; 142.36; 143.24; 144.78; 147.46; 151.39; 167.13 (C=O). MS (+ESI)  $m/z$  (relative intensity) 537 ( $^{79}\text{Br}$ ) ( $[\text{M}-\text{Br}]^+$ , 100%). Anal. calcd for  $\text{C}_{33}\text{H}_{49}\text{N}_2\text{O}_4\text{Br}$ : C, 64.17; H, 8.00; N, 4.50; found: C, 64.31; H, 8.04; N, 4.50.

4.1.2.7.9. *3',5'-Bisethoxycarbonyl-1-hexadecyl-2',6'-dimethyl-1'-prop-2-ynyl-1',4'-dihydro-[3,4]bipyridinyl-1-ium bromide (14)*. Yield: 76%. Mp: 149–151 °C.  $^1\text{H}$  NMR (400 MHz,  $\text{DMSO}-d_6$ )  $\delta$ : 0.85 (t, 3H,  $J=6.6$ ); 1.18 (t, 6H,  $J=6.8$ ); 1.19–1.30 (m, 26H); 1.85 (quint, 2H,  $J=6.9$ ); 2.58 (s, 6H); 3.57 (s, 1H); 4.09 (dq, 4H,  $J=6.6$  and  $J=3.0$ ); 4.59 (s, 2H); 4.64 (t, 2H,  $J=6.9$ ); 5.02 (s, 1H); 8.05 (dd, 1H,  $J=7.8$  and  $J=5.7$ ); 8.36 (d, 1H,  $J=7.8$ ); 8.72 (s, 1H); 8.97 (d, 1H,  $J=5.7$ ).  $^{13}\text{C}$  NMR ( $\text{DMSO}-d_6$ )  $\delta$ : 13.80; 13.96; 15.74; 21.94; 25.11; 28.25; 28.55; 28.62; 28.73; 28.82; 28.84; 28.86; 28.88; 28.89; 28.91; 30.79; 31.14; 36.12; 36.68 (4-C-DHP); 59.93 (3,5-OCH<sub>2</sub>); 60.50 (N<sup>+</sup>-CH<sub>2</sub>); 76.29 (-C≡); 80.12 (≡CH); 103.41 (3,5-C-DHP); 128.06; 142.23; 142.91; 143.76; 146.05; 150.41; 165.88 (C=O). MS (+ESI)  $m/z$  (relative intensity) 593 ( $^{79}\text{Br}$ ) ( $[\text{M}-\text{Br}]^+$ , 100%). Anal. calcd for  $\text{C}_{37}\text{H}_{57}\text{N}_2\text{O}_4\text{Br}$ : C, 65.96; H, 8.53; N, 4.16; found: C, 65.62; H, 8.57; N, 4.03.

4.1.2.7.10. *3',5'-Bisethoxycarbonyl-1-ethoxycarbonylmethyl-2',6'-dimethyl-1'-prop-2-ynyl-1',4'-dihydro-[3,4]bipyridinyl-1-ium bromide (16)*. Yield: 78%. Mp: 157–159 °C.  $^1\text{H}$  NMR (400 MHz,  $\text{CDCl}_3$ )  $\delta$ : 1.28 (t, 6H,  $J=7.0$ ); 1.29 (t, 3H,  $J=7.0$ ); 2.46 (t, 1H,  $J=1.9$ ); 2.71 (s, 6H); 4.14 (q, 4H,  $J=7.0$ ); 4.25 (q, 2H,  $J=7.0$ ); 4.65 (d, 2H,  $J=1.9$ ); 5.20 (s, 1H); 6.35 (s, 2H); 7.88 (dd, 1H,  $J=8.2$  and  $J=5.5$ ); 8.48 (d, 1H,  $J=8.2$ ); 8.77 (s, 1H); 9.09 (d, 1H,  $J=5.5$ ).  $^{13}\text{C}$  NMR ( $\text{CDCl}_3$ )  $\delta$ : 14.49; 14.73; 17.18; 38.25; 38.41 (4-C-DHP); 61.14 (3,5-OCH<sub>2</sub>); 61.64 (N<sup>+</sup>-...OCH<sub>2</sub>); 63.63 (N<sup>+</sup>-CH<sub>2</sub>); 74.46 (-C≡); 80.25 (≡CH);

103.60 (3,5-C-DHP); 127.18; 144.39; 145.50; 146.07; 147.70; 152.18; 166.36 ( $N^+ \dots C=O$ ); 167.40 (3,5-C=O). Anal. calcd for  $C_{25}H_{31}N_2O_6Br$ : C, 56.08; H, 5.84; N, 5.23; found: C, 56.00; H, 5.78; N, 5.09.

4.1.2.7.11. 1-Carboxymethyl-2',6'-dimethyl-3',5'-bisethoxycarbonyl-1'-prop-2'-ynyl-1',4'-dihydro-[3,4']bipyridinyl-1-ium (18). 3',5'-Bisethoxycarbonyl-1-ethoxycarbonylmethyl-2',6'-dimethyl-1'-prop-2'-ynyl-1',4'-dihydro-[3,4']bipyridinyl-1-ium bromide (16) (0.5 g, 0.93 mmol) was dissolved in ethanol (5 mL) and a solution of NaOH (37.2 mg, 0.93 mmol) in water (2.5 mL) was added, then, the reaction mixture was heated to 50 °C for 3 h. The reaction mixture was concentrated in vacuo till approximately half of solvent was evaporated off, after which the residue was mixed with water. The resulting precipitate was filtered off, recrystallized from water and dried in vacuo. Yield: 53% Mp: 105 °C (decomp.).  $^1H$  NMR (200 MHz,  $CDCl_3$ )  $\delta$ : 1.28 (t, 6H,  $J=7.3$ ); 2.49 (t, 1H,  $J=2.3$ ); 2.64 (s, 6H); 4.19 (q, 4H,  $J=7.3$ ); 4.48 (d, 2H,  $J=2.3$ ); 5.05 (s, 2H); 5.22 (s, 1H); 7.71 (dd, 1H,  $J=8.0$  and  $J=5.9$ ); 8.33 (d, 1H,  $J=8.0$ ); 8.42 (s, 1H); 8.56 (d, 1H,  $J=5.9$ ). MS (+ESI)  $m/z$  (relative intensity) 427 ( $[M]^+$ , 100%). Anal. calcd for  $C_{23}H_{26}N_2O_6$ : C, 64.78; H, 6.14; N, 6.35; found: C, 64.39; H, 6.13; N, 6.38.

## 4.2. Biology

### 4.2.1. Intracellular $Ca^{2+}$ measurements

Fluo-4 NW Calcium Assay Kit was purchased from Invitrogen (Sweden), all the others from Sigma–Aldrich (St Louis, MO, USA). A7r5 (rat aorta smooth muscle cells) were obtained from the ATCC cell collection (USA), SH-SY5Y (human neuroblastoma cell line) from the European Collection of Animal Cell Cultures (ECACC, UK). The cells were grown at 37 °C in a humidified atmosphere with 5%  $CO_2$ /95% air in Dulbecco's modified Eagle medium (DMEM), containing 2 mM of glutamine and supplemented with 10% fetal bovine serum. Cells were passaged once a week using 0.25% trypsin, 0.53 mM EDTA solution and grown in 75  $mm^2$  plastic culture flasks until confluence.

For the experiment, SH-SY5Y cells were plated into 96-well plates at a density of 30,000 cells per well and incubated for 24 h. A7r5 cells were seeded into 96-well plates at a density of 10,000 cells per well and incubated for 72 h. Changes in intracellular  $[Ca^{2+}]_i$  concentration were studied using the Fluo-4 NW Calcium Assay Kit, accordingly to the manufacturer's instructions. The SH-SY5Y and A7r5 cells were loaded with Fura-4NW for 45 min. Then, the cells were pre-incubated in the dark for 15 min with the tested compounds at concentrations from 0.8 to 100  $\mu M$ . The compounds were dissolved in DMSO.

Application of carbachol (100 nM) to Fura-4 loaded SH-SY5Y cells was used to stimulate changes in the intracellular  $[Ca^{2+}]_i$  concentration, whereas A7r5 cells were treated with 1.5 mM  $CaCl_2$  and KCl (50 mM) for 5 min to induce an increase in the  $[Ca^{2+}]_i$  concentration. The intracellular  $[Ca^{2+}]_i$  concentration was measured using the fluorescence spectrophotometer's (Thermo Asciant, Finland) settings appropriate for an excitation at 494 nm and an emission at 516 nm. Amlodipine, nimodipine were

used as the positive control.  $IC_{50}$  values as mean  $\pm$  SD were calculated using GraphPad Prism 3.0 software.

### 4.2.2. Evaluation of the total antioxidant activity

The total antioxidant activity of the synthesised 1,4-DHP derivatives was studied using a spectrophotometric quantitation of the antioxidant capacity through the formation of the phosphomolybdenum complex [41]. Stock solutions of the tested compounds and of reference diludine were prepared in ethanol with concentration  $1 \times 10^{-3}$  M just before use.

The reagent solution contains 0.6 M sulphuric acid, 28 mM sodium phosphate, and 4 mM ammonium molybdate solutions in water.

An aliquot of 0.3 mL of the sample solution was combined in an Eppendorf tube with 3 mL of the reagent solution. The tubes were capped and incubated in a thermal block at 95 °C for 90 min. After the samples had been cooled to room temperature, the absorbance of the sample solution of each was measured at 695 nm against a blank sample. A typical blank solution contained 3 mL of the reagent solution and the appropriate volume of ethanol as the solvent, and was incubated under the same conditions as the rest of the samples.

### 4.2.3. Assays in rat liver isolated mitochondria

Male Wistar rats (250–350 g) were obtained from Central Vivarium, Faculty of Medicine, University of Coimbra, Coimbra, Portugal). All the experimental procedures were performed in accordance with the guidelines of Directive 86/609/EEC. "European Convention for the Protection of Vertebrate Animals Used for Experimental and Other Scientific Purposes" (1986) and were approved by the National Ethics Committee. All the chemicals were obtained from Sigma (St Louis, MO, USA).

Liver mitochondria were isolated by differential centrifugation according to the conventional methods. The experimental procedures were performed in accordance to those described previously [15].

Briefly, after washing, the pellet was gently re-suspended in the washing medium at a protein concentration of about 50 mg/mL. The protein content was determined by the biuret method, using bovine serum albumin as a standard.

1,4-DHP derivatives were dissolved in DMSO; concentration did not exceed 0.1% in the medium.

### 4.2.4. Measurement of respiratory activities

Oxygen consumption was monitored polarographically with a Clark-type electrode at 30 °C in a closed glass chamber equipped with a magnetic stirring device. Mitochondria (1 mg/mL) were incubated in a respiratory medium containing 130 mM of sucrose, 5 mM of HEPES (pH 7.2), 50 mM of KCl, 2.5 mM of  $K_2HPO_4$ , and 2.5 mM of  $MgCl_2$  (in the presence and absence of compounds 4 or 12) for 3 min before energisation with 10 mM glutamate/5 mM malate. State-2 respiration (consumption of oxygen in the presence of substrate); state-3 respiration (consumption of oxygen in the presence of substrate and ADP) was induced by the addition of adenosine diphosphate (ADP, 150  $\mu M$ ) and state-4 respiration

(consumption of oxygen after ADP phosphorylation). FCCP (*p*-trifluoromethoxyphenylhydrazon)-stimulated respiration was initiated by the addition of 1  $\mu\text{M}$  of FCCP. The respiratory control ratio (RCR), which is calculated by the ratio between states 3 and 4, is an indicator of the mitochondrial membrane integrity. The ADP/O ratio, which is expressed by the ratio between the amounts of ADP and the oxygen consumed during state-3 respiration, is an index of oxidative phosphorylation efficiency. Respiration rates were calculated assuming that the saturation of oxygen concentration was 250  $\mu\text{M}$  at 30 °C, and the values are expressed in percentage of control (% of control).

#### 4.2.5. $\text{Ca}^{2+}$ -induced mitochondrial membrane transition pore

$\text{Ca}^{2+}$ -induced MPT was evaluated by measuring changes in oxygen consumption using a Clark-type electrode. The reactions were conducted in a medium containing 200 mM of sucrose, 10 mM of MOPS-Tris (pH 7.4), 1 mM of  $\text{KH}_2\text{PO}_4$ , and 10  $\mu\text{M}$  of EGTA, supplemented with 2  $\mu\text{M}$  of rotenone, as previously described [42,43]. Mitochondria (1 mg/mL), previously incubated at 30 °C for 3 min (in the absence and presence of compounds **4** or **12**), were energised with 10 mM succinate, and a single addition of  $\text{Ca}^{2+}$  (100 mol/mg protein) was used to induce MPT. Control assays, in both the absence and presence of  $\text{Ca}^{2+}$ , and in the presence of  $\text{Ca}^{2+}$  plus 0.75 nmol/mg of protein cyclosporin A (CsA) and the compound (when necessary), were also performed. To evaluate the ability of the compounds to increase the susceptibility of mitochondria to MPT induction, we used a  $\text{Ca}^{2+}$  concentration (60 nmol/mg of protein) that did not induce MPT by itself.

#### 4.2.6. Lipid peroxidation

Lipid peroxidation was determined by measuring thiobarbituric acid reactive substances (TBARS), using the routine thiobarbituric acid assay. Aliquots of mitochondrial suspensions (0.5 mL each), removed 10 min after the addition of ADP/ $\text{Fe}^{2+}$ , were added to 0.5 mL of ice cold 40% trichloroacetic acid. Then, 2 mL of 0.67% of aqueous thiobarbituric acid containing 0.01% of 2,6-di-*t*-butyl-*p*-cresol was added. The mixtures were heated at 90 °C for 15 min, then cooled on ice for 10 min, and centrifuged at 850 *g* for 10 min. Controls, in the absence of ADP/ $\text{Fe}^{2+}$ , were performed under the same conditions. The supernatant fractions were collected and lipid peroxidation was estimated spectrophotometrically at 530 nm. As blanks, we used control reactions performed in the absence of mitochondria and ADP/ $\text{Fe}^{2+}$ . The amount of TBARS formed was calculated using a molar extinction coefficient of  $1.56 \times 10^5 \text{ mol}^{-1} \text{ cm}^{-1}$  and expressed as nmol TBARS/mg of protein.

#### 4.2.7. Statistical analysis

The mitochondrial experiments were performed using three independent experiments with different mitochondrial preparations. The values are expressed as means  $\pm$  SE. Means were compared using one-way ANOVA for multiple-comparisons, followed by Tukey's test. Statistical significance was set at  $P < 0.05$ .

#### 4.2.8. Subchronic toxicity in mice

The test was performed in male ICR mice weighing  $20 \pm 2$  g (obtained from the Laboratory of Experimental Animals, Riga Stradins University, Riga, Latvia).

Compound **12** was administered as a single daily intraperitoneal dose of 100 mg/kg for 7 days. Number of animals  $n = 10$ . Control group ( $n = 10$ ) received a saline solution. The behaviour of the mice was observed during 10 days.

All experimental procedures were performed in accordance with the EU Directive 2010/63/EU for animal experiments and were approved by the Animal Ethics Committee of the Food and Veterinary Service (Riga, Latvia).

#### Acknowledgements

This study was supported by ESF project No. 2009/0217/1DP/1.1.1.2.0/09/APIA/VIAA/031; the EuroNanoMed project "CheTherDel"; Portuguese Research Council (FCT), Faculty of Medicine, Centre for Neuroscience and Cell Biology (CNC) and Marine and Environmental Research Centre (IMAR-CMA) of the University of Coimbra, Portugal.

We thank colleagues from the University of Coimbra, particularly Catarina R. Oliveira, António J. M. Moreno and Maria S. Santos for the assistance to perform mitochondrial studies. We obliged also the students from the University of Latvia: Nelda Lenberga, Marta Pavasare, Evija Sidorova, Katrina Hauka for their participation in mitochondrial assays at University of Coimbra, in a framework of ERASMUS programme, as well as Elga Poppela for technical assistance to carry out in vivo test. Also thanks to Dr. Gunars Tirzitis for fruitful discussions, Dr. Brigita Cekavicus for synthesis of reference compounds **1** and **3**.

#### References

- [1] F. Bossert, W. Vater, *Med. Res. Rev.* 9 (1989) 291.
- [2] D.J. Triggle, *Biochem. Pharmacol.* 74 (2007) 1.
- [3] G. Duburs, B. Vigante, A. Plotniece, A. Krauze, A. Sobolevs, J. Briede, V. Klusa, A. Velena, *Chim. Oggi* 26 (2008) 68.
- [4] D.J. Triggle, *Cell. Mol. Neurobiol.* 23 (2003) 293.
- [5] C. Becker, S. Jick, C. Meier, *Neurology* 70 (2008) 1438.
- [6] B. Ritz, S.L. Rhodes, L. Qian, E. Schernhammer, J.H. Olsen, S. Friis, *Ann. Neurol.* 67 (2010) 600.
- [7] K.C. Simon, X. Gao, H. Chen, M.A. Schwarzschild, A. Ascherio, *Mov. Disord.* 25 (2010) 1818.
- [8] T.S. Anekonda, J.F. Quinn, *Biochim. Biophys. Acta, Mol. Basis Dis.* 1812 (2011) 1584.
- [9] T.S. Anekonda, J.F. Quinn, C. Harris, K. Frahler, T.L. Wadsworth, R.L. Woltjer, *Neurobiol. Dis.* 41 (2011) 62.
- [10] D. Paris, C. Bachmeier, N. Patel, A. Quadros, C.H. Volmar, V. Laporte, J. Ganey, D. Beaulieu-Abdelahad, G. Ait-Ghezala, F. Crawford, M.J. Mullan, *Mol. Med.* 17 (2011) 149.
- [11] H. Miyazaki, S. Tanaka, Y. Fujii, K. Shimizu, K. Nagashima, M. Kami-bayashi, T. Uehara, Y. Okuma, Y. Nomura, *Life Sci.* 64 (1999) 869.
- [12] J. Rumaks, J. Pupure, S. Svirskis, S. Isajevs, G. Duburs, I. Kalvins, V. Klusa, *Medicina* 48 (2012) 525.
- [13] V. Klusa, *Drugs Future* 20 (1995) 135.
- [14] A. Fournier, R. Oprisiu-Fournier, J.-M. Serot, O. Godefroy, J.-M. Achard, S. Faure, H. Mazouz, M. Temmar, A. Albu, R. Bordet, O. Hanon, F. Gueyffier, J. Wang, S. Black, N. Sato, *Expert Rev. Neurother.* 9 (2009) 1413.
- [15] M.A.S. Fernandes, M.S. Santos, J.A.F. Vicente, A.J.M. Moreno, A. Velena, G. Duburs, C.R. Oliveira, *Mitochondrion* 3 (2003) 47.
- [16] M.A.S. Fernandes, A.S. Jurado, R.A. Videira, M.S. Santos, A.J.M. Moreno, A. Velena, G. Duburs, C.R. Oliveira, J.A.F. Vicente, *Mitochondrion* 5 (2005) 341.



- [17] M.A.S. Fernandes, S.P.S. Pereira, A.S. Jurado, J.B.A. Custódio, M.S. Santos, A.J.M. Moreno, G. Duburs, J.A.F. Vicente, *Chem. Biol. Interact.* 173 (2008) 195.
- [18] M.A.S. Fernandes, M.S. Santos, A.J.M. Moreno, L. Chernova, A. Krauze, G. Duburs, J.A.F. Vicente, *Toxicol. In Vitro* 23 (2009) 1333.
- [19] O. Weinreb, T. Amit, O. Bar-Am, M.B.H. Youdim, *Prog. Neurobiol.* 92 (2010) 330.
- [20] M.B.H. Youdim, O. Bar Am, M. Yogev-Falach, O. Weinreb, W. Maruyama, M. Naoi, T. Amit, *J. Neurosci. Res.* 79 (2005) 172.
- [21] W. Maruyama, Y. Akao, M.C. Carrillo, K.-i. Kitani, M.B.H. Youdim, M. Naoi, *Neurotoxicol. Teratol.* 24 (2002) 675.
- [22] J.L. Harper, C.S. Camerini-Otero, A.H. Li, S.A. Kim, K.A. Jacobson, J.W. Daly, *Biochem. Pharmacol.* 65 (2003) 329.
- [23] T.I. Rokitskaya, N.V. Sumbatyan, V.N. Tashlitsky, G.A. Korshunova, Y.N. Antonenko, V.P. Skulachev, *Biochim. Biophys. Acta, Biomembr.* 1798 (2010) 1698.
- [24] D. Tirzite, J. Koronova, A. Plotniece, *Biochem. Mol. Biol. Int.* 45 (1998) 849.
- [25] L. Ignatovich, O. Starkova, V. Romanovs, I. Sleiksha, I. Shestakova, J. Popelis, E. Lukevics, *C. R. Chimie* 16 (2013) 621.
- [26] H.H. Fox, J.I. Lewis, W. Wenner, *J. Org. Chem.* 16 (1951) 1259.
- [27] R. Wiley, G. Irick, *J. Org. Chem.* 26 (1961) 593.
- [28] N.V. Makarova, Z.V. Koronova, A.V. Plotniece, D.Y. Tirzite, G.D. Tirzit, G.Y. Duburs, *Chem. Heterocycl. Comp.* 31 (1995) 969.
- [29] N. Makarova, A. Plotnietse, G. Tirzitis, I. Turovskii, G. Dubur, *Chem. Heterocycl. Comp.* 33 (1997) 175.
- [30] A. Hantzsch, *Justus Liebigs Ann. Chem.* 215 (1882) 1.
- [31] M. Masuo, T. Kozo, I. Masaru, F. Masaharu, S. Tadao, K. Ryutarō, T. Toichi, *Ltd. Patent: US3985758 A1*, 1976.
- [32] A.A.P. Meekel, A. Wagenaar, J. Šmisterová, J.E. Kroeze, P. Haadisma, B. Bosgraaf, M.C.A. Stuart, A. Brisson, M.H.J. Ruiters, D. Hoekstra, J.B.F.N. Engberts, *Eur. J. Org. Chem.* 2000 (2000) 665.
- [33] A. Roosjen, J. Šmisterová, C. Driessen, J.T. Anders, A. Wagenaar, D. Hoekstra, R. Hulst, J.B.F.N. Engberts, *Eur. J. Org. Chem.* 2002 (2002) 1271.
- [34] D. Pijper, E. Bulten, J. Šmisterová, A. Wagenaar, D. Hoekstra, J.B.F.N. Engberts, R. Hulst, *Eur. J. Org. Chem.* 2003 (2003) 4406.
- [35] L. Dagnino, M.C. Li-Kwong-Ken, M.W. Wolowyk, H. Wynn, C.R. Triggle, E.E. Knaus, *J. Med. Chem.* 29 (1986) 2524.
- [36] R. Fossheim, K. Svarteng, A. Mostad, C. Romming, E. Shefter, D.J. Triggle, *J. Med. Chem.* 25 (1982) 126.
- [37] L. Kouřimská, J. Pokorný, G. Tirzitis, *Food/Nahrung* 37 (1993) 91.
- [38] G. Tirzitis, D. Tirzite, Z. Hyvonen, *Czech J. Food Sci.* 19 (2001) 81.
- [39] G.V. Belevich, G.Y. Duburs, M.M. Spirin, G.E. Dobrecov, *Biologicheskiiye Membrany* 3 (1986) 368.
- [40] M.G. Rimoli, L. Avallone, S. Zanarone, E. Abignente, A. Mangoni, *J. Heterocycl. Chem.* 39 (2002) 1117.
- [41] P. Prieto, M. Pineda, M. Aguilar, *Anal. Biochem.* 269 (1999) 337.
- [42] J.B.A. Custodio, A.J.M. Moreno, K.B. Wallace, *Toxicol. Appl. Pharmacol.* 152 (1998) 10.
- [43] J.B.A. Custodio, C.M. Palmeira, A.J. Moreno, K.B. Wallace, *Toxicol. Sci.* 43 (1998) 19.

## **Publication**

### **E**

Gene delivery agents possessing antiradical activity: self-assembling cationic amphiphilic 1,4-dihydropyridine derivatives.

*New J. Chem.*, 2013 37(10).

# Gene delivery agents possessing antiradical activity: self-assembling cationic amphiphilic 1,4-dihydropyridine derivatives†

Cite this: DOI: 10.1039/c3nj00272a

Karlis Pajuste,<sup>a</sup> Zanna Hyvönen,<sup>b</sup> Oksana Petrichenko,<sup>c</sup> Dainis Kaldre,<sup>a</sup> Martins Rucins,<sup>a</sup> Brigita Cekavicus,<sup>a</sup> Velta Ose,<sup>d</sup> Baiba Skrivele,<sup>a</sup> Marina Gosteva,<sup>a</sup> Emmanuelle Morin-Picardat,<sup>e</sup> Mara Plotniece,<sup>a</sup> Arkadij Sobolev,<sup>a</sup> Gunars Duburs,<sup>a</sup> Marika Ruponen<sup>b</sup> and Aiva Plotniece\*<sup>a</sup>

Seventeen 1,4-dihydropyridine (1,4-DHP) amphiphiles including differently substituted pyridinium, pyrazinium, *N*-methyl piperidinium or *N*-methyl morpholinium moieties as the cationic head-group of the molecule have been designed and synthesised. 1,4-DHP amphiphiles have been earlier proposed as a promising tool for plasmid DNA (pDNA) delivery *in vitro*. In this work the ability of the 1,4-DHP amphiphiles to self-assemble, to bind pDNA and to transfer it into the cells as well as the cytotoxicity of 1,4-DHP amphiphiles-pDNA complexes was studied. Furthermore, antiradical activity (ARA) of the 1,4-DHP derivatives was determined. We have revealed that all new 1,4-DHP amphiphiles possessed self-assembling properties and formed nanoparticles in an aqueous environment. The structure of the cationic head-group of 1,4-DHP amphiphiles influenced the size of nanoparticles. Additionally, we demonstrated for the first time that the electronic nature of the substituent of the pyridinium as the cationic head-group of the 1,4-DHP amphiphiles strongly affected the ability of these compounds to bind pDNA and transfer it into the cells. The amphiphiles with electron-donating properties possessing substituents at pyridinium moieties were able to bind pDNA and to deliver it more efficiently than amphiphiles containing electron-withdrawing properties possessing substituents at pyridinium moieties. Moreover, in this study we have established that the presence of the cationic part in the molecule was essential for the expression of ARA among tested 1,4-DHP amphiphiles. Cationic 1,4-DHP derivatives containing pyrazinium or *N*-methyl morpholinium substituents in the cationic head-group of the molecule displayed the highest ARA.

Received (in Montpellier, France)

13th March 2013,

Accepted 12th July 2013

DOI: 10.1039/c3nj00272a

[www.rsc.org/njc](http://www.rsc.org/njc)

## Introduction

During the last two decades, development of new non-viral vectors for DNA delivery has become an interesting field attracting more and more researchers. Gene delivery studies have been focused on the design of synthetic cationic compounds, such as cationic amphiphilic ammonium<sup>1,2</sup> or pyridinium<sup>3-6</sup> derivatives, polymers,<sup>7</sup> peptides<sup>8,9</sup> or dendrimers,<sup>10-12</sup> which would be able to

overcome gene delivery barriers both *in vitro* and *in vivo*. Cationic derivatives that possess self-assembling properties and are able to form liposomes in aqueous solutions have received widespread attention in gene delivery. Moreover, these compounds are relatively non-toxic and non-immunogenic, simple to use and easy to produce in large scale.<sup>13,14</sup> However, the main drawback of these cationic compounds, like other non-viral gene delivery systems, is their low transfection efficiency.<sup>15-17</sup> Therefore, there is still a huge need for design and development of more efficient and safer non-viral gene delivery systems.

Complex formation of cationic non-viral vectors with negatively charged DNA is an important prerequisite for successful gene transfer. The chemical structure and shape of cationic compounds have been shown to define their self-assembling and DNA complexation properties, and subsequent gene delivery activity.<sup>18</sup> Therefore, it is highly important to understand the structure-activity relationships.

Previously we have developed multiple cationic 1,4-dihydropyridine (1,4-DHP) amphiphiles with varying lengths of alkyl

<sup>a</sup> Latvian Institute of Organic Synthesis, Aizkraukles str. 21, Riga, LV-1006, Latvia.

E-mail: aiva@osi.lv; Fax: +371-67551335; Tel: +371-67014852

<sup>b</sup> University of Eastern Finland, Yliopistonranta 1C, P.O. Box 1627, Kuopio, FIN-70211, Finland

<sup>c</sup> Faculty of Physics and Mathematics, University of Latvia, Zellu str. 8, Riga, LV-1002, Latvia

<sup>d</sup> Latvian Biomedical Research and Study Centre, Ratsupites str. 1, Riga, LV-1067, Latvia

<sup>e</sup> Centre for Drug Research, Faculty of Pharmacy, University of Helsinki, Viikinkaari 5E, P.O. Box 56, Helsinki, FIN-00014, Finland

† Electronic supplementary information (ESI) available. See DOI: 10.1039/c3nj00272a

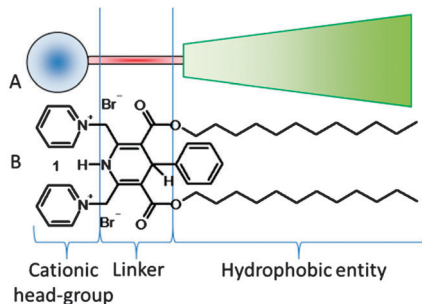


**Fig. 1** General composition of the structure of cationic lipids<sup>21</sup> (A); structure of cationic 1,4-dihydropyridine amphiphile **1** (B).

chains at positions 3 and 5 of the 1,4-DHP ring. These amphiphiles have been demonstrated to condense and efficiently deliver plasmid DNA (pDNA) into different cell lines *in vitro*.<sup>19,20</sup> The structures of these cationic amphiphiles resemble those of other cationic lipids currently used for gene delivery and are composed of a positively charged head-group, a hydrophobic moiety and a linker connecting these two parts (Fig. 1A).<sup>21</sup> In terms of transfection efficacy, dodecyloxy carbonyl substituents at positions 3 and 5 were optimal for these kinds of amphiphiles. Thus, 1,1'-[(3,5-dodecyloxy carbonyl-4-phenyl)-1,4-dihydropyridine-2,6-diyl]dimethylen]-bispyridinium dibromide (1,4-DHP amphiphile **1**, Fig. 1B) was found to be more active than commercially available cationic lipid DOTAP (*N*-(1-(2,3-dioleoyloxy)propyl)-*N,N,N*-trimethyl ammonium methylsulfate) and cationic polymer PEI 25 (polyethyleneimine of 25 kDa).<sup>19,22</sup> The chemical structure of the 1,4-DHP amphiphiles has been revealed to strongly influence their physicochemical and biological properties.<sup>19,20,23</sup>

Pyridinium amphiphiles based on the 1,4-DHP core are attractive because in addition to the self-assembling properties they contain the 1,4-DHP group as an active linker, which according to Triggler<sup>24,25</sup> is an intrinsic structural part of many pharmacologically active compounds and drugs. Earlier it has been reported that several 1,4-DHP derivatives possess antiradical activity (ARA) and antioxidant activity (AOA).<sup>26,27</sup> Antioxidant and antiradical activities were found for an analogue of the cardiovascular drug foridon (riodipine), which contains pyridinium substituents.<sup>27</sup> Noticeably, foridon itself did not possess AOA or ARA. The presence of ARA and AOA is believed to be an advantage for gene carriers since it can prevent DNA from chemical degradation induced by free radical oxidation upon complexation<sup>28,29</sup> or storage<sup>30–32</sup> of the complexes.

Although some structure–activity relationships<sup>19</sup> have been already found for 1,4-DHP amphiphiles, it is rather unclear how the chemical structure affects their self-assembling properties, antiradical activity, pDNA binding ability and properties of formed 1,4-DHP amphiphile–pDNA complexes. Particularly, the effect of the electronic nature of the substituent at the pyridinium as the cationic head-group of the amphiphilic 1,4-DHP molecule on the ability of these compounds to bind pDNA and to deliver it into the cells, as well as to show other activities like ARA, has never been studied before. Understanding of the structure–activity relationships of the 1,4-DHP carriers

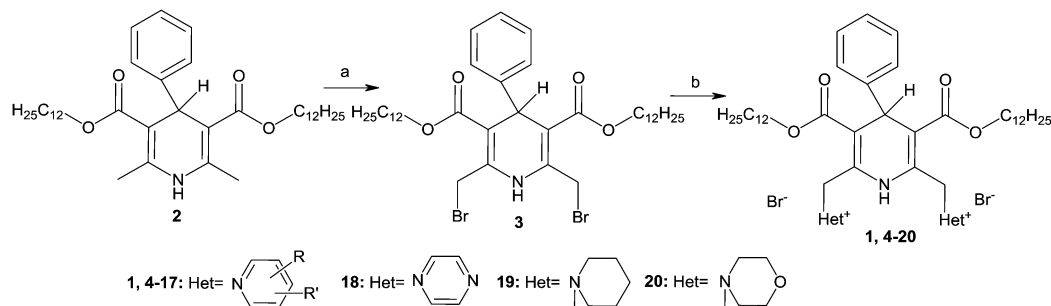
in cells is essential for further improving their design and functionality.

To explore the posed questions we designed and synthesised seventeen polyfunctional pyridinium 1,4-DHP amphiphiles which are structurally closely related to the most efficient 1,4-DHP derivative for pDNA delivery so far termed amphiphile **1** (Fig. 1B). The amphiphiles are synthesised by modification of the substituents at the cationic head-group of the amphiphilic 1,4-DHP molecule, specifically, different pyridinium (containing electron-donating or electron-withdrawing properties possessing substituent) (1,4-DHP amphiphiles **4–17**), pyrazinium (1,4-DHP amphiphile **18**), *N*-methyl piperidinium (1,4-DHP amphiphile **19**) or *N*-methyl morpholinium (1,4-DHP amphiphile **20**) moieties at the 2,6-methylene groups of the 1,4-DHP ring as the cationic head-group of the amphiphile. In the present study the self-assembling properties of the selected 1,4-DHP amphiphiles were characterised by atomic force microscopy (AFM), transmission electron microscopy (TEM) and dynamic light scattering (DLS) measurements. The ability to bind pDNA was determined by gel electrophoresis. Cytotoxicity of 1,4-DHP amphiphile–pDNA complexes was analysed using colorimetric 3-(4,5-dimethylthiazol-2-yl)-2,5-diphenyl-tetrazolium bromide (MTT) assay and the ability to deliver  $\beta$ -galactosidase plasmid into the monkey fibroblasts (CV1-P) cell line was assessed using the *o*-nitrophenylgalactopyranoside (ONPG) method. Furthermore, the ARA of the synthesised compounds was studied by 1,1-diphenyl-2-picrylhydrazyl (DPPH) radical scavenging assay.

## Results and discussion

### Synthesis

The synthesis of the new compounds studied in this work is described in Scheme 1. The synthesis of amphiphilic compounds **1** and **4–20** is achieved *via* a multi-step sequence. The first step of this approach is Hantzsch synthesis of the parent compound 3,5-bis(dodecyloxy carbonyl)-2,6-dimethyl-4-phenyl-1,4-dihydropyridine (**2**).<sup>19,22,33</sup> The second step is bromination of 2,6-methyl groups with *N*-bromosuccinimide (NBS) resulting in the second parent compound 2,6-di(bromomethyl)-3,5-bis(dodecyloxy carbonyl)-4-phenyl-1,4-dihydropyridine (**3**).<sup>19,22,33</sup> Previously Hyvönen *et al.*<sup>19</sup> demonstrated that hydrophobic dodecyloxy carbonyl substituents at positions 3 and 5 of the 1,4-DHP ring are optimal for the expression of transfection efficiency *in vitro*. However, there are no data about the impact of the cationic part of the 1,4-DHP amphiphile on gene delivery properties. In order to investigate the effect of the substituents at the cationic head-group of the amphiphilic 1,4-DHP molecule we modified amphiphile **1** at positions 2 and 6. Nucleophilic substitution of bromine in the parent compound **3** with various pyridine derivatives as well as pyrazine, *N*-methyl morpholine or *N*-methyl piperidine derivatives resulted in the target 1,4-DHP amphiphiles **4–20** (Scheme 1 and Table 1). Substitution reactions were performed at room temperature due to the fact that at temperatures above 50 °C lactonisation of 2,6-di(bromomethyl) substituted 1,4-DHP **3** to 8-phenyl-5,8-dihydro-1*H*,3*H*-difuro-[3,4-*b*:3',4'-*e*]pyridine-1,7(4*H*)-dione occurs.<sup>34</sup>



**Scheme 1** Synthesis of non-viral gene delivery agents – 1,4-DHP amphiphiles **1**, **4–20**. Reagents and conditions: (a) NBS, MeOH;<sup>19,33</sup> (b) substituted pyridine, pyrazine, *N*-methyl piperidine or *N*-methyl morpholine, acetone, r.t. (reaction time and yield of the products are summarised in Table 1).

**Table 1** Structure, yield, reaction time of the synthesis and affinity to the pDNA of 1,4-DHP amphiphiles **1** and **4–20**

Comp.	R	R'	Yield (%)	Reaction time (h)	Charge ratio, <sup>b</sup> ±
<b>1</b> <sup>a</sup>	H	H	78	24	2
<b>4</b>	4-CH <sub>3</sub>	H	68	24	2
<b>5</b>	4-N(CH <sub>3</sub> ) <sub>2</sub>	H	65	24	2
<b>6</b>	4-C(CH <sub>3</sub> ) <sub>3</sub>	H	30	48	2
<b>7</b>	4-NH <sub>2</sub>	H	50	24	2
<b>8</b>	4-CONH <sub>2</sub>	H	45	48	4
<b>9</b>	4-COCH <sub>3</sub>	H	35	48	4
<b>10</b>	4-CN	H	34	48	8
<b>11</b>	3-CH <sub>3</sub>	H	65	24	2
<b>12</b>	3-C <sub>6</sub> H <sub>5</sub>	H	60	48	8
<b>13</b>	3-NH <sub>2</sub>	H	54	24	2
<b>14</b>	3-CONH <sub>2</sub>	H	52	48	4
<b>15</b>	3-COCH <sub>3</sub>	H	36	48	4
<b>16</b>	3-CH <sub>3</sub>	4-CH <sub>3</sub>	47	24	2
<b>17</b>	3-CH <sub>3</sub>	5-CH <sub>3</sub>	64	24	2

Comp.	Het	Yield (%)	Reaction time (h)	Charge ratio, <sup>b</sup> ±
<b>18</b>	pyrazine	17	48	8
<b>19</b>	<i>N</i> -CH <sub>3</sub> piperidine	79	24	>16
<b>20</b>	<i>N</i> -CH <sub>3</sub> morpholine	98	24	>16

<sup>a</sup> The compound was previously reported.<sup>19</sup> <sup>b</sup> Amphiphiles were complexed with pDNA at different charge ratios ±32–0.125. The complexes were incubated for 25 min and gel electrophoresis was performed. Affinity to pDNA is expressed as minimum ± (1,4-DHP amphiphile–pDNA) charge ratio at which pDNA is completely bound by the amphiphile.

The bromine nucleophilic substitution reaction of 2,6-di(bromomethyl)-1,4-DHP **3** occurred easily and in general with 64–78% yield if the pyridine ring contained electron-donating properties possessing substituents (1,4-DHP amphiphiles **4**, **5**, **11** and **17**), with the exception of amphiphiles **6** and **16** (30 and 47% yield, respectively). In the case of pyridines with electron-withdrawing properties possessing substituents the product yield decreased to 17–52% (1,4-DHP amphiphiles **8–10**, **14** and **15**). The differences in the yield of products were rather insignificant due to the variable solubility of 1,4-DHP amphiphiles in acetone, which was used as reaction media. Elemental analysis of obtained products showed that the compounds were rather hygroscopic.

Elemental analysis of 1,4-DHP amphiphiles **4**, **7**, **12**, **14**, **15**, **19** and **20** was in accordance with the structures, and for the rest of the compounds elemental analysis showed that they were crystal hydrates.

The signals of 2,6-methylene groups of synthesised 1,4-DHP amphiphiles **1** and **4–20** in <sup>1</sup>H NMR spectra were usually

observed as an AB-system, which confirmed diastereotopic properties of CH<sub>2</sub>X protons in amphiphiles **1** and **4–20**. This fact is revealed by detailed studies of model compounds whose structures correspond to 1,1'-[(3,5-didodecyloxycarbonyl-4-phenyl-1,4-dihydropyridine-2,6-diyl)dimethylen]-bispyridinium dibromide (**1**) and its analogues with modifications at positions 3 and 5 of the 1,4-DHP ring.<sup>35</sup> In contrast, the signals of protons of 2,6-dimethylene groups of the fully aromatic compound appeared in the <sup>1</sup>H NMR spectrum as a singlet<sup>36</sup> suggesting that the above mentioned hydrogen bonds are not formed in this case.

The structures of synthesised 1,4-DHP amphiphiles **4–20** were established and confirmed by <sup>1</sup>H NMR data. Molecular weights of the synthesised compounds were in good agreement with the calculated values for all 1,4-DHP derivatives. The synthesis and characterisation of the 1,4-DHP amphiphiles **4–20** are given in detail in the Synthesis section. Purities of the studied compounds **1–20** were at least 98% according to high performance liquid chromatography (HPLC) data.

### Self-assembling properties of 1,4-DHP amphiphiles

Self-assembling properties of the compounds are important factors influencing the transfection efficiency. Due to the amphiphilic nature of the 1,4-DHP molecules it is predictable that they assemble spontaneously into nanoparticles in an aqueous environment.

Hyvönen *et al.* reported earlier that double charged 1,4-DHP amphiphiles possess self-assembling properties and were able to form liposomes.<sup>19</sup> The sizes of liposomes formed by amphiphile **1** and its close structural analogues with ester variations at positions 3 and 5 of the 1,4-DHP ring were found to have mean diameters in the range of 50–130 nm.<sup>19</sup> Almost all these compounds efficiently transfected the cells *in vitro*. In this study we tested the self-assembling properties of newly synthesised 1,4-DHP amphiphiles by atomic force microscopy (AFM), transmission electron microscopy (TEM) and dynamic light scattering (DLS) methods.

First we tested the self-assembling properties of all synthesised 1,4-DHP amphiphiles by AFM. According to the obtained data all amphiphiles possessed self-assembling properties and formed nanoparticles in an aqueous environment.

For more detailed studies we selected six 1,4-DHP amphiphiles which readily formed most stable nanoparticles in water. The chosen amphiphiles were **5**, **11**, **12**, **15** and **20** with various structural modifications at the cationic head-group and 1,4-DHP amphiphile **1** for comparison.

The images and vertical profiles of nanoparticles visualised by AFM are displayed in Fig. 2A. The self-assembling properties of the same 1,4-DHP amphiphiles were studied also by TEM using negative staining after treating with uranyl acetate (Fig. 2B).

According to AFM and TEM data, all studied nanoparticles formed by 1,4-DHP amphiphiles dispersed well without any aggregation and were homogeneous in morphology and shape (Fig. 2). The background between the nanoparticles appeared to be unstructured in TEM measurements. According to AFM data

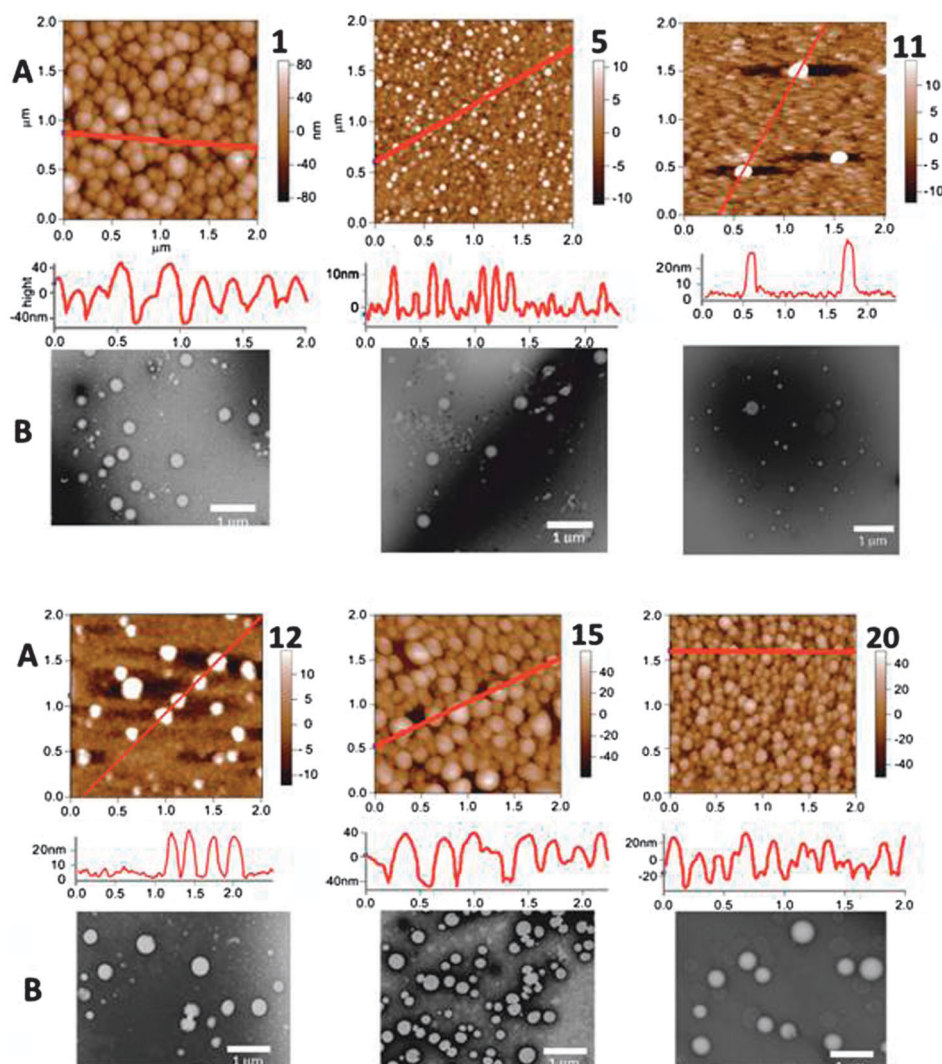


**Fig. 2** AFM images and vertical profiles of nanoparticles formed by 1,4-DHP amphiphiles **1**, **5**, **11**, **12**, **15** and **20** adsorbed on mica plates (A) and TEM images of formed nanostructures for the same amphiphiles **1**, **5**, **11**, **12**, **15** and **20** adsorbed to formvar carbon-coated copper grids and negatively stained with 1% uranyl acetate aqueous solution; bars = 1000 nm (B). The samples were prepared by sonication in an aqueous solution at an amphiphile concentration of 0.5 mg mL<sup>-1</sup>.

**Table 2** Size distribution, polydispersity index (PDI), zeta-potential, Z-average diameter and intensity-weighted size distribution of nanoparticles formed by amphiphiles **1**, **5**, **11**, **12**, **15** and **20** were obtained by DLS measurements. The mean diameter depicts the hydrodynamic diameter of the main population of the tested sample; the PDI value describes polydispersity of the sample; the zeta-potential gives information about the surface charge of nanoparticles; the Z-average diameter represents the average hydrodynamic diameter of all nanoparticles in the sample

Comp.	$D_{[H]}$ Z-aver./nm	PDI	Distr. peak (max) mean $d_{[H]}/nm$ (%)		Zeta-potential/ mV
			Peak 1	Peak 2	
<b>1</b>	113	0.345	151 (98.9)	5210 (1.1)	$82.1 \pm 9.54$
<b>5</b>	100	0.323	151 (96.6)	24.1 (3.4)	$65.9 \pm 13.6$
<b>11</b>	74.8	0.607	147 (88.7)	2.21 (3.4)	$67.0 \pm 11.7$
<b>12</b>	359	0.316	319 (100)	—	$62.0 \pm 10.7$
<b>15</b>	150	0.270	154 (100)	—	$61.0 \pm 11.7$
<b>20</b>	89.9	0.210	113 (100)	—	$59.9 \pm 12.2$

(Fig. 2A) amphiphile **5** formed rather small nanoparticles with an average size of 60–70 nm, whereas the nanoparticles formed by five amphiphiles **1**, **11**, **12**, **15** and **20** were larger with an average diameter up to 170–200 nm. According to the TEM images (Fig. 2B), the average size of the nanoparticles formed by 1,4-DHP amphiphiles **1**, **11**, **12**, **15** and **20** varied between 150 and 350 nm. Nanoparticles formed by 1,4-DHP amphiphile **5** appeared to have an average diameter up to 330 nm. In conclusion, 1,4-DHP amphiphiles were able to self-aggregate and to form nanoparticles in aqueous media with sizes between 60 and 350 nm.

Zeta-potentials for six selected amphiphiles were determined by DLS (Table 2). The obtained data indicated that the nanoparticles formed by selected amphiphiles had quite similar surface characteristics and the surface charges were strongly positive. Zeta-potentials over 30 mV confirm that the formed nanoparticle solutions are also relatively stable.<sup>37</sup>

The hydrodynamic diameters of the nanoparticles formed by selected 1,4-DHP amphiphiles **1**, **5**, **11**, **12**, **15** and **20** in water were determined also by DLS measurements (Table 2 and Fig. 3).

Additionally, for all selected amphiphiles the polydispersity index (PDI) was measured (Table 2). The results revealed that amphiphile **11** possessing a PDI of 0.607 shows rather broad particle size distribution. It seems from the obtained DLS data

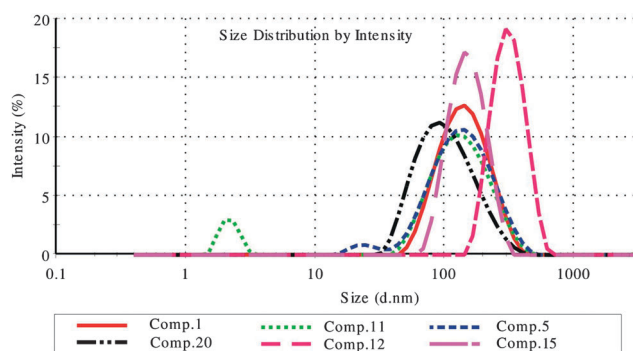


**Fig. 3** Representative dynamic light scattering spectrum (intensity-weighted Gaussian distribution) of nanoparticles formed by 1,4-DHP amphiphiles **1**, **5**, **11**, **12**, **15** and **20** in aqueous solution at 25 °C.

that compound **11** forms micelles (diameter smaller than 5 nm) rather than vesicles in contrast to the other tested amphiphiles. Overall, small changes in the chemical structure of amphiphiles are vitally important for the properties of the formed nanoparticles. It could be assumed that even small changes in the chemical structure of amphiphiles might bring changes in the properties of the formed nanoparticles. For amphiphiles **1**, **5** and **12** PDI values were 0.345, 0.323 and 0.316, while the most homogeneous particles were formed by amphiphiles **15** and **20** with PDI of 0.270 and 0.210, respectively.

The discrepancies in the size of the nanoparticles formed by tested 1,4-DHP amphiphiles and determined by AFM, TEM and DLS methods might be explained by the differences in the measuring principles of these techniques<sup>38</sup> and by the changes which the self-aggregates undergo during the different sample preparation procedures.

In the DLS method the diameter of nanoparticles was measured in the hydrated state, whereas TEM and AFM images were obtained from the dried states of the self-aggregated samples. It is also noticeable that the DLS technique analyses the average size of the whole population of the nanoparticles, whereas AFM and TEM techniques are able to visualise only a small fraction of the nanoparticles. Although the size distributions obtained by AFM, TEM and DLS measurements were in line with each other, the average diameter of the nanoparticles observed by AFM and TEM methods was smaller than the average diameter measured by the DLS method. Similar findings have been reported by other groups related to cationic amphiphiles with a 3,4-dihydro-2(1H)-pyridone spacer.<sup>39</sup>

For self-assembling compounds, the concentration above which micelles and other nanoparticles are formed, called the critical micelle concentration (CMC), is an important characterisation. In this study CMC was determined for tested amphiphiles **1**, **5**, **11** and **15** in aqueous media by the DLS technique according to the procedure described by Topel *et al.*<sup>40</sup> To determine CMC, an aqueous solution of amphiphiles was prepared within the concentration range of 0.5 mg mL<sup>-1</sup> to 0.1 × 10<sup>-2</sup> mg mL<sup>-1</sup> starting from concentrated stock solution, which was subjected to a serial two-fold dilution each time with water. Preliminary CMC values for tested 1,4-DHP amphiphiles **1**, **5**, **11** and **15** are 30, 35, 20 and 15 μM, respectively. In this case small changes in the chemical structure of the amphiphile (in the cationic part) have no a significant influence on CMC values for tested amphiphiles.

Generally, it could be concluded that the structure of the cationic head-group of 1,4-DHP amphiphiles affects the size of the formed nanoparticles.

Further studies on the effect of sample concentration, sonication time and storage conditions on the size and morphology of the nanoparticles as well as CMC determination for all amphiphiles and its influence on the biological properties of compounds are currently ongoing in our group.

#### Affinity of 1,4-DHP amphiphiles to the pDNA

The first step in the gene delivery process is binding of the carrier with the pDNA molecule followed by pDNA condensation

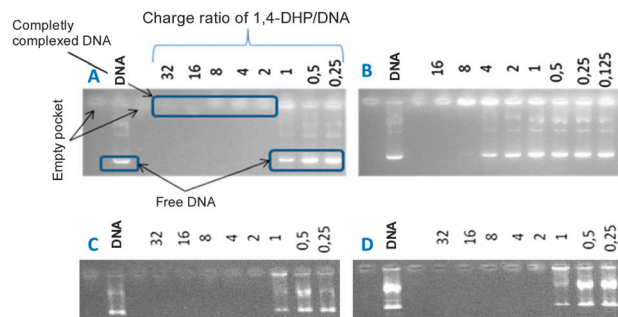


**Fig. 4** Gel electrophoresis of 1,4-DHP amphiphile-pDNA complexes: (A) amphiphile **4**, (B) amphiphile **12**, (C) amphiphile **5** and (D) amphiphile **11**.

and formation of the carrier-pDNA complex. Therefore, the relative pDNA binding affinities of the synthesised 1,4-DHP amphiphiles were evaluated by using gel electrophoresis. In this respect cationic 1,4-DHP amphiphiles were mixed with pDNA at different  $\pm$  charge ratios and the formed complexes were loaded on agarose gel. pDNA complexation was evaluated by monitoring the changes in pDNA migration in agarose gel. The assay is based on the ability of free negatively charged pDNA to migrate into the gel upon application of an electrical field, whereas complexed pDNA lacks this property. For example, 1,4-DHP amphiphiles **4**, **5** and **11** were able to completely bind pDNA at a charge ratio of  $\pm 2$  (Fig. 4A, C and D), whereas for amphiphile **12**, the corresponding charge ratio was  $\pm 8$  (Fig. 4B).

The binding affinities of all studied 1,4-DHP amphiphiles are represented in Table 1. We found that compounds with electron-donating properties possessing substituents in the pyridinium ring (e.g. amphiphiles **1**, **4**–**7**, **11**, **13**, **16** and **17**) were able to bind pDNA at a charge ratio of  $\pm 2$ , whereas 1,4-DHP amphiphiles with electron-withdrawing properties possessing substituents in the pyridinium ring (e.g. amphiphiles **8**–**10**, **14** and **15**) and pyrazinium moiety containing amphiphile **18** complexed pDNA less efficiently (at charge ratios  $\pm 4$  or **8**).

1,4-DHP amphiphiles **19** and **20** containing saturated heterocyclic moieties at the cationic head-group of the molecule, such as *N*-methyl piperidinium or *N*-methyl morpholinium, respectively, were not able to bind pDNA and even at a charge ratio of  $\pm 16$  the formed complexes were loose. Possible explanations for this poor affinity to pDNA may be the steric hindrance caused by *N*-methyl substituents or saturation of heterocyclic systems.

### Transfection efficacy of 1,4-DHP amphiphile-pDNA complexes

Next, we clarified whether the pDNA condensation ability correlated with the transfection efficacy of the synthesised 1,4-DHP amphiphiles. In order to realise this, the synthesised amphiphiles were tested for their ability to deliver the  $\beta$ -galactosidase reporter gene containing pDNA into the monkey fibroblasts (CV1-P). Transfection efficiencies of the novel 1,4-DHP amphiphiles were compared with those of amphiphile **1**, which is known to be the most efficient among the 1,4-DHP derivatives tested so far,<sup>19</sup> as well as with those of common transfection reagents: polymer PEI 25 and cationic lipid DOTAP. Gene transfection efficacy of the most efficient 1,4-DHP amphiphiles is represented in Fig. 5.

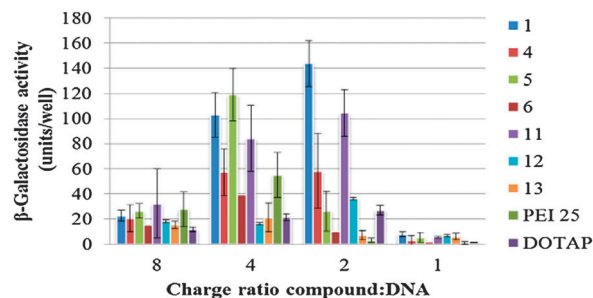


**Fig. 5** Gene transfection efficiency of the selected 1,4-DHP amphiphile-pDNA, PEI 25-pDNA and DOTAP-pDNA complexes. Data on the transfection efficacy of other amphiphiles were negligible and therefore are not shown. The cells were incubated with the complexes for 5 h and  $\beta$ -galactosidase expression was determined 45 h after the exposure. Data are presented as mean  $\pm$  SEM.

The results revealed that some 1,4-DHP amphiphiles showed high gene transfection activity *in vitro*. All tested amphiphiles were most efficient at charge ratios of  $\pm 2$  and **4**. Low transfection efficiency at charge ratio  $\pm 8$  can be explained by the increased cytotoxicity of the amphiphiles, whereas poor transfection of amphiphiles at charge ratio  $\pm 1$  might be due to the weak pDNA binding ability of amphiphiles or formation of loose and large complexes. At a charge ratio of  $\pm 2$  none of the novel 1,4-DHP amphiphiles appeared to be more active than amphiphile **1** although amphiphile **11** with a *meta*-methyl substituent at pyridinium moieties was only slightly less efficient than 1,4-DHP amphiphile **1**. At this charge ratio the transfection efficiency of 1,4-DHP amphiphile **1** was about 5 times better than that of DOTAP and 45 times more effective than that of PEI 25. Transfection efficacy between compounds reduced in the order 1,4-DHP amphiphile **1** > **11** > **4** > **12** > DOTAP > **5** > **6** > **13** > PEI 25.

Interestingly, at a charge ratio of  $\pm 4$ , amphiphile **5** with a *para*-dimethylamino substituent at pyridinium as the cationic head-group was more efficient than 1,4-DHP amphiphile **1**, although the difference was not significant. The activity of amphiphile **11** was again close to that of amphiphile **1**. At a charge ratio of  $\pm 4$  1,4-DHP amphiphile **1** was 1.8 times more effective than PEI 25, whose transfection level was higher at a charge ratio of  $\pm 4$  than at  $\pm 2$  (Fig. 5). In contrast, the activity of DOTAP did not change much and at a charge ratio of  $\pm 4$  it was still 5 times less effective than amphiphile **1**. The transfection efficacy at a charge ratio of  $\pm 4$  reduced in the following order: 1,4-DHP amphiphile **5** > **1** > **11** > **4** > PEI 25 > **6** > DOTAP  $\geq$  **13** > **12**.

Amphiphile **11**, containing a methyl substituent at *meta*-position of pyridinium moieties, was rather efficient at both charge ratios  $\pm 2$  and **4**, whereas amphiphile **4**, containing *para*-methyl substituted pyridinium moieties at the head-group, possessed barely 50% of the activity of amphiphile **1**. Based on the results we conclude that the differences in the transfection efficacy may be explained by the electronic nature of the substituent in the pyridinium rings. In this study, for the first time, we have demonstrated that compounds with electron-donating substituents at *para*- or *meta*-position of pyridinium moieties as the cationic head-group (1,4-DHP amphiphiles **4**, **5**, **11**–**13**) showed high gene transfection efficacy.



### Cytotoxicity of 1,4-DHP amphiphile-pDNA complexes

Cytotoxicity of the amphiphiles towards CV1-P cells was determined using colorimetric 3-(4,5-dimethylthiazol-2-yl)-2,5-diphenyltetrazolium bromide (MTT) assay. The cells were treated with 1,4-DHP amphiphile-pDNA complexes at various  $\pm$  charge ratios for 5 h. After exposure the cells were further incubated for 45 h until the analysis. The cytotoxicity of amphiphile-pDNA in comparison with PEI 25 and DOTAP complexes is summarised in Fig. 6 and expressed as a percentage of viable cells compared to the untreated control (100% of cells were viable). As was expected at low charge ratios ( $\pm 1$  and 2) the cytotoxicity of the complexes was rather low, as more than 80% of the cells were found viable (Fig. 6). At a charge ratio of  $\pm 4$ , most of the complexes formed by 1,4-DHP amphiphiles containing pyridinium moieties with substituents possessing electron-donating properties became more cytotoxic (1,4-DHP amphiphiles 6, 12 and 16) and the cytotoxicity was further increased at a charge ratio of  $\pm 8$  (1,4-DHP amphiphiles 1, 4-6, 11, 12, 16 and 17). The cytotoxicity at higher charge ratios for sure explains the lower transfection efficacy of 1,4-DHP amphiphiles.

In contrast, most of the complexes formed by 1,4-DHP amphiphiles containing pyridinium moieties with electron-withdrawing properties possessing substituents were not so cytotoxic even at higher N/P charge ratios (1,4-DHP amphiphiles 8-10, 14 and 15) as well as pyrazinium moieties containing amphiphile 18. Concerning the negligible transfection efficacy of all complexes formed by 1,4-DHP amphiphiles containing pyridinium moieties with electron-withdrawing properties possessing substituents and their relatively low capacity to bind pDNA (Table 1), it is possible that these 1,4-DHP amphiphiles form more loose complexes which are not able to enter the cells. Therefore toxicity of these compounds is not pronounced; 1,4-DHP amphiphiles 19 and 20 containing saturated *N*-methyl substituted heterocyclic moieties did not display any cytotoxicity. Noticeably, both amphiphiles were completely disabled to bind or condense pDNA (Fig. 6).

### Antiradical activity of 1,4-DHP amphiphiles

Free radicals closely associated with reactive oxygen species (ROS) cause cell aging and death. Antioxidants and radical scavengers play an important role in the defence of the body against ROS. According to the literature, antioxidant or anti-radical substances are able to reduce different radicals and hydrogen peroxide molecules before they react with the other cell organelles,<sup>41</sup> and thus antioxidants may prevent degradation of pDNA and lipids induced by free radicals.<sup>42</sup> During the last few years the AOA and ARA of different nanoparticles and nanoparticle-formed compounds have been very active and attractive research areas.<sup>43-47</sup>

Previously, Tirzitz *et al.* demonstrated ARA for 1,4-DHP derivatives,<sup>26</sup> as well as revealed their singlet oxygen quenching activity, similar to that of  $\alpha$ -tocopherol.<sup>48</sup> Particularly dihydropyridine derivatives are known to be oxidized to appropriate pyridine derivatives; in the case of 1,4-dihyronicotinamide (as part of redox coenzymes NAD-H or NADP-H) reciprocal hydrogen transfer occurs. Additionally some of the dihydropyridine derivatives act as electron and hydrogen donors to oxidants, activated unsaturated compounds, free radicals, reactive oxygen species, reactive nitrogen species, so antiradical and antioxidant properties of DHP derivatives have been discovered.<sup>49</sup> In this study we were interested in whether the novel synthesised 1,4-DHP amphiphiles possess ARA and how the substituent at the cationic head-group of the 1,4-DHP carrier molecule affects the ability to scavenge free radicals. In this respect, both parent 1,4-DHP derivatives 2 and 3, synthesised 1,4-DHP amphiphiles 1, 4-20 as well as PEI 25 and DOTAP were tested as scavengers of the 1,1-diphenyl-2-picrylhydrazyl (DPPH) radical according to the procedure described by Abdelwahed *et al.*<sup>50</sup> This method is widely used due to the stability and simplicity of the reaction system, which allows direct reaction between the radical and a potential antioxidant.<sup>51</sup> The ARA of tested 1,4-DHP derivatives was compared with that of Diludin – a 1,4-DHP derivative (chemical name 2,6-dimethyl-3,5-diethoxycarbonyl-1,4-dihydropyridine) which is unsubstituted at position 4 of

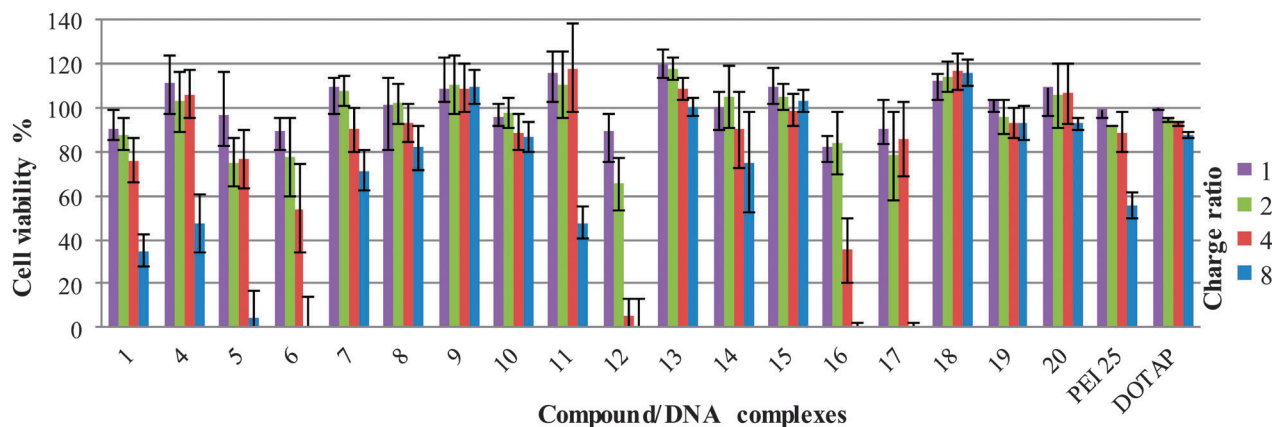


**Fig. 6** Cytotoxicity of 1,4-DHP amphiphile-pDNA, PEI 25-pDNA and DOTAP-pDNA complexes determined by MTT assay. Cell viability at charge ratios  $\pm 1$ , 2, 4 and 8 is displayed as a percentage of survived cells compared to the untreated control (100%). Data are presented as mean  $\pm$  SEM.

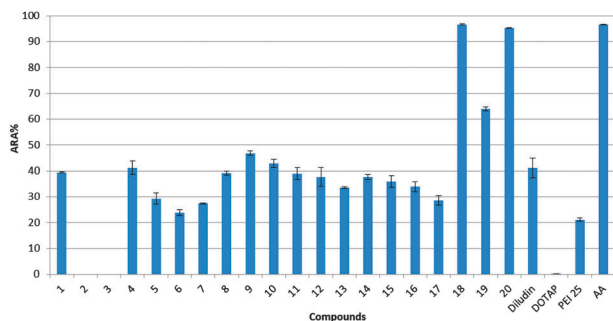


**Fig. 7** ARA of synthesised 1,4-DHP derivatives 1–20, PEI 25, DOTAP, Diludin and AA, evaluated by their ability to react with the DPPH. Results are expressed as a percentage (%) of the DPPH free radical scavenging. The untreated level of the DPPH radical is designated as 100%. Data are presented as mean  $\pm$  SD.

the 1,4-dihydropyridine ring and is a widely known antioxidant<sup>52,53</sup> – and with the activity of ascorbic acid (AA),<sup>54,55</sup> which is a well-known antioxidant and a free radical scavenger. The results showed that among the tested 1,4-DHP derivatives, amphiphiles 1, 4–17 and 19 possessed moderate ARA (25–60%, Fig. 7) which are comparable with the ARA of Diludin (40%, Fig. 7). In contrast, parent compounds 2 and 3 without the cationic head-group in the molecule totally lacked ARA activity, suggesting that the cationic head-group within 1,4-DHP amphiphilic derivatives is an essential structural moiety for expression of ARA. Interestingly, also PEI 25 showed minor ARA (20%, Fig. 7), whereas DOTAP lacked ARA activity, as was expected.

For Hantzsch type 2,6-dimethyl-1,4-dihydropyridine-3,5-dicarboxylates, structurally related to parent 1,4-DHP derivatives 2 and 3, the  $pK_a$  value is considered to be approximately 20.<sup>56</sup> We have, however, demonstrated that 1,4-DHP amphiphile 1 and related derivatives with varying lengths of alkyl chains at positions 3 and 5 and pyridinium as the head-group at positions 2 and 6 show buffering capacity in the pH range of 6–8 and have the  $pK_a$  value approximately at pH 7.<sup>19</sup> Deprotonation of the N–H group of the 1,4-DHP ring is caused by the proximity of positively charged substituents at positions 2 and 6 of the 1,4-DHP ring. In this study we revealed that parent derivatives 2 and 3 with the absence of the cationic head-groups were not able to display ARA. Our observation suggests that the ARA of the tested 1,4-DHP amphiphiles with different cationic substituents at 2,6-positions of the 1,4-DHP ring is related to the ability of their N–H group to protonate/deprotonate at physiological pH. This hypothesis corresponds with the data reported by other groups which particularly claim that the AOA of different indole derivatives depends on the dissociation energy of the N–H bond in their molecules.<sup>57</sup>

1,4-DHP amphiphiles 18 and 20, containing pyrazinium or *N*-methyl morpholinium substituents in the cationic head-group, displayed almost as high ARA as AA (95%, Fig. 7), suggesting that the second heteroatom (nitrogen or oxygen) at the *para*-position of the cationic head-group forming heterocycles is responsible for the high ARA among the studied amphiphiles.

Overall, the results show that the expression of ARA and/or gene delivery by amphiphiles was rather independent and no

certain correlation could be observed. Further experiments on the transgene expression with cells under oxidative stress conditions are needed in order to clarify whether the ARA is a beneficial property for gene delivery agents.

## Conclusions

We have designed and synthesised new 1,4-DHP amphiphiles with variations of the substituents at the cationic head-group of the molecule, containing different substituted pyridinium, pyrazinium, *N*-methyl piperidinium or *N*-methyl morpholinium moieties. The electronic nature of the substituent at the pyridinium as the cationic head-group strongly affects the ability of the 1,4-DHP amphiphiles to bind pDNA and to transfer it into the cells *in vitro*. Additionally, it defines the cytotoxicity of 1,4-DHP–pDNA complexes. Moreover, it was concluded that the cationic head-group within 1,4-DHP amphiphilic derivatives is an essential structural moiety for expression of ARA. These findings on the structure–activity relationships are highly important since 1,4-DHP amphiphiles have been earlier proposed as a promising tool for the delivery of pDNA into target cells *in vitro* and *in vivo*. However, further studies on the effect of the cationic head-group of the 1,4-DHP amphiphiles on their behaviour at different steps of transfection would be essential for developing an optimal structure for efficient transfection.

## Experimental

### General

All chemical reagents were purchased from ACROS, Sigma-Aldrich or Molecular Probes and used without further purification.

TLC was performed on Silica gel 60 F254 Aluminium sheets 20  $\times$  20 cm (Merck). <sup>1</sup>H NMR spectra were recorded with a Varian Mercury (200 MHz or 400 MHz) spectrometer. <sup>13</sup>C NMR spectra were recorded with a Varian Mercury (100 MHz) spectrometer. The chemical shifts of the atoms are reported in parts per million (ppm) relative to the residual signals of the solvent: CDCl<sub>3</sub> ( $\delta$ : 7.26) or DMSO-*d*<sub>6</sub> ( $\delta$ : 2.50) for <sup>1</sup>H NMR spectra and CDCl<sub>3</sub> ( $\delta$ : 77.16) or DMSO-*d*<sub>6</sub> ( $\delta$ : 39.52) for <sup>13</sup>C NMR. Multiplicities are abbreviated as s, singlet; d, doublet; t, triplet; q, quartet; m, multiplet; br, broad. The coupling constants are expressed in Hertz. Infrared spectra were recorded with an IRPrestige-21 FTIR spectrometer (Shimadzu). The Waters Alliance 2695 HPLC system was connected to a Waters 3100 mass detector operating in the ESI positive ion mode on a Waters Xbridge C18 column (5  $\mu$ m, 2.1  $\times$  50 mm) using a gradient elution with methanol–formic acid (0.1% in water) at a flow rate of 0.6 mL min<sup>−1</sup>. The compounds were analysed by HPLC on an Alltima CN column, 4.6  $\times$  150 mm, 5  $\mu$ m (Alltech), using a Waters Alliance 2695 HPLC system equipped with a 2485 UV/Vis detector. The eluent was acetonitrile–phosphate buffer (pH 2.2; 0.05 M) in water (10:90 by volume) at a flow rate of 1 mL min<sup>−1</sup>. Peak areas were determined electronically with a Waters Empower 2 chromatography data system. Melting points of the synthesised compounds were determined on an OptiMelt (SRS Stanford Research Systems). Elemental analyses were performed on an EA 1106 (Carlo Erba Instruments).

## Synthesis

The 3,5-bis(dodecyloxy carbonyl)-2,6-dimethyl-4-phenyl-1,4-dihydropyridine (2) was obtained from the acetoacetic dodecyl ester, benzaldehyde and ammonia by classical Hantzsch synthesis<sup>19</sup> or *via* two-component Hantzsch type cyclisation between 3-oxo-2-[1-phenylmethylidene]-butyric acid dodecyl ester and 3-amino-but-2-enoic acid dodecyl ester using 1-butyl-4-methylpyridinium chloride as the catalyst.<sup>33</sup> Bromination of 2,6-methyl groups of compound 2 with NBS gives 2,6-di(bromomethyl)-3,5-bis(dodecyloxy carbonyl)-4-phenyl-1,4-dihydropyridine (3). <sup>1</sup>H NMR (CDCl<sub>3</sub>, 200 MHz) spectra data of compounds 2 and 3 were identical to those reported in the literature.<sup>19,22,33</sup>

## General procedure for synthesis of amphiphilic

### 1,4-dihydropyridine derivatives 1, 4–20

To a solution of 2,6-di(bromomethyl)-3,5-bis(dodecyloxy carbonyl)-4-phenyl-1,4-dihydropyridine (3) (0.15 g, 0.45 mmol) in dry acetone (30 mL), the corresponding pyridine derivative (or pyrazine, or *N*-methyl piperidine or *N*-methyl morpholine) (0.90 mmol) was added and the resulting mixture was stirred at rt. After cooling, the precipitate was filtered off, washed with dry acetone and crystallised from ethanol. Reaction time and yield of products are summarised in Table 1.

**1,1'-[(3,5-Didodecyloxy carbonyl-4-phenyl-1,4-dihydropyridine-2,6-diyl)dimethylen]-bispyridinium dibromide (1).** *T*<sub>decomp.</sub> 135 °C (41%; *T*<sub>decomp.</sub> 157 °C),<sup>19</sup> <sup>1</sup>H NMR (400 MHz, DMSO-*d*<sub>6</sub>, δ): 0.86 (t, 6H, *J* = 6.6 Hz, 3,5-CH<sub>3</sub>); 1.17–1.29 (m, 36H, 3,5-(CH<sub>2</sub>)<sub>9</sub>); 3.14–1.54 (m, 4H, 3,5-OCH<sub>2</sub>CH<sub>2</sub>); 4.00 (t, 4H, *J* = 6.1 Hz, 3,5-OCH<sub>2</sub>); 5.02 (s, 1H, 4-H); 5.56 and 6.09 (AB-system, 4H, *J* = 14.8 Hz, 2,6-CH<sub>2</sub>); 7.19–7.30 (m, 5H, 4-Ar); 8.10 (dd, 4H, *J* = 7.8 and 6.6 Hz, 3-H Py); 8.58 (t, 2H, *J* = 7.8 Hz, 4-H Py); 8.95 (d, 4H, *J* = 6.6 Hz, 2-H Py); 10.2 (br s, 1H, N-H). <sup>13</sup>C NMR (CDCl<sub>3</sub>, δ): 14.09; 22.66; 25.96; 28.38; 29.27; 29.34; 29.56; 29.62; 29.63; 29.67; 31.89 (4-C-DHP); 39.74; 57.22 (2,6-CH<sub>2</sub>-DHP); 65.56 (3,5-OCH<sub>2</sub>); 110.46 (3,5-C-DHP); 127.52; 128.06; 128.59; 128.87; 137.97; 144.83; 145.45; 146.62; 166.41 (C=O). NMR spectra were in accordance with previously reported spectral data.<sup>33</sup> IR (flm) 3385 (N-H); 1691 (C=O); 1627 (C=C) cm<sup>-1</sup>. MS (+ESI) *m/z* (relative intensity) 766 (<sup>79</sup>Br) ([*M* – 2Br]<sup>+</sup>, 40%); 383 ([*M* – 2Br]<sup>+</sup>/2, 100%). Anal. calcd for C<sub>49</sub>H<sub>71</sub>N<sub>3</sub>O<sub>4</sub>Br<sub>2</sub>·2H<sub>2</sub>O: C, 61.18; H, 7.86; N, 4.37; found: C, 61.42; H, 7.85; N, 4.25.<sup>33</sup>

**1,1'-[(3,5-Didodecyloxy carbonyl-4-phenyl-1,4-dihydropyridine-2,6-diyl)dimethylen]-bis(4-methylpyridinium) dibromide (4).** *T*<sub>decomp.</sub> 135 °C, <sup>1</sup>H NMR (400 MHz, DMSO-*d*<sub>6</sub>, δ): 0.86 (t, 6H, *J* = 6.6 Hz, 3,5-CH<sub>3</sub>); 1.20–1.26 (m, 36H, 3,5-(CH<sub>2</sub>)<sub>9</sub>); 1.47–1.54 (m, 4H, 3,5-OCH<sub>2</sub>CH<sub>2</sub>); 2.61 (s, 6H, CH<sub>3</sub>); 4.02 (t, 4H, *J* = 6.6 Hz, 3,5-OCH<sub>2</sub>); 5.01 (s, 1H, 4-H); 5.51 and 6.01 (AB-system, 4H, *J* = 14.7 Hz, 2,6-CH<sub>2</sub>); 7.19–7.32 (m, 5H, 4-Ar); 7.93 (d, 4H, *J* = 6.5 Hz, 3,5-H Py); 8.80 (d, 4H, *J* = 6.5 Hz, 2,6-H Py); 10.3 (br s, 1H, N-H). <sup>13</sup>C NMR (DMSO-*d*<sub>6</sub>, δ): 13.92; 21.41; 22.10; 25.62; 28.01; 28.56; 28.74; 29.03; 29.06; 29.10; 31.31 (4-C-DHP); 56.71 (2,6-CH<sub>2</sub>-DHP); 64.49 (3,5-OCH<sub>2</sub>); 108.15 (3,5-C-DHP); 127.05; 127.58; 128.12; 128.29; 138.85; 143.61; 145.55; 159.75; 165.61 (C=O). IR (flm) 3404 (N-H); 1695 (C=O); 1630 (C=C) cm<sup>-1</sup>. MS (+ESI) *m/z* (relative intensity) 794 (<sup>79</sup>Br) ([*M* – 2Br]<sup>+</sup>, 30%);

397 ([*M* – 2Br]<sup>+</sup>/2, 100%). Anal. calcd for C<sub>51</sub>H<sub>75</sub>N<sub>3</sub>O<sub>4</sub>Br<sub>2</sub>: C, 64.21; H, 7.92; N, 4.40; found: C, 64.21; H, 7.61; N, 4.28.

**1,1'-[(3,5-Didodecyloxy carbonyl-4-phenyl-1,4-dihydropyridine-2,6-diyl)dimethylen]-bis(4-dimethylaminopyridinium) dibromide (5).** *T*<sub>decomp.</sub> 115 °C, <sup>1</sup>H NMR (200 MHz, DMSO-*d*<sub>6</sub>, δ): 0.85 (t, 6H, *J* = 6.6 Hz, 3,5-CH<sub>3</sub>); 1.17–1.32 (m, 36H, 3,5-(CH<sub>2</sub>)<sub>9</sub>); 1.46–1.59 (m, 4H, 3,5-OCH<sub>2</sub>CH<sub>2</sub>); 3.18 (s, 12H, N-CH<sub>3</sub>); 4.00 (t, 4H, *J* = 6.6 Hz, 3,5-OCH<sub>2</sub>); 4.97 (s, 1H, 4-H); 5.22 and 5.60 (AB-system, 4H, *J* = 14.4 Hz, 2,6-CH<sub>2</sub>); 6.98 (d, 4H, *J* = 7.8 Hz, 3,5-H Py); 7.18–7.28 (m, 5H, 4-Ar); 8.22 (d, 4H, *J* = 7.8 Hz, 2,6-H Py); 10.3 (br s, 1H, N-H). <sup>13</sup>C NMR (DMSO-*d*<sub>6</sub>, δ): 13.93; 22.10; 25.63; 28.03; 28.73; 28.74; 28.94; 29.00; 29.02; 29.04; 29.09; 31.31 (4-C-DHP); 39.79; 53.58 (2,6-CH<sub>2</sub>-DHP); 64.37 (3,5-OCH<sub>2</sub>); 106.95; 107.46 (3,5-C-DHP); 127.37; 128.30; 140.54; 141.74; 143.19; 145.84; 155.86; 165.75 (C=O). IR (flm) 3415 (N-H); 1690 (C=O); 1655 (C=C) cm<sup>-1</sup>. MS (+ESI) *m/z* (relative intensity) 852 (<sup>79</sup>Br) ([*M* – 2Br]<sup>+</sup>, 20%); 426 ([*M* – 2Br]<sup>+</sup>/2, 100%). Anal. calcd for C<sub>53</sub>H<sub>81</sub>N<sub>5</sub>O<sub>4</sub>Br<sub>2</sub>·3H<sub>2</sub>O: C, 59.71; H, 8.22; N, 6.57; found: C, 59.69; H, 8.17; N, 6.48.

**1,1'-[(3,5-Didodecyloxy carbonyl-4-phenyl-1,4-dihydropyridine-2,6-diyl)dimethylen]-bis(4-*tert*-butylpyridinium) dibromide (6).** *T*<sub>decomp.</sub> 120 °C, <sup>1</sup>H NMR (200 MHz, DMSO-*d*<sub>6</sub>, δ): 0.85 (t, 6H, *J* = 6.3 Hz, 3,5-CH<sub>3</sub>); 1.17–1.28 (m, 36H, 3,5-(CH<sub>2</sub>)<sub>9</sub>); 1.36 (s, 18H, CH<sub>3</sub>); 1.40–1.54 (m, 4H, 3,5-OCH<sub>2</sub>CH<sub>2</sub>); 3.98 (t, 4H, *J* = 6.3 Hz, 3,5-OCH<sub>2</sub>); 4.99 (s, 1H, 4-H); 5.65 and 5.96 (AB-system, 4H, *J* = 14.8 Hz, 2,6-CH<sub>2</sub>); 7.14–7.28 (m, 5H, 4-Ar); 8.16 (d, 4H, *J* = 6.6 Hz, 3,5-H Py); 8.95 (d, 4H, *J* = 6.6 Hz, 2,6-H Py); 10.4 (br s, 1H, N-H). <sup>13</sup>C NMR (DMSO-*d*<sub>6</sub>, δ): 13.92; 22.09; 25.56; 27.97; 28.54; 28.72; 29.01; 29.03; 29.07; 29.57; 31.30 (4-C-DHP); 36.36; 56.77 (2,6-CH<sub>2</sub>-DHP); 64.49 (3,5-OCH<sub>2</sub>); 107.99 (3,5-C-DHP); 124.80; 127.11; 127.56; 128.31; 138.57; 143.97; 145.80; 165.66 (C=O); 170.73. IR (flm) 3397 (N-H); 1695 (C=O); 1636 (C=C) cm<sup>-1</sup>. MS (+ESI) *m/z* (relative intensity) 878 (<sup>79</sup>Br) ([*M* – 2Br]<sup>+</sup>, 10%); 439 ([*M* – 2Br]<sup>+</sup>/2, 100%). Anal. calcd for C<sub>57</sub>H<sub>87</sub>N<sub>3</sub>O<sub>4</sub>Br<sub>2</sub>·H<sub>2</sub>O: C, 64.82; H, 8.49; N, 3.98; found: C, 64.82; H, 8.56; N, 3.87.

**1,1'-[(3,5-Didodecyloxy carbonyl-4-phenyl-1,4-dihydropyridine-2,6-diyl)dimethylen]-bis(4-aminopyridinium) dibromide (7).** *T*<sub>decomp.</sub> 213 °C, <sup>1</sup>H NMR (200 MHz, DMSO-*d*<sub>6</sub>, δ): 0.85 (t, 6H, *J* = 5.9 Hz, 3,5-CH<sub>3</sub>); 1.13–1.37 (m, 36H, 3,5-(CH<sub>2</sub>)<sub>9</sub>); 1.42–1.58 (m, 4H, 3,5-OCH<sub>2</sub>CH<sub>2</sub>); 3.99 (t, 4H, *J* = 5.9 Hz, 3,5-OCH<sub>2</sub>); 4.97 (s, 1H, 4-H); 5.18 and 5.54 (AB-system, 4H, *J* = 14.3 Hz, 2,6-CH<sub>2</sub>); 6.80 (d, 4H, *J* = 6.8 Hz, 3,5-H Py); 7.16–7.25 (m, 5H, 4-Ar); 8.12 (d, 4H, *J* = 6.8 Hz, 2,6-H Py); 8.20 (br s, 4H, NH<sub>2</sub>); 10.2 (br s, 1H, N-H). <sup>13</sup>C NMR (DMSO-*d*<sub>6</sub>, δ): 13.93; 22.10; 25.62; 28.03; 28.73; 28.74; 29.01; 29.03; 29.08; 31.31 (4-C-DHP); 53.96 (2,6-CH<sub>2</sub>-DHP); 64.32 (3,5-OCH<sub>2</sub>); 106.86; 109.18 (3,5-C-DHP); 126.95; 127.40; 128.22; 140.48; 142.66; 145.86; 158.71; 165.68 (C=O). IR (flm) 3308 (N-H + NH<sub>2</sub>); 1699 (C=O); 1650 (C=C) cm<sup>-1</sup>. MS (+ESI) *m/z* (relative intensity) 796 (<sup>79</sup>Br) ([*M* – 2Br]<sup>+</sup>, 20%); 498 ([*M* – 2Br]<sup>+</sup>/2, 100%). Anal. calcd for C<sub>49</sub>H<sub>73</sub>N<sub>5</sub>O<sub>4</sub>Br<sub>2</sub>: C, 60.99; H, 7.73; N, 7.22; found: C, 61.12; H, 7.71; N, 7.20.

**1,1'-[(3,5-Didodecyloxy carbonyl-4-phenyl-1,4-dihydropyridine-2,6-diyl)dimethylen]-bis(4-carbamoylpyridinium) dibromide (8).** *T*<sub>decomp.</sub> 240 °C, <sup>1</sup>H NMR (200 MHz, DMSO-*d*<sub>6</sub>, δ): 0.85 (t, 6H, *J* = 6.6 Hz, 3,5-CH<sub>3</sub>); 1.15–1.28 (m, 36H, 3,5-(CH<sub>2</sub>)<sub>9</sub>); 1.41–1.55 (m, 4H, 3,5-OCH<sub>2</sub>CH<sub>2</sub>); 3.97 (t, 4H, *J* = 6.6 Hz, 3,5-OCH<sub>2</sub>); 5.00 (s, 1H, 4-H); 5.68 and 6.07 (AB-system, 4H, *J* = 14.8 Hz, 2,6-CH<sub>2</sub>);

7.17–7.32 (m, 5H, 4-Ar); 8.33 and 8.71 ( $2 \times$  br s,  $2 \times$  2H, NH<sub>2</sub>); 8.39 (d, 4H,  $J = 5.1$  Hz, 3,5-H Py); 9.17 (d, 4H,  $J = 5.1$  Hz, 2,6-H Py); 10.3 (br s, 1H, N-H). <sup>13</sup>C NMR (DMSO-d<sub>6</sub>,  $\delta$ ): 13.92; 22.10; 25.03; 27.32; 28.72; 28.76; 28.95; 29.02; 29.08; 31.31 (4-C-DHP); 61.89 (2,6-CH<sub>2</sub>-DHP); 66.29 (3,5-OCH<sub>2</sub>); 108.33 (3,5-C-DHP); 125.45; 125.63; 127.10; 128.73; 147.03; 148.27; 149.06; 151.50; 163.52 (CONH<sub>2</sub>); 165.11 (C=O). IR (flm) 3445 (N-H + CONH<sub>2</sub>); 1703 (C=O); 1683 (CONH<sub>2</sub>); 1674 (C=C) cm<sup>-1</sup>. MS (+ESI)  $m/z$  (relative intensity) 852 (<sup>79</sup>Br) ([M - 2Br]<sup>+</sup>, 100%); 426 ([M - 2Br]<sup>+</sup>/2, 15%). Anal. calcd for C<sub>51</sub>H<sub>73</sub>N<sub>5</sub>O<sub>6</sub>Br<sub>2</sub>·H<sub>2</sub>O: C, 59.47; H, 7.34; N, 6.80; found: C, 59.37; H, 7.36; N, 6.59.

**1,1'-[(3,5-Didodecyloxy carbonyl-4-phenyl-1,4-dihydropyridine-2,6-diyl)dimethylen]-bis(4-acetylpyridinium) dibromide (9).**  $T_{\text{decomp}}$  156 °C, <sup>1</sup>H NMR (200 MHz, DMSO-d<sub>6</sub>,  $\delta$ ): 0.85 (t, 6H,  $J = 6.2$  Hz, 3,5-CH<sub>3</sub>); 1.14–1.29 (m, 36H, 3,5-(CH<sub>2</sub>)<sub>9</sub>); 1.44–1.58 (m, 4H, 3,5-OCH<sub>2</sub>CH<sub>2</sub>); 2.74 (s, 6H, CH<sub>3</sub>); 3.98 (t, 4H,  $J = 6.2$  Hz, 3,5-OCH<sub>2</sub>); 5.00 (s, 1H, 4-H); 5.70 and 6.14 (AB-system, 4H,  $J = 14.7$  Hz, 2,6-CH<sub>2</sub>); 7.14–7.34 (m, 5H, 4-Ar); 8.43 (d, 4H,  $J = 6.6$  Hz, 3,5-H Py); 9.21 (d, 4H,  $J = 6.6$  Hz, 2,6-H Py); 10.4 (br s, 1H, N-H). <sup>13</sup>C NMR (DMSO-d<sub>6</sub>,  $\delta$ ): 13.92; 22.10; 25.62; 27.45; 27.99; 28.73; 29.03; 29.05; 29.09; 31.31 (4-C-DHP); 57.91 (2,6-CH<sub>2</sub>-DHP); 64.58 (3,5-OCH<sub>2</sub>); 108.37 (3,5-C-DHP); 125.67; 127.16; 127.68; 128.39; 138.41; 145.53; 146.29; 148.98; 165.64 (C=O); 195.49 (COCH<sub>3</sub>). IR (flm) 3393 (N-H); 1694 (C=O + COCH<sub>3</sub>); 1636 (C=C) cm<sup>-1</sup>. MS (+ESI)  $m/z$  (relative intensity) 850 (<sup>79</sup>Br) ([M - 2Br]<sup>+</sup>, 15%); 425 ([M - 2Br]<sup>+</sup>/2, 100%). Anal. calcd for C<sub>53</sub>H<sub>75</sub>N<sub>3</sub>O<sub>6</sub>Br<sub>2</sub>·2H<sub>2</sub>O: C, 60.86; H, 7.61; N 4.02; found: C, 60.91; H, 7.44; N, 3.94.

**1,1'-[(3,5-Didodecyloxy carbonyl-4-phenyl-1,4-dihydropyridine-2,6-diyl)dimethylen]-bis(4-cyanopyridinium) dibromide (10).**  $T_{\text{decomp}}$  150 °C, <sup>1</sup>H NMR (200 MHz, DMSO-d<sub>6</sub>,  $\delta$ ): 0.83 (t, 6H,  $J = 6.6$  Hz, 3,5-CH<sub>3</sub>); 1.15–1.28 (m, 36H, 3,5-(CH<sub>2</sub>)<sub>9</sub>); 1.41–1.55 (m, 4H, 3,5-OCH<sub>2</sub>CH<sub>2</sub>); 3.96 (t, 4H,  $J = 6.6$  Hz, 3,5-OCH<sub>2</sub>); 4.96 (s, 1H, 4-H); 5.60 and 6.15 (AB-system, 4H,  $J = 15.2$  Hz, 2,6-CH<sub>2</sub>); 7.15–7.32 (m, 5H, 4-Ar); 8.68 (d, 4H,  $J = 6.3$  Hz, 3,5-H Py); 9.24 (d, 4H,  $J = 6.3$  Hz, 2,6-H Py); 10.2 (br s, 1H, N-H). <sup>13</sup>C NMR (DMSO-d<sub>6</sub>,  $\delta$ ): 13.92; 22.09; 25.61; 27.99; 28.73; 29.03; 29.05; 29.09; 31.31 (4-C-DHP); 58.46 (2,6-CH<sub>2</sub>-DHP); 64.62 (3,5-OCH<sub>2</sub>); 108.86 (3,5-C-DHP); 114.60 (CN); 127.69; 128.32; 130.71; 130.82; 137.64; 145.36; 146.14; 157.86; 165.58 (C=O). IR (flm) 3405 (N-H); 23 1696 (C=O); 1634 (C=C) cm<sup>-1</sup>. MS (+ESI)  $m/z$  (relative intensity) 816 (<sup>79</sup>Br) ([M - 2Br]<sup>+</sup>, 10%); 408 ([M - 2Br]<sup>+</sup>/2, 100%). Anal. calcd for C<sub>51</sub>H<sub>69</sub>N<sub>5</sub>O<sub>4</sub>Br<sub>2</sub>·H<sub>2</sub>O: C, 61.63; H, 7.20; N, 7.05; found: C, 61.98; H, 7.18; N, 7.27.

**1,1'-[(3,5-Didodecyloxy carbonyl-4-phenyl-1,4-dihydropyridine-2,6-diyl)dimethylen]-bis(3-methylpyridinium) dibromide (11).**  $T_{\text{decomp}}$  160 °C, <sup>1</sup>H NMR (200 MHz, DMSO-d<sub>6</sub>,  $\delta$ ): 0.86 (t, 6H,  $J = 6.6$  Hz, 3,5-CH<sub>3</sub>); 1.16–1.29 (m, 36H, 3,5-(CH<sub>2</sub>)<sub>9</sub>); 1.43–1.56 (m, 4H, 3,5-OCH<sub>2</sub>CH<sub>2</sub>); 2.44 (s, 6H, CH<sub>3</sub>); 3.99 (t, 4H,  $J = 6.6$  Hz, 3,5-OCH<sub>2</sub>); 5.02 (s, 1H, 4-H); 5.50 and 6.07 (AB-system, 4H,  $J = 14.6$  Hz, 2,6-CH<sub>2</sub>); 7.21–7.33 (m, 5H, 4-Ar); 7.99 (dd, 2H,  $J = 8.1$  and  $J = 5.9$  Hz, 5-H Py); 8.44 (d, 2H,  $J = 8.1$  Hz, 4-H Py); 8.76 (d, 2H,  $J = 5.9$  Hz, 6-H Py); 8.79 (s, 2H, 2-H Py); 10.1 (br s, 1H, N-H). <sup>13</sup>C NMR (DMSO-d<sub>6</sub>,  $\delta$ ): 13.93; 17.87; 22.10; 25.59; 28.00; 28.73; 29.01; 29.02; 29.04; 29.09; 31.31 (4-C-DHP); 57.32 (2,6-CH<sub>2</sub>-DHP); 64.52 (3,5-OCH<sub>2</sub>); 108.19 (3,5-C-DHP); 127.10; 127.19; 127.57; 128.29; 138.42; 138.57; 141.87; 143.86; 145.56;

145.65; 165.63 (C=O). IR (flm) 3404 (N-H); 1690 (C=O); 1633 (C=C) cm<sup>-1</sup>. MS (+ESI)  $m/z$  (relative intensity) 794 (<sup>79</sup>Br) ([M - 2Br]<sup>+</sup>, 10%); 397 ([M - 2Br]<sup>+</sup>/2, 100%). Anal. calcd for C<sub>51</sub>H<sub>75</sub>N<sub>3</sub>O<sub>4</sub>Br<sub>2</sub>·3H<sub>2</sub>O: C, 60.77; H, 8.10; N, 4.17; found: C, 60.73; H, 7.77; N, 4.11.

**1,1'-[(3,5-Didodecyloxy carbonyl-4-phenyl-1,4-dihydropyridine-2,6-diyl)dimethylen]-bis(3-phenylpyridinium) dibromide (12).**  $T_{\text{decomp}}$  183 °C, <sup>1</sup>H NMR (200 MHz, DMSO-d<sub>6</sub>,  $\delta$ ): 0.85 (t, 6H,  $J = 6.6$  Hz, 3,5-CH<sub>3</sub>); 1.16–1.27 (m, 36H, 3,5-(CH<sub>2</sub>)<sub>9</sub>); 1.43–1.57 (m, 4H, 3,5-OCH<sub>2</sub>CH<sub>2</sub>); 4.02 (t, 4H,  $J = 6.6$  Hz, 3,5-OCH<sub>2</sub>); 5.06 (s, 1H, 4-H); 5.70 and 6.20 (AB-system, 4H,  $J = 13.3$  Hz, 2,6-CH<sub>2</sub>); 7.19–7.34 (m, 5H, 4-Ar); 7.53–7.61 (m, 6H, 3,4,5-H Ar); 7.73–7.82 (m, 4H, 2,6-H Ar); 8.07 (dd, 2H,  $J = 8.1$  and  $J = 6.6$  Hz, 5-H Py); 8.80 (d, 2H,  $J = 8.1$  Hz, 4-H Py); 8.87 (d, 2H,  $J = 6.6$  Hz, 6-H Py); 9.35 (s, 2H, 2-H Py); 10.4 (br s, 1H, N-H). <sup>13</sup>C NMR (DMSO-d<sub>6</sub>,  $\delta$ ): 13.94; 22.09; 25.58; 28.01; 28.72; 28.99; 29.01; 29.07; 31.30 (4-C-DHP); 57.71 (2,6-CH<sub>2</sub>-DHP); 64.59 (3,5-OCH<sub>2</sub>); 108.27 (3,5-C-DHP); 127.34; 127.38; 127.52; 127.95; 128.36; 129.49; 130.23; 132.85; 138.73; 139.10; 142.16; 143.37; 143.41; 145.47; 165.77 (C=O). IR (flm) 3375 (N-H); 1719 (C=O); 1698 (C=C) cm<sup>-1</sup>. MS (+ESI)  $m/z$  (relative intensity) 918 (<sup>79</sup>Br) ([M - 2Br]<sup>+</sup>, 20%); 459 ([M - 2Br]<sup>+</sup>/2, 100%). Anal. calcd for C<sub>61</sub>H<sub>79</sub>N<sub>3</sub>O<sub>4</sub>Br<sub>2</sub>: C, 67.96; H, 7.39; N, 3.90; found: C, 67.88; H, 7.45; N, 3.86.

**1,1'-[(3,5-Didodecyloxy carbonyl-4-phenyl-1,4-dihydropyridine-2,6-diyl)dimethylen]-bis(3-aminopyridinium) dibromide (13).**  $T_{\text{decomp}}$  198 °C, <sup>1</sup>H NMR (200 MHz, DMSO-d<sub>6</sub>,  $\delta$ ): 0.85 (t, 6H,  $J = 6.6$  Hz, 3,5-CH<sub>3</sub>); 1.08–1.34 (m, 36H, 3,5-(CH<sub>2</sub>)<sub>9</sub>); 1.44–1.58 (m, 4H, 3,5-OCH<sub>2</sub>CH<sub>2</sub>); 4.01 (t, 4H,  $J = 6.6$  Hz, 3,5-OCH<sub>2</sub>); 5.03 (s, 1H, 4-H); 5.38 and 5.96 (AB-system, 4H,  $J = 14.8$  Hz, 2,6-CH<sub>2</sub>); 6.67 (br s, 4H, NH<sub>2</sub>); 7.17–7.31 (m, 5H, 4-Ar); 7.51–7.67 (m, 4H, 4,5-H Py); 8.00 (d, 2H,  $J = 5.1$  Hz, 6-H Py); 8.05 (s, 2H, 2-H Py); 10.3 (br s, 1H, N-H). <sup>13</sup>C NMR (DMSO-d<sub>6</sub>,  $\delta$ ): 13.94; 22.10; 25.60; 28.01; 28.73; 28.74; 29.01; 29.03; 29.04; 29.06; 29.09; 31.31 (4-C-DHP); 57.28 (2,6-CH<sub>2</sub>-DHP); 64.54 (3,5-OCH<sub>2</sub>); 108.01 (3,5-C-DHP); 127.07; 127.52; 127.59; 127.66; 127.76; 128.32; 130.60; 138.93; 145.41; 148.43; 165.55 (C=O). IR (flm) 3295 (N-H + NH<sub>2</sub>); 1694 (C=O); 1623 (C=C) cm<sup>-1</sup>. MS (+ESI)  $m/z$  (relative intensity) 796 (<sup>79</sup>Br) ([M - 2Br]<sup>+</sup>, 10%); 398 ([M - 2Br]<sup>+</sup>/2, 100%). Anal. calcd for C<sub>49</sub>H<sub>73</sub>N<sub>5</sub>O<sub>4</sub>Br<sub>2</sub>·2H<sub>2</sub>O: C, 59.33; H, 7.82; N, 7.06; found: C, 59.71; H, 7.76; N, 6.87.

**1,1'-[(3,5-Didodecyloxy carbonyl-4-phenyl-1,4-dihydropyridine-2,6-diyl)dimethylen]-bis(3-carbamoylpyridinium) dibromide (14).**  $T_{\text{decomp}}$  170 °C, <sup>1</sup>H NMR (200 MHz, DMSO-d<sub>6</sub>,  $\delta$ ): 0.85 (t, 6H,  $J = 5.9$  Hz, 3,5-CH<sub>3</sub>); 1.14–1.28 (m, 36H, 3,5-(CH<sub>2</sub>)<sub>9</sub>); 1.44–1.56 (m, 4H, 3,5-OCH<sub>2</sub>CH<sub>2</sub>); 3.99 (t, 4H,  $J = 5.9$  Hz, 3,5-OCH<sub>2</sub>); 5.01 (s, 1H, 4-H); 5.63 and 6.14 (AB-system, 4H,  $J = 14.8$  Hz, 2,6-CH<sub>2</sub>); 7.21–7.33 (m, 5H, 4-Ar); 8.17 (dd, 2H,  $J = 6.6$  and  $J = 8.1$  Hz, 5-H Py); 8.21 and 8.59 ( $2 \times$  br s,  $2 \times$  2H, NH<sub>2</sub>); 8.94 (d, 2H,  $J = 8.1$  Hz, 4-H Py); 9.02 (d, 2H,  $J = 6.6$  Hz, 6-H Py); 9.35 (s, 2H, 2-H Py); 10.1 (br s, 1H, N-H). <sup>13</sup>C NMR (DMSO-d<sub>6</sub>,  $\delta$ ): 13.94; 22.10; 27.59; 27.98; 28.73; 29.01; 29.03; 29.09; 31.31 (4-C-DHP); 58.00 (2,6-CH<sub>2</sub>-DHP); 64.59 (3,5-OCH<sub>2</sub>); 108.42 (3,5-C-DHP); 127.11; 127.62; 127.73; 128.34; 133.39; 138.33; 143.96; 145.39; 145.51; 145.66; 162.51 (CONH<sub>2</sub>); 165.67 (C=O). IR (flm) 3267 (N-H + CONH<sub>2</sub>); 1694 (C=O + CONH<sub>2</sub>); 1644 (C=C) cm<sup>-1</sup>. MS (+ESI)  $m/z$  (relative intensity) 852 (<sup>79</sup>Br) ([M - 2Br]<sup>+</sup>, 25%);

426 ( $[M - 2Br]^+/2$ , 100%). Anal. calcd for  $C_{51}H_{73}N_5O_6Br_2$ : C, 60.53; H, 7.27; N, 6.92; found: C, 60.53; H, 7.27; N, 6.82.

**1,1'-[(3,5-Didodecyloxy carbonyl-4-phenyl-1,4-dihydropyridine-2,6-diyl)dimethylen]-bis(3-acetylpyridinium) dibromide (15).**  $T_{decomp}$ . 155 °C,  $^1H$  NMR (200 MHz, DMSO- $d_6$ ,  $\delta$ ): 0.85 (t, 6H,  $J = 6.2$  Hz, 3,5-CH<sub>3</sub>); 1.13–1.32 (m, 36H, 3,5-(CH<sub>2</sub>)<sub>9</sub>); 1.44–1.57 (m, 4H, 3,5-OCH<sub>2</sub>CH<sub>2</sub>); 2.73 (s, 6H, CH<sub>3</sub>); 4.00 (t, 4H,  $J = 6.2$  Hz, 3,5-OCH<sub>2</sub>); 5.01 (s, 1H, 4-H); 5.77 and 6.17 (AB-system, 4H,  $J = 14.7$  Hz, 2,6-CH<sub>2</sub>); 7.20–7.30 (m, 5H, 4-Ar); 8.22 (dd, 2H,  $J = 8.1$  and  $J = 6.6$  Hz, 5-H Py); 9.02 (d, 2H,  $J = 8.1$  Hz, 4-H Py); 9.12 (d, 2H,  $J = 6.6$  Hz, 6-H Py); 9.52 (s, 2H, 2-H Py); 10.5 (br s, 1H, N-H).  $^{13}C$  NMR (CDCl<sub>3</sub>,  $\delta$ ): 13.93; 22.09; 25.59; 27.38; 27.98; 28.73; 29.01; 29.02; 29.04; 29.05; 29.09; 31.31 (4-C-DHP); 57.78 (2,6-CH<sub>2</sub>-DHP); 64.62 (3,5-OCH<sub>2</sub>); 108.26 (3,5-C-DHP); 127.18; 127.57; 128.19; 128.38; 134.80; 138.55; 145.08; 145.51; 145.81; 146.70; 165.72 (C=O); 193.02 (COCH<sub>3</sub>). IR (flm) 3396 (N-H); 1694 (C=O); 1683 (CONH<sub>2</sub>); 1630 (C=C)  $cm^{-1}$ . MS (+ESI)  $m/z$  (relative intensity) 850 ( $^{79}Br$ ) ( $[M - 2Br]^+$ , 15%); 425 ( $[M - 2Br]^+/2$ , 100%). Anal. calcd for  $C_{53}H_{75}N_3O_6Br_2$ : C, 63.03; H, 7.48; N, 4.16; found: C, 62.86; H, 7.46; N, 4.07.

**1,1'-[(3,5-Didodecyloxy carbonyl-4-phenyl-1,4-dihydropyridine-2,6-diyl)dimethylen]-bis(3,4-dimethylpyridinium) dibromide (16).**  $T_{decomp}$ . 172 °C,  $^1H$  NMR (200 MHz, DMSO- $d_6$ ,  $\delta$ ): 0.85 (t, 6H,  $J = 6.2$  Hz, 3,5-CH<sub>3</sub>); 1.16–1.27 (m, 36H, 3,5-(CH<sub>2</sub>)<sub>9</sub>); 1.41–1.55 (m, 4H, 3,5-OCH<sub>2</sub>CH<sub>2</sub>); 2.35 (s, 6H, CH<sub>3</sub>); 2.50 (s, 6H, CH<sub>3</sub>); 3.98 (t, 4H,  $J = 6.2$  Hz, 3,5-OCH<sub>2</sub>); 5.00 (s, 1H, 4-H); 5.45 and 5.96 (AB-system, 4H,  $J = 14.7$  Hz, 2,6-CH<sub>2</sub>); 7.18–7.33 (m, 5H, 4-Ar); 7.87 (d, 2H,  $J = 5.9$  Hz, 5-H Py); 8.61–8.72 (m, 4H, 6-H Py + 2-H Py); 10.2 (br s, 1H, N-H).  $^{13}C$  NMR (DMSO- $d_6$ ,  $\delta$ ): 13.93; 16.28; 19.68; 22.10; 28.61; 28.01; 28.74; 29.02; 29.09; 31.31 (4-C-DHP); 56.70 (2,6-CH<sub>2</sub>-DHP); 64.48 (3,5-OCH<sub>2</sub>); 107.97 (3,5-C-DHP); 127.08; 127.59; 127.68; 128.28; 137.35; 138.77; 141.31; 142.49; 145.72; 158.68; 165.63 (C=O). IR (flm) 3465 and 3371 (N-H as two sharp bands); 1694 (C=O); 1639 (C=C)  $cm^{-1}$ . MS (+ESI)  $m/z$  (relative intensity) 822 ( $^{79}Br$ ) ( $[M - 2Br]^+$ , 30%); 411 ( $[M - 2Br]^+/2$ , 100%). Anal. calcd for  $C_{53}H_{79}N_3O_4Br_2 \cdot H_2O$ : C, 63.66; H, 8.16; N, 4.20; found: C, 63.75; H, 8.10; N, 4.16.

**1,1'-[(3,5-Didodecyloxy carbonyl-4-phenyl-1,4-dihydropyridine-2,6-diyl)dimethylen]-bis(3,5-dimethylpyridinium) dibromide (17).**  $T_{decomp}$ . 140 °C,  $^1H$  NMR (200 MHz, DMSO- $d_6$ ,  $\delta$ ): 0.86 (t, 6H,  $J = 6.6$  Hz, 3,5-CH<sub>3</sub>); 1.16–1.29 (m, 36H, 3,5-(CH<sub>2</sub>)<sub>9</sub>); 1.43–1.54 (m, 4H, 3,5-OCH<sub>2</sub>CH<sub>2</sub>); 2.40 (s, 12H, CH<sub>3</sub>); 3.99 (t, 4H,  $J = 6.6$  Hz, 3,5-OCH<sub>2</sub>); 5.01 (s, 1H, 4-H); 5.47 and 6.03 (AB-system, 4H,  $J = 13.5$  Hz, 2,6-CH<sub>2</sub>); 7.18–7.36 (m, 5H, 4-Ar); 8.32 (s, 2H, 4-H Py); 8.62 (s, 4H, 2,6-H Py); 10.1 (br s, 1H, N-H).  $^{13}C$  NMR (DMSO- $d_6$ ,  $\delta$ ): 13.94; 17.73; 22.10; 25.59; 28.01; 28.56; 28.74; 28.95; 29.01; 29.03; 29.04; 29.09; 31.32 (4-C-DHP); 57.19 (2,6-CH<sub>2</sub>-DHP); 64.52 (3,5-OCH<sub>2</sub>); 108.03 (3,5-C-DHP); 127.57; 128.28; 137.14; 137.62; 138.52; 141.26; 145.71; 147.05; 165.68 (C=O). IR (flm) 3388 (N-H); 1690 (C=O); 1633 (C=C)  $cm^{-1}$ . MS (+ESI)  $m/z$  (relative intensity) 822 ( $^{79}Br$ ) ( $[M - 2Br]^+$ , 40%); 411 ( $[M - 2Br]^+/2$ , 100%). Anal. calcd for  $C_{53}H_{79}N_3O_4Br_2 \cdot H_2O$ : C, 63.66; H, 8.16; N, 4.20; found: C, 63.85; H, 8.19; N, 4.11.

**1,1'-[(3,5-Didodecyloxy carbonyl-4-phenyl-1,4-dihydropyridine-2,6-diyl)dimethylen]-bispiazinium dibromide (18).**  $T_{decomp}$ . 185 °C,  $^1H$  NMR (200 MHz, DMSO- $d_6$ ,  $\delta$ ): 0.86 (t, 6H,  $J = 6.6$  Hz, 3,5-CH<sub>3</sub>);

1.16–1.33 (m, 36H, 3,5-(CH<sub>2</sub>)<sub>9</sub>); 1.42–1.58 (m, 4H, 3,5-OCH<sub>2</sub>CH<sub>2</sub>); 4.00 (t, 4H,  $J = 6.6$  Hz, 3,5-OCH<sub>2</sub>); 5.01 (s, 1H, 4-H); 5.62 and 6.20 (AB-system, 4H,  $J = 15.3$  Hz, 2,6-CH<sub>2</sub>); 7.18–7.33 (m, 5H, 4-Ar); 9.14 (d, 4H,  $J = 4.4$  Hz, 3,5-H Pyr); 9.55 (d, 4H,  $J = 4.4$  Hz, 2,6-H Pyr); 10.1 (br s, 1H, N-H).  $^{13}C$  NMR (DMSO- $d_6$ ,  $\delta$ ): 13.93; 22.10; 25.06; 27.98; 28.73; 29.03; 29.05; 29.09; 31.31 (4-C-DHP); 58.26 (2,6-CH<sub>2</sub>-DHP); 64.67 (3,5-OCH<sub>2</sub>); 109.07 (3,5-C-DHP); 127.20; 127.75; 128.34; 136.92; 137.12; 145.28; 150.74; 165.62 (C=O). IR (flm) 3387 (N-H); 1690 (C=O); 1634 (C=C)  $cm^{-1}$ . MS (+ESI)  $m/z$  (relative intensity) 768 ( $^{79}Br$ ) ( $[M - 2Br]^+$ , 20%); 384 ( $[M - 2Br]^+/2$ , 100%). Anal. calcd for  $C_{47}H_{69}N_5O_4Br_2 \cdot H_2O$ : C, 59.68; H, 7.57; N, 7.40; found: C, 59.89; H, 7.46; N, 7.31.

**1,1'-[(3,5-Didodecyloxy carbonyl-4-phenyl-1,4-dihydropyridine-2,6-diyl)dimethylen]-bis(*N*-methylpiperidinium) dibromide (19).**  $T_{decomp}$ . 105 °C,  $^1H$  NMR (200 MHz, CDCl<sub>3</sub>,  $\delta$ ): 0.82 (t, 6H,  $J = 6.2$  Hz, 3,5-CH<sub>3</sub>); 1.19–1.27 (m, 36H, 3,5-(CH<sub>2</sub>)<sub>9</sub>); 1.45–1.67 (m, 12H, 3,5-OCH<sub>2</sub>CH<sub>2</sub> and piperidinium); 1.73–1.92 (m, 4H, piperidinium); 3.13 (s, 6H, N-CH<sub>3</sub>); 3.33–3.48 (m, 4H, piperidinium); 3.55–3.89 (m, 4H, piperidinium); 3.92 (t, 4H,  $J = 6.2$  Hz, 3,5-OCH<sub>2</sub>); 4.78 and 4.86 (AB-system, 4H,  $J = 14.0$  Hz, 2,6-CH<sub>2</sub>); 5.08 (s, 1H, 4-H); 6.98–7.19 (m, 5H, 4-Ar); 9.8 (br s, 1H, N-H).  $^{13}C$  NMR (CDCl<sub>3</sub>,  $\delta$ ): 14.27; 20.48; 20.58; 21.26; 22.84; 26.33; 28.98; 29.54; 29.82; 29.83; 29.87; 32.08 (4-C-DHP); 47.79; 56.70 (2,6-CH<sub>2</sub>-DHP); 62.25; 63.82; (3,5-OCH<sub>2</sub>); 77.36; 109.49 (3,5-C-DHP); 126.07; 126.99; 128.01; 149.27; 149.32; 169.33 (C=O). IR (flm) 3393 (N-H); 1653 (C=O); 1633 (C=C)  $cm^{-1}$ . MS (+ESI)  $m/z$  (relative intensity) 806 ( $^{79}Br$ ) ( $[M - 2Br]^+$ , 40%); 403 ( $[M - 2Br]^+/2$ , 100%). Anal. calcd for  $C_{51}H_{87}N_3O_4Br_2$ : C, 63.41; H, 9.08; N, 4.35; found: C, 63.79; H, 9.29; N, 4.49.

**1,1'-[(3,5-Didodecyloxy carbonyl-4-phenyl-1,4-dihydropyridine-2,6-diyl)dimethylen]-bis(*N*-methylmorpholinium) dibromide (20).**  $T_{decomp}$ . 117 °C,  $^1H$  NMR (400 MHz, CDCl<sub>3</sub>,  $\delta$ ): 0.88 (t, 6H,  $J = 7.1$  Hz, 3,5-CH<sub>3</sub>); 1.24–1.33 (m, 36H, 3,5-(CH<sub>2</sub>)<sub>9</sub>); 1.60–1.66 (m, 4H, 3,5-OCH<sub>2</sub>CH<sub>2</sub>); 3.47–3.55 (m, 2H, morpholinium); 3.65–3.77 (m, 2H, morpholinium); 3.68 (s, 6H, N-CH<sub>3</sub>); 3.96–4.08 (m, 4H, morpholinium); 4.04 (t, 4H,  $J = 7.1$  Hz, 3,5-OCH<sub>2</sub>); 4.09–4.22 (m, 6H, morpholinium); 4.38–4.46 (m, 2H, morpholinium); 5.19 and 5.38 (AB-system, 4H,  $J = 12.4$  Hz, 2,6-CH<sub>2</sub>); 5.20 (s, 1H, 4-H); 7.21 (t, 1H,  $J = 7.5$  Hz, 4-H Ph); 7.44–7.51 (m, 2H, 2,6-H Ph); 7.53–7.59 (m, 2H, 3,5-H Ph); 9.9 (br s, 1H, N-H).  $^{13}C$  NMR (CDCl<sub>3</sub>,  $\delta$ ): 14.26; 22.81; 26.12; 28.54; 29.43; 29.49; 29.72; 29.78; 29.83; 32.05 (4-C-DHP); 39.91; 57.52 (2,6-CH<sub>2</sub>-DHP); 65.70 (3,5-OCH<sub>2</sub>); 77.36; 110.57 (3,5-C-DHP); 127.65; 128.18; 128.76; 145.62; 146.74; 166.59 (C=O). IR (flm) 3447 (N-H); 1688 (C=O); 1636 (C=C)  $cm^{-1}$ . MS (+ESI)  $m/z$  (relative intensity) 810 ( $^{79}Br$ ) ( $[M - 2Br]^+$ , 30%); 405 ( $[M - 2Br]^+/2$ , 100%). Anal. calcd for  $C_{49}H_{83}N_3O_6Br_2$ : C, 60.67; H, 8.62; N, 4.33; found: C, 60.41; H, 8.49; N, 4.25.

### Self-assembling properties of 1,4-DHP amphiphiles

Samples for AFM, TEM and DLS studies were prepared by dispersing selected 1,4-DHP amphiphiles (1, 5, 12, 15 and 20) in an aqueous solution at a concentration of 0.5 mg mL<sup>-1</sup> by sonication using a probe type sonicator (Cole Parmer ultrasonic processor CPX 130W (USA)). The settings were as follows: amplitude 30%, pulse 15 s on, 15 s off, 5 min (amphiphiles 1, 5, 15 and 20) and 15 min (amphiphile 12).

**Atomic force microscopy.** Freshly cleaved mica plates were dipped into the solution of samples and kept for 30 s to allow the nanoparticles formed by 1,4-DHP amphiphiles to stick to the negatively charged surface. The mica samples were dried at room temperature and visualised by AFM in tapping mode with an Asylum Research MFP-3D-BIOTM AFM in dynamic mode using Olympus AC240TM tips. The software *IGOR Pro 6* was used for analysis of AFM images and characterisation of average parameters of obtained nanoparticles.

**Transmission electron microscopy.** The morphology of nanoparticles formed by 1,4-DHP amphiphiles was studied by TEM applying a negative staining technique. One drop of the sample was adsorbed to a formvar carbon-coated copper grid and negatively stained with 1% aqueous solution of uranyl acetate. The grids were examined with a JEM-1230 TEM at 100 kV. The diameter of 400 nanoparticles of each negatively stained sample was measured from electron microscopic micrographs.

**Dynamic light scattering.** The DLS measurements of the nanoparticles formed by compounds were carried in water using a Zetasizer Nano S90 instrument with Malvern Instruments Ltd software.

The zeta-potentials were determined *via* DLS measurements using a Malvern nanoZS apparatus with the following specifications: medium: water; refractive index: 1.330; viscosity: 0.8872 cP; temperature: 25 °C; dielectric constant: 78.5. Nanoparticles: liposomes; refractive index of materials: 1.60. Beam mode F(Ka): 1.5 (Smoluchowski model). Data were analysed using multimodal number distribution software included with the instrument.

The critical micelle concentrations were determined in aqueous media using a Zetasizer Nano S90 instrument with Malvern Instruments Ltd software. A series of solutions of amphiphiles with concentrations ranging from 0.5 mg mL<sup>-1</sup> to 0.1 × 10<sup>-2</sup> mg mL<sup>-1</sup> were prepared from a stock solution of selected 1,4-DHP amphiphiles (1, 5, 11 and 15) at a concentration 0.5 mg mL<sup>-1</sup> obtained as described above. All next samples were prepared starting from the concentrated stock solution, which was subjected to a serial two-fold dilution each time with water. The intensity values of scattered light (kcps) as a function of concentration of amphiphiles were analysed. The scattering intensities detected for amphiphile concentrations below CMC have an approximately constant value corresponding to water. The intensity starts to show a linear increase with concentration at the CMC, since the amount of nanoparticles increases in the solution. The intersection of the best fit lines drawn through the data points is the preliminary CMC value of amphiphiles.

#### Preparation of the carriers and the carrier-pDNA complexes

For DNA binding, transfection and cytotoxicity experiments the liposomal solutions of 1,4-DHP amphiphiles as well as DOTAP were prepared using the thin film hydration method as previously described.<sup>19</sup> Briefly, an appropriate amount of compounds was dissolved in chloroform which was then evaporated until a thin film appeared. The samples were subjected to a stream of nitrogen for 2 h to remove the traces of chloroform. The dried thin films were hydrated with de-ionized water at 45 °C and sonicated with a bath type sonicator until clear liposomal solutions were obtained.

The final concentrations of DHPs were 1.25 mM (relative to the cationic amphiphile). The concentration of DOTAP was 3.2 mM (relative to the cationic lipid). To obtain 0.9 mg mL<sup>-1</sup> polymer solution, the stock of PEI 25 (Sigma) was dissolved in water and pH was adjusted to 7.4.

In order to obtain complexes at N/P ratios ranging from 0.125 to 32 (carrier-pDNA) various amounts of carrier stock solution were gently mixed with 0.6 µg of pDNA. The complexes were prepared in 50 mM MES-50 mM HEPES-75 mM NaCl buffer (pH 7.2). The complexes were allowed to stand at room temperature for 25 min prior to use.

#### Gel electrophoresis

The 1,4-DHP amphiphile-pDNA complexes were prepared at different charge ratios, as described above. After formation, gel running buffer containing bromophenol blue was added to the complexes and complexes were loaded on a 0.9% agarose gel prepared in Tris-borate/EDTA buffer, pH 8.0. The gel was run at 65 V for 3 h. After ethidium bromide (EtBr) staining of the gel, pDNA bands were visualised using an UV transilluminator and photographed (Biometra, Bio-Doc II/NT, Video Documentation System, Göttingen, Germany).

#### Transfection assay

The cells were seeded in growth medium (100 µL) into a 96-well plate (20 000 cells per well). The next day, the medium was replaced with fresh medium without serum (150 µL). The DHP amphiphile-pDNA complexes at different ± charge ratios were added to the cells. The dose of pDNA per well was 0.6 µg. After 5 h incubation at 37 °C, the complexes were removed, the cells were washed with phosphate buffered saline (PBS), and the growth medium was added. After 45 h of incubation, the cells were lysed with 2% Triton X-100 and deep frozen. The β-galactosidase activity in each well was determined spectrophotometrically with an ELx800 automated microplate reader (Bio-Tek Instruments Inc., Winooski, VT, USA) by monitoring the hydrolysis of ONPG at 405 nm.<sup>58</sup> Purified β-galactosidase from *E. coli* was used to generate a standard curve for calculation of the β-galactosidase activity in the samples.

#### Cytotoxicity assay

Cytotoxicity of the 1,4-DHP amphiphile-pDNA complexes was studied using a colorimetric 3-(4,5-dimethylthiazol-2-yl)-2,5-diphenyltetrazolium bromide (MTT) assay.<sup>59</sup> Briefly, the cells were plated on a 96-well plate and transfected as described above. After 45 h incubation (37 °C at 7% CO<sub>2</sub>), the cells were washed with PBS, the growth medium was replaced with serum-free medium and 10 µL of MTT (5 mg mL<sup>-1</sup>) was added per well. The plate was incubated for 2 h at 37 °C and 100 µL of the solubilizing solution composed of 50% of sodium dodecyl sulphate and 50% of dimethylformamide, pH 4.7, was added to the cells. Absorbance at 570 nm was measured immediately using an automatic enzyme-linked immunosorbent assay plate reader (Labsystems Multiscan PLUS, Labssystem, Finland). Results were expressed as a percentage of viable cells compared to the negative control (untreated cells).

### Antiradical activity (ARA) studies: DPPH radical scavenging assay

Free radical scavenging activity of the synthesised 1,4-DHP derivatives 1–20 was evaluated by their ability to react with a stable radical of the 1,1-diphenyl-2-picrylhydrazyl (DPPH). An aliquot (0.5 mL) of the tested 1,4-DHP derivative or ascorbic acid (AA) solution in EtOH was added to 3 mL of freshly prepared DPPH solution in EtOH (0.1 mM). The final concentration of the tested compounds was 0.086 nM and the ratio of the tested compound and DPPH was equimolar. The solution was incubated for 30 min in the dark and changes in the optical density of solution were measured at 517 nm using a UV/Vis Camspec M501 spectrometer (UK). Each assay was performed in triplicate. The scavenging activity was defined as the decrease in sample absorbance versus absorbance of DPPH standard solutions. Results were expressed as a percentage (%) of the DPPH free radical scavenging, which is defined by the following formula:

$$\text{ARA}(\%) = \frac{\text{OD}_{\text{control}} - \text{OD}_{\text{sample}}}{\text{OD}_{\text{control}}} \times 100$$

where  $\text{OD}_{\text{control}}$  is the absorbance of standard solution of DPPH and  $\text{OD}_{\text{sample}}$  is the absorbance value for the sample.

### Cell cultures

CV1-P fibroblast cells derived from African green monkey kidney were cultured in Dulbecco's modified Eagle's medium (Gibco), supplemented with 10% fetal bovine serum and penicillin/streptomycin (100 U mL<sup>-1</sup> and 100 µg mL<sup>-1</sup>, respectively). Cells were maintained at 37 °C (7% CO<sub>2</sub>) and subcultured twice a week.

### Conflict of interest

The authors report no conflicts of interest with respect to this paper.

### Acknowledgements

The authors are thankful for the financial support from the EuroNanoMed project "CheTherDel" and Academia of Finland foundation No. 14127 for K. Pajuste as well as COST action CM1101 for fruitful discussion and possibility for dissemination of preliminary results. We are also grateful to professor A. Urtti for initiation and support of development of these studies, to P. Biryukov (MSc), Z. Alute (MSc) and Dr D. Erts of the Institute of Chemical Physics, University of Latvia, for the use and assistance with the AFM equipment and to the Institute of Physics, University of Latvia, for the use and assistance with the DLS equipment for determination of hydrodynamic diameters of nanoparticles as well as to Dr D. Tirezite for fruitful discussion about ARA results.

### Notes and references

- 1 T. Ren and D. Liu, *Bioorg. Med. Chem. Lett.*, 1999, **9**, 1247–1250.
- 2 E. Fiscaro, C. Compari, E. Duce, G. Donofrio, B. Rozycka-Rozsak and E. Wozniak, *Biochim. Biophys. Acta, Gen. Subj.*, 2005, **1722**, 224–233.
- 3 I. van der Woude, A. Wagenaar, A. A. Meekel, M. B. ter Beest, M. H. Ruiters, J. B. Engberts and D. Hoekstra, *Proc. Natl. Acad. Sci. U. S. A.*, 1997, **94**, 1160–1165.
- 4 A. Roosjen, J. Šmisterová, C. Driessen, J. T. Anders, A. Wagenaar, D. Hoekstra, R. Hulst and J. B. F. N. Engberts, *Eur. J. Org. Chem.*, 2002, 1271–1277.
- 5 M. A. Ilies, W. A. Seitz, I. Ghiviriga, B. H. Johnson, A. Miller, E. B. Thompson and A. T. Balaban, *J. Med. Chem.*, 2004, **47**, 3744–3754.
- 6 M. A. Ilies, W. A. Seitz, B. H. Johnson, E. L. Ezell, A. L. Miller, E. B. Thompson and A. T. Balaban, *J. Med. Chem.*, 2006, **49**, 3872–3887.
- 7 S. H. Wong, *Clin. Chem. Lab. Med.*, 2007, **45**, 799–800.
- 8 H. H. Kim, W. S. Lee, J. M. Yang and S. Shin, *Biochim. Biophys. Acta, Mol. Cell Res.*, 2003, **1640**, 129–136.
- 9 J. C. Rea, R. F. Gibly, A. E. Barron and L. D. Shea, *Acta Biomater.*, 2009, **5**, 903–912.
- 10 B. H. Zinselmeyer, S. P. Mackay, A. G. Schatzlein and I. F. Uchegbu, *Pharm. Res.*, 2002, **19**, 960–967.
- 11 A.-M. Caminade and J.-P. Majoral, *Prog. Polym. Sci.*, 2005, **30**, 491–505.
- 12 C. Dufes, I. F. Uchegbu and A. G. Schatzlein, *Adv. Drug Delivery Rev.*, 2005, **57**, 2177–2202.
- 13 P. L. Felgner, T. R. Gadek, M. Holm, R. Roman, H. W. Chan, M. Wenz, J. P. Northrop, G. M. Ringold and M. Danielsen, *Proc. Natl. Acad. Sci. U. S. A.*, 1987, **84**, 7413–7417.
- 14 D. D. Lasic and N. S. Templeton, *Adv. Drug Delivery Rev.*, 1996, **20**, 221–266.
- 15 C. F. Bennett, D. Mirejovsky, R. M. Crooke, Y. J. Tsai, J. Felgner, C. N. Sridhar, C. J. Wheeler and P. L. Felgner, *J. Drug Targeting*, 1998, **5**, 149–162.
- 16 N. S. Templeton, D. D. Lasic, P. M. Frederik, H. H. Strey, D. D. Roberts and G. N. Pavlakis, *Nat. Biotechnol.*, 1997, **15**, 647–652.
- 17 Y. Sun, I. Migueliz, G. Navarro and C. T. de Ilarduya, *Lett. Drug Des. Discovery*, 2009, **6**, 33–37.
- 18 B. Paul, A. Bajaj, S. S. Indi and S. Bhattacharya, *Tetrahedron Lett.*, 2006, **47**, 8401–8405.
- 19 Z. Hyvönen, A. Plotniece, I. Reine, B. Chekavichus, G. Duburs and A. Urtti, *Biochim. Biophys. Acta, Biomembr.*, 2000, **1509**, 451–466.
- 20 Z. Hyvönen, M. Ruponen, S. Rönkkö, P. Suhonen and A. Urtti, *Eur. J. Pharm. Sci.*, 2002, **15**, 449–460.
- 21 G. Byk, C. Dubertret, V. Escriou, M. Frederic, G. Jaslin, R. Rangara, B. Pitard, J. Crouzet, P. Wils, B. Schwartz and D. Scherman, *J. Med. Chem.*, 1998, **41**, 224–235.
- 22 A. Urtti, Z. Hyvönen, A. Plotniece, N. Makarova, I. Reine, G. Tirezite, B. Vigante, B. Cekavichus, A. Schmidlers, A. Krauze, R. Zhalubovskis, G. Duburs, M. Turunen, S. Ylä-Herttuala, I. Jääskeläinen and M.-R. Toppinen, *WO Patent*, 01/62946 A62941, Int.Cl.62947 C62912N 62915/62987, 62001, 2001 (*Chem. Abstr.* 62001, 62135, 206419h).
- 23 Z. Hyvönen, S. Rönkkö, M.-R. Toppinen, I. Jääskeläinen, A. Plotniece and A. Urtti, *J. Controlled Release*, 2004, **99**, 177–190.
- 24 D. J. Triggle, *Cell. Mol. Neurobiol.*, 2003, **23**, 293–303.
- 25 D. J. Triggle, *Mini-Rev. Med. Chem.*, 2003, **3**, 215–223.

- 26 G. D. Tirzitz and G. J. Duburs, *Chem. Heterocycl. Compd.*, 1972, **1**, 126–127.
- 27 D. Tirzitz, Z. Khyuvonen, A. Shimidlers, G. Tirzitz and G. Duburs, *Pharm. Chem. J.*, 2000, **34**, 297–300.
- 28 J. A. Imlay and S. Linn, *Science*, 1988, **240**, 1302–1309.
- 29 Q. T. Li, M. H. Yeo and B. K. Tan, *Biochem. Biophys. Res. Commun.*, 2000, **273**, 72–76.
- 30 M. D. Molina and T. J. Anchordoquy, *Biochim. Biophys. Acta, Biomembr.*, 2008, **1778**, 2119–2126.
- 31 T. Yoshitomi, A. Hirayama and Y. Nagasaki, *Biomaterials*, 2011, **32**, 8021–8028.
- 32 D. V. Ratnam, D. D. Ankola, V. Bhardwaj, D. K. Sahana and M. N. Kumar, *J. Controlled Release*, 2006, **113**, 189–207.
- 33 K. Pajuste, A. Plotniece, K. Kore, L. Intenberga, B. Cekavicus, D. Kaldre, G. Duburs and A. Sobolev, *Cent. Eur. J. Chem.*, 2011, **9**, 143–148.
- 34 I. P. Skrastinsh, V. V. Kastron, B. S. Chekavichus, A. E. Sausinsh, R. M. Zolotoyabko and G. Y. Dubur, *Chem. Heterocycl. Compd.*, 1991, **9**, 989–994.
- 35 M. Petrova, R. Muhamadejev, B. Vigante, B. Cekavicus, A. Plotniece, G. Duburs and E. Liepinsh, *Molecules*, 2011, **16**, 8041–8052.
- 36 A. Plotniece, K. Pajuste, D. Kaldre, B. Cekavicus, B. Vigante, B. Turovska, S. Belyakov, A. Sobolev and G. Duburs, *Tetrahedron*, 2009, **65**, 8344–8349.
- 37 L. L. Schramm, *Surfactants – Fundamentals and Application in Petroleum Industry*, Cambridge University Press, 2000.
- 38 B. G. Zanetti-Ramos, M. B. Fritzen-Garcia, T. B. Crezynski-Pasa, C. S. D. Oliveira, A. A. Pasa, V. Soldi and R. Borsali, *Part. Sci. Technol.*, 2010, **28**, 472–484.
- 39 R. Smits, Y. Goncharenko, I. Vesere, B. Skrivele, O. Petrichenko, B. Vigante, M. Petrova, A. Plotniece and G. Duburs, *J. Fluorine Chem.*, 2011, **132**, 414–419.
- 40 Ö. Topel, B. A. Çakır, L. Budama and N. Hoda, *J. Mol. Liq.*, 2013, **177**, 40–43.
- 41 A. O. Aytakin, S. Morimura and K. Kida, *J. Biosci. Bioeng.*, 2011, **111**, 212–216.
- 42 K. V. Harish Prashanth, S. M. Dharmesh, K. S. Jagannatha Rao and R. N. Tharanathan, *Carbohydr. Res.*, 2007, **342**, 190–195.
- 43 L. Yang, J.-m. Huang, Y.-g. Zu, C.-h. Ma, H. Wang, X.-w. Sun and Z. Sun, *Food Chem.*, 2011, **128**, 1152–1159.
- 44 Z. Nie, K. J. Liu, C.-J. Zhong, L.-F. Wang, Y. Yang, Q. Tian and Y. Liu, *Free Radical Biol. Med.*, 2007, **43**, 1243–1254.
- 45 X. Kong, L. Jin, M. Wei and X. Duan, *Appl. Clay Sci.*, 2010, **49**, 324–329.
- 46 P. Rajakumar, N. Venkatesan, K. Sekar, S. Nagaraj and R. Rengasamy, *Eur. J. Med. Chem.*, 2010, **45**, 1220–1224.
- 47 P. Basnet, H. Hussain, I. Tho and N. Skalko-Basnet, *J. Pharm. Sci.*, 2012, **101**, 598–609.
- 48 G. Tirzitz, I. Byteva, K. Salokhiddinov, G. Gurinovich and G. Dubur, *Chem. Heterocycl. Compd.*, 1981, **17**, 682–684.
- 49 A. Augustyniak, G. Bartosz, A. Čipak, G. Duburs, L. U. Horáková, W. Łuczaj, M. Majekova, A. D. Odysseos, L. Rackova, E. Skrzydlewska, M. Stefek, M. Štrosová, G. Tirzitz, P. R. Venskutonis, J. Viskupicova, P. S. Vranka and N. Žarković, *Free Radical Res.*, 2010, **44**, 1216–1262.
- 50 A. Abdelwahed, I. Bouhleb, I. Skandrani, K. Valenti, M. Kadri, P. Guiraud, R. Steiman, A.-M. Mariotte, K. Ghedira, F. Laporte, M.-G. Dijoux-Franca and L. Chekir-Ghedira, *Chem.-Biol. Interact.*, 2007, **165**, 1–13.
- 51 T. Noipa, S. Srijaranai, T. Tuntulani and W. Ngeontae, *Food Res. Int.*, 2011, **44**, 798–806.
- 52 L. Kouřimská, J. Pokorný and G. Tirzitz, *Nahrung*, 1993, **37**, 91–93.
- 53 G. Tirzitz, D. Tirzitz and Z. Hyvonen, *Czech J. Food Sci.*, 2001, **19**, 81–84.
- 54 L. S. Roberto, *Food Chem.*, 2008, **107**, 40–43.
- 55 A. Bendich, L. J. Machlin, O. Scandurra, G. W. Burton and D. D. M. Wayner, *Free Radical Biol. Med.*, 1986, **2**, 419–444.
- 56 B. A. Vigante, M. I. Terekhova, Y. Y. Ozols, E. S. Petrov and G. Y. Dubur, *Chem. Heterocycl. Compd.*, 1989, **9**, 1028–1031.
- 57 T. Nishiyama, T. Suzuki, Y. Hashiguchi, S. Shiotsu and M. Fujioka, *Polym. Degrad. Stab.*, 2002, **75**, 549–554.
- 58 J. H. Felgner, R. Kumar, C. N. Sridhar, C. J. Wheeler, Y. J. Tsai, R. Border, P. Ramsey, M. Martin and P. L. Felgner, *J. Biol. Chem.*, 1994, **269**, 2550–2561.
- 59 T. Mosmann, *J. Immunol. Methods*, 1983, **65**, 55–63.



## **Publication**

### **F**

Studies of preparation and stability of liposomes formed by 1',1,-[(3,5-didodecyloxycarbonyl)-4-phenyl-1,4-dihydropyridine-2,6-diil)-dimethylen]bispyridinium dibromide.

*Adv. Materials Research.* 2013, 787, 157-162.

## Studies of Preparation and Stability of Liposomes Formed by 1,1'-[(3,5-didodecyloxycarbonyl-4-phenyl-1,4-dihydropyridine-2,6-diyl)-dimethylen]bispyridinium Dibromide

Rucins Martins<sup>1,a</sup>, Petricenko Oksana<sup>2,b</sup>, Pajuste Karlis<sup>1,c</sup>, Plotniece Mara<sup>1,d</sup>,  
Pajuste Klavs<sup>1,e</sup>, Gosteva Marina<sup>1,f</sup>, Cekavicus Brigita<sup>1,g</sup>, Sobolev Arkadij<sup>1,h</sup>  
and Plotniece Aiva<sup>1,i</sup>

<sup>1</sup>Latvian Institute of Organic Synthesis, Aizkraukles str. 21, Riga, LV-1006, Latvia

<sup>2</sup>Faculty of Physics and Mathematics, University of Latvia, Zellu str. 8, Riga, LV-1002, Latvia

<sup>a</sup>rucins@osi.lv, <sup>b</sup>oksana.petricenko@lu.lv, <sup>c</sup>kpajuste@osi.lv, <sup>d</sup>marapl67@hotmail.com,  
<sup>e</sup>klap@inbox.lv, <sup>f</sup>mmarina@osi.lv, <sup>g</sup>brigita.cekavicus@inbox.lv, <sup>h</sup>arkady@osi.lv, <sup>i</sup>aiva@osi.lv

**Keywords:** 1,4-Dihydropyridine amphiphile, Self-assembling, Liposomes, Gene delivery, AFM, DLS.

**Abstract.** In this work we describe the studies of preparation and stability of liposomes formed by 1,1'-[(3,5-didodecyloxycarbonyl-4-phenyl-1,4-dihydropyridine-2,6-diyl)dimethylen]bispyridinium dibromide, novel lipid-like compound. The influence of the amount of amphiphilic compound, solvent and sonication time was studied. Liposomes were prepared by dispersing of compound in the corresponding media at a selected concentration by sonication using a probe type sonicator and characterised by atomic force microscopy (AFM) and dynamic light scattering (DLS) methods.

### Introduction

Previously, we have developed and studied multiple cationic 1,4-dihydropyridine (1,4-DHP) amphiphiles with different length of alkyl chains at the positions 3 and 5 of the 1,4-DHP ring. These amphiphiles have been demonstrated to condense and efficiently deliver plasmid DNA (pDNA) into different cell lines in vitro [1-4]. The structures of these cationic amphiphiles resemble those of other cationic lipids currently used for gene delivery and are composed of positively charged head-group, hydrophobic moiety and a linker connecting these two parts. It has been shown that dodecyloxycarbonyl substituents as hydrophobic moiety at positions 3 and 5 of the 1,4-DHP ring are optimal for high transfection efficiencies in vitro. Thus, 1,1'-[(3,5-didodecyloxycarbonyl-4-phenyl-1,4-dihydropyridine-2,6-diyl)dimethylen]-bispyridinium dibromide (1,4-DHP amphiphile 1, Fig. 1) was found to be more active than commercially available cationic lipid DOTAP (N-(1-(2,3-dioleoyloxy)propyl)-N,N,N-trimethylammonium methylsulfate) and cationic polymer PEI 25 (polyethyleneimine of 25 kDa) [1].

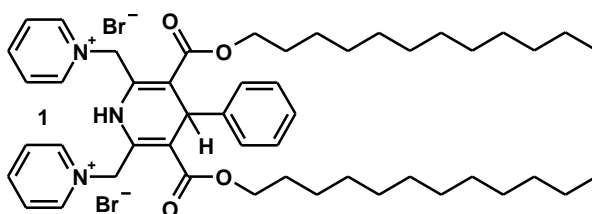


Figure 1. Structure of 1,1'-[(3,5-didodecyloxycarbonyl-4-phenyl-1,4-dihydropyridine-2,6-diyl)dimethylen]-bispyridinium dibromide (1).

Chemical structures of the 1,4-DHP amphiphiles have been revealed to be strongly influent on their physicochemical and biological activities. Pyridinium amphiphiles based on the 1,4-DHP core remain important as in the addition to the self-assembling properties they contain 1,4-DHP group as

an active linker, which according to Trigg is intrinsic structural part within many pharmacologically active compounds and drugs [5, 6]. 1,4-Dihydropyridine derivatives possess a broad range of other biological activities [7, 8].

In the present work we report studies of preparation conditions and stability of liposomes formed by 1,1'-[(3,5-didodecylloxycarbonyl-4-phenyl-1,4-dihydropyridine-2,6-diil)dimethylen]bispyridinium dibromide (1). The influence of the amount of amphiphilic compound, solvent and sonication intensity was studied.

## Materials and Methods

### Synthesis of 1,4-DHP amphiphile

The self-assembling 1,4-DHP amphiphile 1 is obtained according to the method described by Pajuste et al. [9]. The structure of synthesised compound 1 was established and confirmed by <sup>1</sup>H NMR, <sup>13</sup>C NMR, MS and elemental analysis data. Purity of the studied compound was at least 98% according to high performance liquid chromatography (HPLC) data.

### Preparation of liposomes

Briefly: Sample of liposomes was prepared by dispersing of compound 1 in the corresponding media at a selected concentration by sonication using a probe type sonicator, Cole Palmer ultrasonic processor CPX 130W (USA). The settings were following: amplitude 30%, pulse 15 s on, 15 s off, for selected time.

### Studies of liposomes

Atomic Force Microscopy (AFM) - For AFM studies freshly cleaved mica plates were dipped into the solution and kept for 30 s to allow the liposomes to stick to the negatively charged surface. The mica samples were dried at room temperature and observed by AFM in tapping mode with Asylum Research MFP-3D-BIOTM atomic force microscope in dynamic mode using Olympus AC240TM tips. Software IGOR Pro 6 was used for analysis of AFM images and characterisation of average parameters of obtained liposomes.

Dynamic Light Scattering (DLS) - The DLS measurements of the same samples were recorded on an equipment Zetasizer Nano S90 instrument with software of Malvern Instruments Ltd.

## Results

Atomic force microscopy and dynamic light scattering methods were used for characterisation of liposomes formed by 1,4-DHP amphiphile 1. AFM is ideally suited for characterisation of nanoparticles due to possibility of 3D visualization of sample and determination of average size of the nanoparticles [10] as well tapping mode of AFM allows the investigation of soft samples with minimal sample alteration and height resolution 0.1 nm [11]. DLS is a nonintrusive, sensitive method for characterisation of nanoparticles in solution. The main advantages of DLS are rapidity of analysis, no requirement for calibration, and sensitivity [12].

Self-assembling properties of the compounds are important factor influencing the transfection efficiency. Due to the amphiphilic nature of the 1,4-DHP molecules it is predictable that they assemble spontaneously into nanoparticles in aqueous environment. Hyvönen et al. reported earlier that double charged 1,4-DHP amphiphiles possess self-assembling properties and they are able to form liposomes. The sizes of liposomes formed by 1,4-DHP amphiphile 1 and its close structural analogues differing in ester substituents at the positions 3 and 5 of 1,4-DHP ring, were found to have mean diameters in the range of 50-130 nm. Almost all these compounds transfected efficiently the cells in vitro [1]. According to literature data, vesicle size was inversely related to content release properties where increased content release rates were found for smaller vesicle sizes. Liposomes around 100 nm in size are routinely used in vivo. Even small changes in size or a wider size distribution might affect stability and release properties and thus yield in decreased efficacy or unwanted side effects of drug loaded liposomes during in vivo applications [13].

At the beginning, samples from self-assembling compound 1 were prepared in aqueous media at concentrations 0.01 and 0.3 mg/ml and with sonication for 5 min. Stability of liposomes was tested every month during three month period. The obtained liposomes were visualised by AFM as images and vertical profiles of liposomes (Fig. 2).

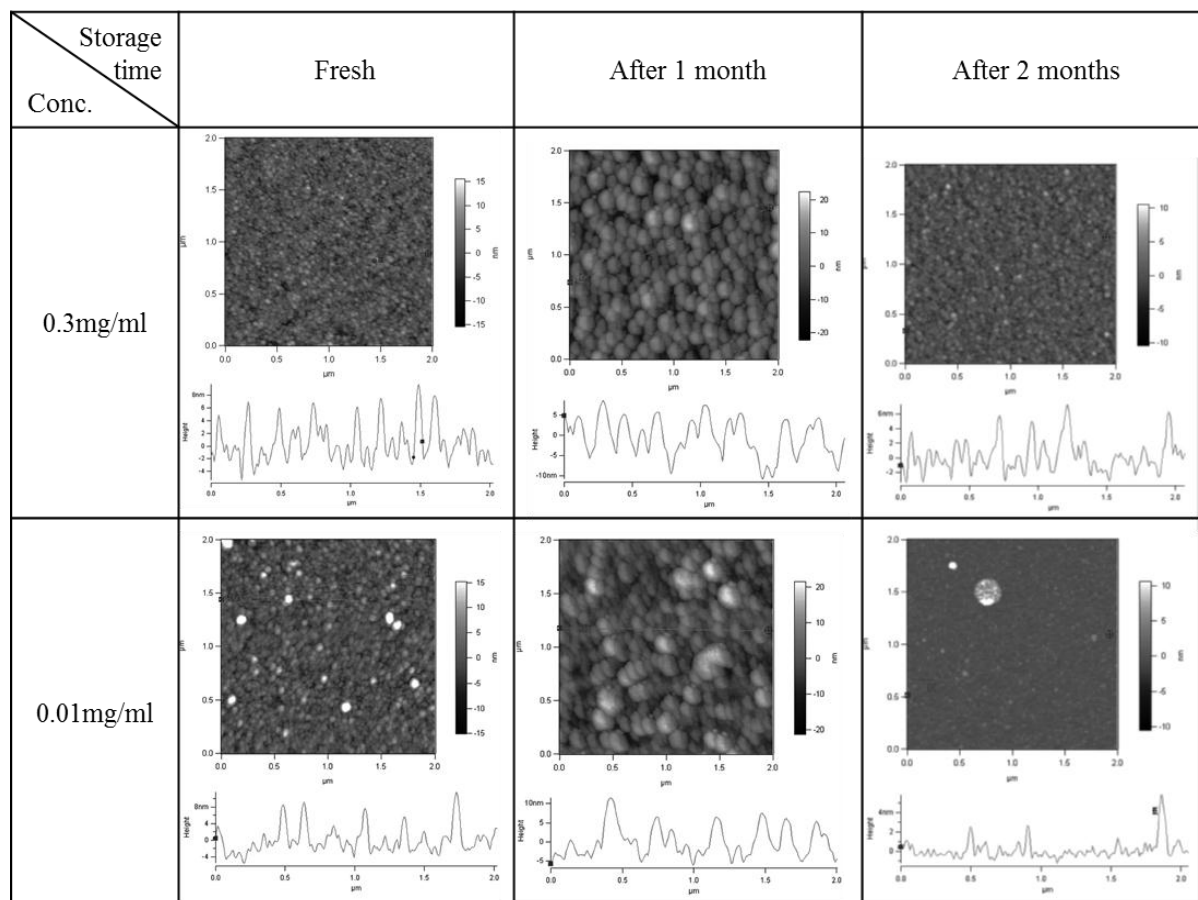


Figure 2. AFM images and vertical profiles of liposomes formed by 1,4-DHP amphiphile 1 at the concentrations 0.01 or 0.3 mg/ml; liposomes adsorbed on a mica plates.

From obtained AFM data it was concluded that liposomes formed by 1,4-DHP amphiphile 1 are with average diameter up to 100-150 nm and are stable at least for one month period.

Additionally, the hydrodynamic diameters of the liposomes formed by 1,4-DHP amphiphile 1 in water were determined also with DLS measurements (Fig. 3).

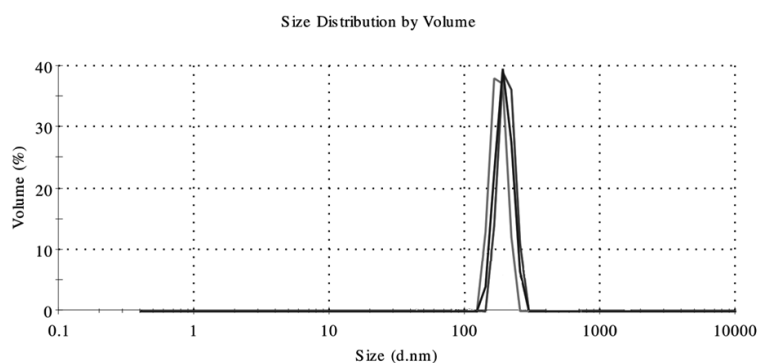


Figure 3. Representative dynamic light scattering spectrum (volume-weighted Gaussian distribution) of liposomes formed by 1,4-DHP amphiphile 1 in aqueous solution at 25°C; the concentration of compound 1 - 0.3 mg/ml and with sonication for 5 min.

We can conclude that the nanoparticles formed by 1,4-DHP amphiphile 1 were monodisperse (Fig. 3) with the average hydrodynamic diameter of 190-195 nm.

For testing of influence of sonication time, samples from 1,4-DHP amphiphile 1 were prepared in aqueous media at concentration 0.1 mg/ml and sonicated for 5 min and 5+15 min. The obtained liposomes were visualised by AFM as images and vertical profiles of liposomes (Fig. 4).

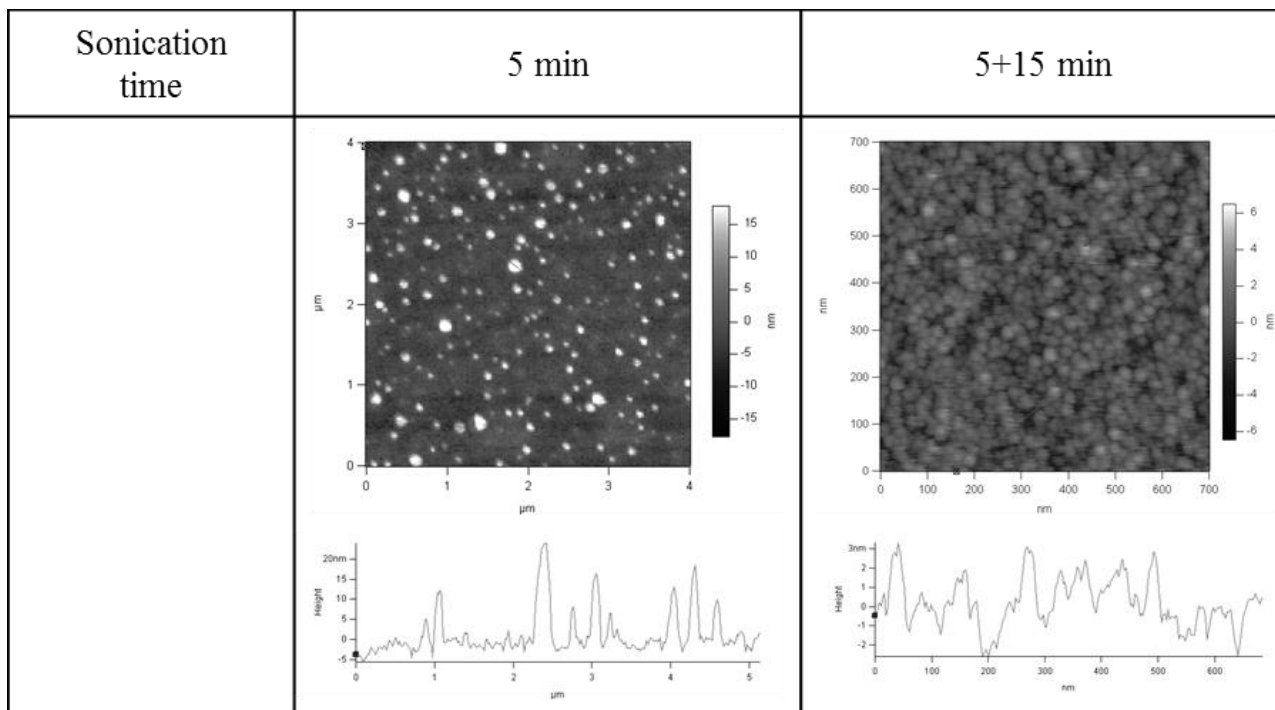


Figure 4. AFM images and vertical profiles of liposomes formed by 1,4-DHP amphiphile 1; sonication time 5 or 5+15 min; liposomes adsorbed on a mica plates.

According to obtained data we can conclude that, longer sonication time (at least 15 min), is essential for preparation of liposomes with rather narrow size distribution, as after short sonication time liposomes were found to be quite different in their sizes and shapes.

Interaction of liposomes with biological systems is very complex and complicated. Factors which influence liposome-cell interactions such as effect of blood or blood components (serum, plasma and proteins) should be studied prior further investigations of 1,4-DHP amphiphile 1. Serum is an important barrier in transfection mediated by cationic carriers. Various components of serum, like negatively charged albumin, complement system and  $\beta$ 2-glycoprotein, may bind to the cationic liposomes leading to their rapid clearance from the circulation [14]. Hyvönen et al. reported earlier that cellular uptake and transfection activity of 1,4-DHP amphiphile formed lipoplexes were clearly reduced in the presence of serum [3], however there is no information about physical characterisation of liposomes under these conditions. As the primary screening test of these interactions: mixing of liposomes formed by 1,4-DHP amphiphile 1 with different medias used in biological test systems. Studies of these mixtures with physicochemical methods were performed and obtained results are presented in Fig. 5.

Samples from self-assembling compound 1 were prepared in various biological medias, for example, Dulbecco's Modified Eagle Medium (DMEM) and DMEM + fetal bovine serum (FBS) - medias for tests with cell cultures; phosphate buffer (PBS). Studies were performed by AFM and DLS methods.

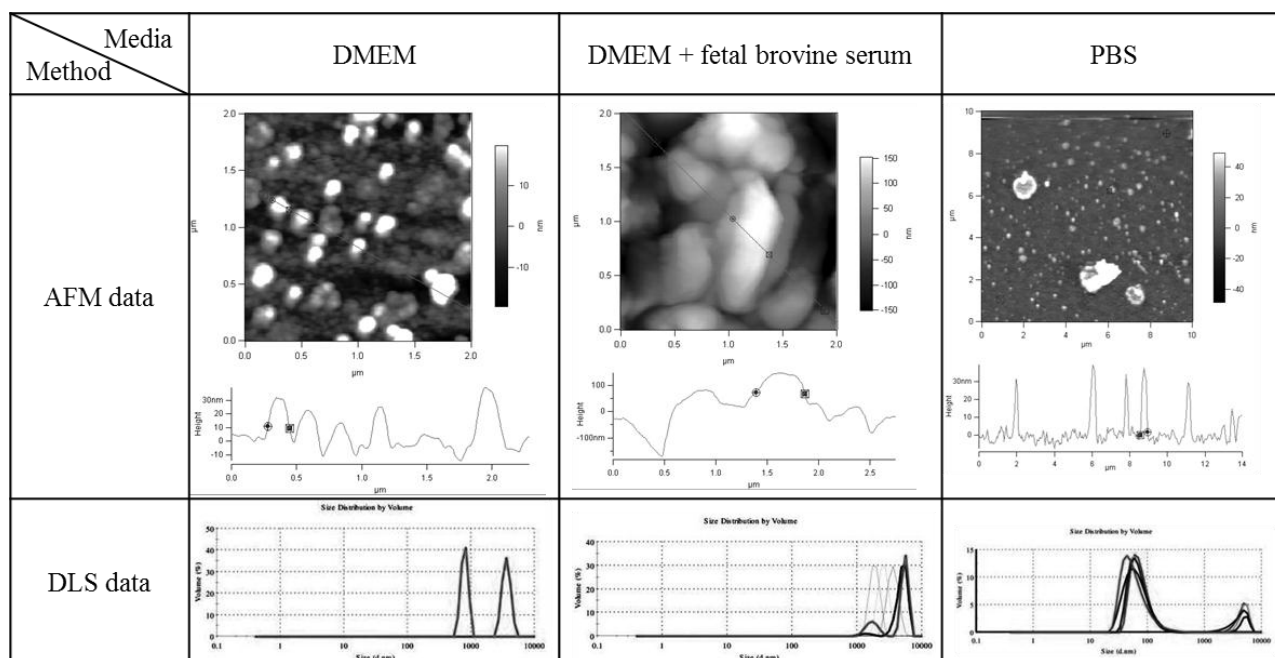


Figure 5. AFM images and vertical profiles and DLS data of liposomes formed by 1,4-DHP amphiphile 1 in different biological media. The samples were prepared by sonication in media solution at a concentration of 1,4-DHP amphiphile 1 at 0.3 mg/ml.

According to the obtained results we can conclude that in the DMEM media at the presence of FBS 1,4-DHP amphiphile 1 formed complexes. Incorporation of PEG-modified lipids into liposomes is well-known and widely used technique to reduce the rate of protein binding on the complex surface, helping to stabilize the structures. In the nearest future our research group is planning to carry out PEG-ylation of liposomes by non-covalent bounding to exclude complexation.

In all cases with DLS method the diameter of liposomes was measured in hydrated state, whereas AFM images were obtained from dried states of the self-aggregated samples. It is also should be admitted that DLS technique detects the average sizes of the whole population of the liposomes, whereas AFM technique is able to visualise only a small fraction of the liposomes. Although the size distribution obtained by AFM and DLS measurements was in line with each other, the average diameters of the liposomes observed by AFM methods were smaller than the average diameters measured by DLS method.

## Summary

From obtained AFM data it can be concluded that the average size of liposomes formed by 1,1'-[(3,5-didodecyloxycarbonyl-4-phenyl-1,4-dihydropyridine-2,6-diyl)dimethylen]-bispyridinium dibromide is about 100-150 nm diameter. Formed liposomes are stable for at least of one month period. According to DLS data liposomes formed by 1,4-dihydropyridine amphiphile 1 in aqueous media are monodisperse with the average hydrodynamic diameter of 190-195 nm. Interaction of liposomes with biological systems is very complicated, obviously liposomes formed by 1,4-DHP amphiphile complexed with fetal bovine serum in the biological system. However, further studies of influence of the size and stability of liposomes formed by 1,4-DHP amphiphile or their compositions with other lipids on their behaviour at different steps of transfection as well as characterisation of liposomes would be beneficial for developing the new efficient delivery agents.

## Acknowledgements

This study was supported by the EuroNanoMed project "CheTherDel", travel grant from ERAF project 2010/0193/2DP/2.1.1.2.0/ 10/APIA/VIAA/002. We are also grateful to M.Sc. P. Biryukov,

M.Sc. Z. Alute and Dr. D. Erts of the Institute of Chemical Physics, University of Latvia for the use and assistance with the AFM equipment and to the Institute of Physics, to University of Latvia for the use and assistance with the DLS equipment.

### Conflict of interest

The authors report no conflicts of interest with respect to this paper.

### References

- [1] Z. Hyvönen, A. Plotniece, I. Reine, B. Chekavichus, G. Duburs and A. Urtti, *Biochim. Biophys. Acta, Biomembr.*, 1509 (2000) 451.
- [2] Z. Hyvönen, M. Ruponen, S. Rönkkö, P. Suhonen and A. Urtti, *Eur. J. Pharm. Sci.*, 15 (2002) 449.
- [3] Z. Hyvönen, S. Rönkkö, M.-R. Toppinen, I. Jääskeläinen, A. Plotniece and A. Urtti, *J. Controlled Release*, 99 (2004) 177.
- [4] A. Urtti, Z. Hyvönen, A. Plotniece, N. Makarova, I. Reine, G. Tirzitis, B. Vigante, B. Cekavicus, Shmidlers, A. Krauze, R. Zhalubovskis, G. Duburs, M. Turunen, S. Ylä-Herttuala, I. Jääskeläinen and M.-R. Toppinen, in, 2001, pp. WO Patent 01/62946 A62941, Int.Cl.62947 C62912N 62915/62987, 62001, Chem. Abstr. 62001, 62135, 206419h.
- [5] D.J. Triggle, *Cell. Mol. Neurobiol.*, 23 (2003) 293.
- [6] D.J. Triggle, *Mini-Rev. Med. Chem.*, 3 (2003) 215.
- [7] G. Duburs, B. Vīgante, A. Plotniece, A. Krauze, A. Sobolevs, J. Briede, V. Kluša and A. Velēna, *Chimica Oggi*, 26 (2008) 68.
- [8] M. Cindric, A. Cipak, J. Serly, A. Plotniece, M. Jaganjac, L. Mrakovcic, T. Lovakovic, A. Dedic, I. Soldo, G. Duburs, N. Zarkovic and J. Molnar, *Anticancer Res.*, 30 (2010) 4063.
- [9] K. Pajuste, A. Plotniece, K. Kore, L. Intenberga, B. Cekavicus, D. Kaldre, G. Duburs and A. Sobolev, *Central European Journal of Chemistry*, 9 (2011) 143.
- [10] I. Montasser, H. Fessi and A.W. Coleman, *Eur. J. Pharm. Biopharm.*, 54 (2002) 281.
- [11] E.I. Goksu, J.M. Vanegas, C.D. Blanchette, W.C. Lin and M.L. Longo, *Biochim. Biophys. Acta*, 1788 (2009) 254.
- [12] S.K. Brar and M. Verma, *Trac-trend anal. chem.*, 30 (2011) 4.
- [13] M. Hossann, T. Wang, M. Wiggenghorn, R. Schmidt, A. Zengerle, G. Winter, H. Eibl, M. Peller, M. Reiser, R.D. Issels and L.H. Lindner, *J. Controlled Release*, 147 (2010) 436.
- [14] S.C. Semple, A. Chonn and P.R. Cullis, *Adv. Drug Delivery Rev.*, 32 (1998) 3.

**Advanced Materials Researches, Engineering and Manufacturing Technologies in Industry**

10.4028/www.scientific.net/AMR.787

**Studies of Preparation and Stability of Liposomes Formed by 1,1'-[(3,5-didodecylloxycarbonyl-4-phenyl-1,4-dihydropyridine-2,6-diil)-dimethylen]Bispyridinium Dibromide**

10.4028/www.scientific.net/AMR.787.157